Volume 31, Number 1 January 2023
ISSN:1521-1398 PRINT,1572-9206 ONLINE

Journal of Computational Analysis and Applications

EUDOXUS PRESS,LLC

Journal of Computational Analysis and Applications
ISSNno.'s:1521-1398 PRINT,1572-9206 ONLINE

SCOPE OF THE JOURNAL

An international publication of Eudoxus Press, LLC
(published quarterly) www.eudoxuspress.com.

Editor in Chief: George Anastassiou
Department of Mathematical Sciences,
University of Memphis, Memphis, TN 38152-3240, U.S.A
ganastss@memphis.edu, ganastss2@gmail.com
http://web0.msci.memphis.edu/~ganastss/jocaaa/

The main purpose of "J.Computational Analysis and Applications" is to publish high quality research articles from all subareas of Computational Mathematical Analysis and its many potential applications and connections to other areas of Mathematical Sciences. Any paper whose approach and proofs are computational,using methods from Mathematical Analysis in the broadest sense is suitable and welcome for consideration in our journal, except from Applied Numerical Analysis articles. Also plain word articles without formulas and proofs are excluded. The list of possibly connected mathematical areas with this publication includes, but is not restricted to: Applied Analysis, Applied Functional Analysis, Approximation Theory, Asymptotic Analysis, Difference Equations, Differential Equations, Partial Differential Equations, Fourier Analysis, Fractals, Fuzzy Sets, Harmonic Analysis, Inequalities, Integral Equations, Measure Theory, Moment Theory, Neural Networks, Numerical Functional Analysis, Potential Theory, Probability Theory, Real and Complex Analysis, Signal Analysis, Special Functions, Splines, Stochastic Analysis, Stochastic Processes, Summability, Tomography, Wavelets, any combination of the above, e.t.c.

"J.Computational Analysis and Applications" is a peer-reviewed Journal. See the instructions for preparation and submission **of articles to JOCAAA.**

Journal of Computational Analysis and Applications(JoCAAA) is published by **EUDOXUS PRESS,LLC**,1424 Beaver Trail Drive,Cordova,TN38016,USA,anastassioug@yahoo.com http://www.eudoxuspress.com. **Annual Subscription Prices**:For USA and Canada,Institutional:Print $500, Electronic OPEN ACCESS. Individual:Print $250. For any other part of the world add $150 more(handling and postages) to the above prices for Print. No credit card payments.

JoCAAA is reviewed and abstracted by Elsevier-Scopus, available also via EBSCO publishing and EBSCO.

Editorial Board
Associate Editors of Journal of Computational Analysis and Applications

George Cybenko
Thayer School of Engineering
Dartmouth College
8000 Cummings Hall,
Hanover, NH 03755-8000
603-646-3843 (X 3546 Secr.)
e-mail:george.cybenko@dartmouth.edu
Approximation Theory and Neural Networks

Sever S. Dragomir
School of Computer Science and Mathematics, Victoria University,
PO Box 14428,
Melbourne City,
MC 8001, AUSTRALIA
Tel. +61 3 9688 4437
Fax +61 3 9688 4050
e-mail: sever.dragomir@vu.edu.au
Inequalities, Functional Analysis, Numerical Analysis, Approximations, Information Theory, Stochastics.

Oktay Duman
TOBB University of Economics and Technology,
Department of Mathematics, TR-06530, Ankara, Turkey,
e-mail: oduman@etu.edu.tr
Classical Approximation Theory, Summability Theory, Statistical Convergence and its Applications

J .A. Goldstein
Department of Mathematical Sciences
The University of Memphis
Memphis, TN 38152
901-678-3130
e-mail: jgoldste@memphis.edu
Partial Differential Equations, Semigroups of Operators

H. H. Gonska
Department of Mathematics
University of Duisburg
Duisburg, D-47048
Germany
011-49-203-379-3542
e-mail: heiner.gonska@uni-due.de
Approximation Theory, Computer Aided Geometric Design

John R. Graef
Department of Mathematics
University of Tennessee at Chattanooga
Chattanooga, TN 37304 USA
e-mail: John-Graef@utc.edu
Ordinary and functional differential equations, difference equations, impulsive systems, differential inclusions, dynamic equations on time scales, control theory and their applications

Weimin Han
Department of Mathematics
University of Iowa
Iowa City, IA 52242-1419
319-335-0770
e-mail: whan@math.uiowa.edu
Numerical analysis, Finite element method, Numerical PDE, Variational inequalities, Computational mechanics

Tian-Xiao He
Department of Mathematics and Computer Science
P.O. Box 2900, Illinois Wesleyan University
Bloomington, IL 61702-2900, USA
Tel (309)556-3089
Fax (309)556-3864
e-mail: the@iwu.edu
Approximations, Wavelet, Integration Theory, Numerical Analysis, Analytic Combinatorics

Margareta Heilmann
Faculty of Mathematics and Natural Sciences, University of Wuppertal
Gaußstraße 20
D-42119 Wuppertal, Germany,
heilmann@math.uni-wuppertal.de
Approximation Theory (Positive Linear Operators)

Xing-Biao Hu
Institute of Computational Mathematics
AMSS, Chinese Academy of Sciences
Beijing, 100190, CHINA
e-mail: hxb@lsec.cc.ac.cn
Computational Mathematics

Seda Karateke
Department of Computer Engineering,
Faculty of Engineering,
Istanbul Topkapi University,
Istanbul, Zeytinburnu 34087, Turkey
e-mail: sedakarateke@topkapi.edu.tr
Approximation Theory, Neural Networks

Vassilis Papanicolaou
Department of Mathematics
National Technical University of Athens
Zografou campus, 157 80
Athens, Greece
tel: +30(210) 772 1722
Fax +30(210) 772 1775
e-mail: papanico@math.ntua.gr
Partial Differential Equations, Probability

Choonkil Park
Department of Mathematics
Hanyang University
Seoul 133-791
S. Korea,
e-mail: baak@hanyang.ac.kr
Functional Equations

Svetlozar (Zari) Rachev,
Professor of Finance, College of Business, and Director of Quantitative Finance Program,
Department of Applied Mathematics & Statistics
Stonybrook University
312 Harriman Hall, Stony Brook, NY 11794-3775
tel: +1-631-632-1998,
svetlozar.rachev@stonybrook.edu

Alexander G. Ramm
Mathematics Department
Kansas State University
Manhattan, KS 66506-2602
e-mail: ramm@math.ksu.edu
Inverse and Ill-posed Problems, Scattering Theory, Operator Theory, Theoretical Numerical Analysis, Wave Propagation, Signal Processing and Tomography

Tomasz Rychlik
Polish Academy of Sciences
Instytut Matematyczny PAN
00-956 Warszawa, skr. poczt. 21
ul. Śniadeckich 8
Poland
e-mail: trychlik@impan.pl
Mathematical Statistics, Probabilistic Inequalities

Boris Shekhtman
Department of Mathematics
University of South Florida
Tampa, FL 33620, USA
Tel 813-974-9710
e-mail: shekhtma@usf.edu
Approximation Theory, Banach spaces, Classical Analysis

T. E. Simos
Department of Computer Science and Technology
Faculty of Sciences and Technology
University of Peloponnese
GR-221 00 Tripolis, Greece
Postal Address:
26 Menelaou St.
Anfithea - Paleon Faliron
GR-175 64 Athens, Greece
e-mail: tsimos@mail.ariadne-t.gr
Numerical Analysis

Jagdev Singh
JECRC University, Jaipur, India
jagdevsinghrathore@gmail.com
Fractional Calculus, Mathematical Modelling, Special Functions, Numerical Methods

H. M. Srivastava
Department of Mathematics and Statistics
University of Victoria
Victoria, British Columbia V8W 3R4
Canada
tel.250-472-5313; office,250-477-6960 home, fax 250-721-8962
e-mail: harimsri@math.uvic.ca
Real and Complex Analysis, Fractional Calculus and Appl., Integral Equations and Transforms, Higher Transcendental Functions and Appl.,q-Series and q-Polynomials, Analytic Number Th.

I. P. Stavroulakis
Department of Mathematics
University of Ioannina
451-10 Ioannina, Greece
e-mail: ipstav@cc.uoi.gr
Differential Equations
Phone +3-065-109-8283

Jessada Tariboon
Department of Mathematics
King Mongut's University of Technology N. Bangkok
1518 Pracharat 1 Rd., Wongsawang,
Bangsue, Bangkok, Thailand 10800
e-mail: jessada.t@sci.kmutnb.ac.th
Time scales

Differential/Difference Equations, Fractional Differential Equations

Manfred Tasche
Department of Mathematics
University of Rostock
D-18051 Rostock, Germany
manfred.tasche@mathematik.uni-rostock.de
Numerical Fourier Analysis, Fourier Analysis, Harmonic Analysis, Signal Analysis, Spectral Methods, Wavelets, Splines, Approximation Theory

Juan J. Trujillo
University of La Laguna
Departamento de Analisis Matematico
C/Astr.Fco.Sanchez s/n
38271. LaLaguna. Tenerife.
SPAIN
Tel/Fax 34-922-318209
e-mail: Juan.Trujillo@ull.es
Fractional: Differential Equations-Operators-Fourier Transforms, Special functions, Approximations, and Applications

Xiao-Jun Yang
State Key Laboratory for Geomechanics and Deep Underground Engineering, China
University of Mining and Technology, Xuzhou 221116, China
Local Fractional Calculus and Applications, Fractional Calculus and Applications, General Fractional Calculus and Applications, Variable-order Calculus and Applications, Viscoelasticity and Computational methods for Mathematical Physics.dyangxiaojun@163.com

Xiang Ming Yu
Department of Mathematical Sciences
Southwest Missouri State University
Springfield, MO 65804-0094
417-836-5931
e-mail: xmy944f@missouristate.edu
Classical Approximation Theory, Wavelets

Richard A. Zalik
Department of Mathematics
Auburn University
Auburn University, AL 36849-5310
USA.
Tel 334-844-6557 office
Fax 334-844-6555
e-mail: zalik@auburn.edu
Approximation Theory, Chebychev Systems, Wavelet Theory

Ahmed I. Zayed
Department of Mathematical Sciences
DePaul University
2320 N. Kenmore Ave.
Chicago, IL 60614-3250
773-325-7808
e-mail: azayed@condor.depaul.edu
Shannon sampling theory, Harmonic analysis and wavelets, Special functions and orthogonal polynomials, Integral transforms

Ding-Xuan Zhou
Department Of Mathematics
City University of Hong Kong
83 Tat Chee Avenue
Kowloon, Hong Kong
852-2788 9708,Fax:852-2788 8561
e-mail: mazhou@cityu.edu.hk
Approximation Theory, Spline functions, Wavelets

Xin-long Zhou
Fachbereich Mathematik, Fachgebiet Informatik
Gerhard-Mercator-Universitat Duisburg
Lotharstr.65, D-47048 Duisburg, Germany
e-mail:Xzhou@informatik.uni-duisburg.de
Fourier Analysis, Computer-Aided Geometric Design, Computational Complexity, Multivariate Approximation Theory, Approximation and Interpolation Theory

Instructions to Contributors
Journal of Computational Analysis and Applications

An international publication of Eudoxus Press, LLC, of TN.

Editor in Chief: George Anastassiou

Department of Mathematical Sciences
University of Memphis
Memphis, TN 38152-3240, U.S.A.

1. Manuscripts files in Latex and PDF and in English, should be submitted via email to the Editor-in-Chief:

Prof.George A. Anastassiou
Department of Mathematical Sciences
The University of Memphis
Memphis,TN 38152, USA.
Tel. 901.678.3144
e-mail: ganastss@memphis.edu

Authors may want to recommend an associate editor the most related to the submission to possibly handle it.

Also authors may want to submit a list of six possible referees, to be used in case we cannot find related referees by ourselves.

2. Manuscripts should be typed using any of TEX,LaTEX,AMS-TEX,or AMS-LaTEX and according to EUDOXUS PRESS, LLC. LATEX STYLE FILE. (Click HERE to save a copy of the style file.)They should be carefully prepared in all respects. Submitted articles should be brightly typed (not dot-matrix), double spaced, in ten point type size and in 8(1/2)x11 inch area per page. Manuscripts should have generous margins on all sides and should not exceed 24 pages.

3. Submission is a representation that the manuscript has not been published previously in this or any other similar form and is not currently under consideration for publication elsewhere. A statement transferring from the authors(or their employers,if they hold the copyright) to Eudoxus Press, LLC, will be required before the manuscript can be accepted for publication.The Editor-in-Chief will supply the necessary forms for this transfer.Such a written transfer of copyright,which previously was assumed to be implicit in the act of submitting a manuscript,is necessary under the U.S.Copyright Law in order for the publisher to carry through the dissemination of research results and reviews as widely and effective as possible.

4. The paper starts with the title of the article, author's name(s) (no titles or degrees), author's affiliation(s) and e-mail addresses. The affiliation should comprise the department, institution (usually university or company), city, state (and/or nation) and mail code.

The following items, 5 and 6, should be on page no. 1 of the paper.

5. An abstract is to be provided, preferably no longer than 150 words.

6. A list of 5 key words is to be provided directly below the abstract. Key words should express the precise content of the manuscript, as they are used for indexing purposes.

The main body of the paper should begin on page no. 1, if possible.

7. All sections should be numbered with Arabic numerals (such as: 1. INTRODUCTION) .
Subsections should be identified with section and subsection numbers (such as 6.1. Second-Value Subheading).
If applicable, an independent single-number system (one for each category) should be used to label all theorems, lemmas, propositions, corollaries, definitions, remarks, examples, etc. The label (such as Lemma 7) should be typed with paragraph indentation, followed by a period and the lemma itself.

8. Mathematical notation must be typeset. Equations should be numbered consecutively with Arabic numerals in parentheses placed flush right, and should be thusly referred to in the text [such as Eqs.(2) and (5)]. The running title must be placed at the top of even numbered pages and the first author's name, et al., must be placed at the top of the odd numbed pages.

9. Illustrations (photographs, drawings, diagrams, and charts) are to be numbered in one consecutive series of Arabic numerals. The captions for illustrations should be typed double space. All illustrations, charts, tables, etc., must be embedded in the body of the manuscript in proper, final, print position. In particular, manuscript, source, and PDF file version must be at camera ready stage for publication or they cannot be considered.

Tables are to be numbered (with Roman numerals) and referred to by number in the text. Center the title above the table, and type explanatory footnotes (indicated by superscript lowercase letters) below the table.

10. List references alphabetically at the end of the paper and number them consecutively. Each must be cited in the text by the appropriate Arabic numeral in square brackets on the baseline.
References should include (in the following order):
initials of first and middle name, last name of author(s)
title of article,

name of publication, volume number, inclusive pages, and year of publication.

Authors should follow these examples:

Journal Article

1. H.H.Gonska,Degree of simultaneous approximation of bivariate functions by Gordon operators, (journal name in italics) *J. Approx. Theory*, 62,170-191(1990).

Book

2. G.G.Lorentz, (title of book in italics) *Bernstein Polynomials* (2nd ed.), Chelsea,New York,1986.

Contribution to a Book

3. M.K.Khan, Approximation properties of beta operators,in(title of book in italics) *Progress in Approximation Theory* (P.Nevai and A.Pinkus,eds.), Academic Press, New York,1991,pp.483-495.

11. All acknowledgements (including those for a grant and financial support) should occur in one paragraph that directly precedes the References section.

12. Footnotes should be avoided. When their use is absolutely necessary, footnotes should be numbered consecutively using Arabic numerals and should be typed at the bottom of the page to which they refer. Place a line above the footnote, so that it is set off from the text. Use the appropriate superscript numeral for citation in the text.

13. After each revision is made please again submit via email Latex and PDF files of the revised manuscript, including the final one.

14. Effective 1 Nov. 2009 for current journal page charges, contact the Editor in Chief. Upon acceptance of the paper an invoice will be sent to the contact author. The fee payment will be due one month from the invoice date. The article will proceed to publication only after the fee is paid. The charges are to be sent, by money order or certified check, in US dollars, payable to Eudoxus Press, LLC, to the address shown on the Eudoxus homepage.

No galleys will be sent and the contact author will receive one (1) electronic copy of the journal issue in which the article appears.

15. This journal will consider for publication only papers that contain proofs for their listed results.

Characteristics of Mexican hat wavelet transform in a class of generalized quotient space

Abhishek Singh*,[1], Aparna Rawat[1] and Shubha Singh[2]

December 24, 2022

Abstract

In this paper, Mexican hat wavelet transformation is defined on the space of tempered generalized quotients by employing the structure of exchange property. We study the exchange property for the Mexican hat wavelet transform by applying the theory of the Mexican hat wavelet transform of distributions. Further, different properties of Mexican hat wavelet transform are investigated on the space of tempered generalized quotients.

Key words: Wavelet transform; Exchange property; Distribution space; Tempered generalized quotient

Mathematics Subject Classification(2010): 44A15; 44A35; 46F99; 54B15

[1]

1 Introduction

The wavelet transform $(Wf)(b,a)$ of a square integrable function f, is given by

$$(Wf)(b,a) = \int_{-\infty}^{\infty} f(t)\overline{\psi_{b,a}}(t)dt, \tag{1.1}$$

where

$$\psi_{b,a}(t) = (\sqrt{a})^{-1}\psi\left(\frac{t-b}{a}\right), \quad b,t \in \mathbb{R}^n, \text{ and } a > 0. \tag{1.2}$$

The inversion formula for (1.1) is given by

$$\frac{2}{C_\psi}\int_0^\infty \left[\int_{-\infty}^{\infty} (\sqrt{a})^{-1}(Wf)(b,a)\psi\left(\frac{x-b}{a}\right)db\right]\frac{da}{a^2} = f(x), \quad x \in \mathbb{R}^n, \tag{1.3}$$

[1]* Corresponding author (mathdras@gmail.com) [1]Department of Mathematics and Statistics, Banasthali Vidhyapith, Banasthali, India
[2]Department of Physics, Banaras Hindu University, Varanasi

where the admissibility condition C_ψ is given by

$$\frac{C_\psi}{2} = \int_0^\infty \frac{|\hat{\psi}(u)|^2}{|u|} dv = \int_0^\infty \frac{|\hat{\psi}(-u)|^2}{|u|} du < \infty \qquad [3, \text{p. } 64].$$

The Mexican hat wavelet is constructed by taking the negative second derivative of a Gaussian function and is given by [24]

$$\psi(t) = e^{-(\frac{t^2}{2})}(1-t^2) = -\frac{d^2}{dt^2} e^{-(\frac{t^2}{2})} \tag{1.4}$$

such that

$$\psi_{b,a}(t) = -a^{\frac{3}{2}} D_t^2 e^{-\frac{(b-t)^2}{2a^2}}, \qquad \left(D_t = \frac{d}{dt}\right). \tag{1.5}$$

Thus, (1.1) can be reduced to

$$(Wf)(b,a) = -a^{\frac{3}{2}} \int_{\mathbb{R}} f(t)\ D_t^2 e^{-\frac{(b-t)^2}{2a^2}} dt, \qquad a \in \mathbb{R}_+ \tag{1.6}$$

which then, under certain conditions on f is

$$(Wf)(b,a) = -a^{\frac{3}{2}} \int_{\mathbb{R}} f^{(2)}(t)\ \ e^{-\frac{(b-t)^2}{2a^2}} dt, \qquad a \in \mathbb{R}_+. \tag{1.7}$$

Let a function $k_a(b-t)$ be defined by

$$k_a(b-t) = \frac{1}{\sqrt{2\pi a}} e^{\left(\frac{-(b-t)^2}{2a}\right)}, \tag{1.8}$$

where $t \in \mathbb{R},\ b = \sigma + i\omega$ and $a \in \mathbb{R}_+$. Then

$$D_t^2 k_{a^2}(b-t) = \frac{1}{\sqrt{2\pi a}} D_t^2 \left(e^{\frac{-(b-t)^2}{2a^2}}\right). \tag{1.9}$$

Therefore, by (1.5)

$$\psi_{b,a}(t) = -(2\pi)^{\frac{1}{2}} a^{\frac{5}{2}} D_t^2 k_{a^2}(b-t)$$

and hence the Mexican hat wavelet transform is given by

$$\begin{aligned}
(Wf)(b,a) &= (2\pi)^{\frac{1}{2}} a^{\frac{5}{2}} \int_{\mathbb{R}} f(t) D_t^2 k_{a^2}(b-t) dt \\
&= (2\pi)^{\frac{1}{2}} a^{\frac{5}{2}} \int_{\mathbb{R}} f^{(2)}(t) k_{a^2}(b-t) dt \\
&= (2\pi)^{\frac{1}{2}} a^{\frac{5}{2}} (f^{(2)} * k_{a^2})(b), \quad b \in \mathbb{C},\ a \in \mathbb{R}_+,
\end{aligned} \tag{1.10}$$

where $k_{a^2}(b-t) = \frac{1}{\sqrt{2\pi a}} e^{\frac{-(b-t)^2}{2a^2}}$.

The most general theory of the MHWT is investigated on the generalized function space $(\mathscr{W}^{\gamma}_{\alpha,\beta})'$ developed by Pathak *et al.* [8]. It is proved that the MHWT $(Wf)(b,a)$ of $f \in (\mathscr{W}^{\gamma}_{\alpha,\beta})'$, is given by $\langle f^{(2)}(t), k_{a^2}(b-t)\rangle$ is an analytic function in the strip $\frac{\alpha}{\gamma} < \text{Re } b < \frac{\beta}{\gamma}$ for some $\alpha, \beta, \gamma \in \mathbb{R}$.

Recently, the wavelet transform has been comprehensively studied in many functions, distributions, and tempered distribution spaces. Several interesting properties and applications in generalized function spaces have been developed (See, for example, [6, 9, 10, 11, 12, 13, 17, 18, 19, 20, 21]. On the other hand, Mikusiński's algebraic approach gave a new transformation to the theory of functional analysis. The space of generalized quotients (Boehmians) is the recent generalization of the Schwartz distribution and the motivation for the expansion is in the core of Mikusiński operators. Its application to function spaces with the involvement of convolution provides different generalized function spaces. Hence, many integral transforms have been investigated in such spaces [1, 5, 7, 14, 15, 16, 22, 23].

Let $\mathscr{S}(\mathbb{R}^n)$ and $\mathscr{S}(\mathbb{R}^n \times \mathbb{R}_+)$ be the spaces of functions with continuous derivatives which are rapidly decreasing on $\mathbb{R}^n$ and $\mathbb{R}^n \times \mathbb{R}_+$. The dual of $\mathscr{S}$ is represented by $\mathscr{S}'$ that is known as the space of tempered distributions. The spaces $\mathscr{S}$ and $\mathscr{S}'$ have been introduced and developed in [2]. The class $\mathscr{S}'$ of tempered distributions is contained in $(\mathscr{W}^{\gamma}_{\alpha,\beta})'$. Therefore the Mexican hat wavelet transform theory can be made applicable to $\mathscr{S}'$. Further, the Mexican hat wavelet transform can be expanded to the space of tempered generalized quotient, as the space is a natural expansion of tempered distributions. Here, we extend the Mexican hat wavelet transformation to a class of generalized quotient space that have quotients of sequences in the form of f_n/φ_n, where the numerator contains terms of the sequence from some set $\mathscr{S}'$ and the denominator is a delta sequence such that it satisfies the following condition

$$f_n * \varphi_m = f_m * \varphi_m, \quad \forall m, n \in \mathbb{N}. \tag{1.11}$$

Further, the delta sequences are defined as sequences of functions $\{\varphi_n\} \in \mathscr{S}$ that satisfies

1. $\int_{\mathbb{R}^n} \varphi_n(x)dx = 1$ for all $n = 1, 2, 3, \cdots$.

2. There exists a constant $C > 0$ such that

$$\int_{\mathbb{R}^n} |\varphi_n(x)|\, dx \leq C \text{ for all } n = 1, 2, 3, \cdots.$$

3. $\lim_{n\to\infty} \int_{\|x\|\geq\epsilon} \|x\|^k \, |(\varphi_j(x))|\, dx = 0$ for every $k \in \mathbb{N}$ and $\epsilon > 0$.

In particular, we extend the transformation to generalized quotient space by defining an exchange property for the Mexican hat wavelet transform. In the

next section, we introduce some of the basic results required for the investigation of MHWT on the generalized quotient space. Section 3 describes some algebraic properties of MHWT in the context of tempered generalized quotients.

2 The exchange property

In this section, the space of tempered generalized quotients is constructed by applying the exchange property. This construction for generalized quotients indicates that the role of convergence is not necessary.

Theorem 2.1. *For a function $f \in \mathscr{S}'$ and $t \in \mathbb{R}$,*

$$(Wf)(b,a) = (2\pi)^{\frac{1}{2}} a^{\frac{5}{2}} (f^{(2)} * k_{a^2})(b) = (2\pi)^{\frac{1}{2}} a^{\frac{5}{2}} \lim_{n\to\infty} ((f^{(2)} * k_{a^2}) e^{-\frac{t^2}{2n}})(b).$$

Proof. Consider,

$$\begin{aligned}
(2\pi)^{\frac{1}{2}} a^{\frac{5}{2}} \lim_{n\to\infty} ((f^{(2)} * k_{a^2}) e^{-\frac{t^2}{2n}})(b) &= (2\pi)^{\frac{1}{2}} a^{\frac{5}{2}} \lim_{n\to\infty} \int_{\mathbb{R}} f^{(2)}(t) k_{a^2}(b) e^{-\frac{t^2}{2n}} dt \\
&= a^{\frac{3}{2}} \lim_{n\to\infty} \int_{\mathbb{R}} f^{(2)}(t) e^{-\frac{(b-t)^2}{2a^2}} e^{-\frac{t^2}{2n}} dt \\
&= a^{\frac{3}{2}} \int_{\mathbb{R}} f^{(2)}(t) e^{-\frac{(b-t)^2}{2a^2}} dt.
\end{aligned}$$

Therefore,

$$(Wf)(b,a) = (2\pi)^{\frac{1}{2}} a^{\frac{5}{2}} \lim_{n\to\infty} ((f^{(2)} * k_{a^2}) e^{-\frac{t^2}{2n}})(b).$$

□

Theorem 2.2. *For $f \in \mathscr{S}'$ and $\varphi \in \mathscr{S}$, we have*

$$(W(f * \varphi))(b,a) = (Wf)(b,a) * \varphi.$$

Proof. By using [4, Lemma 4.3.8], $(f * \varphi) \in \mathscr{S}'$ and hence $(W(f * \varphi))(b,a)$ is defined. Also, by Theorem 2.1

$$(W(f * \varphi))(b,a) = (2\pi)^{\frac{1}{2}} a^{\frac{5}{2}} \lim_{n\to\infty} (((f^{(2)} * \varphi) * k_{a^2}) e^{-\frac{t^2}{2n}})(b).$$

Consider,

$$\begin{aligned}
(2\pi)^{\frac{1}{2}} a^{\frac{5}{2}} (((f^{(2)} * \varphi) * k_{a^2}) e^{-\frac{t^2}{2n}})(b) &= (2\pi)^{\frac{1}{2}} a^{\frac{5}{2}} \int_{\mathbb{R}} (f^{(2)} * \varphi)(t) k(b-t, a^2) e^{-\frac{t^2}{2n}} \, dt \\
&= a^{\frac{3}{2}} \int_{\mathbb{R}} (f^{(2)} * \varphi)(t) e^{-\frac{(b-t)^2}{2a^2}} e^{-\frac{t^2}{2n}} \, dt \\
&= a^{\frac{3}{2}} \int_{\mathbb{R}} \langle f^{(2)}(s), \varphi(t-s) \rangle e^{-\frac{(b-t)^2}{2a^2}} e^{-\frac{t^2}{2n}} \, dt \\
&= a^{\frac{3}{2}} \int_{\mathbb{R}} \langle f^{(2)}(s), \varphi(t-s) \rangle \psi_n(t) dt, \qquad (2.1)
\end{aligned}$$

where $\psi_n(t) = e^{-\frac{(b-t)^2}{2a^2}} e^{-\frac{t^2}{2n}}$.

By [8, Lemma 4.3], we have

$$a^{\frac{3}{2}} \int_{-m}^{m} \langle f^{(2)}(s), \varphi(t-s)\rangle \psi_n(t)dt = a^{\frac{3}{2}} \left\langle f^{(2)}(s), \int_{-m}^{m} \varphi(t-s)\psi_n(t)dt \right\rangle, \ \forall m > 0,$$

which converges to

$$a^{\frac{3}{2}} \left\langle f^{(2)}(s), \int_{-m}^{m} \varphi(t-s)\psi_n(t)dt \right\rangle \text{ as } m \to \infty,$$

Therefore,

$$\begin{aligned} \int_{-\infty}^{\infty} \langle f^{(2)}(s), \varphi(t-s)\rangle e^{-\frac{(b-t)^2}{2a^2}} e^{-\frac{t^2}{2n}}\, dt &= \left\langle f^{(2)}(s), \int_{-\infty}^{\infty} \varphi(t-s)\psi_n(t)\, dt \right\rangle \\ &= \langle f^{(2)}(s), (\varphi * \psi_n)(s)\rangle. \end{aligned} \tag{2.2}$$

Let us now consider,

$$\begin{aligned} (2\pi)^{\frac{1}{2}} a^{\frac{5}{2}} ((f^{(2)} * k_{a^2}) * \varphi)(b) &= (2\pi)^{\frac{1}{2}} a^{\frac{5}{2}} \int_{\mathbb{R}} (f^{(2)} * k_{a^2})(b-t)\varphi(t)\, dt \\ &= (2\pi)^{\frac{1}{2}} a^{\frac{5}{2}} \int_{-M}^{M} \langle f^{(2)}(s), k_{a^2}(b-t-s)\rangle \varphi(t)\, dt, \end{aligned}$$

where supp $\varphi \subseteq [-P, P]$. Now by [8, Lemma 4.3],

$$\begin{aligned} (2\pi)^{\frac{1}{2}} a^{\frac{5}{2}} ((f^{(2)} * k_{a^2}) * \varphi)(b) &= (2\pi)^{\frac{1}{2}} a^{\frac{5}{2}} \int_{-M}^{M} \langle f^{(2)}(s), k_{a^2}(b-t-s)\rangle \varphi(t)\, dt \\ &= (2\pi)^{\frac{1}{2}} a^{\frac{5}{2}} \left\langle f^{(2)}(s), \int_{-\infty}^{\infty} k_{a^2}(b-t-s)\varphi(t)\, dt \right\rangle \\ &= (2\pi)^{\frac{1}{2}} a^{\frac{5}{2}} \left\langle f^{(2)}(s), \int_{-\infty}^{\infty} \frac{1}{\sqrt{2\pi}a} \psi(t-s)\varphi(t)\, dt \right\rangle \\ &= a^{\frac{3}{2}} \left\langle f^{(2)}(s), \int_{-\infty}^{\infty} \psi(t-s)\varphi(t)\, dt \right\rangle \\ &= a^{\frac{3}{2}} \langle f^{(2)}(s), (\varphi * \psi)(s)\rangle. \end{aligned} \tag{2.3}$$

From (2.2) and (2.3), we obtain

$$(W(f * \varphi))(b, a) = (Wf)(b, a) * \varphi.$$

□

Definition 2.3. For a family $\{\varphi_j\}_{j\in J}$, where $\varphi_j \in \mathcal{S}$, we define

$$M\left(\{\varphi_j\}_J \right) = \{x \in \mathbb{R}^n : \varphi_j(x) = 0, \ \ \forall j \in J\}. \tag{2.4}$$

A family of pairs $\{(f_j, \varphi_j)\}_J$, where $f_j \in \mathcal{S}'$ and $\varphi_j \in \mathcal{S}$, have the exchange property if

$$f_j * \varphi_k = f_k * \varphi_j, \forall j, k \in J. \tag{2.5}$$

Let set $\mathcal{A}$ denotes the collection of $\{(f_j, \varphi_j)\}_J$, where $f_j \in \mathcal{S}'(\mathbb{R}^n)$ and $\varphi_j \in \mathcal{S}(\mathbb{R}^n)$, $\forall j \in J$, with exchange property such that $M\left(\{\varphi_j\}_J\right) = \emptyset$.

If $M\left(\{\varphi_j\}_J\right) = \emptyset$ and $M\left(\{\lambda_k\}_K\right) = \emptyset$, then $M\left(\{\varphi_j * \lambda_k\}_{J\times K}\right) = \emptyset$.

Theorem 2.4. *If $\{(f_j, \varphi_j)\}_J \in \mathcal{A}$, then there exists a unique $F \in \mathcal{S}'(\mathbb{R}^n \times \mathbb{R}_+)$ such that F is the Mexican hat wavelet transform of the family of functions $\{(f_j, \varphi_j)\}_J$, i.e., $F = (W\{(f_j, \varphi_j)\}_J)$.*

Proof. Let us consider family of sequences $\{(f_j, \varphi_j)\}_J \in \mathcal{A}$, where $f_j \in \mathscr{S}'(\mathbb{R}^n)$ and $\varphi \in \mathscr{S}$, $\forall j \in J$, with exchange property such that $|\varphi(x)| > \epsilon$, for some $\epsilon > 0$, and $x \in M(\{\varphi_j\}_J)^c$. Then, in some open neighborhood of x, we define

$$F = \frac{(Wf_j)}{\varphi_j}. \tag{2.6}$$

Case 1: We show that for some open neighborhood of x we have a quotient F that is unique in that neighborhood, i.e., F does not depend on $j \in J$. Let U and V be some open neighborhood of x such that $|\varphi_j(x)| > \epsilon$, $\forall x \in U$ and $|\varphi_k(x)| > \epsilon$, $\forall x \in V$. Then since $\{(f_j, \varphi_j)\} \in \mathcal{A}$, hence it satisfy the exchange property and therefore,

$$f_j * \varphi_k = f_k * \varphi_j, \ \forall j, k \in J. \tag{2.7}$$

Applying Mexican hat wavelet transform to (2.7), we get

$$\begin{aligned} (W(f_j * \varphi_k)) &= (W(f_k * \varphi_j)) \\ (Wf_j) * \varphi_k &= (Wf_k) * \varphi_j \quad \text{(by Theorem 2.2)} \\ \frac{(Wf_j)}{\varphi_j} &= \frac{(Wf_k)}{\varphi_k}. \end{aligned} \tag{2.8}$$

Hence, we get a quotient $F = \dfrac{(Wf_j)}{\varphi_j}$ on $U \cap V$.

Case 2: We need to show that $F \in \mathscr{S}'(\mathbb{R}^n \times \mathbb{R}_+)$ is unique. From (2.6) and (2.8), for any $j, k \in J$, we have

$$(Wf_k) = F\varphi_k, \ \forall k \in J \tag{2.9}$$

such that there exists a unique $F \in \mathscr{S}'(\mathbb{R}^n \times \mathbb{R}_+)$ which implies exchange property.

Clearly, for a total sequence, say $\{\varphi_j\}_{\mathbb{N}}$, where $\varphi_j \in \mathcal{S}(\mathbb{R}^n)$ for all $j \in \mathbb{N}$, there is an $f_j \in \mathcal{S}'(\mathbb{R}^n)$ such that $(Wf_j) = \varphi_j F$. Hence, $\{(f_j, \varphi_j)\}_{\mathbb{N}} \in \mathcal{A}$ and $F = (W(\{(f_j, \varphi_j)\}_{\mathbb{N}}))$. □

For the family of pairs of sequences $\{(f_j,\varphi_j)\}_J$, $\{(g_k,\lambda_k)\}_K \in \mathcal{A}$ has an Equivalence Relation, i.e., $\{(f_j,\varphi_j)\}_J$ $\{(g_k,\phi_k)\}_K$ if

$$f_j * \lambda_k = g_k * \varphi_j, \quad \forall j \in J,\ k \in K. \tag{2.10}$$

Theorem 2.5. *Let* $\{(f_j,\varphi_j)\}_J, \{(g_k,\lambda_k)\}_K \in \mathcal{A}$. *Then* $\{(f_j,\varphi_j)\}_J \sim \{(g_k,\lambda_k)\}_K$ *iff* $(W(\{(f_j,\varphi_j)\}_J)) = (W(\{(g_k,\lambda_k)\}_K))$.

Proof. Let $\{(f_j,\varphi_j)\}_J \sim \{(g_k,\lambda_k)\}_K$, hence, they satisfy the exchange property, defined as

$$f_j * \lambda_k = g_k * \varphi_k,\ \forall j \in J, k \in K.$$

Let F and G denotes the Mexican hat wavelet transform of some family of sequences such that $F = (W(\{(f_j,\varphi_j)\}_J))$ and $G = (W(\{(g_k,\lambda_k)\}_K))$. Now, consider,

$$\begin{aligned}
\varphi_j F * \lambda_k &= (Wf_j) * \lambda_k \\
&= (W(f_j * \lambda_k)) \\
&= (W(g_k * \varphi_j)) \\
&= (Wg_k) * \varphi_j \\
&= \lambda_k G * \varphi_j.
\end{aligned}$$

Now, by applying Lemma 2, we get $F = G$.
Conversely, we need to show that the family of sequences $\{(f_j,\varphi_j)\}_J$ and $\{(g_k,\lambda_k)\}_K$ are equivalent. Let us consider

$$\begin{aligned}
& F = G \\
\implies\ & (Wf_j) * \lambda_k = (Wg_k) * \varphi_j \\
\implies\ & (W(f_j * \lambda_k)) = (W(g_k * \varphi_j)) \\
\implies\ & f_j * \lambda_k = g_k * \varphi_j.
\end{aligned} \tag{2.11}$$

Hence, $\{(f_j,\varphi_j)\}_J \sim \{(g_k,\lambda_k)\}_K$. □

From the above theorem it is shown that there is an equivalence relation on $\mathcal{A}$ and hence splits $\mathcal{A}$ into equivalence classes. The equivalence class contains the generalized quotient $\frac{f_n}{\varphi_n}$ and is denoted by $\left[\frac{f_n}{\varphi_n}\right]$. These equivalence classes are called generalized quotients or Boehmians and the space of all such generalized quotients is denoted by $\mathcal{B}$.

Definition 2.6. Let $X = \left[\frac{f_n}{\varphi_n}\right] \in \mathscr{B}$, then the MHWT of X as a generalized quotient is defined by,

$$Y = (WX)(b,a) = \left[\frac{(Wf_n)(b,a)}{\varphi_n}\right].$$

It is well defined since, if $X = \left[\frac{f_n}{\varphi_n}\right] = Y = \left[\frac{g_n}{\psi_n}\right]$ in $\mathscr{B}$, then

$$\begin{aligned} f_m * \psi_n &= g_n * \varphi_m \ \ \forall m, n \in \mathbb{N} \\ (W(f_m * \psi_n))(b,a) &= (W(g_n * \varphi_m))(b,a) \\ (Wf_m)(b,a) * \psi_n &= (Wg_n)(b,a) * \varphi_m \quad \text{(by Theorem 2.2)} \\ \left[\frac{(Wf_n)(b,a)}{\varphi_n}\right] &= \left[\frac{(Wg_n)(b,a)}{\psi_n}\right]. \end{aligned}$$

Further, by considering the map $f \ \to \left[\frac{f*\delta_n}{\delta_n}\right]$, any $f \in \mathcal{W}'(-\infty,\infty)$ can be considered as an element of $\mathscr{B}$ by [4, Theorem 4.3.9], i.e., if $X = \left[\frac{f*\delta_n}{\delta_n}\right]$, then

$$(WX)(b,a) = \left[\frac{W(f*\delta_n)(b,a)}{\delta_n}\right] = \left[\frac{(Wf)(b,a)*\delta_n}{\delta_n}\right] = (Wf)(b,a).$$

This definition extends the theory of MHWT to more general spaces than $(\mathscr{W}^{\gamma}_{\alpha,\beta})'$.

From Theorem 2.4 and Theorem 2.5, it is clear that the Mexican hat wavelet transform is a bijection from the space of generalized quotients to the space of distributions.

Theorem 2.7. *For every $\mathcal{X} \in \mathcal{B}_{\mathscr{S}'(\mathbb{R}^n)}$ there exists a delta sequence (φ_n) such that $\mathcal{X} = [\{(f_n, \varphi_n)\}_{\mathbb{N}}]$ for some $f_n \in \mathscr{S}'(\mathbb{R}^n)$.*

Proof. Let $(\phi_n) \in \mathscr{S}(\mathbb{R}^n)$, be a delta sequence and $X \in \mathcal{B}_{\mathscr{S}'(\mathbb{R}^n)}$. Then, $(WX) * \phi_n \in \mathscr{S}'$, since $(WX) \in \mathscr{S}'$. Consequently, $(WX) * \phi_n = (Wg_n)$ for some $g_n \in \mathscr{S}'$. Therefore, we have

$$X = \left[\frac{g_n * \phi_n}{\phi_n * \phi_n}\right]. \tag{2.12}$$

Hence, $f_n = (g_n * \phi_n) \in \mathscr{S}'$ and by using the property of delta sequences $\phi_n * \phi_n \in \mathscr{S}$ is a delta sequence. This completes the proof. □

Conclusions

The space of generalized quotients includes regular operators, distributions, ultra-distributions and also objects which are neither regular operators nor distributions. It may be concluded here that the space of tempered generalized quotient is constructed in a simple way by using the exchange property. This new construction is further used to represent the Mexican hat wavelet transform of tempered generalized quotients with its algebraic properties. This space of generalized quotient can be applied to examine Mexican hat wavelet transformation on various manifolds.

Acknowledgement

The first author (AS) is supported by National Board for Higher Mathematics(DAE), Government of India, through sanction No. 02011/7/2022 NBHM(R.P.)/ R&D-II/10010 and the third author is supported by DST under WOS-A, Government of India.

References

[1] Arteaga, C. and Marrero, I. (2012). The Hankel Transform of Tempered Boehmians via the Exchange Property. *Applied Mathematics and Computation*, **219**(3), 810-818.

[2] Atanasiu, D. and Mikusiński, P. (2005). On the Fourier transform and the Exchange Property. *International Journal of Mathematics and Mathematical Sciences*, **16**,2579-2584.

[3] Chui, C. K. (1992). *An Introduction to Wavelets*. New York: Academic Press.

[4] Kalpakam NV (1998) Topics in the theory of Boehmians and their integral transforms. (Doctoral dissertation)

[5] Loonker, D., Banerji, P.K., Debnath, L. (2010). On the Hankel transform for Boehmians. *Integral Transforms and Special Functions*, **21**(7), 479-486.

[6] Mala, A., Singh, A., Banerji, P. K. (2018). Wavelet transform of L c, d-space. Integral Transforms and Special Functions, 29(6), 431-441.

[7] Mikusiński, P. (1983). Convergence of Boehmains. *Japanese Journal of Mathematics*, **9**(1), 159-179.

[8] Pathak RS, Singh Abhishek (2016) Mexican hat Wavelet Transform of Distributions. Integral Transforms Special Functions, 27(6):468-483

[9] Pathak, R. S., and Singh, A. (2016). Distributional Wavelet Transform. *Proceedings of the National Academy of Sciences, India Section A: Physical Sciences*, **86**(2), 273-277.

[10] Pathak, R. S., Singh, A. (2016). Wavelet transform of Generalized functions in $K'\{M_p\}$ spaces. *Proceedings Mathematical Sciences*, **126**(2), 213-226.

[11] Pathak, R. S., Singh, A. (2017) Wavelet transform of Beurling-Bjrck type ultradistributions. *Rendiconti del Seminario Matematico della Universita di Padova*, **137**(1), 211-222.

[12] Pathak, R. S., Singh, A. (2019) PaleyWienerSchwartz type theorem for the wavelet transform. *Applicable Analysis*, **98**(7), 1324-1332.

[13] Rawat, A., Singh, A. (2021). Mexican hat wavelet transform of generalized functions in $\mathcal{G}'$ spaces. Proceedings-Mathematical Sciences, 131(2), 1-13.

[14] Roopkumar, R. (2003). Wavelet Analysis on a Boehmian Space. *International Journal of Mathematics and Mathematical Sciences*, **15**, 917-926.

[15] Roopkumar, R. (2009). Convolution Theorems for Wavelet Transform on Tempered Distributions and their extension to Tempered Boehmians. *Asian-European Journal of Mathematics*, **2**(1), 117-127.

[16] Singh, A. (2015). On the Exchange Property for the Hartley Transform. *Italian J. Pure Appl. Math*, **35**, 373-380.

[17] Singh, A., Mala, A. (2019). The continuous wavelet transform on ultradistribution spaces. In Colloquium Mathematicum (Vol. 157, pp. 189-201). Instytut Matematyczny Polskiej Akademii Nauk.

[18] Singh, A., Raghuthaman, N., Rawat, A., Singh, J. (2020). Representation theorems for the Mexican hat wavelet transform. Mathematical Methods in the Applied Sciences, 43(7), 3914-3924.

[19] Singh, A. (2020). Distributional Mexican hat wavelet transform. The Journal of Analysis, 28(2), 533-544.

[20] Singh, A., Raghuthaman, N., Rawat, A. (2021). PaleyWienerSchwartz Type Theorem for Ultradistributional Wavelet Transform. Complex Analysis and Operator Theory, 15(4), 1-11.

[21] Singh, A. (2021). Some Characterizations of Wavelet Transform. National Academy Science Letters, 44(2), 143-145.

[22] Singh, A., Rawat, A., Dhawan, S. (2022). On the exchange property for the wavelet transform. The Journal of Analysis, 1-9.

[23] Singh, A., Rawat, A., Singh, S., Banerji, P. K. (2022). On the wavelet transform for boehmians. Proceedings of the National Academy of Sciences, India Section A: Physical Sciences, 92(3), 331-336.

[24] Srivastava, H. M., Singh, A., Rawat, A., Singh, S. (2021). A family of Mexican hat wavelet transforms associated with an isometry in the heat equation. Mathematical Methods in the Applied Sciences, 44(14), 11340-11349.

Maxwell Cattaneo double diffusive convection (DDC) in a viscoelastic fluid layer

Monal Bharty[1], Atul. K. Srivastava[2], Hrisikesh Mahato[3]
Department of Mathematics, School of Natural Sciences,
Central University of Jharkhand,
Ranchi−825305, India
Emails: priyabharty58@gmail.com[1], atulshaswat@gmail.com[2]
hrishikesh.mahato@cuj.ac.in[3]

December 28, 2022

Abstract

The onset of Maxwell-Cattaneo DDC in a viscoelastic fluid layer is studied using linear stability analysis with the help of normal mode technique. The parabolic advection diffusion equation, which presupposes classical fickian diffusion for both heat and salt, controls the evaluation of temperature and salinity. Analytically, the onset criteria for stationary and oscillatory convection is derived. Since the onset of stationary (steady case) convection is unaffected by Maxwell-Cattaneo effects as well as visco-elastic parameters, oscillatory convection rather than stationary convection is the key to visualize the effects of different parameters in this paper. Two different scenarios for oscillatory convection have been discussed (i) when Maxwell-Cattaneo coefficient for salinity $C_S = 0$ and (ii) when Maxwell-Cattaneo coefficient for temperature $C_T = 0$. Also a comparative study for these two cases i.e. $C_S = 0$ and $C_T = 0$ is performed for different controlling parameters like relaxation parameter (λ_1), retardation parameter (λ_2), diffusion ratio (τ), solutal Rayleigh number (Ra_S) and Prandtl number (Pr) with the help of graphs.

Keywords

DDC, Maxwell-Cattaneo Effect (M-C Effect), Viscoelastic binary fluid, Rayleigh number, Thermal Convection.

1 Introduction

The viscoelastic fluid flow is of significant importance in many fields of science, engineering, and technology, including geophysics, bioengineering, and the

processing of materials in the nuclear, chemical, and petroleum sectors [15][4]. Unique patterns of instabilities, such as overstability, which cannot be predicted or seen in Newtonian fluid, are present in viscoelastic fluids. For almost 40 years [5], the literature has explored the nature of convective motions in a thin horizontal layer of viscoelastic fluid heated from below in the context of the classical Rayleigh-Benard convection geometry. The key papers by Vest and Arpaci [5] provided the first thorough study of the linear stability of a layer of an upper-convected Maxwell fluid, in which stress exhibits an elastic response to strain typified by a single viscous relaxation period. Due to the high viscosity of the polymeric fluids, flow instability and turbulence are much less common than in Newtonian fluids. For a very long time, it has been widely accepted that in realistic experimental conditions, oscillatory convection cannot occur in viscoelastic fluids .However, recent studies on the elastic behaviour of single long DNA strands in buffer solutions have revealed how to make a fluid in which oscillatory viscoelastic convection might be observed. Recently, this notion was confirmed by Kolodner [21], who found oscillatory convection in DNA suspensions in annular geometry. Theoretically, these studies reignite interest in heat convection in viscoelastic fluids.
Sushila et. al. [25] studied a hybrid analytical algorithm for the thin film flow problem that arises in non-Newtonian fluid. They looked at the thin film flow of a third-grade fluid down an inclined plane in their paper. For the local fractional transport equation that occurs in fractal porous media, in [14], a an effective computational technique is presented. Mehta et. al. [22] investigated heat generation/absorption and the effect of joule heating on radiating MHD mixed convection stagnation point flow along vertical stretched sheet embedded in a permeable medium. The use of an unique fractional derivative in the analysis of heat and mass transfer for the slipping flow of viscous fluid with SWCNT's subject to Newtonian heating is explored by [17]. Whereas heat and mass transfer fractional second grade fluid with slippage and ramped wall temperature using Caputo-Fabrizio fractional derivative approach is investigated by [24].
Due to a variety of real-world situations where the Fourier law of heat flux is insufficient, the dynamics of Maxwell-Cattaneo (or non-fourier) fluids have drawn interest. In his investigation of the theory of gases, Maxwell argued that the relationship between heat flow and temperature gradient not only contain a finite relaxation time but also not be instantaneous. In the case of solid, Cattaneo [3] established a comparable relation, which Oldroyd [11] developed further. Later additions were important, such as those by Fox [20] and Carrassi, Morro[18]. The classical Fourier law of heat conduction expresses the heat flux within a medium is proportional to the local temperature gradient in the system. i.e.

$$V_T = -K\nabla T \tag{1}$$

In which V_T is heat flux, T is temperature and K the thermal conductivity. A well consequence of this law is that the heat purturbation propagate with a infinite velocity. To eliminate this unphysical feature, Maxwell-Cattaneo law is

one of the various modifications fourier law and takes the form:

$$\tau_T \frac{DV_T}{Dt} = -V_T - K\nabla T \tag{2}$$

Where the relaxation time is τ_T and the thermal conductivity is K. The derivative $\frac{D}{Dt}$ here represents the time derivative following the motion so that:

$$\frac{DV_T}{Dt} = \left(\frac{\partial}{\partial t} + V.\nabla\right) V_T \tag{3}$$

Where t is time and V is velocity. When a finite speed heatwave [6],[1],[2] is solved by the inclusion of finite relaxation periods, the parabolic heat equation of Fourier fluids, in which heat diffuses at infinite speed, is transformed into a hyperbolic heat equation. The significance of the thermal relaxation term is typically expressed by the dimensionless Maxwell-Cattaneo coefficient C_T, which is the ratio of the thermal relaxation time to twice the thermal diffusion time.

$$C_T = \frac{\tau_T K}{2\rho C_P d^2} = \frac{\tau_T \kappa}{2d^2} = \frac{\left(\frac{\tau_T}{2}\right)}{\tau_\kappa} \tag{4}$$

where thermal diffusion time is $\tau_\kappa (= \frac{d^2}{\kappa})$, density is ρ, specific heat at constant pressure is C_P, length is d and thermal diffusivity is κ. Thus the classical Fourier law has $C_T = 0$.

Numerous physical scenarios have been investigated when it comes to the Maxwell-Cattaneo heat transport effect, including nano-fluid and nano-material [7], biological tissue [26] and stellar interiors [16] in the context of DDC. Many factors, including the coefficient definition, affect the Maxwell-Cattaneo effect's potential importance. Eltayeb [9] discussed convection instabilities of Maxwell-Cattaneo fluids. In his study, he used three distinct forms of the time derivative of the heat flux to explore the linear and weakly nonlinear stabilities of a horizontal layer of fluid obeying the Maxwell-Cattaneo relationship of heat flux and temperature. While Eltayeb, Hughes, and Proctor [10] have examined the convection instability of a Maxwell-Cattaneo fluid in the presence of a vertical magnetic field and have discussed about the instability of a Benard layer under a vertical uniform magnetic field. The DDC of Maxwell-Cattaneo fluid has been studied by Hughes, Proctor and Eltayeb [8]. The consequences of include the Maxwell-Cattaneo (M-C) effects on the commencement of DDC, in which two factors alter the density of a fluid but diffuse at separate rates, were investigated in that study. For both temperature and salinity they considered Maxwell-Cattaneo effect. The modified salinity evolution equation is expressed as:

$$\tau_{\mathscr{C}} \frac{DV_{\mathscr{C}}}{Dt} = -V_{\mathscr{C}} - \kappa_{\mathscr{C}} \nabla \mathscr{C} \tag{5}$$

by analogy with temperature equation when M-C effect is included. where $\mathscr{C}$

is salt concentration, κ is salinity diffusivity, $\tau_{\mathscr{C}}$ the relaxation time for salinity and $V_{\mathscr{C}}$ is salt flux. Most of the above discussed work is related with the Newtonian fluid.
The onset of DDC in viscoelastic fluid (non-Newtonian fluid)layer is investigated by Malashetty and Swamy [19]. They analysed the stability of a binary viscoelastic fluid layer using linear and weakly nonlinear methods in that study. In view of importance viscoelastic fluid as discussed above, in this paper we carry out a linear stability analysis for a Maxwell-Cattaneo DDC in a viscoelastic fluid layer. Here, we focus on the scenario in which the M-C coefficients are extremely small, driven by geophysical and astrophysical concerns. Therefore, even when $C_T, C_S << 1$, new mechanisms for oscillatory instability might develop, given that the initial gradients of temperature and salinity are relatively significant. This is because the modified equations now describe singular perturbations in the time domain.
The work is presented in the following way. The physical problem is discussed in sect. 2 with a brief mathematical formulation. In sect. 3, the linear stability analysis in oscillatory convection for two cases i.e ($C_T = 0$ and $C_S = 0$) for the free-free boundaries is covered. The results and discussion are included in sect. 4, where we described results shown with the help of graph drawn for different parameters by fixing the values of all other parameters and discussed whether these parameters stabilise or destabilise the system. Last but not least, sect. 5 brings to a close a few key aspects of the analysis.

2 Mathematical model

2.1 The physical domain

We consider DDC in a horizontal layer of an incompressible binary viscoelastic Maxwell-Cattaneo fluid confined between two parallel horizontal planes at $z = 0$ and $z = \mathrm{d}$, a distance d apart with the vertically downward gravity g acting on it. Origin is set in the lower boundary of a Cartesian frame of reference, horizontal component x and vertical component z increases upwards. The surfaces are stretched indefinitely in both x and y directions while maintaining a consistent temperature gradient ΔT across the porous layer. To account for the impact of density fluctuations, we presum that the Oberbeck-Boussinesq approximation is used.

2.2 Governing equations

The momentum equation is modelled using the viscoelastic fluid of the Oldroyd type. The basic governing equations are

$$\left(1+\lambda_1\frac{\partial}{\partial t}\right)\left[\rho_0\left(\frac{\partial V}{\partial t}+V.\nabla V\right)+\nabla p-\rho g\right]=\mu\left(1+\lambda_2\frac{\partial}{\partial t}\right)\nabla^2 V \quad (6)$$

$$\left(\frac{\partial T}{\partial t} + (V.\nabla)T\right) = -\nabla.V_T \tag{7}$$

$$\tau_T\left(\frac{\partial U_T}{\partial t} + \nabla.(VU_T)\right) = -U_T - K\nabla^2 T \tag{8}$$

$$\left(\frac{\partial \mathscr{C}}{\partial t} + (V.\nabla)\mathscr{C}\right) = -\nabla.V_{\mathscr{C}} \tag{9}$$

$$\tau_{\mathscr{C}}\left(\frac{\partial U_{\mathscr{C}}}{\partial t} + \nabla.(VU_{\mathscr{C}})\right) = -U_{\mathscr{C}} - K_{\mathscr{C}}\nabla^2\mathscr{C} \tag{10}$$

$$\nabla.V = 0 \tag{11}$$

where $U_T = \nabla.V_T$, $U_{\mathscr{C}} = \nabla.V_{\mathscr{C}}$, $V = (u, v, w)$ is velocity, μ is viscosity, λ_1 is relaxation parameter, λ_2 is retardation parameter, ρ is density, K is thermal conductivity, $K_{\mathscr{C}}$ is salt conductivity, V_T is heat flux and $V_{\mathscr{C}}$ is salt flux. The formula for the relationship between reference density, temperature, and salinity is:-

$$\rho = \rho_0\left[1 - \beta_T(T - T_0) + \beta_{\mathscr{C}}(\mathscr{C} - \mathscr{C}_0)\right] \tag{12}$$

Temperature and salinity's appropriate boundary conditions are:-

$$T = T_0 + \Delta T \text{ at } z = 0 \text{ and } T = T_0 \text{ at } z = d \tag{13}$$

$$\mathscr{C} = \mathscr{C}_0 + \Delta\mathscr{C} \text{ at } z = 0 \text{ and } \mathscr{C} = \mathscr{C}_0 \text{ at } z = d \tag{14}$$

2.3 Initial state

It is considered that the fluid is in a quiescent initial state, which is represented by

$$V_b = (0,0,0), P = P_b(z), T = T_b(z), \mathscr{C} = \mathscr{C}_b(z), \rho = \rho_b(z), \quad V_{T_b} = (0,0,V_T(z)), V_{\mathscr{C}_b} = (0,0,V_{\mathscr{C}}(z)) \tag{15}$$

Using (2.3) in Eqs. (6) − (12) yield

$$\frac{dp_b}{dz} = -\rho_b g, \frac{d^2T_b}{dz^2} = 0, \frac{d^2\mathscr{C}_b}{dz^2} = 0 \tag{16}$$

The initial state solution for temperature and salinity fields are given by:-

$$T_b(z) = T_l - \Delta T\frac{z}{d}, \mathscr{C}_b(z) = \mathscr{C}_l - \Delta\mathscr{C}\frac{z}{d} \tag{17}$$

2.4 Perturbed state

On the initial state, we superimpose a disturbance of the type:-

$$\begin{aligned} V = V_b(z) + V'(x, y.z, t), T = T_b(z) + T'(x, y, z.t), \mathscr{C} = \mathscr{C}_b(z) + \mathscr{C}'(x, y, z, t), \\ P = P_b(z) + P'(x, y, z, t), \rho = \rho_b(z) + \rho'(x, y, z, t), V_T = V_{T_b} + V'_T(x, y, z, t), \\ V_{\mathscr{C}} = V_{\mathscr{C}_b} + V'_{\mathscr{C}}(x, y, z, t) \end{aligned} \tag{18}$$

where perturbations are indicated by primes. Introducing (18) in Eqs. (6) – (11), and using basic state from Eq. (16), The resulting equations are then non-dimensionalized using the following transformations

$$(x, y, z) = d(x^*, y^*, z^*), t = \frac{d^2}{\kappa_{Tz}} t^*, \lambda_1 = \frac{\kappa_{Tz}}{d^2}\lambda_1 *, (V') = \frac{\kappa_{Tz}}{d}(V^*), P' = \frac{\mu \kappa_{Tz}}{K_z} P^*,$$

$$\lambda_2 = \frac{\kappa_{Tz}}{d^2}\lambda_2 *, V_T = \Delta T \frac{K}{d} V_T^*, V_{\mathscr{C}} = \Delta T \frac{\kappa}{d} V_{\mathscr{C}}^*, T' = (\Delta T) T^*, \mathscr{C}' = (\Delta \mathscr{C}) \mathscr{C}^* \tag{19}$$

After eliminating the asterisks for simplicity, we arrived at the non-dimensional, linear governing equations, which are

$$\left(1 + \lambda_1 \frac{\partial}{\partial t}\right)\left[\frac{1}{Pr}\frac{\partial}{\partial t}\nabla^2 V - Ra_T \nabla_1^2 T + Ra_S \nabla_1^2 \mathscr{C}\right] - \left(1 + \lambda_2 \frac{\partial}{\partial t}\right)\nabla^4 V = 0 \tag{20}$$

$$\frac{\partial T}{\partial t} = w - U_T \tag{21}$$

$$2C_T \frac{\partial U_T}{\partial t} = -U_T - \nabla^2 T \tag{22}$$

$$\frac{\partial \mathscr{C}}{\partial t} = w - U_{\mathscr{C}} \tag{23}$$

$$2C_S \frac{\partial U_{\mathscr{C}}}{\partial t} = -U_{\mathscr{C}} - \tau \nabla^2 \mathscr{C} \tag{24}$$

where the Prandtl number Pr, thermal Rayleigh number Ra_T, solutal Rayleigh number Ra_S, Diffusivity ratio τ, Maxwell-Cattaneo coefficient for temperature C_T and Maxwell-Cattaneo coefficient for salinity $C_{\mathscr{C}}$ are defined as: $Pr = \frac{\nu}{\kappa_{T_Z}}$, $Ra_T = \frac{\beta_T g \Delta T d K_Z \nu}{\kappa_{T_Z}}$, $Ra_S = \frac{\beta_S g \Delta \mathscr{C} d K_Z \nu}{\kappa_{T_Z}}$, $\tau = \frac{\kappa_{\mathscr{C}}}{\kappa}$, $C_T = \frac{\tau_T \kappa}{2d^2}$, $C_S = \frac{\tau_{\mathscr{C}} \kappa_{\mathscr{C}}}{2d^2}$, and u, v and w are x, y and z component of velocity respectively.
The boundaries are assumed to be impermeable, isothermal and stress free, therefore we have the following conditions

$$w = \frac{\partial^2 w}{\partial z^2} = T = \mathscr{C} = 0 \text{ at } z = 0, 1. \tag{25}$$

3 Linear Stability Analysis

In this part, we employ linear theory to forecast the thresholds of both marginal and oscillatory convections. Assuming that the amplitudes are small enough, the time-dependent periodic disturbances in a horizontal plane are used to solve the eigenvalue problem specified by Eqs. (20)–(24) subject to the boundary conditions (20) is solved as follows:

$$\begin{pmatrix} w \\ T \\ \mathscr{C} \\ U_T \\ U_{\mathscr{C}} \end{pmatrix} = \begin{pmatrix} W(z) \\ \Theta(z) \\ \Phi(z) \\ \zeta(Z) \\ \gamma(Z) \end{pmatrix} e^{i(lx+my)+\sigma t} \tag{26}$$

where the growth rate is represented by the complex quantity σ and the horizontal wave numbers l and m. W, Θ, Φ, ζ and γ are the amplitudes of stream function, temperature field, solute field, heat flux and solute flux respectively.

$$\left[(1+\lambda_1\sigma)\left(\frac{\sigma}{Pr}(D^2-a^2)\right)+(1+\lambda_2\sigma)(D^2-a^2)^2\right]W+(1+\lambda_1\sigma)Ra_Ta^2\Theta \\ -(1+\lambda_1\sigma)Ra_Sa^2\Phi=0 \tag{27}$$

$$-W+\sigma\Theta+\zeta=0 \tag{28}$$

$$(D^2-a^2)\Theta+(2C_T\sigma+1)\zeta=0 \tag{29}$$

$$-W+\sigma\Phi+\gamma=0 \tag{30}$$

$$\tau(D^2-a^2)\Phi+(2C_S\sigma+1)\gamma=0 \tag{31}$$

where $D=\frac{d}{dz}$ and $a^2=l^2+m^2$. on the free boundary. we take the solution of Eqn. (27)-(31) satisfying the boundary condition for free-free case:

$$[W(z),\Theta(z),\Phi(z),\zeta(z),\gamma(z)]=[W_0,\Theta_0,\Phi_0,\zeta_0,\gamma_0]\sin(n\pi z),(n=1,2,3,...) \tag{32}$$

Substituting Eq. (32) into (27)-(31), and considering $n=1$, we get a matrix equation

$$\begin{bmatrix} M_1 & -a^2Ra_T & a^2Ra_S & 0 & 0 \\ -1 & \sigma & 0 & 1 & 0 \\ 0 & -\alpha & 0 & 2C_T\sigma+1 & 0 \\ -1 & 0 & \sigma & 0 & 1 \\ 0 & 0 & -\tau\alpha & 0 & 2C_S\sigma+1 \end{bmatrix} \begin{bmatrix} W_0 \\ \Theta_0 \\ \Phi_0 \\ \zeta_0 \\ \gamma_0 \end{bmatrix} = \begin{bmatrix} 0 \\ 0 \\ 0 \\ 0 \\ 0 \end{bmatrix} \tag{33}$$

where $\alpha=a^2+\pi^2$, $M_1=\left[\frac{-\sigma}{Pr}+\frac{(1+\lambda_2\sigma)\alpha}{(1+\lambda_1\sigma)}\right]\alpha$.

For non-trivial solution of W, Θ, Φ, ζ and γ, we need to make the determinant of the above matrix as zero, we get

$$Ra_T=\left(\sigma+\frac{\alpha}{(2C_T\sigma+1)}\right)\left[\frac{M_1}{a^2}-\frac{Ra_S(2C_S\sigma+1)}{\sigma(2C_S\sigma+1)+\tau\alpha}\right] \tag{34}$$

3.1 Stationary state

We have $\sigma = 0$ at the stability margin for the direct bifurcation, or stable onset. The Rayleigh number at which a marginally stable steady mode occurs therefore becomes

$$Ra_T^{st} = \frac{\alpha^3}{a^2} - \frac{Ra_S}{\tau} \tag{35}$$

We obtained the result which is comparable to that of Turner [13]. This result also indicate that stationary Rayleigh number is independent of the viscoelastic parameters and Maxwell-Cattaneo coefficients. The stationary Rayleigh number Ra_T^{st} given by Eq. (35) attains the critical value

$$Ra_{T,C}^{st} = \frac{27}{4}\pi^4 - \frac{Ra_S}{\tau} \tag{36}$$

for the wave number $a_c = \frac{\pi}{\sqrt{2}}$.
When $Ra_S = 0$, Eq. (36) gives

$$Ra_{T,C}^{st} = \frac{27}{4}\pi^4 \tag{37}$$

which is classical outcome of Newtonian fluid layer mentioned in the book of Chandrashekhar [23].

3.2 Oscillatory motion

In general, σ, the growth rate, is a complex quantity with the formula $\sigma = \sigma_r + i\omega$. While the system will become unstable for $\sigma_r > 0$, it is always stable for $\sigma_r < 0$. $\sigma_r = 0$ for the neutral stability state.

1. The case of C_S=0

we put C_S=0 in Eq. (34), and get

$$Ra_T = \left(\sigma + \frac{\alpha}{2C_T\sigma + 1}\right)\left[\left(\frac{-\sigma\alpha}{Pra^2} + \frac{(1+\lambda_2\sigma)\alpha^2}{(1+\lambda_1\sigma)a^2}\right) - \frac{Ra_S}{\sigma + \tau\alpha}\right] \tag{38}$$

then put $\sigma = i\omega$(ω is real) in Eq. (38) and get

$$Ra_T = \Pi_1 + (i\omega)\,\Pi_2 \tag{39}$$

The expression for Π_1 is given by

$$\Pi_1 = D_1 - D_2 - D_3 + D_4 - D_5$$

The fact that Ra_T is a physical quantity proves that it is real. Hence, from Eq. (39) it follows that either $\omega = 0$ (steady onset) or $\Pi_2 = 0$ ($\omega \neq 0$, oscillatory onset). For oscillatory onset $\Pi_2 = 0(\omega \neq 0)$ and this provides a dispersion relation of the form

$$B_1\left(\omega^2\right)^3 + B_2\left(\omega^2\right)^2 + B_3\left(\omega^2\right) + B_4 = 0 \tag{40}$$

where the constants $B_1 = Q_1, B_2 = Q_1Q_7 + Q_2 - Q_3Q_5 - Q_3Q_8, B_3 = Q_2Q_7 - Q_4Q_5 - Q_3Q_6 - Q_3Q_7Q_8 - Q_4Q_8 + Q_9 + Q_3Q_{10}, B_4 = -Q_4Q_6 - Q_4Q_7Q_8 + Q_7Q_9 + Q_4Q_{10}$

Now Eq. (39) with $\Pi_2 = 0$, gives oscillatory Rayleigh number Ra_T^{osc} at the margin of stability as

$$Ra_T^{osc} = \Pi_1. \tag{41}$$

Also, to cause the oscillatory convection, ω^2 must be positive. The symbols $D_1, D_2, D_3, D_4, D_5, Q_1, Q_2, Q_3, Q_4, Q_5, Q_6, Q_7, Q_8, Q_9, Q_{10}, Q_{11}, Q_{12}, Q_{13}, Q_{14}$, Q_{15}, Q_{16} and Π_2 are defined in Appendix-I

2. The case of C_T=0

we put C_T=0 in Eq. (34), and get

$$Ra_T = (\sigma + \alpha)\left[\left(\frac{-\sigma\alpha}{Pra^2} + \frac{(1+\lambda_2\sigma)\alpha^2}{1+\lambda_1\sigma)a^2}\right) - \frac{Ra_S(2C_S\sigma+1)}{(\sigma(2C_S\sigma+1)+\tau\alpha)}\right] \tag{42}$$

then put $\sigma = i\omega(\omega$ is real) in Eq. (42) and get

$$Ra_T = \Pi_1' + (i\omega)\,\Pi_2' \tag{43}$$

The expression for Π_1' is given by

$$\Pi_1' = F_1 - F_2 + F_3 + F_4 - F_5$$

For oscillatory onset $\Pi_2' = 0$ ($\omega \neq 0$) and this provides a dispersion relation of the form

$$C_1\left(\omega^2\right)^3 + C_2\left(\omega^2\right)^2 + C_3\left(\omega^2\right) + C_4 = 0 \tag{44}$$

where the constants $C_1 = P_1P_6^2 - P_2P_6^2P_7$, $C_2 = P_1 + 2P_2P_5P_6P_7 - P_2P_7 - P_3P_6^2P_7 + P_6^2P_8 + P_2P_6P_9$, $C_3 = P_1P_5^5 - 2P_1P_5P_6 - P_2P_4 - P_2P_5^2P_7 + 2P_3P_5P_6P_7 - P_3P_7 - 2P_5P_6P_8 + P_8 - P_2P_5P_9 + P_3P_6P_9 + P_2P_9$, $C_4 = -P_3P_4 - P_3P_5^2P_7 + P_5^2P_8 - P_3P_5P_9 + P_3P_9$

Now Eq. (43) with $\Pi_2' = 0$, gives oscillatory Rayleigh number Ra_T^{osc} at the margin of stability as

$$Ra_T^{osc} = \Pi_1'. \tag{45}$$

Also, to cause the oscillatory convection, ω^2 must be positive. The symbols $F_1, F_2, F_3, F_4, F_5, P_1, P_2, P_3, P_4, P_5, P_6, P_7, P_8, P_9, P_{10}, P_{11}, P_{12}, P_{13}, P_{14}$ and Π_2' are defined in Appendix-I

4 Result and discussion

In this paper, Linear stability has been investigated in the presence of Maxwell-Cattaneo DDC for viscoelastic fluid. The onset of instability is examined for various controlling parameters such as Prandtl number (Pr), diffusivity ratio (τ),

relaxation parameter(λ_1), retardation parameter (λ_2), solutal Rayleigh number (Ra_S), Maxwell-Cattaneo coefficient for temperature (C_T) and Maxwell-Cattaneo coefficient for salinity (C_S). In most physical contexts, the Maxwell-Cattaneo effect is so negligible that we have concentrated on the case where C is smaller than 1, where C is used in the discussion to signify either C_T or C_S. Because C is so small, the Maxwell-Cattaneo effect only manifests itself for concomitantly strong heat and salinity gradients.

In the (a, Ra_T) plane, Fig. 1(a)-(f) illustrate the neutral curves of oscillatory convection for C_S, λ_1, λ_2, τ, Pr and Ra_S when $C_T = 0$ while Fig 1(a')-(f') illustrate the neutral curves when $C_S = 0$ for C_T, λ_1, λ_2, τ, Pr and Ra_S. Fig. 1(a) illustrates how C_S affects the system's stability whereas the impact of C_T is depicted in Fig. 1(a'). With a rise in C_S, the minimum Rayleigh number increases, but with a rise in C_T, the minimum Rayleigh number decreases. So, clearly it is shown that C_S has stabilizing while C_T has destabilizing effect on the stability of the system.

Fig. 1(b) and Fig. 1(b') show the influence of relaxation parameter λ_1 on the stability of the system for $C_T = 0$ and $C_S = 0$ respectively. We can see that raising λ_1 causes the lowest value of the Rayleigh number, Ra_T, is decreases, indicating that λ_1 has a destabilising influence on the Maxwell-Cattaneo DDC in viscoelastic fluid for both situations, where ($C_T = 0$ and $C_S = 0$). Also, it is shown graphically that for different values of λ_1 the case $C_S = 0$ is more stable as compare to $C_T = 0$. Fig. 1(c) and Fig. 1(c') demonstrate that when the value of λ_2 grows, the lowest Rayleigh number similarly rises, stabilising the system. For different values of λ_2, $C_S = 0$ case is more stable. Viscoelastic parameter behaviour is clear and consistent with what [12] said.

The influence of diffusion ratio τ on the system's stability is depicted in Fig 1(d) for $C_T = 0$ and in Fig 1(d') for $C_S = 0$. It is shown the minimum of critical Rayleigh number rises with rise in the value of (τ). It occurs because $\tau = \frac{\kappa_{\mathscr{C}}}{\kappa}$ has an inverse relationship to thermal diffusivity κ. Therefore, when the diffusivity ratio τ increases, the value of thermal diffusivity falls, implying an increase in the Rayleigh number. Also, for different values of τ, $C_S = 0$ is more stable.

Fig 1(e) and Fig 1 (e') show graphs for various values of Prandtl number Pr when $C_T = 0$ and $C_S = 0$ respectively. For the case $C_T = 0$, the system becomes stabilised as a result of the minimum of Ra_T value increasing together with the value of Prandtl number Pr. The fact that Pr is inversely proportional to thermal diffusivity explains it. It has been demonstrated that as the value of Pr increases, the minimum Rayleigh number drops and the system becomes unstable as a result for $C_S = 0$.

The graphs for various Ra_S values on the (a, Ra_T) plane for $C_T = 0$ and $C_S = 0$ are shown in Fig 1(f) and Fig 1(f') respectively. So, for $C_T = 0$, as Ra_S values rise, the minimum of Rayleigh number rises as well, which causes the system to stabilise. It has been seen that the system becomes unstable when the value of Ra_S rises because the minimum Rayleigh number decreases for $C_S = 0$.

5 Conclusion

We have attempted to understand the onset of Maxwell-Cattaneo DDC in a binary viscoelastic fluid layer. With the use of the normal mode technique, linear stability analysis for stationary and oscillatory convection is carried out in this study. Because the Maxwell-Cattaneo coefficients have no effect on stationary states, we have generated graphs for oscillatory convection rather than stationary convection.
The conclusions are as follows.

1. The onset of oscillatory convection is found to be delayed by C_S, λ_2, τ, Pr, and Ra_S, whereas the onset of oscillatory convection is found to be advanced by increasing the value of λ_1, which decreases the value of Rayleigh number corresponding to oscillaory convection in the case of $C_T = 0$.

2. λ_2, τ are found to delay the onset of oscillatory convection whereas on increasing the value of C_T, λ_1, Pr and Ra_S the value of Rayleigh number corresponding to oscillaory convection decreases, thus it advances the onset of convection for the case $C_S = 0$.

According to Maxwell-Cattaneo law, there is currently relatively limited study being done on thermal instability. The Maxwell-Cattaneo law for heat flux and temperature relation with various external effects, such as Electrohydrodynamics, radiation, rotation, etc., can therefore be applied to diverse types of fluids in the future.

Appendix-I

$D_1 = \omega^2 Q_8 \left(1 - \frac{Q_{11}}{Q_{16}\omega^2+1}\right)$, $D_2 = \frac{\omega^2 Q_{12}}{Q_3\omega^2+Q_4}\left(1 - \frac{Q_{11}}{Q_{16}\omega^2+1}\right)$, $D_3 = \frac{\omega^2 Q_{13}}{Q_7+\omega^2}\left(1 - \frac{Q_{11}}{Q_{16}\omega^2+1}\right)$, $D_4 = \frac{\omega^2 Q_{14}}{(Q_3\omega^2+Q_4)(Q_{16}\omega^2+1)}$, $D_5 = \frac{Q_5}{(Q_7+\omega^2)(Q_{16}\omega^2+1)}$, $Q_1 = 4C_T^2\alpha^2\lambda_1\lambda_2$, $Q_2 = \lambda_1\lambda_2\alpha^2 - 2C_T\lambda_1\lambda_2\alpha^2$, $Q_3 = \lambda_1^2 a^2$, $Q_4 = a^2$, $Q_5 = 4Ra_S C_T^2\tau\alpha$, $Q_6 = Ra_S\tau\alpha - 2C_T Ra_S\tau\alpha$, $Q_7 = \tau^2\alpha^2$, $Q_8 = \frac{\alpha}{Pra^2}$, $Q_9 = \alpha^3(\lambda_2-\lambda_1)$ $Q_{10} = \alpha Ra_S$, $Q_{11} = 2C_T$, $Q_{12} = (\lambda_2 - \lambda_1)\alpha^2$, $Q_{13} = Ra_S$, $Q_{14} = \alpha^3\lambda_1\lambda_2$, $Q_{15} = Ra_S\tau\alpha^2$, $Q_{16} = 4C_T^2$, $\Pi_2 = \frac{(Q_1\omega^4+Q_2\omega^2)}{(Q_3\omega^2+Q_4)} - \frac{(Q_5\omega^2+Q_6)}{Q_7+\omega^2} - Q_8 + \frac{Q_9}{(Q_3\omega^2+Q_4)} + \frac{Q_{10}}{(Q_7+\Omega^2)}$, $F_1 = \omega^2 P_{10}$, $F_2 = \frac{P_{11}\omega^2}{P_2\omega^2+P_3}$, $F_3 = \frac{\omega^2 Q_{13}((Q_5-Q_6\omega^2)-1)}{(Q_5-Q_6\omega^2)^2+\omega^2}$, $F_4 = \frac{\omega^2 Q_{12}}{Q_2\omega^2+Q_3}$, $F_5 = \frac{Q_9+Q_4(Q_5-Q_6\omega^2)}{(Q_5-Q_6\omega^2)^2+\omega^2}$, $P_1 = \alpha^2\lambda_1\lambda_2$, $P_2 = a^2\lambda_1^2$, $P_3 = a^2$, $P_4 = Ra_S\tau\alpha$, $P_5 = \tau\alpha$, $P_6 = 2C_S$, $P_7 = \frac{\alpha^2}{Pra^2}$, $P_8 = (\lambda_2 - \lambda_1)\alpha^3$, $P_9 = 2Ra_S\alpha C_S$, $P_{10} = \frac{\alpha}{a^2 Pr}$, $P_{11} = (\lambda_2 - \lambda_1)\alpha^2$, $P_{12} = \alpha^3\lambda_1\lambda_2$, $P_{13} = 2C_S Ra_S$, $P_{14} = Ra_S\alpha$, $\Pi_2' = \frac{P_1\omega^2}{P_2\omega^2+P_3} - \frac{P_4}{(P_5-P_6\omega^2)^2+\omega^2} - P_7 + \frac{P_8}{P_2\omega^2+P_3} - \frac{P_9((P_5-P_6\omega^2)-1)}{(P_5-P_6\omega^2)^2+\omega^2}$

Acknowledgment

Author, Monal Bharty, sincerely thanks Central University of Jharkhand for providing financial support in the form of a research fellowship. This work is only presented in the 5th International Conference on Mathematical Modelling,

Applied Analysis and Computation-2022 (ICMMAAC-22) held in JECRC University, Jaipur (India).

References

[1] B. Straughan, *Heat waves*, New York, NY: Springer, 2011.

[2] B. Straughan, Tipping points in Cattaneo-Christov thermohaline convection, *Proc. R. Soc. A*, 467, 7–18 (2011).

[3] C. Cattaneo, Sulla conduzione del calore, *Atti Mat. Fis. Univ. Modena*, 3, 83–101 (1948).

[4] C.W. Horton, F.T. Rogers, Convection currents in a porous medium. *J. Appl. Phys.*, 16, 367-370 (1945).

[5] C.M. Vest, V.S. Arpaci, Overstability of a viscoelastic fluid layer heated from below, *J.Fluid Mech*, 36, 613-623 (1969).

[6] D.D. Joseph, L.Preziosi, Heat waves, *Rev.Mod. Phys.*, 61, 41–73 (1989).

[7] D. Jou, A. Sellitto, FX. Alvarez, Heat waves and phonon-wall collisions, *nanowires. Proc. R. Soc. A*, 467, 2520–2533 (2011).

[8] D.W. Hughes, M.R.E. Proctor, I.A. Eltayeb, Maxwell–Cattaneo double-diffusive convection:limiting cases, *J. Fluid Mech.*, vol. 927 (2021).

[9] I. A. Eltayeb, Convective instabilities of Maxwell–Cattaneo fluids, *Proc. R. Soc. A*, 473 (2017) https://doi.org/10.1098/rspa.2016.0712

[10] I. A. Eltayeb, D. W. Hughes, M. R. E. Proctor, The convective instability of a Maxwell–Cattaneo fluid in the presence of a vertical magnetic field, *Proc. R. Soc. A*, 476 (2020) https://doi.org/10.1098/rspa.2020.0494

[11] J.G. Oldroyd, On the formulation of rheological equations of state, *Proc. R. Soc. Lond. A*, 200, 523–541 (1950).

[12] J. Kang, Fu, Ceji. Fu, W. Tan, Thermal convective instability of viscoelastic fluids in a rotating porous layer heated from below, *J. Non-Newtonian Fluid Mechanics*, 166, 93-101 (2011).

[13] J.S. Turner, *Buoyancy Effects in Fluids*, Cambridge University Press, London, 1973.

[14] J. Singh, An efficient computational method for local fractional transport equation occurring in fractal porous media, *Comput. Appl. Math*, 39, 137(2020).

[15] J.Zhou, I. Papautsky, Viscoelastic microfluidics: progress and challenges, *Microsyst and Nanoeng*, 6, 1-24 (2020).

[16] L. Herrera, N. Falcón, Heat waves and thermohaline instability in a fluid, *Phys. Lett. A*, 201, 33–37 (1995).

[17] M. Ahmad, M. I. Asjad, J. Singh, Application of novel fractional derivative to heat and mass transfer analysis for the slippage flow of viscous fluid with SWCNT's subject to Newtonian heating, *Math. Methods Appl. Sci*, (2021) https://doi.org/10.1002/mma.7332

[18] M. Carrassi, A. Morro, A modified Navier-Stokes equation, and its consequences on sound dispersion, *Nuovo Cimento B*, 9, 321–343 (1972).

[19] M.S. Malashetty, M. Swamy, The onset of double diffusive convection in a viscoelastic fluid layer, *Int. J. Non Newtonian Fluid Mech.*, vol. 165, 1129-1138 (2010).

[20] N. Fox, Low temperature effects and generalized thermoelasticity, *IMA J. Appl. Maths*, 5, 373–386 (1969).

[21] P. Kolodner, Oscillatory convection in viscoelastic DNA suspensions, *J.Non- Newtonian Fluid Mech*, 75, 167–192 (1998).

[22] R. Mehta, R. Kumar, H. Rathore, J. Singh, Joule heating effect on radiating MHD mixed convection stagnation point flow along vertical stretching sheet embedded in a permeable medium and heat generation/absorption, *Heat Transfer (Wiley)*, 51(8), 7369-7386 (2022).

[23] S. Chandrasekhar, *Hydrodynamic and Hydromagnetic Stability*, Dover, New York, 1981.

[24] S. U. Haq, S. U. Jan, S. I. A. Shah, I. Khan, J. Singh, Heat and mass transfer of fractional second grade fluid with slippage and ramped wall temperature using Caputo-Fabrizio fractional derivative approach, *AIMS Mathematics*, 5(4), 3056-3088 (2020).

[25] Sushila, J. Singh, D. Kumar, D. Baleanu, A hybrid analytical algorithm for thin film flow problem occurring in non-Newtonian fluid mechanics, *Ain Shams Eng. J*, 12(2), 2297-2302 (2021).

[26] W. Dai, H. Wang, PM. Jordan, RE. Mickens, A. Bejan, A mathematical model for skin burn injury induced by radiation heating, *Int. J. Heat Mass Transfer*, 51, 5497–5510 (2008).

Figure 1: Oscillatory neutral stablity curves for different values of: 1(a) Maxwell-Cattaneo coefficient for solute C_S when $C_T = 0$; 1(a') Maxwell-Cattaneo coefficient for temperature C_T when $C_S = 0$.

Figure 2: Oscillatory neutral stability curves for different values of: 1(b) relaxation parameter λ_1 when $C_T = 0$; 1(b') relaxation parameter λ_1 when $C_S = 0$.

Figure 3: Oscillatory neutral stability curves for different values of: 1(c) retardation parameter λ_2 when $C_T = 0$; 1(c') retardation parameter λ_2 when $C_S = 0$.

Figure 4: Oscillatory neutral stability curves for different values of: 1(d) diffusivity ratio τ when $C_T = 0$; 1(d') diffusivity ratio τ when $C_S = 0$.

Figure 5: Oscillatory neutral stability curves for different values of: 1(e) Prandtl number Pr when $C_T = 0$; 1(e') Prandtl number Pr when $C_S = 0$.

Figure 6: Oscillatory neutral stability curves for different values of: 1(f) solutal Rayleigh number Ra_S when $C_T = 0$; 1(f') solutal Rayleigh number Ra_S when $C_S = 0$.

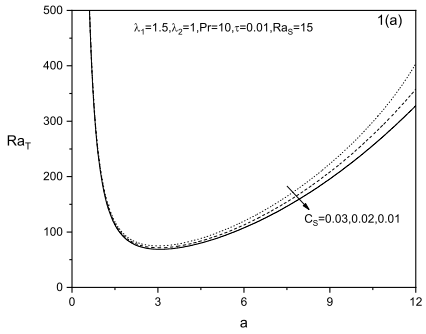

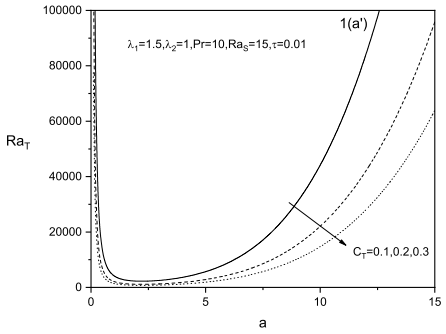

Figure 1

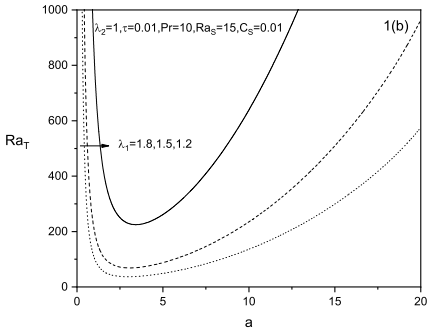

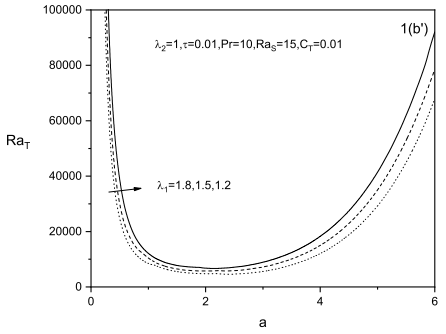

Figure 2

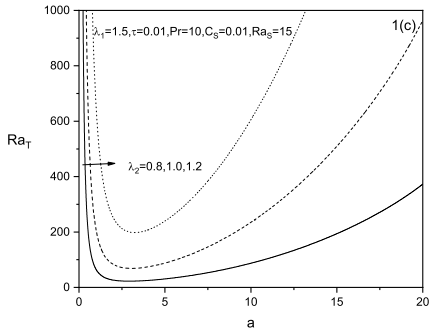

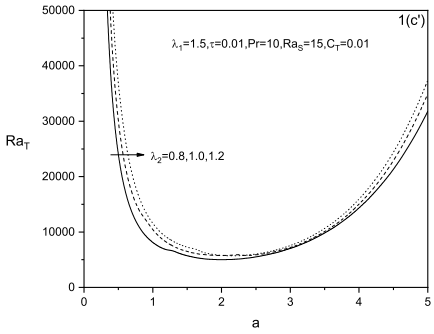

Figure 3

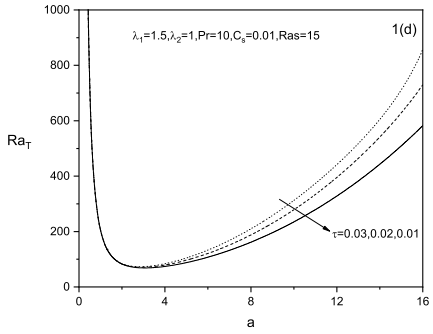

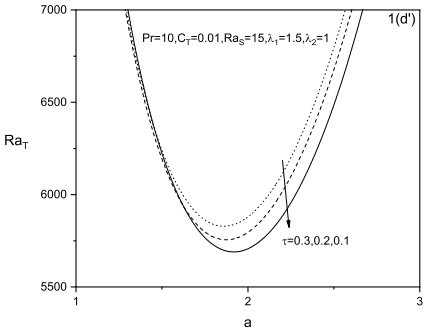

Figure 4

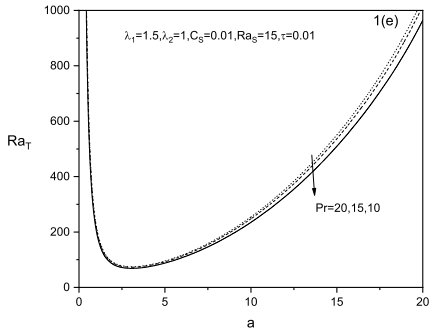

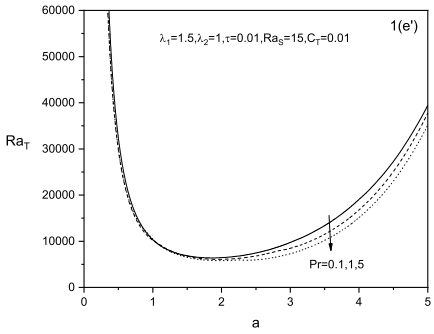

Figure 5

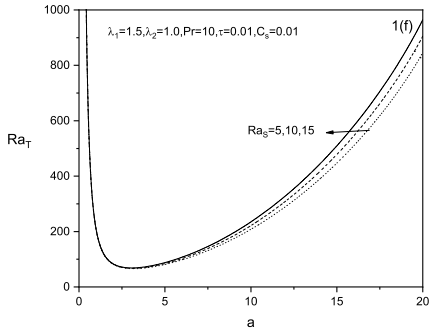

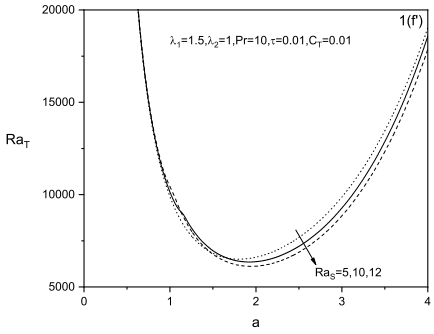

Figure 6

Some New Results for the $\mathcal{M}$-Transform Involving the Incomplete H- and $\overline{H}$-Functions

Sanjay Bhatter[1], Sapna Meena[1], Jagdev Singh[2] and Sunil Dutt Purohit[3,*]

[1]Department of Mathematics, Malaviya National Institute of Technology, Jaipur, India.
sbhatter.maths@mnit.ac.in, sapnabesar1996@gmail.com

[2]Department of Mathematics, JECRC University, Jaipur, India.
jagdevsinghrathore@gmail.com

[3]Department of HEAS (Mathematics), Rajasthan Technical University, Kota, India.
sunil_a_purohit@yahoo.com

Abstract

In this paper, we construct some new image formulas for the incomplete H-and $\overline{H}$-functions under the Akel's $\mathcal{M}$-transform. We also provide image formulas for the incomplete Meijer's G-functions, incomplete Fox-Wright functions and Fox's H-function, as special cases of our main findings in corollaries.

Key Words and Phrases. Incomplete gamma function; $\mathcal{M}$-transform; Incomplete H-functions; Incomplete $\overline{H}$-functions; Mellin-Barnes type contour; Incomplete Fox-Wright generalized hypergeometric functions.
MSC2010. 26A33, 33B20,33C60, 33E20, 44A40 .

1 Introduction and Preliminaries

Integral transforms have been useful in solving numerous differential and integral problems for many years. It is possible to convert differential and integral operators from one domain under consideration into multiplication operators in another domain by using the right integral transform.

The Laplace transform, the Fourier integral transform, the Mellin transform are the classical integral transforms used to solve differential equations, integral equations, and in analysis and the theory of functions. For further information, see the research papers [5, 10, 12, 13].

*Corresponding author

Akel's $\mathcal{M}$-transform

Akel in [1] recently, introduced the following $\mathcal{M}$-transform in this sequence:

$$\mathcal{M}_{\rho,m}[f(x)](u,v,w)=\int_0^\infty \frac{e^{-ux-\frac{v}{x}}}{(x^m+w^m)^\rho}f(wx)\,dx, \tag{1}$$

with $\rho\in\mathbb{C},\mathfrak{Re}(\rho)>0,m\in\mathbb{N}$ and $u,v\in\mathbb{C}$, $w\in\mathbb{R}^+$ are called the transform variables.

The $\mathcal{M}$-transform given by (1), depends on a number of parameters, so that it covers many known integral transforms as its special cases. This transform has the duality relations with well-known transforms such as the Laplace transform, the natural transform and the Srivastava-Luo-Raina $\mathbb{M}$-transform.
This transform is a precious tool for solving certain initial and boundary value problems with certain variable coefficients. Additional ionformation on this transform, may be found in [1].

The incomplete H-and $\overline{H}$-functions

The incomplete H-functions $\gamma_{\mathsf{p},\,\mathsf{q}}^{\mathsf{m},\,\mathsf{n}}$ and $\Gamma_{\mathsf{p},\,\mathsf{q}}^{\mathsf{m},\,\mathsf{n}}$ have studied and defined by Srivastava et al. [13] in the form of Mellin-Barness contour integral as follow:

$$\gamma_{\mathsf{p},\,\mathsf{q}}^{\mathsf{m},\,\mathsf{n}}(z)=\gamma_{\mathsf{p},\,\mathsf{q}}^{\mathsf{m},\,\mathsf{n}}\left[z\,\middle|\,\begin{matrix}(\mathfrak{g}_1,\nu_1,y),(\mathfrak{g}_\mathsf{j},\nu_\mathsf{j})_{2,\mathsf{p}}\\(\mathfrak{h}_\mathsf{j},\omega_\mathsf{j})_{1,\mathsf{q}}\end{matrix}\right]=(2\pi\iota)^{-1}\int_{\pounds} g(\vartheta,y)\;z^{-\vartheta}\;d\vartheta, \tag{2}$$

and

$$\Gamma_{\mathsf{p},\,\mathsf{q}}^{\mathsf{m},\,\mathsf{n}}(z)=\Gamma_{\mathsf{p},\,\mathsf{q}}^{\mathsf{m},\,\mathsf{n}}\left[z\,\middle|\,\begin{matrix}(\mathfrak{g}_1,\nu_1,y),(\mathfrak{g}_\mathsf{j},\nu_\mathsf{j})_{2,\mathsf{p}}\\(\mathfrak{h}_\mathsf{j},\omega_\mathsf{j})_{1,\mathsf{q}}\end{matrix}\right]=(2\pi\iota)^{-1}\int_{\pounds} G(\vartheta,y)\;z^{-\vartheta}\;d\vartheta, \tag{3}$$

where,

$$g(\vartheta,y)=\frac{\gamma(1-\mathfrak{g}_1-\nu_1\vartheta,y)\prod_{\mathsf{j}=1}^{\mathsf{m}}\Gamma(\mathfrak{h}_\mathsf{j}+\omega_\mathsf{j}\vartheta)\prod_{\mathsf{j}=2}^{\mathsf{n}}\Gamma(1-\mathfrak{g}_\mathsf{j}-\nu_\mathsf{j}\vartheta)}{\prod_{\mathsf{j}=\mathsf{m}+1}^{\mathsf{q}}\Gamma(1-\mathfrak{h}_\mathsf{j}-\omega_\mathsf{j}\vartheta)\prod_{\mathsf{j}=\mathsf{n}+1}^{\mathsf{p}}\Gamma(\mathfrak{g}_\mathsf{j}+\nu_\mathsf{j}\vartheta)}, \tag{4}$$

and

$$G(\vartheta,y)=\frac{\Gamma(1-\mathfrak{g}_1-\nu_1\vartheta,y)\prod_{\mathsf{j}=1}^{\mathsf{m}}\Gamma(\mathfrak{h}_\mathsf{j}+\omega_\mathsf{j}\vartheta)\prod_{\mathsf{j}=2}^{\mathsf{n}}\Gamma(1-\mathfrak{g}_\mathsf{j}-\nu_\mathsf{j}\vartheta)}{\prod_{\mathsf{j}=\mathsf{m}+1}^{\mathsf{q}}\Gamma(1-\mathfrak{h}_\mathsf{j}-\omega_\mathsf{j}\vartheta)\prod_{\mathsf{j}=\mathsf{n}+1}^{\mathsf{p}}\Gamma(\mathfrak{g}_\mathsf{j}+\nu_\mathsf{j}\vartheta)}. \tag{5}$$

This family of incomplete H-functions characterized as (2) and (3) exist for $x\geq 0$, according to the conditions specified by Srivastava [13].

Srivastava in [13] developed a generalisation for the family of incomplete H-functions, referred as the incomplete $\overline{H}$-functions, which is described by:

$$\begin{aligned}\overline{\gamma}_{\mathsf{p},\,\mathsf{q}}^{\mathsf{m},\,\mathsf{n}}(z) &= \overline{\gamma}_{\mathsf{p},\,\mathsf{q}}^{\mathsf{m},\,\mathsf{n}}\left[z\,\middle|\,\begin{matrix}(\mathfrak{g}_1,\nu_1;\mathfrak{G}_1;y),\,(\mathfrak{g}_\mathfrak{j},\nu_\mathfrak{j};\mathfrak{G}_\mathfrak{j})_{2,\,\mathsf{n}},\,(\mathfrak{g}_\mathfrak{j},\nu_\mathfrak{j})_{\mathsf{n}+1,\,\mathsf{p}}\\ (\mathfrak{h}_\mathfrak{j},\omega_\mathfrak{j})_{1,\mathsf{m}},\,(\mathfrak{h}_\mathfrak{j},\omega_\mathfrak{j};\mathfrak{H}_\mathfrak{j})_{\mathsf{m}+1,\,\mathsf{q}}\end{matrix}\right]\\ &= (2\pi\iota)^{-1}\int_{\pounds}\overline{g}(\vartheta,y)\,z^{-\vartheta}\,d\vartheta,\end{aligned}\tag{6}$$

and

$$\begin{aligned}\overline{\Gamma}_{\mathsf{p},\,\mathsf{q}}^{\mathsf{m},\,\mathsf{n}}(z) &= \overline{\Gamma}_{\mathsf{p},\,\mathsf{q}}^{\mathsf{m},\,\mathsf{n}}\left[z\,\middle|\,\begin{matrix}(\mathfrak{g}_1,\nu_1;\mathfrak{G}_1;y),\,(\mathfrak{g}_\mathfrak{j},\nu_\mathfrak{j};\mathfrak{G}_\mathfrak{j})_{2,\,\mathsf{n}},\,(\mathfrak{g}_\mathfrak{j},\nu_\mathfrak{j})_{\mathsf{n}+1,\,\mathsf{p}}\\ (\mathfrak{h}_\mathfrak{j},\omega_\mathfrak{j})_{1,\mathsf{m}},\,(\mathfrak{h}_\mathfrak{j},\omega_\mathfrak{j};\mathfrak{H}_\mathfrak{j})_{\mathsf{m}+1,\,\mathsf{q}}\end{matrix}\right]\\ &= (2\pi\iota)^{-1}\int_{\pounds}\overline{G}(\vartheta,y)\,z^{-\vartheta}\,d\vartheta,\end{aligned}\tag{7}$$

where

$$\overline{g}(\vartheta,y)=\frac{[\gamma(1-\mathfrak{g}_1-\nu_1\vartheta,y)]^{\mathfrak{G}_1}\prod_{\mathsf{j}=1}^{\mathsf{m}}\Gamma(\mathfrak{h}_\mathfrak{j}+\omega_\mathfrak{j}\vartheta)\prod_{\mathsf{j}=2}^{\mathsf{n}}[\Gamma(1-\mathfrak{g}_\mathfrak{j}-\nu_\mathfrak{j}\vartheta)]^{\mathfrak{G}_\mathfrak{j}}}{\prod_{\mathsf{j}=\mathsf{m}+1}^{\mathsf{q}}[\Gamma(1-\mathfrak{h}_\mathfrak{j}-\omega_\mathfrak{j}\vartheta)]^{\mathfrak{H}_\mathfrak{j}}\prod_{\mathsf{j}=\mathsf{n}+1}^{\mathsf{p}}\Gamma(\mathfrak{g}_\mathfrak{j}+\nu_\mathfrak{j}\vartheta)},\tag{8}$$

and

$$\overline{G}(\vartheta,y)=\frac{[\Gamma(1-\mathfrak{g}_1-\nu_1\vartheta,y)]^{\mathfrak{G}_1}\prod_{\mathsf{j}=1}^{\mathsf{m}}\Gamma(\mathfrak{h}_\mathfrak{j}+\omega_\mathfrak{j}\vartheta)\prod_{\mathsf{j}=2}^{\mathsf{n}}[\Gamma(1-\mathfrak{g}_\mathfrak{j}-\nu_\mathfrak{j}\vartheta)]^{\mathfrak{G}_\mathfrak{j}}}{\prod_{\mathsf{j}=\mathsf{m}+1}^{\mathsf{q}}[\Gamma(1-\mathfrak{h}_\mathfrak{j}-\omega_\mathfrak{j}\vartheta)]^{\mathfrak{H}_\mathfrak{j}}\prod_{\mathsf{j}=\mathsf{n}+1}^{\mathsf{p}}\Gamma(\mathfrak{g}_\mathfrak{j}+\nu_\mathfrak{j}\vartheta)}.\tag{9}$$

Numerous authors are actively working on the development and wide variety of implications for these incomplete functions, such as in [3, 15], authors established modified saigo fractional integral operators involving the product of a general class of multivariable polynomials and the multivariable H-function and an integral operator involving the family of incomplete H-function in its kernel, respectively. The authors of [11] investigated applications of the incomplete H-function on the influence of environmental pollution on the occurrence of biological populations, whereas the authors of [6,7] developed an equation of internal blood pressure involving incomplete $\overline{H}$-functions and specific expansion formulae for the incomplete H-functions.
The main purpose of this paper is to give new image formulas for incomplete H- and $\overline{H}$-functions under Akel's $\mathcal{M}$-transform. And by giving suitable values to the involved parameters, we also present some special cases of our main findings.

The paper is organized in the following way. In Section 2, we establish the Akel's $\mathcal{M}$-transform image formulae for the incomplete H- and $\overline{H}$-functions. In Section 3 , we derive some interesting and important special cases of our main findings. Finally, a brief conclusion in Section 4.

2 The $\mathcal{M}$-Transform of Incomplete H- and $\overline{H}$-Functions

In this segment, we establish new image formulas for the incomplete H- and $\overline{H}$-functions under the Akel's $\mathcal{M}$-transform.

Theorem 1. *If $\rho \in \mathbb{C}, \mathfrak{Re}(\rho) > 0, m \in \mathbb{N}$ and $u, v \in \mathbb{C}$, $w \in \mathbb{R}^+$, then the following image formula exists for $\gamma_{\mathsf{p},\,\mathsf{q}}^{\mathsf{m},\,\mathsf{n}}[z]$:*

$$\mathcal{M}_{\rho,m}\left\{\gamma_{\mathsf{p},\,\mathsf{q}}^{\mathsf{m},\,\mathsf{n}}\left[zx \;\middle|\; \begin{matrix}(\mathfrak{g}_1,\nu_1,y),(\mathfrak{g}_\mathsf{j},\nu_\mathsf{j})_{2,\mathsf{p}}\\(\mathfrak{h}_\mathsf{j},\omega_\mathsf{j})_{1,\mathsf{q}}\end{matrix}\right]\right\}(u,v,w) = \frac{w^{-m\rho}}{u\,m}\,\frac{1}{2\pi\iota}\int_{\pounds}\mathbb{B}\left(\rho-\frac{\xi}{m},\frac{\xi}{m}\right)(uw)^{\xi}$$
$$\gamma_{\mathsf{p}+1,\,\mathsf{q}}^{\mathsf{m},\,\mathsf{n}+1}\left[z\frac{w}{u} \;\middle|\; \begin{matrix}(\mathfrak{g}_1,\nu_1,y),(\xi,1)_{uv},(\mathfrak{g}_\mathsf{j},\nu_\mathsf{j})_{2,\mathsf{p}}\\(\mathfrak{h}_\mathsf{j},\omega_\mathsf{j})_{1,\mathsf{q}}\end{matrix}\right]d\xi. \tag{10}$$

Here, $\mathbb{B}(x,y)$ represents the classical Euler-Beta function.

Proof. To get the result (1), first we take the L.H.S of (10) and use the definition (1), we have

$$\mathcal{M}_{\rho,m}\left\{\gamma_{\mathsf{p},\,\mathsf{q}}^{\mathsf{m},\,\mathsf{n}}\left[zx \;\middle|\; \begin{matrix}(\mathfrak{g}_1,\nu_1,y),(\mathfrak{g}_\mathsf{j},\nu_\mathsf{j})_{2,\mathsf{p}}\\(\mathfrak{h}_\mathsf{j},\omega_\mathsf{j})_{1,\mathsf{q}}\end{matrix}\right]\right\}(u,v,w) = \int_0^\infty \frac{e^{-ux-\frac{v}{x}}}{(x^m+w^m)^\rho}\,\gamma_{\mathsf{p},\,\mathsf{q}}^{\mathsf{m},\,\mathsf{n}}(zw\,x)\,dx$$
$$= \int_0^\infty \frac{e^{-ux-\frac{v}{x}}}{(x^m+w^m)^\rho}\,\frac{1}{2\pi\iota}\int_{\pounds} g(\vartheta,y)z^{-\vartheta}(wx)^{-\vartheta}\,d\vartheta\,dx$$

On interchanging the orders of the integration

$$= \frac{1}{2\pi\iota}\int_{\pounds} g(\vartheta,y)z^{-\vartheta}\int_0^\infty \frac{e^{-ux-\frac{v}{x}}}{(x^m+w^m)^\rho}(wx)^{-\vartheta}\,dx\,d\vartheta$$

Now, on utilizing [1, pg. 6, Eqn. (2.11)], we get

$$= \frac{1}{2\pi\iota}\int_{\pounds} g(\vartheta,y)z^{-\vartheta}\,\frac{w^{-\vartheta-m\rho}\,u^{\vartheta-1}}{m\,\Gamma(\rho)}\,H_{1,\,2}^{2,\,1}\left[u\,w \;\middle|\; \begin{matrix}(1,\frac{1}{m})\\(1-\vartheta,1)_{uv},(\rho,\frac{1}{m})\end{matrix}\right]d\vartheta$$
$$= \frac{w^{-m\rho}}{um\,\Gamma(\rho)}\frac{1}{2\pi\iota}\int_{\pounds} g(\vartheta,y)\left(z\frac{w}{u}\right)^{-\vartheta}\frac{1}{2\pi\iota}\int_{-\iota\infty}^{+\iota\infty}(u\,w)^{\xi}\Gamma(\frac{\xi}{m})\Gamma_{uv}(1-\xi-\vartheta)\Gamma(\rho-\frac{\xi}{m})d\xi\,d\vartheta$$

On changing the order of the integrations and after some adjustment of terms

$$= \frac{w^{-m\rho}}{u\,m}\,\frac{1}{2\pi\iota}\int_{\pounds}\frac{\Gamma(\frac{\xi}{m})\,\Gamma(\rho-\frac{\xi}{m})}{\Gamma(\rho)}\,(uw)^{\xi}\,\frac{1}{2\pi\iota}\int_{\pounds} g(\vartheta,y)\,\Gamma_{uv}(1-\xi-\vartheta)\left(z\frac{w}{u}\right)^{-\vartheta}d\vartheta\,d\xi, \tag{11}$$

using (2), we obtain the required R.H.S of (10). □

Theorem 2. *If $\rho \in \mathbb{C}, \mathfrak{Re}(\rho) > 0, m \in \mathbb{N}$ and $u, v \in \mathbb{C}$, $w \in \mathbb{R}^+$, then the following image formula exists for $\Gamma^{\mathsf{m},\,\mathsf{n}}_{\mathsf{p},\,\mathsf{q}}[z]$:*

$$\mathcal{M}_{\rho,m}\left\{\Gamma^{\mathsf{m},\,\mathsf{n}}_{\mathsf{p},\,\mathsf{q}}\left[zx\,\middle|\,\begin{matrix}(\mathfrak{g}_1,\nu_1,y),(\mathfrak{g}_\mathsf{j},\nu_\mathsf{j})_{2,\mathsf{p}}\\(\mathfrak{h}_\mathsf{j},\omega_\mathsf{j})_{1,\mathsf{q}}\end{matrix}\right]\right\}(u,v,w)=\frac{w^{-m\rho}}{u\,m}\,\frac{1}{2\pi\iota}\int_{\pounds}\mathbb{B}\left(\rho-\frac{\xi}{m},\frac{\xi}{m}\right)(uw)^{\xi}$$
$$\Gamma^{\mathsf{m},\,\mathsf{n}+1}_{\mathsf{p}+1,\,\mathsf{q}}\left[z\frac{w}{u}\,\middle|\,\begin{matrix}(\mathfrak{g}_1,\nu_1,y),(\xi,1)_{uv},(\mathfrak{g}_\mathsf{j},\nu_\mathsf{j})_{2,\mathsf{p}}\\(\mathfrak{h}_\mathsf{j},\omega_\mathsf{j})_{1,\mathsf{q}}\end{matrix}\right]d\xi. \tag{12}$$

Here, $\mathbb{B}(x,y)$ represents the classical Euler-Beta function.

Proof. To get the result (12), we take the Akel's $\mathcal{M}$-transform presented in (1) of (3), then on interchanging the order of the integrations and making use of the known result given in [1, p. 6, Eq. (2.11)], and after some small arrangements of the terms, we easily get the right hand side assertion of (12). □

Theorem 3. *If $\rho \in \mathbb{C}, \mathfrak{Re}(\rho) > 0, m \in \mathbb{N}$ and $u, v \in \mathbb{C}$, $w \in \mathbb{R}^+$, then the following image formula exists for $\overline{\gamma}^{\mathsf{m},\,\mathsf{n}}_{\mathsf{p},\,\mathsf{q}}[z]$:*

$$\mathcal{M}_{\rho,m}\left\{\overline{\gamma}^{\mathsf{m},\,\mathsf{n}}_{\mathsf{p},\,\mathsf{q}}\left[zx\,\middle|\,\begin{matrix}(\mathfrak{g}_1,\nu_1;\mathfrak{G},y),(\mathfrak{g}_\mathsf{j},\nu_\mathsf{j};\mathfrak{G}_\mathsf{j})_{2,\mathsf{n}},(\mathfrak{g}_\mathsf{j},\nu_\mathsf{j})_{\mathsf{n}+1,\mathsf{p}}\\(\mathfrak{h}_\mathsf{j},\omega_\mathsf{j})_{1,\mathsf{m}},(\mathfrak{h}_\mathsf{j},\omega_\mathsf{j};\mathfrak{H}_\mathsf{j})_{\mathsf{m}+1,\mathsf{q}}\end{matrix}\right]\right\}(u,v,w)$$
$$=\frac{w^{-m\rho}}{u\,m}\,\frac{1}{2\pi\iota}\int_{\pounds}\mathbb{B}\left(\rho-\frac{\xi}{m},\frac{\xi}{m}\right)(uw)^{\xi}$$
$$\overline{\gamma}^{\mathsf{m},\,\mathsf{n}+1}_{\mathsf{p}+1,\,\mathsf{q}}\left[z\frac{w}{u}\,\middle|\,\begin{matrix}(\mathfrak{g}_1,\nu_1;\mathfrak{G},y),(\xi,1;1)_{uv},(\mathfrak{g}_\mathsf{j},\nu_\mathsf{j};\mathfrak{G}_\mathsf{j})_{2,\mathsf{n}},(\mathfrak{g}_\mathsf{j},\nu_\mathsf{j})_{\mathsf{n}+1,\mathsf{p}}\\(\mathfrak{h}_\mathsf{j},\omega_\mathsf{j})_{1,\mathsf{m}},(\mathfrak{h}_\mathsf{j},\omega_\mathsf{j};\mathfrak{H}_\mathsf{j})_{\mathsf{m}+1,\mathsf{q}}\end{matrix}\right]d\xi. \tag{13}$$

Here, $\mathbb{B}(x,y)$ represents the classical Euler-Beta function.

Proof. To get the result (3), first we take the L.H.S of (13) and use the definition (1), we have

$$\mathcal{M}_{\rho,m}\left\{\overline{\gamma}^{\mathsf{m},\,\mathsf{n}}_{\mathsf{p},\,\mathsf{q}}\left[zx\,\middle|\,\begin{matrix}(\mathfrak{g}_1,\nu_1;\mathfrak{G}_1;y),\,(\mathfrak{g}_\mathsf{j},\nu_\mathsf{j};\mathfrak{G}_\mathsf{j})_{2,\,\mathsf{n}},\,(\mathfrak{g}_\mathsf{j},\nu_\mathsf{j})_{\mathsf{n}+1,\,\mathsf{p}}\\(\mathfrak{h}_\mathsf{j},\omega_\mathsf{j})_{1,\mathsf{m}},\,(\mathfrak{h}_\mathsf{j},\omega_\mathsf{j};\mathfrak{H}_\mathsf{j})_{\mathsf{m}+1,\,\mathsf{q}}\end{matrix}\right]\right\}(u,v,w)$$
$$=\int_0^\infty\frac{e^{-ux-\frac{v}{x}}}{(x^m+w^m)^\rho}\,\overline{\gamma}^{\mathsf{m},\,\mathsf{n}}_{\mathsf{p},\,\mathsf{q}}(zw\,x)\,dx$$
$$=\int_0^\infty\frac{e^{-ux-\frac{v}{x}}}{(x^m+w^m)^\rho}\,\frac{1}{2\pi\iota}\int_{\pounds}\overline{g}(\vartheta,y)z^{-\vartheta}(wx)^{-\vartheta}\,d\vartheta\,dx$$

On interchanging the orders of the integration

$$=\frac{1}{2\pi\iota}\int_{\pounds}\overline{g}(\vartheta,y)z^{-\vartheta}\int_0^\infty\frac{e^{-ux-\frac{v}{x}}}{(x^m+w^m)^\rho}(wx)^{-\vartheta}\,dx\,d\vartheta$$

Now, on utilizing [1, pg. 6, Eqn. (2.11)], we get

$$= \frac{1}{2\pi\iota}\int_{\pounds} \overline{g}(\vartheta,y)z^{-\vartheta}\,\frac{w^{-\vartheta-m\rho}\,u^{\vartheta-1}}{m\,\Gamma(\rho)}\,H^{2,\,1}_{1,\,2}\left[u\,w\;\middle|\;\begin{matrix}(1,\frac{1}{m})\\(1-\vartheta,1)_{uv},(\rho,\frac{1}{m})\end{matrix}\right]d\vartheta$$

$$= \frac{w^{-m\rho}}{um\,\Gamma(\rho)}\frac{1}{2\pi\iota}\int_{\pounds}\overline{g}(\vartheta,y)\left(z\frac{w}{u}\right)^{-\vartheta}\frac{1}{2\pi\iota}\int_{-\iota\infty}^{+\iota\infty}(u\,w)^{\xi}\Gamma(\frac{\xi}{m})\Gamma_{uv}(1-\xi-\vartheta)\Gamma(\rho-\frac{\xi}{m})d\xi\,d\vartheta$$

On changing the order of the integrations and after some adjustment of terms

$$= \frac{w^{-m\rho}}{u\,m}\,\frac{1}{2\pi\iota}\int_{\pounds}\frac{\Gamma(\frac{\xi}{m})\,\Gamma(\rho-\frac{\xi}{m})}{\Gamma(\rho)}\,(uw)^{\xi}\,\frac{1}{2\pi\iota}\int_{\pounds}\overline{g}(\vartheta,y)\,\Gamma_{uv}(1-\xi-\vartheta)\left(z\frac{w}{u}\right)^{-\vartheta}d\vartheta\,d\xi, \tag{14}$$

using (6), we obtain the required R.H.S of (13). □

Theorem 4. *If $\rho\in\mathbb{C},\mathfrak{Re}(\rho)>0,m\in\mathbb{N}$ and $u,v\in\mathbb{C}$, $w\in\mathbb{R}^{+}$, then the following image formula exists for $\overline{\Gamma}^{\mathsf{m},\,\mathsf{n}}_{\mathsf{p},\,\mathsf{q}}[z]$:*

$$\mathcal{M}_{\rho,m}\left\{\overline{\Gamma}^{\mathsf{m},\,\mathsf{n}}_{\mathsf{p},\,\mathsf{q}}\left[zx\;\middle|\;\begin{matrix}(\mathfrak{g}_1,\nu_1;\mathfrak{G},y),(\mathfrak{g}_{\mathsf{j}},\nu_{\mathsf{j}};\mathfrak{G}_{\mathsf{j}})_{2,\mathsf{n}},(\mathfrak{g}_{\mathsf{j}},\nu_{\mathsf{j}})_{\mathsf{n}+1,\mathsf{p}}\\(\mathfrak{h}_{\mathsf{j}},\omega_{\mathsf{j}})_{1,\mathsf{m}},(\mathfrak{h}_{\mathsf{j}},\omega_{\mathsf{j}};\mathfrak{H}_{\mathsf{j}})_{\mathsf{m}+1,\mathsf{q}}\end{matrix}\right]\right\}(u,v,w)$$

$$= \frac{w^{-m\rho}}{u\,m}\,\frac{1}{2\pi\iota}\int_{\pounds}\mathbb{B}\left(\rho-\frac{\xi}{m},\frac{\xi}{m}\right)(uw)^{\xi}$$

$$\overline{\Gamma}^{\mathsf{m},\,\mathsf{n}+1}_{\mathsf{p}+1,\,\mathsf{q}}\left[z\frac{w}{u}\;\middle|\;\begin{matrix}(\mathfrak{g}_1,\nu_1;\mathfrak{G},y),(\xi,1;1)_{uv},(\mathfrak{g}_{\mathsf{j}},\nu_{\mathsf{j}};\mathfrak{G}_{\mathsf{j}})_{2,\mathsf{n}},(\mathfrak{g}_{\mathsf{j}},\nu_{\mathsf{j}})_{\mathsf{n}+1,\mathsf{p}}\\(\mathfrak{h}_{\mathsf{j}},\omega_{\mathsf{j}})_{1,\mathsf{m}},(\mathfrak{h}_{\mathsf{j}},\omega_{\mathsf{j}};\mathfrak{H}_{\mathsf{j}})_{\mathsf{m}+1,\mathsf{q}}\end{matrix}\right]d\xi. \tag{15}$$

Here, $\mathbb{B}(x,y)$ represents the classical Euler-Beta function.

Proof. To get the result (15), we take the Akel's $\mathcal{M}$-transform presented in (1) of (7), then on interchanging the order of the integrations and making use of the known result given in [1, p. 6, Eq. (2.11)], and after some small arrangements of the terms, we easily get the right hand side assertion of (15). □

3 Special Cases

In this section, we derive some interesting and important special cases of our main findings by giving some particular values to the parameters involved in the definitions of $\mathcal{M}$-transform (1) and incomplete H-functions (2) and (3).
(1) Taking $\mathsf{n}=\mathsf{p}$, $\mathsf{m}=1$, substitute q with $\mathsf{q}+1$ and choosing appropriate parameters such as $z=-z$, $\mathfrak{g}_{\mathsf{j}}\to(1-\mathfrak{g}_{\mathsf{j}})$ $(\mathsf{j}=1,\cdots,\mathsf{p})$, and $\mathfrak{h}_{\mathsf{j}}\to(1-\mathfrak{h}_{\mathsf{j}})$ $(\mathsf{j}=1,\cdots,\mathsf{q})$, the incomplete H-functions (2) and (3) convert, respectively, to the incomplete Fox-Wright ${}_{\mathsf{p}}\Psi^{(\gamma)}_{\mathsf{q}}$- and ${}_{\mathsf{p}}\Psi^{(\Gamma)}_{\mathsf{q}}$-functions (see [13, Eqs. (6.3)

and (6.4)]):

$$\gamma_{\mathsf{p},\,\mathsf{q}+1}^{1,\,\mathsf{p}}\left[-z\,\middle|\,\begin{matrix}(1-\mathfrak{g}_1,\nu_1,y),(1-\mathfrak{g}_\mathsf{j},\nu_\mathsf{j})_{2,\mathsf{p}}\\(0,1),(1-\mathfrak{h}_\mathsf{j},\omega_\mathsf{j})_{1,\mathsf{q}}\end{matrix}\right]={}_{\mathsf{p}}\Psi_{\mathsf{q}}^{(\gamma)}\left[\begin{matrix}(\mathfrak{g}_1,\nu_1,y),(\mathfrak{g}_\mathsf{j},\nu_\mathsf{j})_{2,\mathsf{p}}\,;\\(\mathfrak{g}_\mathsf{j},\omega_\mathsf{j})_{1,\mathsf{q}}\,;\end{matrix}\quad z\right] \tag{16}$$

and

$$\Gamma_{\mathsf{p},\,\mathsf{q}+1}^{1,\,\mathsf{p}}\left[-z\,\middle|\,\begin{matrix}(1-\mathfrak{g}_1,\nu_1,y),(1-\mathfrak{g}_\mathsf{j},\nu_\mathsf{j})_{2,\mathsf{p}}\\(0,1),(1-\mathfrak{h}_\mathsf{j},\omega_\mathsf{j})_{1,\mathsf{q}}\end{matrix}\right]={}_{\mathsf{p}}\Psi_{\mathsf{q}}^{(\Gamma)}\left[\begin{matrix}(\mathfrak{g}_1,\nu_1,y),(\mathfrak{g}_\mathsf{j},\nu_\mathsf{j})_{2,\mathsf{p}}\,;\\(\mathfrak{g}_\mathsf{j},\omega_\mathsf{j})_{1,\mathsf{q}}\,;\end{matrix}\quad z\right]. \tag{17}$$

Using above relations (16) and (17), in (10) and (12), respectively, we will get the following corollaries.

Corollary 1. *If $\rho\in\mathbb{C},\mathfrak{Re}(\rho)>0,m\in\mathbb{N}$ and $u,v\in\mathbb{C}$, $w\in\mathbb{R}^+$, then the following image formulae exist for ${}_{\mathsf{p}}\Psi_{\mathsf{q}}^{(\gamma)}[z]$ and ${}_{\mathsf{p}}\Psi_{\mathsf{q}}^{(\Gamma)}[z]$:*

$$\mathcal{M}_{\rho,m}\left\{{}_{\mathsf{p}}\Psi_{\mathsf{q}}^{(\gamma)}\left[zx\,\middle|\,\begin{matrix}(\mathfrak{g}_1,\nu_1,y),(\mathfrak{g}_\mathsf{j},\nu_\mathsf{j})_{2,\mathsf{p}}\\(\mathfrak{h}_\mathsf{j},\omega_\mathsf{j})_{1,\mathsf{q}}\end{matrix}\right]\right\}(u,v,w)=\frac{w^{-m\rho}}{u\,m}\,\frac{1}{2\pi\iota}\int_{\pounds}\mathbb{B}\left(\rho-\frac{\xi}{m},\frac{\xi}{m}\right)(uw)^{\xi}$$
$${}_{\mathsf{p}+1}\Psi_{\mathsf{q}}^{(\gamma)}\left[z\frac{w}{u}\,\middle|\,\begin{matrix}(\mathfrak{g}_1,\nu_1,y),(\xi,1)_{uv},(\mathfrak{g}_\mathsf{j},\nu_\mathsf{j})_{2,\mathsf{p}}\\(\mathfrak{h}_\mathsf{j},\omega_\mathsf{j})_{1,\mathsf{q}}\end{matrix}\right]d\xi \tag{18}$$

and

$$\mathcal{M}_{\rho,m}\left\{{}_{\mathsf{p}}\Psi_{\mathsf{q}}^{(\Gamma)}\left[zx\,\middle|\,\begin{matrix}(\mathfrak{g}_1,\nu_1,y),(\mathfrak{g}_\mathsf{j},\nu_\mathsf{j})_{2,\mathsf{p}}\\(\mathfrak{h}_\mathsf{j},\omega_\mathsf{j})_{1,\mathsf{q}}\end{matrix}\right]\right\}(u,v,w)=\frac{w^{-m\rho}}{u\,m}\,\frac{1}{2\pi\iota}\int_{\pounds}\mathbb{B}\left(\rho-\frac{\xi}{m},\frac{\xi}{m}\right)(uw)^{\xi}$$
$${}_{\mathsf{p}+1}\Psi_{\mathsf{q}}^{(\Gamma)}\left[z\frac{w}{u}\,\middle|\,\begin{matrix}(\mathfrak{g}_1,\nu_1,y),(\xi,1)_{uv},(\mathfrak{g}_\mathsf{j},\nu_\mathsf{j})_{2,\mathsf{p}}\\(\mathfrak{h}_\mathsf{j},\omega_\mathsf{j})_{1,\mathsf{q}}\end{matrix}\right]d\xi. \tag{19}$$

Here, $\mathbb{B}(x,y)$ indicates the classical Euler-Beta function.

(2) Letting $(\nu_\mathsf{j})_{1,\mathsf{p}}=1=(\omega_\mathsf{j})_{1,\mathsf{q}}$, the functions (2) and (3) convert into Meijer's incomplete ${}^{(\gamma)}G_{\mathsf{p},\,\mathsf{q}}^{\mathsf{m},\,\mathsf{n}}$- and ${}^{(\Gamma)}G_{\mathsf{p},\,\mathsf{q}}^{\mathsf{m},\,\mathsf{n}}$- functions:

$$\gamma_{\mathsf{p},\,\mathsf{q}}^{\mathsf{m},\,\mathsf{n}}(z)\left[z\,\middle|\,\begin{matrix}(\mathfrak{g}_1,1,y),(\mathfrak{g}_\mathsf{j},1)_{2,\mathsf{p}}\\(\mathfrak{h}_\mathsf{j},1)_{1,\mathsf{q}}\end{matrix}\right]={}^{(\gamma)}G_{\mathsf{p},\,\mathsf{q}}^{\mathsf{m},\,\mathsf{n}}\left[z\,\middle|\,\begin{matrix}(\mathfrak{g}_1,y),(\mathfrak{g}_\mathsf{j})_{2,\mathsf{p}}\\(\mathfrak{h}_\mathsf{j})_{1,\mathsf{q}}\end{matrix}\right] \tag{20}$$

and

$$\Gamma_{\mathsf{p},\,\mathsf{q}}^{\mathsf{m},\,\mathsf{n}}(z)\left[z\,\middle|\,\begin{matrix}(\mathfrak{g}_1,1,y),(\mathfrak{g}_\mathsf{j},1)_{2,\mathsf{p}}\\(\mathfrak{h}_\mathsf{j},1)_{1,\mathsf{q}}\end{matrix}\right]={}^{(\Gamma)}G_{\mathsf{p},\,\mathsf{q}}^{\mathsf{m},\,\mathsf{n}}\left[z\,\middle|\,\begin{matrix}(\mathfrak{g}_1,y),(\mathfrak{g}_\mathsf{j})_{2,\mathsf{p}}\\(\mathfrak{h}_\mathsf{j})_{1,\mathsf{q}}\end{matrix}\right]. \tag{21}$$

Using above relations (20) and (21) in (10) and (12), respectively, we get the following corollaries.

Corollary 2. *If $\rho \in \mathbb{C}, \mathfrak{Re}(\rho) > 0, m \in \mathbb{N}$ and $u, v \in \mathbb{C}$, $w \in \mathbb{R}^+$, then the following image formulae exist for ${}^{(\gamma)}G^{\mathsf{m},\,\mathsf{n}}_{\mathsf{p},\,\mathsf{q}}[z]$ and ${}^{(\Gamma)}G^{\mathsf{m},\,\mathsf{n}}_{\mathsf{p},\,\mathsf{q}}[z]$, respectively:*

$$\mathcal{M}_{\rho,m}\left\{ {}^{(\gamma)}G^{\mathsf{m},\,\mathsf{n}}_{\mathsf{p},\,\mathsf{q}}\left[zx \,\middle|\, \begin{matrix}(\mathfrak{g}_1,1,y),(\mathfrak{g}_\mathsf{j},1)_{2,\mathsf{p}}\\(\mathfrak{h}_\mathsf{j},1)_{1,\mathsf{q}}\end{matrix}\right]\right\}(u,v,w) = \frac{w^{-m\rho}}{u\,m}\,\frac{1}{2\pi\iota}\int_{\mathcal{L}} \mathbb{B}\left(\rho-\frac{\xi}{m},\frac{\xi}{m}\right)(uw)^{\xi}$$
$${}^{(\gamma)}G^{\mathsf{m},\,\mathsf{n}+1}_{\mathsf{p}+1,\,\mathsf{q}}\left[z\frac{w}{u} \,\middle|\, \begin{matrix}(\mathfrak{g}_1,1,y),(\xi,1)_{uv},(\mathfrak{g}_\mathsf{j},1)_{2,\mathsf{p}}\\(\mathfrak{h}_\mathsf{j},1)_{1,\mathsf{q}}\end{matrix}\right] d\xi \tag{22}$$

and

$$\mathcal{M}_{\rho,m}\left\{ {}^{(\Gamma)}G^{\mathsf{m},\,\mathsf{n}}_{\mathsf{p},\,\mathsf{q}}\left[zx \,\middle|\, \begin{matrix}(\mathfrak{g}_1,1,y),(\mathfrak{g}_\mathsf{j},1)_{2,\mathsf{p}}\\(\mathfrak{h}_\mathsf{j},1)_{1,\mathsf{q}}\end{matrix}\right]\right\}(u,v,w) = \frac{w^{-m\rho}}{u\,m}\,\frac{1}{2\pi\iota}\int_{\mathcal{L}} \mathbb{B}\left(\rho-\frac{\xi}{m},\frac{\xi}{m}\right)(uw)^{\xi}$$
$${}^{(\Gamma)}G^{\mathsf{m},\,\mathsf{n}+1}_{\mathsf{p}+1,\,\mathsf{q}}\left[z\frac{w}{u} \,\middle|\, \begin{matrix}(\mathfrak{g}_1,1,y),(\xi,1)_{uv},(\mathfrak{g}_\mathsf{j},1)_{2,\mathsf{p}}\\(\mathfrak{h}_\mathsf{j},1)_{1,\mathsf{q}}\end{matrix}\right] d\xi. \tag{23}$$

Here, $\mathbb{B}(x,y)$ indicates the classical Euler-Beta function.

(3) If we put $y = 0$ in (3), we get the Fox's H-function

$$\Gamma^{\mathsf{m},\,\mathsf{n}}_{\mathsf{p},\,\mathsf{q}}\left[z \,\middle|\, \begin{matrix}(\mathfrak{g}_1,\nu_1,0),(\mathfrak{g}_\mathsf{j},\nu_\mathsf{j})_{2,\mathsf{p}}\\(\mathfrak{h}_\mathsf{j},\omega_\mathsf{j})_{1,\mathsf{q}}\end{matrix}\right] = H^{\mathsf{m},\,\mathsf{n}}_{\mathsf{p},\,\mathsf{q}}\left[z \,\middle|\, \begin{matrix}(\mathfrak{g}_\mathsf{j},\nu_\mathsf{j})_{1,\mathsf{p}}\\(\mathfrak{h}_\mathsf{j},\omega_\mathsf{j})_{1,\mathsf{q}}\end{matrix}\right]. \tag{24}$$

Using relation (24), we obtain the subsequent corollaries.

Corollary 3. *If $\rho \in \mathbb{C}, \mathfrak{Re}(\rho) > 0, m \in \mathbb{N}$ and $u, v \in \mathbb{C}$, $w \in \mathbb{R}^+$, then the following image formula exists for $H^{\mathsf{m},\,\mathsf{n}}_{\mathsf{p},\,\mathsf{q}}[z]$:*

$$\mathcal{M}_{\rho,m}\left\{ H^{\mathsf{m},\,\mathsf{n}}_{\mathsf{p},\,\mathsf{q}}\left[zx \,\middle|\, \begin{matrix}(\mathfrak{g}_\mathsf{j},\nu_\mathsf{j})_{1,\mathsf{p}}\\(\mathfrak{h}_\mathsf{j},\omega_\mathsf{j})_{1,\mathsf{q}}\end{matrix}\right]\right\}(u,v,w) = \frac{w^{-m\rho}}{u\,m}\,\frac{1}{2\pi\iota}\int_{\mathcal{L}} \mathbb{B}\left(\rho-\frac{\xi}{m},\frac{\xi}{m}\right)(uw)^{\xi}$$
$$H^{\mathsf{m},\,\mathsf{n}+1}_{\mathsf{p}+1,\,\mathsf{q}}\left[z\frac{w}{u} \,\middle|\, \begin{matrix}(\xi,1)_{uv},(\mathfrak{g}_\mathsf{j},\nu_\mathsf{j})_{1,\mathsf{p}}\\(\mathfrak{h}_\mathsf{j},\omega_\mathsf{j})_{1,\mathsf{q}}\end{matrix}\right] d\xi. \tag{25}$$

Here, $\mathbb{B}(x,y)$ indicates the classical Euler-Beta function.

(4) If we put $v = 0$ in (1), then the Akel's $\mathcal{M}$-transform converts into the Srivastava-Luo-Raina $\mathbb{M}$-transform (see [1]):

$$\mathcal{M}_{\rho,m}[f(x)](u,0,w) = \mathbb{M}_{\rho,m}[f(x)](u,w), \tag{26}$$

here, $\mathbb{M}_{\rho,m}[f(x)](u,w)$ is the Srivastava-Luo-Raina $\mathbb{M}$-transform, defined in [14]. Using relation (26) in (10) and (12), we obtain the results derived by Bansal et

al. [2, p. 720, Eqs. (2.1) and (2.2)],

$$\mathbb{M}_{\rho,m}\left\{\gamma_{\mathsf{p},\,\mathsf{q}}^{\mathsf{m},\,\mathsf{n}}\left[zx\,\middle|\,\begin{matrix}(\mathfrak{g}_1,\nu_1,y),(\mathfrak{g}_\mathfrak{j},\nu_\mathfrak{j})_{2,\mathsf{p}}\\(\mathfrak{h}_\mathfrak{j},\omega_\mathfrak{j})_{1,\mathsf{q}}\end{matrix}\right]\right\}(u,w)=\frac{w^{-m\rho}}{u\,m}\,\frac{1}{2\pi\iota}\int_{\pounds}\mathbb{B}\left(\rho-\frac{\xi}{m},\frac{\xi}{m}\right)(uw)^{\xi}$$
$$\gamma_{\mathsf{p}+1,\,\mathsf{q}}^{\mathsf{m},\,\mathsf{n}+1}\left[z\frac{w}{u}\,\middle|\,\begin{matrix}(\mathfrak{g}_1,\nu_1,y),(\xi,1),(\mathfrak{g}_\mathfrak{j},\nu_\mathfrak{j})_{2,\mathsf{p}}\\(\mathfrak{h}_\mathfrak{j},\omega_\mathfrak{j})_{1,\mathsf{q}}\end{matrix}\right]d\xi \tag{27}$$

and

$$\mathbb{M}_{\rho,m}\left\{\Gamma_{\mathsf{p},\,\mathsf{q}}^{\mathsf{m},\,\mathsf{n}}\left[zx\,\middle|\,\begin{matrix}(\mathfrak{g}_1,\nu_1,y),(\mathfrak{g}_\mathfrak{j},\nu_\mathfrak{j})_{2,\mathsf{p}}\\(\mathfrak{h}_\mathfrak{j},\omega_\mathfrak{j})_{1,\mathsf{q}}\end{matrix}\right]\right\}(u,w)=\frac{w^{-m\rho}}{u\,m}\,\frac{1}{2\pi\iota}\int_{\pounds}\mathbb{B}\left(\rho-\frac{\xi}{m},\frac{\xi}{m}\right)(uw)^{\xi}$$
$$\Gamma_{\mathsf{p}+1,\,\mathsf{q}}^{\mathsf{m},\,\mathsf{n}+1}\left[z\frac{w}{u}\,\middle|\,\begin{matrix}(\mathfrak{g}_1,\nu_1,y),(\xi,1),(\mathfrak{g}_\mathfrak{j},\nu_\mathfrak{j})_{2,\mathsf{p}}\\(\mathfrak{h}_\mathfrak{j},\omega_\mathfrak{j})_{1,\mathsf{q}}\end{matrix}\right]d\xi. \tag{28}$$

Remark. *If we take $v = 0$ in* (18) *and* (19)*, then we get the known results obtained by Bansal et al. [2, p. 720-721, Eqs. (2.3) and (2.4)].*

4 Conclusion

In this paper, we have derived image formulas for the incomplete H- and $\overline{H}$-functions under the Akel's $\mathcal{M}$-transform. Furthermore, from our key findings various special cases can be evaluated by giving suitable values to the involved parameters and variables with applications in engineering and science, some of which are clearly indicated in section 3.

References

[1] M. Akel, A new gneneralized integral transform and applications, *arXiv preprint* arXiv:2207.13093, 2022.

[2] M. K. Bansal, D. Kumar, J. Singh, A. Tassaddiq, and K. S. Nisar, Some new results for the Srivastava−Luo−Raina $\mathbb{M}$-transform pertaining to the incomplete H-functions, *AIMS Math*, **5**(1), 717-722, 2020.

[3] M.K. Bansal, S. Lal, D. Kumar, S. Kumar, and J. Singh, Fractional differential equation pertaining to an integral operator involving incomplete Hfunction in the kernel, *Mathematical Methods in the Applied Sciences*, 1-8, 2020.

[4] B. Davis, *Integral Transforms and Their Applications*, 3rd ed.; Springer: New York, NY, USA, 2002.

[5] L. Debnath and D. Bhatta, *Integral Transforms and Their Applications*, Third Edi- tion, Chapman and Hall (CRC Press), Taylor and Francis Group, London and New York, 2016.

[6] N. Jangid, S. Joshi, S.D. Purohit, and D.L. Suthar, Fractional derivatives and expansion formulae of incomplete H and $\overline{H}$-functions, *Advances in the Theory of Nonlinear Analysis and its Application*, **5**(2), 193-202, 2021.

[7] D. Kumar, M.K. Bansal, K.S. Nisar, and J. Singh, Mathematical modelling of internal blood pressure involving incomplete $\overline{H}$-functions, *Journal of Interdisciplinary Mathematics*, **22**(7), 1213-1221, 2019.

[8] A.M. Mathai, R.K. Saxena, and H.J. Haubold, *The H-function theory and applications*, Springer-Verlag, New York, 2010.

[9] A.M. Mathai, R.K. Saxena, *The H-function with applications in statistics and other disciplines*, Wiley Eastern Limited, New Delhi; John Wiley ans Sons, New York, 1978.

[10] S. Meena, S. Bhatter, K. Jangid, and S.D. Purohit, Certain integral transforms concerning the product of family of polynomials and generalized incomplete functions, *Moroccan Journal of Pure and Applied Analysis*, **6**(2), 243-254, 2020.

[11] S.D. Purohit, A.M. Khan, D.L. Suthar, and S. Dave, The impact on raise of environmental pollution and occurrence in biological populations pertaining to incomplete H-function, *National Academy Science Letters*, **44**(3), 263-266, 2021.

[12] I.N. Sneddon, *The use of integral transforms*, Tata McGraw-Hill, New York, 1974.

[13] H.M. Srivastava, R.K. Saxena, and R.K. Parmar, Some families of the incomplete H-functions and the incomplete $\overline{H}$-functions and associated integral transforms and operators of fractional calculus with applications, *Rus. J. Math. Phys.*, **25**, 116-138, 2018.

[14] H.M. Srivastava, M.J. Luo, R.K. Raina, A new integral transform and its applications, *Acta Math. Sci.*, **35**, 1386-1400, 2015.

[15] D. L. Suthar, B. Debalkie, and M. Andualem, Modified Saigo fractional integral operators involving multivariable H-function and general class of multivariable polynomials, *Advances in Difference Equations*, **1**(2019), 1-11, 2019.

Approximate solutions of space and time fractional telegraph equations using Taylor series expansion method

*Shweta Dubey, †S. Chakraverty, and ‡M. Kundu

December 29, 2022

The study investigates the telegraph equations by considering space and time fractional derivatives. Caputo's concept of fractional derivatives is used here. We are focusing to generalize the solutions of integer order telegraph equations to fractional order telegraph equations. In this case, approximate solutions for fractional order telegraph equations have been obtained using Taylor series expansion. Additionally, it has been shown quantitatively how the solutions converge by using the number of terms in the series solutions.

Keywords

Telegraph equation, Caputo fractional derivative, Taylor series.

Mathematics Subject Classification

65M99

1 Introduction

Recent research suggests that fractional order derivatives are essential for a wide range of physical phenomena viz. rheology, damping law, heat-diffusion, wave dynamics, signal processing, etc. Researchers have used different types of analytical and numerical methods to handle such problems. Techniques including modified extended tanh method [1], novel analytical technique [2], coupled transformation method [3], Galerkin and collocation methods [4], etc. are some

*shwetadubey9452@gmail.com (Department of Mathematics, National Institute of Technology Rourkela, India)

†sne_ chak@yahoo.com (Department of Mathematics, National Institute of Technology Rourkela, India)

‡mkundu@nitrkl.ac.in (Department of Chemical Engineering, National Institute of Technology Rourkela, India)

recent endeavors in this paradigm. Moreover, the semi-analytical homotopy perturbation method (HPM) has been used to tackle fractional models such as the heat-conduction equation [5], convection-diffusion problem [6], and wave equation [7] etc. Additionally, Dubey et al. have used local fractional natural homotopy analysis method [8, 9] and some coupling techniques such as the local fractional variational iteration technique with the local fractional natural transform [10] and local fractional homotopy perturbation method with local fractional natural transform operator [11] to solve various types of physical problems.

The studied of fractional telegraph equations (FTEs) have gained popularity due to various applications they can be applied to, such as modeling reaction diffusion, transmission and propagation of electrical signals, etc.

The general FTE [12] is given as,

$$D_x^p \phi(x,t) = aD_t^q \phi(x,t) + bD_t^r \phi(x,t) + c\phi(x,t) + h(x,t)$$

,

where $1 < p,\ q \leq 2,\ 0 < r \leq 1,\ x,t \geq 0,\ \phi(0,t) = f_1(t),\ \phi_x(0,t) = f_2(t)$ and a, b, c are constants.

Various authors have solved telegraph equations using different numerical and analytical techniques. The analytical solution for FTE with respect to time has been obtained by chen et al. [13] by using method of separating variables. The space-fractional telegraph equation (SFTE) and time-fractional telegraph equation (TFTE) and related telegraph process have been disscussed by Orsingher and Zaho [14] and Orsingher and Beghin [15]. Moreover, some other methods such as variational iteration method [16], HPM [17], differential transform method [18] have also been used to handle FTEs.

The Taylor series expansion method (TSEM) is applied by Demir et al. [19] for different fractional partial differential equation (PDE). In this study, we use Taylor series of an analytical solution of the integer order differential equation. This Taylor series solution can be reach out to the approximate or exact solution of fractional differential equation (FDE). Our approach changes the terms of Taylor series expansion for derivatives in the sense of fractionals and integers so that their relationship remains unaltered. Applications of this method demonstrate that it may be used to solve any differential equation derived from FDEs with ease and effectiveness, provided that the differential equation has an analytical or approximative solution. Here, the Caputo concept of the fractional derivative is utilised.

Here, Taylor series is applied on SFTEs and TFTEs. Firstly, the Taylor series expansion for analytical solution obtained from integer order telegraph

equation is determined and then the expansion has been extended for FDE.

The rest of the paper follows this format: Methodology of the Taylor series expansion method is described in Section 2. Section 3 includes solutions of SFTEs and TFTEs. This section also covers convergency tables and graphical solutions. Finally, Section 4 concludes this article with a brief summary.

2 Taylor series expansion method

In this section, TSEM has been discussed to handle space and time fractional PDEs.

2.1 Fundamental approach to solve space-fractional PDEs

Let us consider a genaral form space-fractional PDE as

$$D_x^{\alpha}\phi(x,t) = \eta\left(\phi, \frac{\partial\phi}{\partial t}, \cdots \frac{\partial^n\phi}{\partial t^n}, x, t\right), \quad k-1 < \alpha \leq k,\, x > 0,\, t > 0. \tag{1}$$

To find the solution of Eq. (1), we must first calculate the solution to its integer order version by using the expression $\alpha = k$, which is represented as

$$D_x^{k}\phi(x,t) = \eta\left(\phi, \frac{\partial\phi}{\partial t}, \cdots \frac{\partial^n\phi}{\partial t^n}, x, t\right), \quad t > 0,\, x > 0. \tag{2}$$

From the exact answer of Eq. (1), one can get the approximation or exact solution (2). To do this, we must modify the terms in the Taylor series expansion of integer order differential equation (2). In the infinite Taylor series expansion of the solution of Eq. (2), the first k terms remain the same. Moreover, the fractional derivative with respect to x is used in place of the integer order derivative with respect to x in order to maintain the relationship between the terms of the Taylor series and to satisfy the boundary conditions of the fractional differential equation.

To solve Eq. (2) with respect to x, a primitive Taylor series form is shown below.

$$\phi(x,t) = \sum_{n=0}^{\infty} \frac{\partial^n\phi(0,t)}{\partial x^n}\frac{x^n}{n!}. \tag{3}$$

The solution of Eq. (1) is thus expressed in the following way:

$$\phi(x,t) = \sum_{n=0}^{k-1} \frac{\partial^n\phi(0,t)}{\partial x^n}\frac{x^n}{n!} + \sum_{n=1}^{\infty}\sum_{j=0}^{k-1} \frac{\partial^{kn+j}\phi(0,t)}{\partial x^{kn+j}}\frac{x^{n\alpha+j}}{\Gamma(n\alpha+j+1)}. \tag{4}$$

2.2 Fundamental approach to solve time-fractional PDEs

Let us consider a genaral form time-fractional PDE as

$$D_t^{\alpha}\phi(x,t) = \eta\left(\phi, \frac{\partial\phi}{\partial x}, \cdots \frac{\partial^n\phi}{\partial x^n}, x, t\right), \quad k-1 < \alpha \leq k,\, t > 0. \tag{5}$$

For obtaing the solution of Eq. (5), we have to determine the solution for integer order form of Eq. (5) by taking $\alpha = k$, which is written as

$$D_t^{k}\phi(x,t) = \eta\left(\phi, \frac{\partial\phi}{\partial x}, \cdots \frac{\partial^n\phi}{\partial x^n}, x, t\right), \quad t > 0. \tag{6}$$

If we alter the terms of the Taylor series expansion in the solution of the integer order differential equation, we can obtain the approximate or precise solution of Equation (5) from the exact solution of Eq. (6). The initial k terms of the infinite Taylor series expansion of solution of Eq. (6) are unaltered. Additionally, in order to maintain the relationship between the terms of the Taylor series and to satisfy the boundary conditions of the fractional differential equation, the integer order derivative with respect to t is substituted by the fractional derivative with respect to t.

For the solution of Eq. (6) with regard to t, the sketched Taylor series form is shown below.

$$\phi(x,t) = \sum_{n=0}^{\infty} \frac{\partial^n\phi(x,0)}{\partial t^n}\frac{t^n}{n!}. \tag{7}$$

Then the solution of Eq. (5) is given in the following format.

$$\phi(x,t) = \sum_{n=0}^{k-1} \frac{\partial^n\phi(x,0)}{\partial t^n}\frac{t^n}{n!} + \sum_{n=1}^{\infty}\sum_{j=0}^{k-1} \frac{\partial^{kn+j}\phi(x,0)}{\partial t^{kn+j}}\frac{t^{n\alpha+j}}{\Gamma(n\alpha+j+1)}. \tag{8}$$

3 Numerical examples

3.1 Solution of SFTE

Take a look at a general SFTE example [20].

$$\frac{\partial^{2\alpha}\phi}{\partial x^{2\alpha}} = \frac{\partial^2\phi}{\partial t^2} + 4\frac{\partial\phi}{\partial t} + 4\phi \quad t \geq 0,\, 0 < \alpha \leq 1, \tag{9}$$

with initial conditions

$$\phi(0,t) = 1 + e^{-2t},\ \phi_x(0,t) = 2. \tag{10}$$

The exact solution of Eq. (9) with initial conditions (10) is given as

$$\phi(x,t) = e^{2x} + e^{-2t}. \tag{11}$$

The Taylor series expansion of the exact solution (11) is below.

$$\phi(x,t) = \left(e^{-2t} + 1 + 2x + \frac{4x^2}{2!} + \frac{8x^3}{3!} + \cdots\right). \tag{12}$$

As discussed in the procedure, the solution to Eq. (9) is given by

$$\phi(x,t) = \left(1 + e^{-2t} + \frac{2x^{\alpha}}{\Gamma(\alpha+1)} + \frac{4x^{2\alpha}}{\Gamma(2\alpha+1)} + \frac{8x^{3\alpha}}{\Gamma(3\alpha+1)} + \cdots\right). \tag{13}$$

To demonstrate how well the approach works, we will check its convergence by increasing the number of terms in the series solution. In perspective of this, Convergency Table 1 contains values for the fractional value α, with $\alpha = 0.8$ and a fixed value of $t = 0.1$, while x ranges from 0 to 1.

Table 1: Convergency chart for the solution of the SFTE.

x	$\phi(x, t = 0.1)$						
	3 terms	5 terms	7 terms	9 terms	13 terms	16 terms	17 terms
0	1.818730	1.818730	1.818730	1.818730	1.818730	1.818730	1.818730
0.1	2.159061	2.240025	2.241460	2.241473	2.241473	2.241473	2.241473
0.2	2.411281	2.680719	2.694812	2.695188	2.695194	2.695194	2.695194
0.3	2.638323	3.195128	3.249704	3.252453	3.252541	3.252541	3.252541
0.4	2.850420	3.793880	3.937923	3.949311	3.949894	3.949895	3.949895
0.5	3.052055	4.483454	4.791251	4.825739	4.828286	4.828291	4.828291
0.6	3.245725	5.268850	5.843929	5.929557	5.938111	5.938144	5.938144
0.7	3.433014	6.154317	7.133256	7.318560	7.342541	7.342702	7.342703
0.8	3.615007	7.143644	8.699801	9.062343	9.121244	9.121873	9.121876
0.9	3.792495	8.240293	10.587472	11.244084	11.374845	11.376950	11.376964
1.0	3.966073	9.447488	12.843557	13.962366	14.230392	14.236641	14.236689

The surface of the graph in Fig. 1 depicts the exact solution of the telegraph equation given in Eq. (11) for $\alpha = 1$. Further, the surface of graphs in Figs. 2 and 3 show the approximate solutions of the SFTE for $\alpha = 0.5$ and 0.3 respectively.

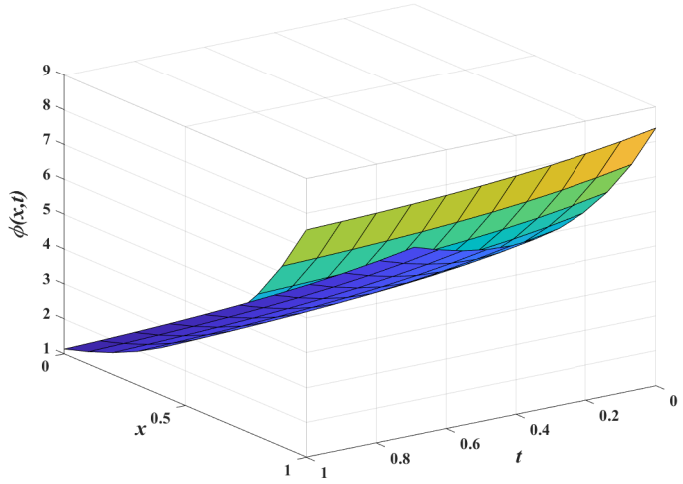

Figure 1: Exact solution of SFTE (11) for $\alpha = 1$

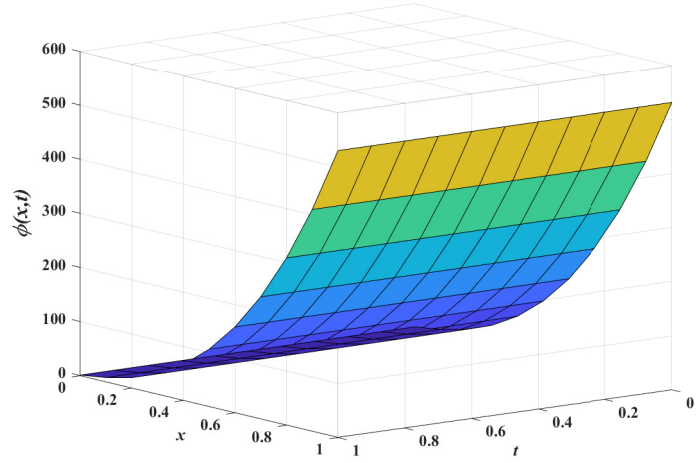

Figure 2: Approximate solution of SFTE (13) for $\alpha = 0.3$

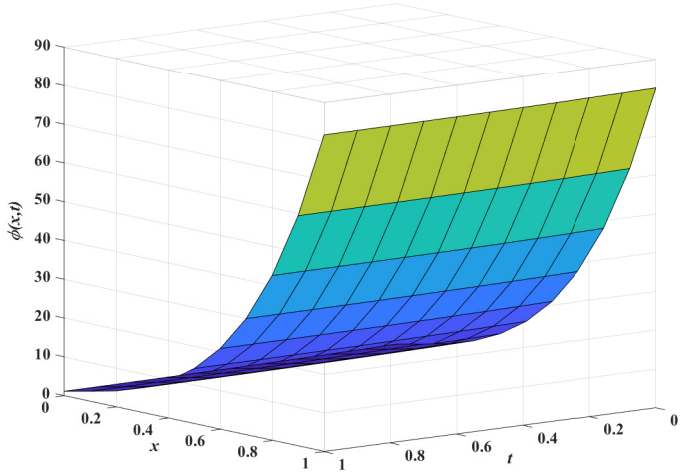

Figure 3: Approximate solution of SFTE (13) for $\alpha = 0.5$

3.2 Solution of TFTE

Take a look at the following TFTE [20],

$$\frac{\partial^\alpha \phi(x,t)}{\partial t^\alpha} = \frac{\partial^2 \phi(x,t)}{\partial x^2} - \frac{\partial \phi(x,t)}{\partial t} - \phi(x,t), \quad x,t \geq 0,\ 0 < \alpha \leq 2 \tag{14}$$

with initial conditions

$$\phi(x,0) = e^{-x}, \quad \phi_t(x,0) = -e^{-x}. \tag{15}$$

This equation has the following exact solution for $\alpha = 2$,

$$\phi(x,t) = e^{-(x+t)}. \tag{16}$$

The Taylor series expansion for exact solution (16) as below

$$\phi(x,t) = e^{-2t}\left(1 - t + \frac{4x^2}{2!} + \frac{8x^3}{3!} + \cdots\right). \tag{17}$$

The method allows us to arrive at the following solution to Eq. (14),

$$\phi(x,t) = e^{-x}\left(1 - t + \frac{t^\alpha}{\Gamma(\alpha+1)} - \frac{t^{\alpha+1}}{\Gamma(\alpha+2)} + \frac{t^{2\alpha}}{\Gamma(2\alpha+1)} - \frac{t^{2\alpha+1}}{\Gamma(2\alpha+2)} + \cdots\right). \tag{18}$$

Here, we examine whether the approximation solution for the fractional value of α is convergent. The calculated values of $\phi(x,t)$ for $\alpha = 1.7, x = 0.1$, and t ranging from 0 to 1 are shown in Table 2. This table indicates that the computed result $\phi(x,t)$ converges up to four places of decimal in the approximation of the tenth term.

The graphical illustration for exact and approximate solutions has been shown. The graph in Fig. 4 has been plotted for the exact solution (16). In Figs. 5 and 6, the surfaces of the graphs show the approximate solutions (18) for $\alpha = 1.2$ and 1.7.

Table 2: Convergency chart for the solution of the TFTE.

t	$\phi(x=0.1,t)$						
	2 terms	3 terms	4 terms	5 terms	6 terms	7 terms	8 terms
0	0.9048374	0.9048374	0.9048374	0.9048374	0.9048374	0.9048374	0.9048374
0.1	0.8426171	0.8499774	0.8482249	0.8485619	0.8485076	0.8485151	0.8485142
0.2	0.7888023	0.8057117	0.8016857	0.8024599	0.8023350	0.8023524	0.8023503
0.3	0.7390122	0.7665189	0.7599697	0.7612292	0.7610260	0.7610542	0.7610508
0.4	0.6920779	0.7309256	0.7216762	0.7234549	0.7231680	0.7232079	0.7232030
0.5	0.6473983	0.6981743	0.6860848	0.6884097	0.6880347	0.6880868	0.6880804
0.6	0.6045998	0.6677937	0.6527476	0.6556410	0.6551744	0.6552392	0.6552313
0.7	0.5634244	0.6394591	0.6213556	0.6248370	0.6242755	0.6243535	0.6243440
0.8	0.5236826	0.6129314	0.5916817	0.5957681	0.5951090	0.5952006	0.5951894
0.9	0.4852285	0.5880266	0.5635508	0.5682577	0.5674985	0.5676040	0.5675911
1.0	0.4479456	0.5645982	0.5368238	0.5421650	0.5413035	0.5414232	0.5414086

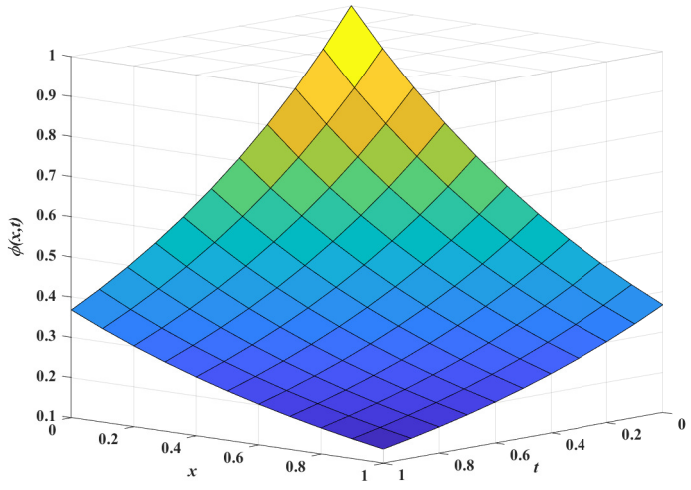

Figure 4: Exact solution of TFTE (16) for $\alpha = 2$

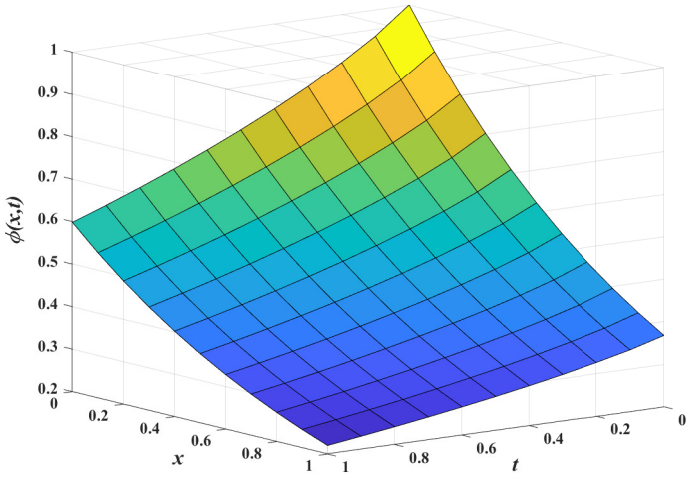

Figure 5: Approximate solution of TFTE (18) for $\alpha = 1.2$

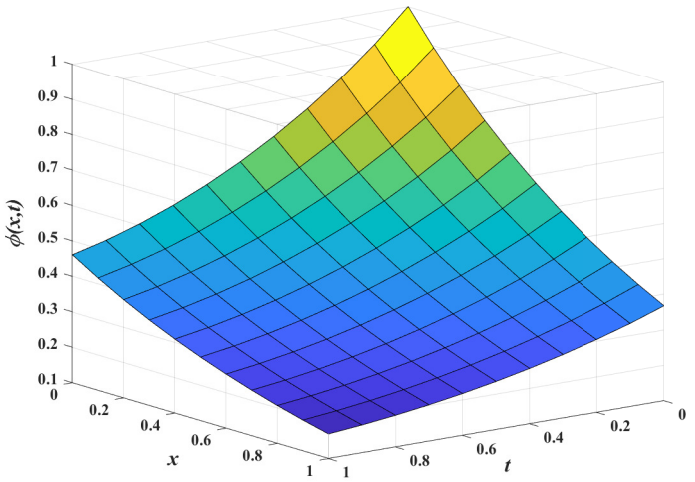

Figure 6: Approximate solution of TFTE (18) for $\alpha = 1.7$

4 Conclusion

If the integer order PDEs have analytical solutions, the Taylor series expansion method works well enough for fractional order PDEs. Numerical examples of this method demonstrate that it may be used to solve any differential equation derived from FDEs with ease and effectiveness, provided that the differential equation has an analytical or approximative solution. By extending the Taylor series expansion of the analytical solution, this study has determined the approximate solutions of the SFTE and TFTE. Furthermore, the infinitive series solution obtained in numerical examples 3.1 and 3.2 is identical to that given in [20], confirming the validity of the considered method. Additionally, the convergency Tables 1 and 2 demonstrate the efficacy of the method. As we can observe that the recorded values in Tables 1 and 2 are being closure enough if the number of terms increases. Furthermore, a graphic illustration is used to show both the exact and approximative solutions for integer and fractional values of α. Using the MATLAB programme, the 3D graphs for the solution of SFTE and TFTE are shown. The discussed method can also be used to analyse ODEs and PDEs with fractional derivatives with exponential and Mittag-Leffler kernels in future iterations of the research.

References

[1] S. Dubey and S. Chakraverty, "Application of modified extended tanh method in solving fractional order coupled wave equations," *Mathematics and Computers in Simulation*, vol. 198, pp. 509–520, 2022.

[2] R. M. Jena, S. Chakraverty, and D. Baleanu, "A novel analytical technique for the solution of time-fractional ivancevic option pricing model," *Physica A: Statistical Mechanics and its Applications*, vol. 550, p. 124380, 2020.

[3] S. Edeki, R. Jena, S. Chakraverty, and D. Baleanu, "Coupled transform method for time-space fractional black-scholes option pricing model," *Alexandria Engineering Journal*, vol. 59, no. 5, pp. 3239–3246, 2020.

[4] E. Zayed, Y. Amer, and R. Shohib, "The fractional complex transformation for nonlinear fractional partial differential equations in the mathematical physics," *Journal of the Association of Arab Universities for Basic and Applied Sciences*, vol. 19, pp. 59–69, 2016.

[5] S. Dubey and S. Chakraverty, "Homotopy perturbation method for solving fuzzy fractional heat-conduction equation," in *Advances in Fuzzy Integral and Differential Equations*. Springer, 2022, pp. 159–169.

[6] S. Momani and A. Yıldırım, "Analytical approximate solutions of the fractional convection–diffusion equation with nonlinear source term by he's homotopy perturbation method," *International Journal of Computer Mathematics*, vol. 87, no. 5, pp. 1057–1065, 2010.

[7] S. Dubey and S. Chakraverty, "Solution of fractional wave equation by homotopy perturbation method," *Wave Dynamics*, p. 263, 2022.

[8] V. P. Dubey, J. Singh, A. M. Alshehri, S. Dubey, and D. Kumar, "Analysis of local fractional coupled helmholtz and coupled burgers' equations in fractal media," *AIMS Mathematics*, vol. 7, no. 5, pp. 8080–8111, 2022.

[9] V. P. Dubey, D. Kumar, H. M. Alshehri, S. Dubey, and J. Singh, "Computational analysis of local fractional lwr model occurring in a fractal vehicular traffic flow," *Fractal and Fractional*, vol. 6, no. 8, p. 426, 2022.

[10] V. P. Dubey, J. Singh, A. M. Alshehri, S. Dubey, and D. Kumar, "Forecasting the behavior of fractional order bloch equations appearing in nmr flow via a hybrid computational technique," *Chaos, Solitons & Fractals*, vol. 164, p. 112691, 2022.

[11] V. P. Dubey, D. Kumar, J. Singh, A. M. Alshehri, and S. Dubey, "Analysis of local fractional klein-gordon equations arising in relativistic fractal quantum mechanics," *Waves in Random and Complex Media*, pp. 1–21, 2022.

[12] D. KUMAR, J. SINGH, and S. KUMAR, "Analytic and approximate solutions of space-time fractional telegraph equations via laplace transform," *Walailak Journal of Science and Technology (WJST)*, vol. 11, no. 8, pp. 711–728, 2014.

[13] J. Chen, F. Liu, and V. Anh, "Analytical solution for the time-fractional telegraph equation by the method of separating variables," *Journal of Mathematical Analysis and Applications*, vol. 338, no. 2, pp. 1364–1377, 2008.

[14] E. Orsingher and X. Zhao, "The space-fractional telegraph equation and the related fractional telegraph process," *Chinese Annals of Mathematics*, vol. 24, no. 01, pp. 45–56, 2003.

[15] E. Orsingher and L. Beghin, "Time-fractional telegraph equations and telegraph processes with brownian time," *Probability Theory and Related Fields*, vol. 128, no. 1, pp. 141–160, 2004.

[16] A. Sevimlican, "An approximation to solution of space and time fractional telegraph equations by he's variational iteration method," *Mathematical Problems in Engineering*, vol. 2010, 2010.

[17] A. Yıldırım, "He's homotopy perturbation method for solving the space-and time-fractional telegraph equations," *International Journal of Computer Mathematics*, vol. 87, no. 13, pp. 2998–3006, 2010.

[18] J. Biazar and M. Eslami, "Analytic solution for telegraph equation by differential transform method," *Physics Letters A*, vol. 374, no. 29, pp. 2904–2906, 2010.

[19] A. Demir, S. Erman, B. Özgür, and E. Korkmaz, "Analysis of fractional partial differential equations by taylor series expansion," *Boundary Value Problems*, vol. 2013, no. 1, pp. 1–12, 2013.

[20] S. Dubey and S. Chakraverty, "Hybrid techniques for approximate analytical solution of space-and time-fractional telegraph equations," *Pramana*, vol. 97, no. 1, pp. 1–13, 2023.

An $M/G/1$ Feedback retrial queue with working vacation and a waiting server

S.Pazhani Bala Murugan[1] and R.Keerthana[2]
[1,2]Department of Mathematics, Annamalai University,
Annamalainagar-608002, Tamilnadu, India.
*Corresponding Author E-Mail: spbm1966@gmail.com

December 27, 2022

Abstract

An $M/G/1$ feedback retrial queue with working vacation and a waiting server is taken into consideration in this study. Both retrial times and service times are assumed to follow general distribution and the waiting server follows an exponential distribution. During the working vacation period customers are served at a lesser rate of service. Before going for a vacation the server waits for some arbitrary amount of time and so is called a waiting server. We obtain the probability generating function (PGF) for the number of customers and the mean number of customers in the invisible waiting area by utilizing the supplementary variable technique. We compute the mean waiting time. Out of interest a few special cases are conferred. Numerical outcomes are exhibited.

Keywords: Retrial queue, Working vacation, Supplementary variable technique, Waiting server, Feedback.

Mathematics Subject Classification 2010: 60K25, 90B22

1 Introduction

Retrial queues are expressed by the fact that if a customer observed that the server is occupied then they are entered into the invisible waiting area called an orbit. In recent years numerous researchers have examined the retrial queue. For a more in-depth analysis of the retrial queues, we can refer[1,2,3].
In Queueing theory queueing models with server vacation has a most impactful application. In addition to the vacation strategy Servi and Finn [4] developed a newest vacation strategy, called as Working Vacation (WV). In the WV period the server provides a lesser rate of service to the customers than during the regular service period. Wu and Takagi [5] examined M/G/1/Multiple Working

Vacation (MWV). Pazhani Bala Murugan and Santhi[7] studied the $M/G/1$ retrial queue with MWV. For a comprehensive study on WV we can refer [8]. Whenever the system becomes empty the server leaves from the regular service period (RS) and goes on a WV, but in a waiting server model the server wait for a arbitrary amount of time before going to WV.
The server wait option is representative of many queueing mechanisms used in real life, especially when interacting with people. For a detailed study on waiting server model we can refer [9,10,11]. In queueing models, some customers rejoin the orbit after receiving the service to receive it again out of dissatisfaction. This is referred to as feedback. For a broad analysis of feedback retrial queues we can refer[12,13,14,15].
In this article, we consider an $M/G/1$ feedback retrial queue with multiple WV and a waiting server. This article has the following structure. We explain the model in segment 2. In segment 3 performance measures are established. Segment 4 discusses some special cases. In segment 5 numerical outcomes are exhibited . The conclusion is given in segment 6.

2 Model Description

We examined an $M/G/1$ retrial queue with switch over time to working vacation where the primary customer's arrival follows a Poisson process with a rate of λ and service discipline is first-in-first-out(FIFO). If an approaching customer discovers that the server is occupied, then they exit the service area because we assume that there is no waiting area and they join the orbit. At a service completion instant, only the customer at the head of the orbit is permitted to approach the server. The retrial time follows a general distribution with a distribution function G(x) for the regular service period, let $g(x)$ and $G^*(\theta)$ signifies the pdf and LST respectively, and for WV period, let $L(x), l(x), L^*(\theta)$ signifies the distribution function, pdf and LST respectively. On the service completion epoch of each customer, if there is a contest between the primary customer and an orbit customer. The service time in the RS period follows a general distribution with the distribution function $R_s(x), r_s(x)$ and $R_s^*(\theta)$ as its pdf and LST respectively. The service delivered in the WV period follows a general distribution with $W_v(x), w_v(x), W_v^*(\theta)$ as its distribution function, pdf, LST. The server waits for an arbitrary period of time once the orbit turns empty, which follows an exponential distribution with a rate of α. After completion of the waiting time, the server goes for WV, which follows an exponential distribution with a rate of β. After getting the service, customers either rejoin the orbit with probability m or depart the system with probability $n(= 1 - m)$. Inter-arrival times, retrial times, service time in RS periods and WV periods are all presumed to be independent of one another.
Let's use the subsequent random variables.
$O(t)$- Size of the orbit at time "t".
$G^0(t), R_s^0(t)$- the remaing retrial time and remaining service time in RS period.
$L^0(t), W_v^0(t)$- the remaing retrial time and remaining service time in WV period.

At time "t" the four distinct states of the server are

$$E(t) = \begin{cases} 0 \text{ - if the server is not being occupied in WV} \\ 1 \text{ - if the server is not being occupied in RS period} \\ 2 \text{ - if the server is being occupied in WV} \\ 3 \text{ - if the server is being occupied in RS period} \end{cases}$$

so that the supplementary variables $L^0(t), G^0(t), W_v^0(t)$ and $R_s^0(t)$ are introduced in order to obtain the bivariate Markov Processes $\{(O(t), B(t)); t \geq 0\}$, where

$$B(t) = \begin{cases} L^0(t), & \text{if } E(t) = 0; \\ G^0(t), & \text{if } E(t) = 1; \\ W_v^0(t), & \text{if E(t)=2;} \\ R_s^0(t), & \text{if E(t)=3.} \end{cases}$$

$$\begin{aligned}
W_{0,0} &= \lim_{t\to\infty} P[O(t) = 0,\ E(t) = 0] \\
R_{0,0} &= \lim_{t\to\infty} P[O(t) = 0,\ E(t) = 1] \\
W_{0,h} &= \lim_{t\to\infty} P[O(t) = h,\ E(t) = 0,\ x < L^0(t) \leq x + dx];\ h \geq 1 \\
R_{0,h} &= \lim_{t\to\infty} P[O(t) = h,\ E(t) = 1,\ x < G^0(t) \leq x + dx];\ h \geq 1 \\
W_{1,h} &= \lim_{t\to\infty} P[O(t) = h,\ E(t) = 2,\ x < W_v^0(t) \leq x + dx];\ h \geq 0 \\
R_{1,h} &= \lim_{t\to\infty} P[O(t) = h,\ E(t) = 3,\ x < R_s^0(t) \leq x + dx];\ h \geq 0
\end{aligned}$$

The above mentioned are the limiting probabilities which we have defined.

$$R_s^*(\theta) = \int_0^\infty e^{-\theta x} r_s(x)dx \qquad W_v^*(\theta) = \int_0^\infty e^{-\theta x} w_v(x)dx$$

$$L^*(\theta) = \int_0^\infty e^{-\theta x} l(x)dx \qquad G^*(\theta) = \int_0^\infty e^{-\theta x} g(x)dx$$

$$W_{0,h}^*(\theta) = \int_0^\infty e^{-\theta x} W_{0,h}(x)dx \qquad W_{0,h}^*(0) = \int_0^\infty W_{0,h}(x)dx$$

$$W_{1,h}^*(\theta) = \int_0^\infty e^{-\theta x} W_{1,h}(x)dx \qquad W_{1,h}^*(0) = \int_0^\infty W_{1,h}(x)dx$$

$$R_{0,h}^*(\theta) = \int_0^\infty e^{-\theta x} R_{0,h}(x)dx \qquad R_{0,h}^*(0) = \int_0^\infty R_{0,h}(x)dx$$

$$R_{1,h}^*(\theta) = \int_0^\infty e^{-\theta x} R_{1,h}(x)dx \qquad R_{1,h}^*(0) = \int_0^\infty R_{1,h}(x)dx$$

$$W_0^*(z,\theta)=\sum_{h=1}^{\infty}W_{0,h}^*(\theta)z^h \qquad W_0^*(z,0)=\sum_{h=1}^{\infty}W_{0,h}^*(0)z^h$$
$$W_0(z,0)=\sum_{h=1}^{\infty}W_{0,h}(0)z^h \qquad W_1^*(z,\theta)=\sum_{h=0}^{\infty}W_{1,h}^*(\theta)z^h$$
$$W_1^*(z,0)=\sum_{h=0}^{\infty}W_{1,h}^*(0)z^h \qquad W_1(z,0)=\sum_{h=0}^{\infty}W_{1,h}(0)z^h$$
$$R_0^*(z,\theta)=\sum_{h=1}^{\infty}R_{0,h}^*(\theta)z^h \qquad R_0^*(z,0)=\sum_{h=1}^{\infty}R_{0,h}^*(0)z^h$$
$$R_0(z,0)=\sum_{h=1}^{\infty}R_{0,h}(0)z^h \qquad R_1^*(z,\theta)=\sum_{h=0}^{\infty}R_{1,h}^*(\theta)z^h$$
$$R_1^*(z,0)=\sum_{h=0}^{\infty}R_{1,h}^*(0)z^h \qquad R_1(z,0)=\sum_{h=0}^{\infty}R_{1,h}(0)z^h$$

The above mentioned are the Laplace Steiltjes Transform and PGF which we have defined.
In steady state the system was illustrated by the subsequent differential difference equations:

$$\lambda W_{0,0} = nW_{1,0}(0)+\alpha R_{0,0} \tag{1}$$
$$-\frac{d}{dx}W_{0,h}(x) = -(\beta+\lambda)W_{0,h}(x)+nW_{1,h}(0)l(x) + mW_{1,h-1}(0)l(x);\quad h\geq 1 \tag{2}$$
$$-\frac{d}{dx}W_{1,0}(x) = -(\lambda+\beta)W_{1,0}(x)+W_{0,1}(0)w_v(x)+\lambda W_{0,0}w_v(x) \tag{3}$$
$$-\frac{d}{dx}W_{1,h}(x) = -(\lambda+\beta)W_{1,h}(x)+\lambda W_{1,h-1}(x)+W_{0,h+1}(0)w_v(x) + \lambda\int_0^{\infty}W_{0,h}(x)dx\ w_v(x); h\geq 1 \tag{4}$$
$$(\lambda+\alpha)R_{0,0} = nR_{1,0}(0) \tag{5}$$
$$-\frac{d}{dx}R_{0,h}(x) = -\lambda R_{0,h}(x)+nR_{1,h}(0)g(x)+mR_{1,h-1}(0)g(x) + \beta\int_0^{\infty}W_{0,h}(x)dx\ g(x);\quad h\geq 1 \tag{6}$$
$$-\frac{d}{dx}R_{1,0}(x) = -\lambda R_{1,0}(x)+R_{0,1}(0)r_s(x)+\beta r_s(x)\int_0^{\infty}W_{1,0}(x)dx \tag{7}$$

$$-\frac{d}{dx}R_{1,h}(x) = -\lambda R_{1,h}(x) + \lambda R_{1,h-1}(x) + \beta r_s(x)\int_0^\infty W_{1,h}(x)dx$$
$$+R_{0,h+1}(0)r_s(x) + \lambda r_s(x)\int_0^\infty R_{0,h}(x)dx; \quad h \geq 1 \tag{8}$$

Taking the LST from (2) to (8) on both sides results

$$\theta W^*_{0,h}(\theta) - W_{0,h}(0) = (\lambda+\beta)W^*_{0,h}(\theta) - nW_{1,h}(0)L^*(\theta)$$
$$-mW_{1,h-1}(0)L^*(\theta); \quad h \geq 1 \tag{9}$$

$$\theta W^*_{1,0}(\theta) - W_{1,0}(0) = (\lambda+\beta)W^*_{1,0}(\theta) - W_{0,1}(0)W^*_v(\theta)$$
$$-\lambda W_{0,0}W^*_v(\theta) \tag{10}$$

$$\theta W^*_{1,h}(\theta) - W_{1,h}(0) = (\lambda+\beta)W^*_{1,h}(\theta) - W_{0,h+1}(0)W^*_v(\theta)$$
$$-\lambda W^*_{1,h-1}(\theta) - \lambda W^*_{0,h}(0)W^*_v(\theta); \quad h \geq 1 \tag{11}$$

$$\theta R^*_{0,h}(\theta) - R_{0,h}(0) = \lambda R^*_{0,h}(\theta) - nR_{1,h}(0)G^*(\theta) - \beta G^*(\theta)W^*_{0,h}(0)$$
$$-mR_{1,h-1}(0)G^*(\theta); \quad h \geq 1 \tag{12}$$

$$\theta R^*_{1,0}(\theta) - R_{1,0}(0) = \lambda R^*_{1,0}(\theta) - R_{0,1}(0)R^*_s(\theta) - \beta R^*_s(\theta)W^*_{1,0}(0)$$
$$-\lambda R_{0,0}R^*_s(\theta) \tag{13}$$

$$\theta R^*_{1,h}(\theta) - R_{1,h}(0) = \lambda R^*_{1,h}(\theta) - \lambda R^*_{1,h-1}(\theta) - R^*_s(\theta)R_{0,h+1}(0)$$
$$-\beta R^*_s(\theta)W^*_{1,h}(0) - \lambda R^*_s(\theta)R^*_{0,h}(0); \quad h \geq 1 \tag{14}$$

Summing over h from 1 to infinity $\times$ (9) with z^h and results,

$$W^*_0(z,\theta)[\theta - (\lambda+\beta)] = W_0(z,0) - L^*(\theta)[(n+mz)W_1(z,0)$$
$$-nW_{1,0}(0)] \tag{15}$$

Summing over h from 1 to infinity $\times$ (11) with z^h and comprise with (10) results,

$$W^*_1(z,\theta)[\theta - (\lambda+\beta-\lambda z)] = W_1(z,0) - \frac{W^*_v(\theta)}{z}W_0(z,0)$$
$$-\lambda W_{0,0}W^*_v(\theta) - \lambda W^*_v(\theta)W^*_0(z,0) \tag{16}$$

Placing $\theta = \lambda + \beta$ in (15), results

$$W_0(z,0) = L^*(\lambda+\beta)[(n+mz)W_1(z,0) - nW_{1,0}(0)] \tag{17}$$

Placing $\theta = 0$ and (Sub.) (17) in (15), results

$$W^*_0(z,0) = \frac{(1-L^*(\lambda+\beta))((n+mz)W_1(z,0) - nW_{1,0}(0))}{\lambda+\beta} \tag{18}$$

Placing $\theta = \lambda + \beta - \lambda z$ and (Sub.) (17) and (18) in (16), results

$$W_1(z,0) = \frac{\left[\begin{array}{r}[\lambda z(\lambda+\beta)W_{0,0} - n[L^*(\lambda+\beta)(\lambda+\beta-\lambda z) \\ +\lambda z]W_{1,0}(0)]W_v^*(\lambda+\beta-\lambda z)\end{array}\right]}{Dr_1(z)} \tag{19}$$

(Sub.)(19) in (17), results

$$W_0(z,0) = \frac{\left[\begin{array}{r}(\lambda+\beta)z[(n+mz)\lambda W_v^*(\lambda+\beta-\lambda z)W_{0,0} \\ -nW_{1,0}(0)]L^*(\lambda+\beta)\end{array}\right]}{Dr_1(z)} \tag{20}$$

Let $f(z) = (\lambda+\beta)z - W_v^*(\lambda+\beta-\lambda z)(L^*(\lambda+\beta)(\lambda+\beta-\lambda z)+\lambda z)$, for $f(z) = 0$ we obtain $f(0) < 0$ and $f(1) > 0$ which $\Rightarrow$ that $\exists$ a real root $z_1 \in (0,1)$.
At $z = z_1(20)$ is converted in to

$$W_{1,0}(0) = \lambda W_v^*(\lambda - \lambda z_1 + \beta)(n+mz)W_{0,0} \tag{21}$$

(Sub.) (21) in (19), results

$$W_1(z,0) = \frac{\lambda W_v^*(\lambda+\beta-\lambda z)UP(z)}{Dr_1(z)}W_{0,0} \tag{22}$$

where,

$$UP(z) = z(\lambda+\beta) - (n+mz)W_v^*(\lambda+\beta-\lambda z_1)[\lambda z + L^*(\lambda+\beta)(\lambda+\beta-\lambda z)]$$

(Sub.) (21) in (20), results

$$W_0(z,0) = \frac{\left[\begin{array}{r}\Big[(n+mz)\lambda z(\lambda+\beta)[W_v^*(\lambda+\beta-\lambda z) \\ -W_v^*(\lambda-\lambda z_1+\beta)]\Big]L^*(\lambda+\beta)\end{array}\right]}{Dr_1(z)} \tag{23}$$

(Sub.) (21) and (22) in (18), results

$$W_0^*(z,0) = \frac{\left[\begin{array}{r}\Big[(1-L^*(\lambda+\beta))\lambda z(n+mz)[W_v^*(\lambda+\beta-\lambda z) \\ -W_v^*(\lambda+\beta-\lambda z_1)]\Big]\end{array}\right]}{Dr_1(z)} \tag{24}$$

Placing $\theta = 0$ and (Sub.) (22), (23) and (24) in (16), results

$$W_1^*(z,0) \;=\; \frac{W_{0,0}\lambda(1-W_v^*(\lambda+\beta-\lambda z))UP(z)}{(\lambda+\beta-\lambda z)Dr_1(z)} \tag{25}$$

Summing over h from 1 to infinity $\times$ (12) with z^h and results

$$\begin{aligned} R_0^*(z,\theta)(\theta-\lambda) &= R_0(z,0)-G^*(\theta)[(n+mz)R_1(z,0)-nR_{1,0}(0)] \\ &\quad -W_0^*(z,0)\beta G^*(\theta) \end{aligned} \tag{26}$$

(Sub.) $W_{1,0}(0)=(n+mz)\lambda W_v^*(\lambda+\beta-\lambda z_1)W_{0,0}$ in (1), we get

$$\alpha R_{0,0} = \lambda(1-(n+mz)W_v^*(\lambda+\beta-\lambda z_1))W_{0,0}$$

Placing $\theta=\lambda$ and (Sub.) $R_{1,0}(0)=\lambda(1-(n+mz)W_v^*(\lambda+\beta-\lambda z_1))W_{0,0}-\lambda R_{0,0}$ in (26), results

$$\begin{aligned} R_0(z,0) &= [(n+mz)R_1(z,0)-\lambda(1-(n+mz)W_v^*(\lambda+\beta-\lambda z_1))W_{0,0} \\ &\quad -\lambda R_{0,0}+\beta W_0^*(z,0)]G^*(\lambda) \end{aligned} \tag{27}$$

Summing over h from 1 to infinity $\times$ (14) with z^h and comprise with (13) results

$$R_1^*(z,\theta)[\theta-\lambda+\lambda z)] = R_1(z,0)-\left[\frac{R_0(z,0)}{z}+\beta W_1^*(z,0)+\lambda R_0^*(z,0)+\lambda R_{0,0}\right]R_s^*(\theta) \tag{28}$$

Placing $\theta=0$ and (Sub.) (27) and
$nR_{1,0}(0)=(1-(n+mz)W_v^*(\lambda+\beta-\lambda z_1))\lambda W_{0,0}-\lambda R_{0,0}$ in (26), results

$$\begin{aligned} R_0^*(z,0) &= \Big[(n+mz)R_1(z,0)-(1-(n+mz)W_v^*(\lambda+\beta-\lambda z_1))\lambda W_{0,0} \\ &\quad -\lambda R_{0,0}+\beta W_0^*(z,0)\Big]\Big[\frac{(1-G^*(\lambda))}{\lambda}\Big] \end{aligned} \tag{29}$$

Placing $\theta=\lambda-\lambda z$ and (Sub.) (27) and (29) in (28), results

$$R_1(z,0)=\frac{\left[\begin{array}{r} R_s^*(\lambda-\lambda z)\Big[\beta z W_1^*(z,0)+\beta[(1-z)G^*(\lambda)+z]W_0^*(z,0) \\ -[(1-(n+mz)W_v^*(\lambda+\beta-\lambda z_1))\lambda W_{0,0}+\lambda R_{0,0}] \\ [(1-z)G^*(\lambda)+z]+\lambda z R_{0,0}\Big] \end{array}\right]}{z-(n+mz)R_s^*(\lambda-\lambda z)[z+G^*(\lambda)(1-z)]} \tag{30}$$

(Sub.) (30) in (27), results

$$R_0(z,0)=\frac{\left[\begin{array}{r} zG^*(\lambda)\ \Big[\beta(n+mz)R_s^*(\lambda-\lambda z)W_1^*(z,0)+\beta W_0^*(z,0) \\ -\lambda(1-(n+mz)W_v^*(\lambda+\beta-\lambda z_1))W_{0,0} \\ -\lambda(1-(n+mz)R_s^*(\lambda-\lambda z))R_{0,0}\Big] \end{array}\right]}{z-(n+mz)R_s^*(\lambda-\lambda z)\big[(1-z)G^*(\lambda)+z\big]} \tag{31}$$

(Sub.) (30) in (29), results

$$R_0^*(z,0) = \frac{\begin{bmatrix}(1-G^*(\lambda))z\ [\beta W_1^*(z,0)(n+mz)R_s^*(\lambda-\lambda z)+\beta W_0^*(z,0) \\ -\lambda(1-(n+mz)W_v^*(\lambda+\beta-\lambda z_1))W_{0,0} \\ -\lambda(1-(n+mz)R_s^*(\lambda-\lambda z))R_{0,0}]\end{bmatrix}}{\lambda\big\{z-(n+mz)R_S^*(\lambda-\lambda z)\big[(1-z)G^*(\lambda)+z\big]\big\}} \tag{32}$$

Placing $\theta = 0$ and (Sub.) (30), (31) and (32) in (28), results

$$R_1^*(z,0) = \frac{\begin{bmatrix}\Big\{W_0^*(z,0)[G^*(\lambda)(1-z)+z]\beta+\lambda z R_{0,0}-[G^*(\lambda)(1-z)+z] \\ \times[\lambda(1-(n+mz)W_v^*(\lambda+\beta-\lambda z_1))W_{0,0}+\lambda R_{0,0}] \\ +\beta W_1^*(z,0)z\Big\}(1-R_s^*(\lambda-\lambda z))\end{bmatrix}}{(\lambda-\lambda z)\ \Big[\ z-(n+mz)R_s^*(\lambda-\lambda z)[z+G^*(\lambda)(1-z)]\Big]} \tag{33}$$

We define $W_v(z) = W_0^*(z,0) + W_1^*(z,0) + W_{0,0}$

$$\begin{aligned}W_v(z) =& \frac{W_{0,0}}{(\lambda+\beta-\lambda z)D_1(z)}\Big\{\lambda z(W_v^*(\lambda+\beta-\lambda z)-W_v^*(\lambda+\beta-\lambda z_1)) \\ &\times(\lambda+\beta-\lambda z)(1-L^*(\lambda+\beta))+\lambda(1-W_v^*(\lambda+\beta-\lambda z)) \\ &\times[z(\lambda+\beta)-[\lambda z+L^*(\lambda+\beta)(\lambda+\beta-\lambda z)]W_v^*(\lambda+\beta-\lambda z_1) \\ &\times(n+mz)]+(\lambda+\beta-\lambda z)[z(\lambda+\beta)-(n+mz)W_v^*(\lambda+\beta-\lambda z) \\ &\times(\lambda z+L^*(\lambda+\beta)(\lambda+\beta-\lambda z))]\Big\}\end{aligned} \tag{34}$$

when the server is on WV period, as the PGF for the number of customers in orbit.
(Sub.) (24) and (25) in (32), results

$$\begin{aligned}R_0^*(z,0) =& \frac{z(1-G^*(\lambda))W_{0,0}}{(\lambda+\beta-\lambda z)Dr_1(z)Dr_2(z)}\Big\{\beta(n+mz)(1-W_v^*(\lambda+\beta-\lambda z)) \\ &\times R_s^*(\lambda-\lambda z)\big\{(\lambda+\beta)z-(n+mz)W_v^*(\lambda+\beta-\lambda z_1)[\lambda z \\ &+(\lambda+\beta-\lambda z)L^*(\lambda+\beta)]\big\}+\beta z(\lambda+\beta-\lambda z)(1-L^*(\lambda+\beta)) \\ &\times(n+mz)(W_v^*(\lambda+\beta-\lambda z)-W_v^*(\lambda+\beta-\lambda z_1))-(\lambda+\beta-\lambda z) \\ &\times(1-(n+mz)W_v^*(\lambda+\beta-\lambda z_1))\big\{(\lambda+\beta)z-W_v^*(\lambda+\beta-\lambda z) \\ &\times(n+mz)[\lambda z+(\lambda+\beta-\lambda z)L^*(\lambda+\beta)]\big\}-\frac{\lambda}{\alpha}(\lambda+\beta-\lambda z) \\ &\times(1-(n+mz)W_v^*(\lambda+\beta-\lambda z_1))(1-(n+mz)R_s^*(\lambda-\lambda z)) \\ &\times\big\{(\lambda+\beta)z-W_v^*(\lambda+\beta-\lambda z)[\lambda z+(\lambda+\beta-\lambda z)L^*(\lambda+\beta)]\big\}\Big\}\end{aligned} \tag{35}$$

(Sub.) (24), (25) in (33), results

$$
\begin{aligned}
R_1^*(z,0) &= \frac{(1-R_s^*(\lambda-\lambda z))W_{0,0}}{Dr_2(z)(\lambda+\beta-\lambda z)Dr_1(z)}\Big\{[\lambda z+G^*(\lambda)(\lambda+\beta-\lambda z)](n+mz)\\
&\times[1-L^*(\lambda+\beta)][W_v^*(\lambda+\beta-\lambda z)-W_v^*(\beta+\lambda-\lambda z_1)]\beta z\\
&-(1-(n+mz)W_v^*(\lambda+\beta-\lambda z_1))[\lambda z+G^*(\lambda)(\lambda+\beta-\lambda z)]\\
&\times\Big\{(\lambda+\beta)z-(n+mz)W_v^*(\lambda+\beta-\lambda z)[\lambda z+(\lambda+\beta-\lambda z)\\
&\times L^*(\lambda+\beta)]\Big\}+(W_v^*(\lambda+\beta-\lambda z)-W_v^*(\lambda+\beta-\lambda z_1))\beta z\\
&\times(\lambda+\beta)L^*(\lambda+\beta)-\frac{\lambda}{\alpha}(1-(n+mz)W_v^*(\lambda+\beta-\lambda z_1))G^*(\lambda)\\
&\times(\lambda+\beta-\lambda z)\Big\{(\lambda+\beta)z-[\lambda z+(\lambda+\beta-\lambda z)L^*(\lambda+\beta)]\\
&\times W_v^*(\lambda+\beta-\lambda z)(n+mz)\Big\}+m\Big[[\lambda\beta z^2W_v^*(\lambda+\beta-\lambda z_1)\\
&+\beta^2zW_v^*(\lambda+\beta-\lambda z_1)W_v^*(\lambda+\beta-\lambda z)L^*(\lambda+\beta)\\
&\times+W_v^*(\lambda+\beta-\lambda z_1)\lambda\beta zL^*(\lambda+\beta)W_v^*(\lambda+\beta-\lambda z)(1-z)]\\
&\times(n+mz)-[\beta^2z^2+\lambda\beta z^2]W_v^*(\lambda+\beta-\lambda z)\Big]\Big\} \qquad (36)
\end{aligned}
$$

We define $R_S(z)=R_0^*(z,0)+R_1^*(z,0)+R_{0,0}$

$$
\begin{aligned}
R_S(z) &= \frac{W_{0,0}}{(\lambda+\beta-\lambda z)(Dr_1(z)Dr_2(z))}\Big\{z(1-G^*(\lambda))\Big\{(1-W_v^*(\lambda+\beta-\lambda z))\\
&\times R_s^*(\lambda-\lambda z)\beta(n+mz)\Big[(\lambda+\beta)z-(n+mz)W_v^*(\lambda+\beta-\lambda z_1)\\
&\times[\lambda z+(\lambda+\beta-\lambda z)L^*(\lambda+\beta)]\Big]+\beta z(1-L^*(\lambda+\beta))(\lambda+\beta-\lambda z)\\
&\times(n+mz)(W_v^*(\lambda+\beta-\lambda z)-W_v^*(\lambda+\beta-\lambda z_1))-(\lambda+\beta-\lambda z)\\
&\times(1-(n+mz)W_v^*(\lambda+\beta-\lambda z_1))\Big[(\lambda+\beta)z-W_v^*(\lambda+\beta-\lambda z)\\
&\times[\lambda z+(\lambda+\beta-\lambda z)L^*(\lambda+\beta)](n+mz)\Big]\Big\}+(1-R_s^*(\lambda-\lambda z))\\
&\times\Big\{[\lambda z+(\lambda+\beta-\lambda z)G^*(\lambda)][W_v^*(\lambda+\beta-\lambda z)-W_v^*(\lambda+\beta-\lambda z_1)]\\
&\times\beta z(n+mz)[1-L^*(\lambda+\beta)]-(1-(n+mz)W_v^*(\lambda+\beta-\lambda z_1))\\
&\times[\lambda z+G^*(\lambda)(\lambda+\beta-\lambda z)][(\lambda+\beta)z-(n+mz)W_v^*(\lambda+\beta-\lambda z)\\
&\times[\lambda z+L^*(\lambda+\beta)(\lambda+\beta-\lambda z)]]+\beta z(\lambda+\beta)(W_v^*(\lambda+\beta-\lambda z)\\
&-W_v^*(\lambda+\beta-\lambda z_1))L^*(\lambda+\beta)\Big\}+m\Big[[\beta^2zW_v^*(\lambda+\beta-\lambda z_1)\\
&\times W_v^*(\lambda+\beta-\lambda z)L^*(\lambda+\beta)+\lambda\beta z^2W_v^*(\lambda+\beta-\lambda z_1)+(1-z)\\
&\times\lambda\beta zW_v^*(\lambda+\beta-\lambda z_1)L^*(\lambda+\beta)](n+mz)-[\beta^2z^2+\lambda\beta z^2]\\
&\times W_v^*(\lambda+\beta-\lambda z)\Big]+\frac{\lambda}{\alpha}(\lambda+\beta-\lambda z)(1-W_v^*(\lambda+\beta-\lambda z_1))\\
&\times(n+mz)[(\lambda+\beta)z-(n+mz)W_v^*(\lambda+\beta-\lambda z)[\lambda z+L^*(\lambda+\beta)\\
&\times(\lambda+\beta-\lambda z)][mG^*(\lambda)R_s^*(\lambda-\lambda z)-G^*(\lambda)](1-z)\Big\} \qquad (37)
\end{aligned}
$$

where,

$$\begin{aligned} Dr_1(z) &= z(\lambda+\beta)-(n+mz)W_v^*(\lambda+\beta-\lambda z)[\lambda z \\ &\quad +L^*(\lambda+\beta)(\lambda+\beta-\lambda z)] \qquad (38) \\ Dr_2(z) &= z-(n+mz)R_s^*(\lambda-\lambda z)[G^*(\lambda)(1-z)+z] \qquad (39) \end{aligned}$$

when the server is on RS period, as the PGF for the number of customers in the orbit.
Again, we define $R(z) = R_S(z) + W_v(z)$

$$\begin{aligned} R(z) &= \frac{W_{0,0}}{(\lambda+\beta-\lambda z)D_1(z)D_2(z)}\Bigg\{z(1-G^*(\lambda))\Big[(1-W_v^*(\lambda+\beta-\lambda z))\beta \\ &\quad \times(n+mz)R_s^*(\lambda-\lambda z)\big[(\lambda+\beta)z-(n+mz)W_v^*(\lambda+\beta-\lambda z_1)[\lambda z \\ &\quad +(\lambda+\beta-\lambda z)L^*(\lambda+\beta)\big]\big]+\beta z(\lambda-\lambda z)(n+mz)(1-L^*(\lambda+\beta)) \\ &\quad \times(W_v^*(\lambda+\beta-\lambda z)-W_v^*(\lambda+\beta-\lambda z_1))-(\lambda+\beta-\lambda z)(1-(n+mz) \\ &\quad \times W_v^*(\lambda+\beta-\lambda z_1))\big[(\lambda+\beta)z-(n+mz)W_v^*(\lambda+\beta-\lambda z)[L^*(\lambda+\beta) \\ &\quad \times(\lambda+\beta-\lambda z)+\lambda z]\big]\Big]+(1-R_s^*(\lambda-\lambda z))\Big[[\lambda z+(\lambda+\beta-\lambda z)G^*(\lambda)] \\ &\quad \times\beta z(n+mz)[1-L^*(\lambda+\beta)][W_v^*(\lambda+\beta-\lambda z)-W_v^*(\lambda+\beta-\lambda z_1)] \\ &\quad -(1-(n+mz)W_v^*(\lambda+\beta-\lambda z_1))[\lambda z+G^*(\lambda)(\lambda+\beta-\lambda z)]\big[(\lambda+\beta)z \\ &\quad -(n+mz)W_v^*(\lambda+\beta-\lambda z)[\lambda z+(\lambda+\beta-\lambda z)L^*(\lambda+\beta)]\big]+(\lambda+\beta) \\ &\quad \times\beta z(W_v^*(\lambda+\beta-\lambda z))-W_v^*(\lambda+\beta-\lambda z_1))L^*(\lambda+\beta)+m\Big\{[\lambda\beta z^2 \\ &\quad \times W_v^*(\lambda+\beta-\lambda z_1)+\beta^2 z W_v^*(\lambda+\beta-\lambda z_1)W_v^*(\lambda+\beta-\lambda z)L^*(\lambda+\beta) \\ &\quad +W_v^*(\lambda+\beta-\lambda z_1)\lambda\beta z W_v^*(\lambda+\beta-\lambda z)L^*(\lambda+\beta)(1-z)](n+mz) \\ &\quad -[\beta^2z^2+\lambda\beta z^2]W_v^*(\lambda+\beta-\lambda z)\Big]+\frac{\lambda}{\alpha}(\lambda+\beta-\lambda z)(1-(n+mz) \\ &\quad \times W_v^*(\lambda+\beta-\lambda z_1))[(\lambda+\beta)z-(n+mz)W_v^*(\lambda+\beta-\lambda z)[\lambda z \\ &\quad +(\lambda+\beta-\lambda z)L^*(\lambda+\beta)][mG^*(\lambda)R_s^*(\lambda-\lambda z)-G^*(\lambda)](1-z)\big] \\ &\quad +\Big[(\lambda+\beta-\lambda z)(W_v^*(\lambda+\beta-\lambda z)-W_v^*(\lambda+\beta-\lambda z_1))(1-L^*(\lambda+\beta)) \\ &\quad \times\lambda z+\lambda(1-W_v^*(\lambda+\beta-\lambda z))[z(\lambda+\beta)-(n+mz)W_v^*(\lambda+\beta-\lambda z_1) \\ &\quad \times(\lambda z+L^*(\lambda+\beta)(\lambda+\beta-\lambda z))]+(\lambda+\beta-\lambda z)[z(\lambda+\beta)-(n+mz) \\ &\quad \times W_v^*(\lambda+\beta-\lambda z)(\lambda z+L^*(\lambda+\beta)(\lambda+\beta-\lambda z))]\Big]\Big[z-R_s^*(\lambda-\lambda z) \\ &\quad \times[z+(1-z)G^*(\lambda)]\Big]\Bigg\} \qquad (40) \end{aligned}$$

where $Dr_1(z)$ and $Dr_2(z)$ are given in (38) and (39) as the PGF for the number of customers in the orbit. Make use of the normalizing condition $R(1) = 1$ to findout that $W_{0,0}$ araise in (41). Using L'Hospitals rule and (Sub.) $z = 1$ in

(40) results,

$$W_{0,0} = \frac{1-\rho_s}{\left[\begin{array}{l} \left\{\dfrac{O}{\beta G^*(\lambda)[\lambda+\beta-W_v^*(\beta)(\lambda+\beta L^*(\lambda+\beta))]}\right\} \\ -\left\{\dfrac{P+mT}{G^*(\lambda)[\lambda+\beta-W_v^*(\beta)(\lambda+\beta L^*(\lambda+\beta))]}\right\} \\ +\left\{\dfrac{\beta W_v^*(\lambda+\beta-\lambda z_1)L^*(\lambda+\beta)(1-G^*(\lambda))}{G^*(\lambda)[\lambda+\beta-W_v^*(\beta)(\lambda+\beta L^*(\lambda+\beta))]}+Q\right\} \end{array}\right]} \tag{41}$$

$$R_{0,0} = \frac{\lambda}{\alpha}(1-W_v^*(\lambda+\beta-\lambda z_1))W_{0,0} \tag{42}$$

where,

$$\begin{aligned} O &= (\lambda-\lambda W_v^*(\lambda+\beta-\lambda z_1)+\beta)[\lambda+\beta G^*(\lambda) \\ &\quad -W_v^*(\beta)(\lambda+\beta L^*(\lambda+\beta))] \\ P &= \lambda E(R_s)W_v^*(\beta)[\lambda+\beta-W_v^*(\lambda+\beta-\lambda z_1)(\lambda+\beta L^*(\lambda+\beta))] \\ T &= \beta[L^*(\lambda+\beta)[W_v^*(\lambda+\beta-\lambda z)-W_v^*(\lambda+\beta-\lambda z_1)] \\ &\quad -W_v^*(\lambda+\beta-\lambda z)[1-L^*(\lambda+\beta)W_v^*(\lambda+\beta-\lambda z_1)]] \\ &\quad -\frac{\lambda}{\beta^2}(1-W_v^*(\lambda+\beta-\lambda z_1))\Big[1+\frac{\beta}{\alpha}\Big] \\ Q &= \frac{\lambda}{\alpha}(1-W_v^*(\lambda+\beta-\lambda z_1))G^*(\lambda) \\ \rho_s &= \frac{\lambda E(R_s)}{G^*(\lambda)}-\frac{m}{G^*(\lambda)} \end{aligned}$$

$E(R_s)$ is the mean service time and the system's stability condition $\rho_s < 1$ is obtained from (41).

3 The Model's Performance Measures

Mean Orbit Length in WV period:
We assume that W_v - mean orbit size and L_v - mean waiting time of the customer in the orbit during WV period.
Then

$$\begin{aligned} W_v &= \frac{d}{dz}W_v(z)\Big|_{z=1} \\ &= \frac{d}{dz}[W_1^*(z,0)+W_0^*(z,0)]\Big|_{z=1} \\ &= \frac{d}{dz}\left[\frac{S(z)}{(\lambda+\beta-\lambda z)Dr_1(z)}+\frac{K(z)}{Dr_1(z)}\right]W_{0,0}\Big|_{z=1} \end{aligned}$$

$$= \left[\begin{array}{c} \left[\begin{array}{c} Dr_1(z)(\lambda+\beta-\lambda z)S'(z) \\ -S(z)[(\lambda+\beta-\lambda z)Dr_1'(z) - Dr_1(z)\lambda] \end{array} \right] \\ \hline Dr_1(z))^2(\lambda+\beta-\lambda z) \\ + \left[\dfrac{K'(z)Dr_1(z) - Dr_1'(z)K(z)}{(Dr_1(z))^2} \right] \end{array} \right] W_{0,0}\Big|_{z=1}$$

where,

$$\begin{aligned} K(z) &= \lambda z(1-L^*(\lambda+\beta))(n+mz)[W_v^*(\lambda+\beta-\lambda z) - W_v^*(\lambda+\beta-\lambda z_1)] \\ Dr_1(z) &= z(\lambda+\beta) - (n+mz)W_v^*(\lambda+\beta-\lambda z)(L^*(\lambda+\beta) \\ &\quad (\lambda+\beta-\lambda z)+\lambda z) \\ S(z) &= \lambda(1-W_v^*(\lambda+\beta-\lambda z))\big[z(\lambda+\beta) - (n+mz)W_v^*(\lambda+\beta-\lambda z_1) \\ &\quad \times(L^*(\lambda+\beta)(\lambda+\beta-\lambda z)+\lambda z)\big] \end{aligned}$$

Differentiating $S(z), K(z)$ and $Dr_1(z)$ with respect to z, we get

$$\begin{aligned} S'(z) &= \lambda^2 W_v^{*'}(\lambda+\beta-\lambda z)[z(\lambda+\beta) - (n+mz)W_v^*(\lambda+\beta-\lambda z_1) \\ &\quad \times(\lambda+\beta-\lambda z)L^*(\lambda+\beta)+\lambda z] + (1-W_v^*(\lambda+\beta-\lambda z))\lambda \\ &\quad \times[\lambda+\beta-(n+mz)(\lambda-\lambda L^*(\lambda+\beta))W_v^*(\lambda+\beta-\lambda z_1)] \\ &\quad -m[(\lambda+\beta-\lambda z)L^*(\lambda+\beta)+\lambda z]W_v^*(\lambda+\beta-\lambda z_1) \\ K'(z) &= (1-L^*(\lambda+\beta))(n+mz)\lambda[W_v^*(\lambda+\beta-\lambda z) - W_v^*(\lambda+\beta-\lambda z_1)] \\ &\quad +(n+mz)\lambda z(1-L^*(\lambda+\beta))(-\lambda W_v^{*'}(\lambda+\beta-\lambda z)) \\ &\quad +m\lambda z(1-L^*(\lambda+\beta))[W_v^*(\lambda+\beta-\lambda z) - W_v^*(\lambda+\beta-\lambda z_1)] \\ Dr_1'(z) &= (\lambda+\beta)+(n+mz)\lambda W_v^{*'}(\lambda+\beta-\lambda z)(\lambda z+(n+mz)L^*(\lambda+\beta) \\ &\quad (\lambda+\beta-\lambda z)) - W_v^*(\lambda+\beta-\lambda z)(\lambda-\lambda L^*(\lambda+\beta)) \\ &\quad -m(\lambda z+(n+mz)L^*(\lambda+\beta)(\lambda+\beta-\lambda z))W_v^*(\lambda+\beta-\lambda z) \end{aligned}$$

At $z=1$ L_v turns

$$= \left[\begin{array}{c} \left[\dfrac{\beta Dr_1(1)S'(1) - S(1)[\beta Dr_1'(1) - \lambda Dr_1(1)]}{(\beta Dr_1(1))^2} \right] \\ + \left[\dfrac{Dr_1(1)K'(1) - K(1)Dr_1'(1)}{(Dr_1(1))^2} \right] \end{array} \right] W_{0,0}$$

we know that $L_v = \dfrac{W_v}{\lambda}$
where,

$$\begin{aligned} S(1) &= \lambda(1-W_v^*(\beta))[\beta+\lambda-W_v^*(\lambda+\beta-\lambda z_1)(\lambda+\beta L^*(\lambda+\beta))] \\ S'(1) &= \lambda^2 W_v^{*'}(\beta)[\lambda+\beta-W_v^*(\lambda+\beta-\lambda z_1)(\lambda+\beta L^*(\lambda+\beta))] \\ &\quad +\lambda(1-W_v^*(\beta))[\lambda+\beta-W_v^*(\lambda+\beta-\lambda z_1)(\lambda-\lambda L^*(\lambda+\beta))] \\ &\quad -m(\lambda+\beta L^*(\lambda+\beta))W_v^*(\lambda+\beta-\lambda z_1) \end{aligned}$$

$$\begin{aligned}
K(1) &= \lambda(1-L^*(\lambda+\beta))(W_v^*(\beta)-W_v^*(\beta-\lambda z_1+\lambda)) \\
K'(1) &= \lambda(1-L^*(\lambda+\beta))\big[W_v^*(\beta)-W_v^*(\beta+\lambda-\lambda z_1)-W_v^{*'}(\beta)\lambda \\
&\quad +m[W_v^*(\beta)-W_v^*(\beta+\lambda-\lambda z_1)]\big] \\
Dr_1(1) &= \beta-(\lambda+\beta L^*(\lambda+\beta))W_v^*(\beta)+\lambda \\
Dr_1'(1) &= \beta+[\lambda W_v^{*'}(\beta)+mW_v^*(\beta)][\lambda+L^*(\lambda+\beta)\beta] \\
&\quad +\lambda-[\lambda-\lambda L^*(\lambda+\beta)]W_v^*(\beta)
\end{aligned}$$

Mean Orbit Length in RS period:
We assume that L_s - mean orbit size and W_s - mean waiting time of the customer in the orbit during WV period.

$$\begin{aligned}
L_s &= \frac{d}{dz}R_S(z)\Big|_{z=1} \\
&= \frac{d}{dz}[R_1^*(z,0)+R_0^*(z,0)]\Big|_{z=1} \\
&= \frac{d}{dz}\left[\frac{Nr_1(z)(1-G^*(\lambda))+Nr_2(z)Nr_3(z)}{Dr_1(z)(\lambda+\beta-\lambda z)Dr_2(z)}\right]W_{0,0}\Big|_{z=1}
\end{aligned}$$

$$L_s = \frac{\left[\begin{array}{r}\big[Dr_2'(z)2Nr_1'(z)(\lambda Dr_1(z)-(\lambda+\beta-\lambda z)Dr_1'(z)) \\ +(\lambda+\beta-\lambda z)Dr_1(z)Nr_1''(z)(Dr_2'(z)-Dr_2''(z)Nr_1'(z))\big] \\ \times(1-G^*(\lambda))+2(\lambda+\beta-\lambda z)Nr_2'(z)Dr_2'(z)(Nr_3'(z)Dr_1(z) \\ -Nr_3(z)Dr_1'(z))+Nr_3(z)[2\lambda Nr_2'(z)Dr_2'(z)+(\lambda+\beta-\lambda z) \\ Dr_2'(z)Nr_2''(z)-(\lambda+\beta-\lambda z)Dr_2''(z)Nr_2'(z)]Dr_1(z)\end{array}\right]}{2(Dr_1(z)(\lambda+\beta-\lambda z)Dr_2'(z))^2}W_{0,0}\Big|_{z=1}$$

where,

$$\begin{aligned}
Nr_1(z) &= \beta z(n+mz)R_s^*(\lambda-\lambda z)(1-W_v^*(\lambda+\beta-\lambda z))\big\{(\lambda+\beta)z \\
&\quad -(n+mz)W_v^*(\lambda+\beta-\lambda z_1)[(\lambda+\beta-\lambda z)L^*(\lambda+\beta)+\lambda z]\big\} \\
&\quad +(\lambda+\beta-\lambda z)\beta z^2(n+mz)(1-L^*(\lambda+\beta))[W_v^*(\lambda+\beta-\lambda z) \\
&\quad -W_v^*(\lambda+\beta-\lambda z_1)]-(1-(n+mz)W_v^*(\lambda+\beta-\lambda z_1))\big\{(\lambda+\beta) \\
&\quad \times z-(n+mz)W_v^*(\lambda+\beta-\lambda z)[(\lambda+\beta-\lambda z)L^*(\lambda+\beta)+\lambda z]\big\} \\
&\quad \times z(\lambda+\beta-\lambda z)-\frac{z\lambda}{\alpha}(1-(n+mz)R_s^*(\lambda-\lambda z))(\lambda+\beta-\lambda z) \\
&\quad \times(1-(n+mz)W_v^*(\lambda+\beta-\lambda z_1))\big\{(\lambda+\beta)z-(n+mz) \\
&\quad \times W_v^*(\lambda+\beta-\lambda z)[(\lambda+\beta-\lambda z)L^*(\lambda+\beta)+\lambda z]\big\} \\
Nr_2(z) &= (1-R_s^*(\lambda-\lambda z)) \\
Dr_1(z) &= (\lambda+\beta)z-(n+mz)W_v^*(\lambda+\beta-\lambda z)[L^*(\lambda+\beta) \\
&\quad \times(\lambda+\beta-\lambda z)+\lambda z] \\
Dr_2(z) &= z-(n+mz)R_s^*(\lambda-\lambda z)[(1-z)G^*(\lambda)+z]
\end{aligned}$$

$$
\begin{aligned}
Nr_3(z) &= \beta z[(\lambda+\beta-\lambda z)G^*(\lambda)+\lambda z](1-L^*(\lambda+\beta))(W_v^*(\lambda+\beta-\lambda z)\\
&\quad -W_v^*(\lambda+\beta-\lambda z_1))-(1-W_v^*(\lambda+\beta-\lambda z_1))[(\lambda+\beta-\lambda z)\\
&\quad \times G^*(\lambda)+\lambda z]\{(\lambda+\beta)z-W_v^*(\lambda+\beta-\lambda z)(\lambda+\beta-\lambda z)L^*(\lambda+\beta)\\
&\quad +\lambda z)\}+\beta z(\lambda+\beta)(W_v^*(\lambda+\beta-\lambda z)-W_v^*(\lambda+\beta-\lambda z_1))\\
&\quad \times L^*(\lambda+\beta)-\frac{\lambda}{\alpha}(1-W_v^*(\lambda+\beta-\lambda z_1))G^*(\lambda)(\lambda+\beta-\lambda z)\\
&\quad \times\big\{(\lambda+\beta)z-W_v^*(\lambda+\beta-\lambda z)[\lambda z+(\lambda+\beta-\lambda z)L^*(\lambda+\beta)\big\}\\
&\quad +m\Big[\big[\lambda\beta z^2W_v^*(\lambda+\beta-\lambda z_1)+\beta^2zW_v^*(\lambda+\beta-\lambda z_1)L^*(\lambda+\beta)\\
&\quad \times W_v^*(\lambda+\beta-\lambda z)+\lambda\beta zW_v^*(\lambda+\beta-\lambda z_1)W_v^*(\lambda+\beta-\lambda z)\\
&\quad \times L^*(\lambda+\beta)(1-z)\big](n+mz)-[\beta^2z^2+\lambda\beta z^2]W_v^*(\lambda+\beta-\lambda z)\Big]
\end{aligned}
$$

At $z=1$ L_s turns

$$
L_s=\frac{\begin{bmatrix}(1-G^*(\lambda))\big[2Nr_1'(1)Dr_2'(1)(\lambda Dr_1(1)-\beta Dr_1'(1))+\beta Dr_1(1)\\ (Dr_2'(1)Nr_1''(1)-Nr_1'(1)Dr_2''(1))\big]+2\beta Nr_2'(1)Dr_2'(1)\\ (Dr_1(1)Nr_3'(1)-Nr_3(1)Dr_1'(1))+Nr_3(1)Dr_1(1)[2\lambda\\ Nr_2'(1)Dr_2'(1)+\beta Dr_2'(1)Nr_2''(1)-\beta Nr_2'(1)Dr_2''(1)]\end{bmatrix}}{2(\beta Dr_1(1)Dr_2'(1))^2}W_{0,0}
$$

as it is known that $W_s=\dfrac{L_s}{\lambda}$,
where,

$$
\begin{aligned}
Nr_1'(1) &= -\beta\lambda W_v^*(\beta)+\beta\lambda E(R_s)(1-W_v^*(\beta))[\lambda+\beta-\beta W_v^*(\lambda+\beta-\lambda z_1)\\
&\quad \times L^*(\lambda+\beta)-\lambda W_v^*(\lambda+\beta-\lambda z_1)]-\beta^2L^*(\lambda+\beta)W_v^*(\beta)+\beta^2\\
&\quad \times L^*(\lambda+\beta)W_v^*(\lambda+\beta-\lambda z_1)+\lambda[\beta+\lambda-\beta W_v^*(\beta)L^*(\lambda+\beta)\\
&\quad -\lambda W_v^*(\beta)]-\lambda^2W_v^*(\lambda+\beta-\lambda z_1)+\lambda^2W_v^*(\lambda+\beta-\lambda z_1)W_v^*(\beta)\\
&\quad +\lambda\beta W_v^*(\lambda+\beta-\lambda z_1)W_v^*(\beta)L^*(\lambda+\beta)+\frac{\lambda}{\alpha}[-m+\lambda E(R_s)]\\
&\quad \times\beta(1-W_v^*(\lambda+\beta-\lambda z_1))\{(\lambda+\beta)-W_v^*(\beta)[\lambda+\beta L^*(\lambda+\beta)]\}\\
&\quad +\beta m\{(\lambda+\beta)-W_v^*(\beta)[\lambda+\beta L^*(\lambda+\beta)]\}W_v^*(\lambda+\beta-\lambda z_1)\\
Nr_3(1) &= (1-W_v^*(\beta))\{\beta G^*(\lambda)W_v^*(\lambda+\beta-\lambda z_1)(\lambda+\beta L^*(\lambda+\beta))-\beta\lambda\\
&\quad -\beta\lambda G^*(\lambda)-\beta^2G^*(\lambda)\}+(1-W_v^*(\lambda+\beta-\lambda z_1))\{\beta\lambda W_v^*(\beta)\\
&\quad \times L^*(\lambda+\beta)-\lambda^2(1-W_v^*(\beta))\}+\beta^2L^*(\lambda+\beta)(W_v^*(\beta)\\
&\quad -W_v^*(\lambda+\beta-\lambda z_1))-\frac{\lambda}{\alpha}\beta G^*(\lambda)(1-W_v^*(\lambda+\beta-\lambda z_1))\\
&\quad \times\{\lambda+\beta-W_v^*(\beta)(L^*(\lambda+\beta)\beta+\lambda)\}+\big\{\lambda\beta W_v^*(\lambda+\beta-\lambda z_1)\\
&\quad -\beta W_v^*(\beta)[\lambda+\beta-\beta W_v^*(\lambda+\beta-\lambda z_1)L^*(\lambda+\beta)]\big\}m\\
Nr_2'(1) &= -\lambda E(R_s)
\end{aligned}
$$

$$
\begin{aligned}
Nr_1''(1) &= (W_v^*(\beta) - W_v^*(\lambda+\beta-\lambda z_1))[(1-L^*(\lambda+\beta))(\beta\lambda(1-G^*(\lambda)) \\
&\quad +\beta^2 G^*(\lambda)) + \beta^2 L^*(\lambda+\beta)] + G^*(\lambda)(\lambda+\beta+\lambda W_v^*(\beta)) \\
&\quad \times(\beta W_v^*(\lambda+\beta-\lambda z_1) - \lambda) - \beta\lambda L^*(\lambda+\beta)(1-W_v^*(\lambda+\beta-\lambda z_1)) \\
&\quad \times(W_v^*(\beta) + \beta W_v^{*'}(\beta)) + G^*(\lambda) W_v^*(\lambda+\beta-\lambda z_1)[\lambda+\beta-\beta W_v^*(\beta) \\
&\quad \times L^*(\lambda+\beta) + \lambda W_v^*(\beta)]\lambda - \beta G^*(\lambda)[\lambda+\beta-\lambda^2 W_v^{*'}(\beta) + \lambda W_v^*(\beta)] \\
&\quad +[\lambda W_v^{*'}(\beta)(\beta L^*(\lambda+\beta)-\lambda) + \lambda W_v^*(\beta) W^*(\lambda+\beta)][\beta G^*(\lambda) \\
&\quad \times W_v^*(\lambda+\beta-\lambda z_1) - \lambda(1-W_v^*(\lambda+\beta-\lambda z_1))] + \frac{\lambda}{\alpha} G^*(\lambda) \\
&\quad \times(1-W_v^*(\lambda+\beta-\lambda z_1))\big\{\lambda(\lambda+\beta) - \lambda^2 W_v^*(\beta) - 2\lambda\beta W_v^*(\beta) \\
&\quad \times L^*(\lambda+\beta) - \lambda^2\beta W_v^{*'}(\beta) - \lambda\beta^2 W_v^{*'}(\beta) L^*(\lambda+\beta) + \lambda\beta W_v^*(\beta) \\
&\quad -\beta(\lambda+\beta)\big\} + m\Big[\beta W_v^*(\lambda+\beta-\lambda z_1)\Big[[L^*(\lambda+\beta)\beta+\lambda] \\
&\quad \times[3(W_v^*(\beta) - W_v^{*'}(\beta) - \lambda E(R_s)) + m(1-W_v^*(\beta)) - 4] \\
&\quad -3(1-W_v^*(\beta))[\lambda - \lambda L^*(\lambda+\beta)]\Big] + \beta(\lambda+\beta)\Big[2(1-W_v^*(\beta) \\
&\quad +\lambda W_v^{*'}(\beta)) + \lambda E(R_s)[2+W_v^*(\beta)]\Big] + \beta[1-L^*(\lambda+\beta)][2(2\beta-\lambda) \\
&\quad \times[W_v^*(\beta) - W_v^*(\lambda+\beta-\lambda z_1)] - \lambda\beta W_v^{*'}(\beta)] - \lambda\beta^2[1-L^*(\lambda+\beta)] \\
&\quad \times W_v^*(\beta) + (\lambda+\beta) W_v^*(\lambda+\beta-\lambda z_1)(3\beta-2\lambda) + [L^*(\lambda+\beta)\beta+\lambda] \\
&\quad \times\Big[\beta\lambda W_v^{*'}(\beta)[3W_v^*(\lambda+\beta-\lambda z_1) - 2] + W_v^*(\beta)[W_v^*(\lambda+\beta-\lambda z_1) \\
&\quad \times(2\lambda - m\beta - \beta) + \beta]\Big]\frac{\lambda}{\alpha}\Big[\{(\lambda+\beta)(1-W_v^*(\lambda+\beta-\lambda z_1))[\beta+2\beta \\
&\quad -\lambda + \lambda\beta E(R_s)] - 2\beta m W_v^*(\lambda+\beta-\lambda z_1)\} + \Big\{[\lambda\beta(W_v^{*'}(\beta) \\
&\quad -E(R_s)) - m\beta W_v^*(\beta) - 2\beta + \lambda](1-W_v^*(\lambda+\beta-\lambda z_1)) + 2\beta m \\
&\quad \times W_v^*(\lambda+\beta-\lambda z_1)\Big\}[L^*(\lambda+\beta)\beta+\lambda] - \beta(1-W_v^*(\lambda+\beta-\lambda z_1)) \\
&\quad \times[\lambda - \lambda L^*(\lambda+\beta)] W_v^*(\beta)\Big]\Big] \\
Dr_1(1) &= \beta + \lambda - (\lambda + \beta L^*(\lambda+\beta)) W_v^*(\beta) \\
Dr_1'(1) &= \beta + [\lambda W_v^{*'}(\beta) + m W_v^*(\beta)][\lambda + L^*(\lambda+\beta)\beta] \\
&\quad +\lambda - [\lambda - \lambda L^*(\lambda+\beta)] W_v^*(\beta) \\
Dr_2'(1) &= G^*(\lambda) - E(R_s)\lambda - m \\
Dr_2''(1) &= -2(1-G^*(\lambda))[\lambda E(R_s) + m] - E(R_s^2)\lambda^2 - 2\lambda m E(R_s) \\
Nr_2''(1) &= -\lambda^2 E(R_s^2)
\end{aligned}
$$

$$
\begin{aligned}
Nr_3'(1) &= \{(1-W_v^*(\beta))(2\beta\lambda E(R_s)+\beta\lambda^2 E(R_s^2))+2\beta\lambda^2 E(R_s)W_v^{*'}(\beta)\}\\
&\times[\lambda+\beta-W_v^*(\lambda+\beta-\lambda z_1)(\lambda+\beta L^*(\lambda+\beta))]+2\beta\lambda E(R_s)\\
&\times(1-W_v^*(\beta))[\lambda+\beta+\lambda W_v^*(\lambda+\beta-\lambda z_1)(L^*(\lambda+\beta)-1)]\\
&+2\beta\lambda[W_v^{*'}(\beta)(\lambda+\beta L^*(\lambda+\beta))+(1-W_v^*(\beta))(2-L^*(\lambda+\beta)\\
&\times W_v^*(\lambda+\beta-\lambda z_1))]+2\beta^2 L^*(\lambda+\beta)(W_v^*(\lambda+\beta-\lambda z_1)\\
&-W_v^*(\beta))+2\lambda^2(1-W_v^*(\beta))(1-W_v^*(\lambda+\beta-\lambda z_1))+2\lambda[\lambda\\
&+\lambda W_v^{*'}(\beta)(\lambda+\beta L^*(\lambda+\beta))+\lambda W_v^*(\beta)(L^*(\lambda+\beta)-1)]\\
&\times(1-W_v^*(\lambda+\beta-\lambda z_1))+\frac{\lambda^2}{\alpha}(1-W_v^*(\lambda+\beta-\lambda z_1))\{[\lambda+\beta\\
&-W_v^*(\beta)[\lambda+\beta L^*(\lambda+\beta)]][4\beta+\lambda\beta-1]E(R_s)+2\beta\lambda W_v^{*'}(\beta)\\
&\times[\lambda+\beta L^*(\lambda+\beta)]E(R_s)+\lambda\beta E(R_s^2)[\lambda+\beta-W_v^*(\beta)\\
&(\lambda+\beta L^*(\lambda+\beta))]\}
\end{aligned}
$$

4 Special cases

(a) If the service time distribution follows an exponential distribution, no retrial, no service among the vacation period and there is no feedback then, the present model will be remodeled as analysis of M/M/1 queue with server vacations and a waiting server.
(b) If the server does not wait after the completion of the RS period and there is no feedback then, the present model will be remodeled as an M/G/1 retrial queue with multiple working vacation.

5 Numerical results

The curved graph constructed in Figure 1 and the values tabulated in the Table 1 are obtained by setting the fixed values $\mu_v = 3.6$, $\mu_s = 9.8$, $\mu_{vr} = 3.5$, $\mu_{sr} = 5.3$, $\alpha = 1$, $m = 0.4$ and altering the values of λ from 1 to 2 incremented with 0.2 and increasing the values of β from 0.3 to 1.1 in steps of 0.4, we observed that as λ rises L_v falls and hence the stability of the model is verified.

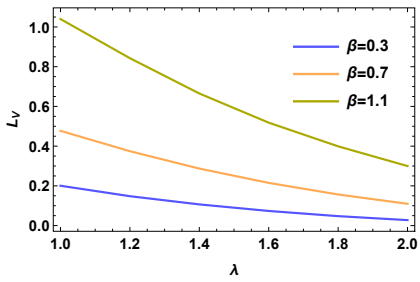

Figure 1: λ versus L_v

λ	$\beta = 0.3$	$\beta = 0.7$	$\beta = 1.1$
1.0	0.2006	0.4771	1.0399
1.2	0.1479	0.3744	0.8428
1.4	0.1066	0.2870	0.6651
1.6	0.0737	0.2149	0.5181
1.8	0.0475	0.1566	0.3990
2.0	0.0275	0.1097	0.2997

Table 1: λ versus L_v

The curved graph constructed in Figure 2 and the values tabulated in the Table 2 are obtained by setting the fixed values $\mu_v = 6.6$, $\mu_s = 10.8$, $\mu_{vr} = 3.5$, $\mu_{sr} = 5.3$, $\alpha = 1.7$, $m = 0.3$ and altering the values of λ from 1 to 2 incremented with 0.2 and increasing the values of β from 0.2 to 0.6 in steps of 0.2. We observed that as λ rises W_v falls which is expected.

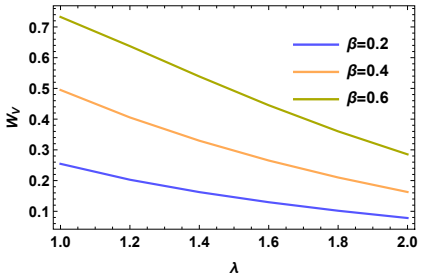

Figure 2: λ versus W_v

λ	$\beta = 0.2$	$\beta = 0.4$	$\beta = 0.6$
1.0	0.2545	0.4949	0.7325
1.2	0.2027	0.4054	0.6375
1.4	0.1624	0.3297	0.5388
1.6	0.1295	0.2652	0.4451
1.8	0.1018	0.2100	0.3602
2.0	0.0781	0.1628	0.2853

Table 2: λ versus W_v

The curved graph constructed in Figure 3 and the values tabulated in the Table 3 are obtained by setting the fixed values $\mu_v = 0.1$, $\mu_s = 10$, $\mu_{vr} = 1.5$, $\mu_{sr} = 4.5$, $\alpha = 0.6$, $m = 0.3$ and altering the values of λ from 1 to 2 incremented with 0.2 and increasing the values of β from 1.3 to 1.7 in steps of 0.2. We observed that as λ rises L_s also rises which shows the stability of the model.

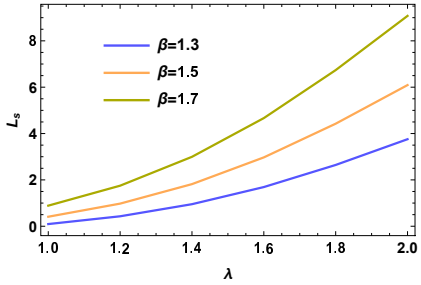

Figure 3: λ versus L_s

λ	$\beta = 1.3$	$\beta = 1.5$	$\beta = 1.7$
1.0	0.0939	0.4101	0.8883
1.2	0.4295	0.9762	1.7499
1.4	0.9517	1.8173	2.9956
1.6	1.6909	2.9705	4.6665
1.8	2.6447	4.4248	6.7373
2.0	3.7557	6.0909	9.0768

Table 3: λ versus L_s

The curved graph constructed in Figure 4 and the values tabulated in the Table 4 are obtained by setting the fixed values $\mu_v = 9.3$, $\mu_s = 11$, $\mu_{vr} = 4.5$, $\mu_{sr} = 5.5$, $\alpha = 1.5$, $m = 0.5$ and altering the values of λ from 1 to 2 incremented with 0.2 and increasing the values of β from 0.3 to 0.5 in steps of 0.1. From the graph, we studied that as λ rises W_s falls which shows the stability of the model.

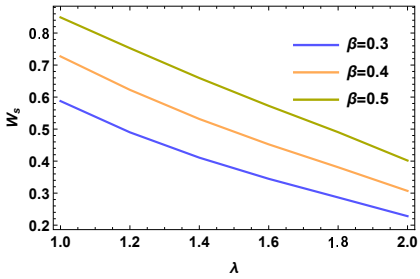

Figure 4: λ versus W_s

λ	$\beta = 0.3$	$\beta = 0.4$	$\beta = 0.5$
1.0	0.5875	0.7271	0.8489
1.2	0.4899	0.6225	0.7527
1.4	0.4107	0.5315	0.6595
1.6	0.3447	0.4523	0.5726
1.8	0.2865	0.3808	0.4904
2.0	0.2280	0.3069	0.4018

Table 4: λ versus W_s

6 Conclusion

In this paper, an $M/G/1$ feedback retrial queue with working vacation and a waiting server is evaluated. We obtained the PGF for the number of customers and the mean number of customers in the orbit. We worked out the mean waiting time. We also derived the performance measures. We performed some particular cases. We illustrated some numerical results.

References

[1] Yang T. and Templeton J.G.C., *A Survey on Retrial Queue*, Queue. Syst., 2 (1987), 201-233.

[2] Falin G.I., *A Survey on Retrial Queues*, Queueing Systems Theory and Applications, 7 (1990), 127-168.

[3] Falin G.I. and Templeton J.G.C., *Retrial queues*, Chapman and Hall, London, (1997).

[4] Servi L. and Finn S., "M/M/1 queue with working vacations (M/M/1/WV)", *Perform. Eval*, 50 (2002), 41-52 .

[5] Wu D. and Takagi H., "M/G/1 queue with multiple working vacations", *Perform. Eval*, 63 (2006), 654-681.

[6] Kalyanaraman R. and Pazhani Bala Murugan S., "A single server retrial queue with vacation", *J.Appl.Math.and Informatics*, 26(3-4) (2008), 721-732.

[7] Pazhani Bala Murugan S. and Santhi K., "An M//G/1 retrial queue with multiple working vacation", *International Journal of Mathematics and its Applications*, 4(2-D) (2016), 35-48.

[8] Chandrasekaran V.M., Indhira K., Saravanarajan M.C. and Rajadurai P., "A survey on working vacation queueing models", *International Journal of Pure and Applied Mathematics*, 106(6) (2016), 33-41.

[9] Gupta P. and Kumar N., Performance Analysis of Retrial Queueing Model with Working Vacation, Interruption, Waiting Server, Breakdown and Repair, *J. Sci. Res.,* 13(3) (2021), 833-844.

[10] Boxma O.J., Schlegel S. and Yechiali U., "M/G/1 queue with waiting server timer and vacations", *American Mathematical Society Translations*, 2(207) (2002), 25-35.

[11] Kalidass K. and Kasturi Ramanath, "Time dependent analysis of M/M/1 queue with server vacations and a waiting server", *QTNA*, August, (2011), 23-26.

[12] Krishna Kumar B., Pavai madheswari and Vijayakumar A., "The M/G/1 retrial queue with feedback and starting failures", *Applied Mathematical modelling*, 26 (2002), 1057-1075.

[13] Jau-chuan ke, Fu-min chang, "Modified vacation Policy for M/G/1 retrial queue with balking and feedback", *Computers and Industrial Engineering*, 57 (2009), 433-443.

[14] Rajadurai P., Saravanarajan M. C. and Chandrasekaran V.M., "A study on M/G/1 feedback retrial queue with subject to server breakdown and repain under multiple working vacation policy", Alexandria University, *Alexandria Engineering Journal*, 57 (2018), 947-962.

[15] Gnanasekar M.M.N. and Indhira K., Analysis of an M/G/1 Retrial Queue with Delayed Repair and Feedback under Working Vacation policy with Impatient Customers, *Mathematical Models: Methods and Applications*, 14(10) 2022, 1-18.

[16] Artalejo J.R.,*Accessible bibliography on retrial queue*, Math. Comput. Modell., 30 (1999), 1-6.

[17] Artalejo J.R. and Falin G., *Standard and retrial queueing systems: A Comparitive Analysis*, Rev. Math. Comput., 15 (2002), 101-129.

[18] Gomez-Corral A., "Stochastic analysis of a single server retrial queue with general retrial time", *Naval Res. Log.*, 46 (1999), 561-581.

[19] Medhi J., *Stochastic Models in Queueing Theory*, Second Edition (2003).

An Application of Incomplete I-Functions with Two Variables to Solve the Nonlinear Differential Equations Using S-Function

Rahul Sharma[1], Jagdev Singh[2], Devendra Kumar[3], Yudhveer Singh[4*]

December 28, 2022

Department of Mathematics, Amity School of Applied Sciences, Amity University Rajasthan, Jaipur-303002, Rajasthan, India[1]
Department of Mathematics, JECRC University, Jaipur-303905, Rajasthan, India[2]
Department of Mathematics, University of Rajasthan, Jaipur-302004, Rajasthan, India[3]
Amity Institute of Information Technology, Amity University Rajasthan, Jaipur-303002, Rajasthan, India[4]

Abstract

In this article, we evaluate the approximate solutions of Nonlinear Differential Equations (NoLDEs) with the association of S-function, incomplete H-functions (IHFs) and incomplete I-functions (IIFs) with two variables by using the Hermite, Legendre and Jacobi polynomials. Here, we introduce incomplete I-functions with two variables. The NoLDEs are significantly applicable in fluid dynamics, vibration problems, population dynamics, electromagnetism, chemical kinetics, combustion theory, economics and finance. Recently, it was implemented to solve the resistance less circuit with a nonlinear capacitor under influence of external periodic force.

This method is established as an application of improper integrals, polynomials and special functions. The obtained results are helpful to get the solution of various problems of mathematical physics and engineering in approximate aspects.

Keywords: Incomplete H-functions, Incomplete I-functions, q-Gamma functions, S-function, Laplace transform, Improper Integral.
MSC2020: 33B20, 33D05, 33E12, 44A10.

1 Introduction and Preliminaries:

Earlier, Nonlinear differential equations play remarkable roles in the field of Engineering and Physics. Numerous authors have given their outputs to solving

these equations by several methods. In the nineteen century, many Mathematicians like Gadre [9], Saxena et al. [16], Srivastava [24] and Srivastava et al. [25] worked on NoLDEs system. In last two decades many more authors such as Chaurasia et al. [5], Sharma [17], Singh [20], Singh et al. [21, 22, 23], Bansal et al. [1, 2, 3, 4] and Kumar et al. [11, 12] have also paid their attention in this branch of Applied Mathematics.

In the section 1, we defined the incomplete H-functions, incomplete I-functions with two variables and S-function. Section 2, shows some important theorems that will be used to solve the NoLDEs given in the section 3.

Special functions are well known tool which are uses in various fields of Engineering and Physics. The incomplete Gamma functions (IGFs) $\gamma(s,y)$ and $\Gamma(s,y)$ are investigated by Prym [14]. The incomplete Gamma functions are base of the recently developed incomplete forms of special functions like incomplete H-functions, incomplete $\overline{H}$-functions, incomplete I-functions and incomplete $\aleph$-functions.

The incomplete Gamma functions $\gamma(s,y)$ and $\Gamma(s,y)$ are defined, by

$$\gamma(s,y)=\int_0^y t^{s-1}e^{-t}dt, \quad (\mathbb{R}(s)>0;\ y\geq 0). \tag{1}$$

$$\Gamma(s,y)=\int_y^\infty t^{s-1}e^{-t}dt, \quad (y\geq 0;\ \mathbb{R}(s)>0\ when\ y=0). \tag{2}$$

The IGFs holds the decomposition formula $\gamma(s,y)+\Gamma(s,y)=\Gamma(s)$, here $\Gamma(.)$ is well known gamma function.

Pochhammer symbol $(\mu)_\lambda$ defined as:

$$(\mu)_\lambda=\frac{\Gamma(\mu+\lambda)}{\Gamma(\mu)}=\begin{cases}1, & \text{if} \quad \lambda=0;\mu\in\mathbb{C}\backslash\{0\}\\ (\mu)(\mu+1)\dots(\mu+n-1), & \text{if} \quad \lambda=n\in\mathbb{N};\mu\in\mathbb{C},\end{cases} \tag{3}$$

provided $\Gamma(\mu)$ exists. Here $\mathbb{C}$ and $\mathbb{N}$ are as usual denote the set of complex and natural numbers respectively.

Definition 1: In terms of the incomplete gamma functions (IGFs) $\Gamma(s,x)$ and $\gamma(s,x)$, the IHFs [26] is defined $\gamma_{P,Q}^{M,N}(z)$ and $\Gamma_{P,Q}^{M,N}(z)$ as follows:

$$\begin{aligned}\gamma_{P,Q}^{M,N}(z)&=\gamma_{P.Q}^{M,N}\left[z\left|\begin{matrix}(f_1,F_1,t),(f_j,F_j)_{2,P}\\(w_j,W_j)_{1,Q}\end{matrix}\right.\right]\\&:=\frac{1}{2\pi i}\int_L\varphi(s,t)z^s ds,\end{aligned} \tag{4}$$

where

$$\varphi(s,t)=\frac{\gamma(1-f_1+F_1s,t)\prod_{j=1}^M\Gamma(w_j-W_js)\prod_{j=2}^N\Gamma(1-f_j+F_js)}{\prod_{j=M+1}^Q\Gamma(1-w_j+W_js)\prod_{j=N+1}^P\Gamma(f_j-F_js)}, \tag{5}$$

and

$$\Gamma_{P,Q}^{M,N}(z) = \Gamma_{P,Q}^{M,N}\left[z \,\middle|\, \begin{matrix}(f_1,F_1,t),(f_j,F_j)_{2,P}\\(w_j,W_j)_{1,Q}\end{matrix}\right] := \frac{1}{2\pi i}\int_L \phi(s,t)z^s ds, \tag{6}$$

where

$$\phi(s,t) = \frac{\Gamma(1-f_1+F_1 s,t)\prod_{j=1}^{M}\Gamma(w_j-W_j s)\prod_{j=2}^{N}\Gamma(1-f_j+F_j s)}{\prod_{j=M+1}^{Q}\Gamma(1-w_j+W_j s)\prod_{j=N+1}^{P}\Gamma(f_j-F_j s)}, \tag{7}$$

The IHFs $\gamma_{P,Q}^{M,N}(z)$ and $\Gamma_{P,Q}^{M,N}(z)$ are exist for all $t \geq 0$ and for more existing conditions (see, [26]).

Definition 2: We introduce the incomplete I-functions with two variables ${}^{(\Gamma)}I_{p_l,q_l,r;p_{l^{(1)}},q_{l^{(1)}},r_{(1)};p_{l^{(2)}},q_{l^{(2)}},r_{(2)}}^{0,n:m_1,n_1;m_2,n_2}$ as follows:

$${}^{(\Gamma)}I_{p_l,q_l,r;p_{l^{(1)}},q_{l^{(1)}},r_{(1)};p_{l^{(2)}},q_{l^{(2)}},r_{(2)}}^{0,n:m_1,n_1;m_2,n_2}\left[\begin{matrix}z_1\\z_2\end{matrix}\,\middle|\,\begin{matrix}\left(e_1,E_1^{(1)},E_1^{(2)},x\right),\left(e_j,E_j^{(1)},E_j^{(2)}\right)_{2,n}\\ \ldots,\left(f_{jl},F_{jl}^{(1)},F_{jl}^{(2)}\right)_{m+1,q_l},\end{matrix}\right.$$

$$\begin{matrix},\left(e_{jl},E_{jl}^{(1)},E_{jl}^{(2)}\right)_{n+1,p_l},(e_j^{(1)},E_j^{(1)})_{1,n_1},\left(e_{jl^{(1)}}^{(1)},E_{jl^{(1)}}^{(1)}\right)_{n_1+1,p_l^{(1)}},\\ \left(f_j^{(1)},F_j^{(1)}\right)_{1,m_1},\left(f_{jl^{(1)}}^{(1)},F_{jl^{(1)}}^{(1)}\right)_{m_1+1,q_l^{(1)}},\end{matrix}$$

$$\left.\begin{matrix}(e_j^{(2)},E_j^{(2)})_{1,n_2},\left(e_{jl^{(2)}}^{(2)},E_{jl^{(2)}}^{(2)}\right)_{n_2+1,p_l^{(2)}}\\ \left(f_j^{(2)},F_j^{(2)}\right)_{1,m_2},\left(f_{jl^{(2)}}^{(2)},F_{jl^{(2)}}^{(2)}\right)_{m_2+1,q_l^{(2)}}\end{matrix}\right]$$

$$= \frac{1}{(2\pi\omega)^2}\int_{L_1}\int_{L_2}\theta\left(\xi_1,\xi_2,x\right)z_1^{\xi_1}z_2^{\xi_2}\theta_1(\xi_1)\theta_2(\xi_2)d\xi_1 d\xi_2 \quad (\omega=\sqrt{-1}), \tag{8}$$

where

$$\theta\left(\xi_1,\xi_2,x\right) = \frac{\Gamma(1-e_1+\sum_{i=1}^{2}E_j^{(i)}\xi_i,x)\prod_{j=2}^{n}\Gamma(1-e_j+\sum_{i=1}^{2}E_j^{(i)}\xi_i)}{\sum_{i=1}^{r}\left[\prod_{j=n+1}^{p_l}\Gamma\left(e_{jl}-\sum_{i=1}^{2}E_{jl}^{(i)}\xi_i\right)\prod_{j=1}^{q_l}\Gamma\left(1-f_{jl}+\sum_{i=1}^{2}F_{jl}^{(i)}\xi_i\right)\right]},$$

and,

$$\theta_i(\xi_i) = \frac{\prod_{j=1}^{m_i}\Gamma(f_j^{(i)}-F_j^{(i)}\xi_i)\prod_{j=1}^{n_i}\Gamma(1-e_j^{(i)}+E_j^{(i)}\xi_i)}{\sum_{i^{(i)}=1}^{r^{(i)}}\left[\prod_{j=m_i+1}^{q_{l^{(i)}}}\Gamma\left(1-f_{jl^{(i)}}^{(i)}+F_{jl^{(i)}}^{(i)}\xi_i\right)\prod_{j=n_i+1}^{p_{i^{(i)}}}\Gamma\left(e_{jl^{(i)}}^{(i)}-E_{jl^{(i)}}^{(i)}\xi_i\right)\right]}, \ (i=1,2).$$

Now, We can define lower form of the incomplete I-function with two variables

${}^{(\gamma)}I^{0,n:m_1,n_1;m_2,n_2}_{p_l,q_l,r;p_{l^{(1)}},q_{l^{(1)}},r_{(1)};p_{l^{(2)}},q_{l^{(2)}},r_{(2)}}$ as follows:

$$
{}^{(\gamma)}I^{0,n:m_1,n_1;m_2,n_2}_{p_l,q_l,r;p_{l^{(1)}},q_{l^{(1)}},r_{(1)};p_{l^{(2)}},q_{l^{(2)}},r_{(2)}}\left[\begin{array}{c|l} z_1 & \left(e_1,E_1^{(1)},E_1^{(2)},x\right),\left(e_j,E_j^{(1)},E_j^{(2)}\right)_{2,n} \\ z_2 & \ldots,\left(f_{jl},F_{jl}^{(1)},F_{jl}^{(2)}\right)_{m+1,q_l}, \end{array}\right.
$$

$$
\left(e_{jl},E_{jl}^{(1)},E_{jl}^{(2)}\right)_{n+1,p_l},(e_j^{(1)},E_j^{(1)})_{1,n_1},\left(e_{jl^{(1)}}^{(1)},E_{jl^{(1)}}^{(1)}\right)_{n_1+1,p_l^{(1)}},
$$
$$
\left(f_j^{(1)},F_j^{(1)}\right)_{1,m_1},\left(f_{jl^{(1)}}^{(1)},F_{jl^{(1)}}^{(1)}\right)_{m_1+1,q_l^{(1)}},
$$

$$
\left.\begin{array}{l}(e_j^{(2)},E_j^{(2)})_{1,n_2},\left(e_{jl^{(2)}}^{(2)},E_{jl^{(2)}}^{(2)}\right)_{n_2+1,p_l^{(2)}} \\ \left(f_j^{(2)},F_j^{(2)}\right)_{1,m_2},\left(f_{jl^{(2)}}^{(2)},F_{jl^{(2)}}^{(2)}\right)_{m_2+1,q_l^{(2)}}\end{array}\right]
$$

$$
=\frac{1}{(2\pi\omega)^2}\int_{L_1}\int_{L_2}\theta\left(\xi_1,\xi_2,x\right)z_1^{\xi_1}z_2^{\xi_2}\theta_1(\xi_1)\theta_2(\xi_2)d\xi_1d\xi_2\quad(\omega=\sqrt{-1}),
$$

where
$\theta\left(\xi_1,\xi_2,x\right)=\frac{\gamma(1-e_1+\sum_{i=1}^2E_j^{(i)}\xi_i,x)\prod_{j=2}^n\Gamma(1-e_j+\sum_{i=1}^2E_j^{(i)}\xi_i)}{\sum_{i=1}^r\left[\prod_{j=n+1}^{p_l}\Gamma\left(e_{jl}-\sum_{i=1}^2E_{jl}^{(i)}\xi_i\right)\prod_{j=1}^{q_l}\Gamma\left(1-f_{jl}+\sum_{i=1}^2F_{jl}^{(i)}\xi_i\right)\right]}$,

and,
$\theta_i(\xi_i)=\frac{\prod_{j=1}^{m_i}\Gamma(f_j^{(i)}-F_j^{(i)}\xi_i)\prod_{j=1}^{n_i}\Gamma(1-e_j^{(i)}+E_j^{(i)}\xi_i)}{\sum_{i^{(i)}=1}^{r^{(i)}}\left[\prod_{j=m_i+1}^{q_{l^{(i)}}}\Gamma\left(1-f_{jl^{(i)}}^{(i)}+F_{jl^{(i)}}^{(i)}\xi_i\right)\prod_{j=n_i+1}^{p_{i^{(i)}}}\Gamma\left(e_{jl^{(i)}}^{(i)}-E_{jl^{(i)}}^{(i)}\xi_i\right)\right]},\ (i=1,2).$

Decomposition formula satisfying in case of incomplete I-functions with two variables defined in (1) and (2) as ${}^{(\gamma)}I_Q^P[z_i]+{}^{(\Gamma)}I_Q^P[z_i]=I_Q^P[z_i]$.

Here, $z_i\neq 0;\ f_j\ (j=1,\ldots,p);\ e_j\ (j=1,\ldots,q);\ e_j^{(i)}\ (j=1,\ldots,n_i);\ e_{jl^{(i)}}^{(i)}\ (j=n_i+1,\ldots,p_{l^{(i)}});\ f_j^{(i)}\ (j=1,\ldots,m_i);\ f_{jl^{(i)}}^{(i)}\ (j=m_i+1,\ldots,q_{l^{(i)}});\ i=1,\ 2$ are complex numbers and $E_j,\ F_j,\ E_{jl^{(i)}}^{(i)},\ F_{jl^{(i)}}^{(i)}$ are positive real numbers for standardization purpose such that

$$
A_l^{(i)}=\sum_{j=1}^nE_j^{(i)}+\sum_{j=n+1}^{p_i}E_{jl}^{(i)}+\sum_{j=1}^{n_i}E_j^{(2)}+\sum_{j=n_i+1}^{p_{i(i)}}E_{jl^{(i)}}^{(i)}
$$
$$
-\sum_{j=1}^{q_i}F_{jl^{(i)}}^{(i)}-\sum_{j=1}^{m_i}F_j^{(i)}-\sum_{j=m_i+1}^{q_{i(i)}}F_{jl^{(i)}}^{(i)}\leq 0\quad(i=1,2),
$$

The integral path is a contour starting from $L-l\infty$ to $L+l\infty$ and the poles of $\Gamma(f_j^{(i)}-F_j^{(i)}\xi_i),\ j=1,\ldots,m_i,\ i=1,2$ are separated from those of $\Gamma(1-a_j+\sum_{i=1}^2E_j^{(i)}\xi_i),\ j=1,\ldots,n$ and $\Gamma(1-e_j^{(i)}+E_j^{(i)}\xi_i),\ j=1,\ldots,n_i,\ i=1,2$

to the left of the contour L_k. The existence conditions for multiple Mellin-Barnes contours can be obtained with the help of two variables I-function [18] as $|argz_i| < \frac{\pi}{2}\bar{A}_i^{(i)}$, where

$$\bar{A}_l^{(k)} = \sum_{j=1}^{n} E_j^{(i)} - \sum_{j=n+1}^{p_l} E_{jl}^{(i)} - \sum_{j=1}^{q_l} F_{jl}^{(i)} + \sum_{j=1}^{n_i} E_j^{(i)} - \sum_{j=n_i+1}^{p_{l^{(i)}}} E_{jl^{(i)}}^{(i)} + \sum_{j=1}^{m_i} F_j^{(i)} - \sum_{j=m_i+1}^{q_{l^{(i)}}} F_{jl^{(i)}}^{(i)} > 0 \quad (i = 1, 2).$$

for more detail conditions (see [13, 18, 10, 19]).

Definition 3: The S-function introduced and investigated by Saxena et al. [7] and defined as:

$$\underset{(p,q)}{\overset{(a,b,c,d,e)}{\mathrm{S}}}(y) = \underset{(p,q)}{\overset{(a,b,c,d,e)}{\mathrm{S}}}(\alpha_1, \alpha_2, \ldots, \alpha_p; \beta_1, \beta_2, \ldots, \beta_q; y) = \sum_{n=0}^{\infty} \frac{(\alpha_1)_n \ldots (\alpha_p)_n}{(\beta_1)_n \ldots (\beta_q)_n} \frac{(c)_{nd,e}}{\Gamma_e(na+b)} \frac{y^n}{n!}, \tag{9}$$

where $e \in \mathbb{R}$; $a, b, c, d \in \mathbb{C}$; $Re(a) > 0, \alpha_i$ $(i = 1, 2, \ldots, p)$, β_j $(j = 1, 2, \ldots, q)$, $Re(a) > eRe(d)$ and $p < q + 1$. Pochhammer symbol $(\mu)_\lambda$ defined in (3).
Here, the k-Pochhammer symbol $(y)_{n,k}$ and k-Gamma function $\Gamma_q(y)$ defined by Diaz et al. [6].
If we put $c = d = e = 1$ in S-function, it reduces to the generalized M-series. Similarly, we can convert S-function to other functions named Generalized k-Mittag-Leffler function, k-function, generalized Mittag-Leffler function and Mittag-Leffler function.

2 Theorems

In this section, we use the linear approximation of the Hermite, Legendre and Jacobi polynomials to obtain the approximate solution of general NoLDEs which given below:

$$\ddot{\mathrm{x}} + \omega \underset{(p,q)}{\overset{(a,b,c,d,e)}{\mathrm{S}}} \left[y \left(\frac{x}{L} \right)^{2\Lambda'} \right] \Gamma_{P,Q}^{M,N} \left[z \left(\frac{x}{L} \right)^{2\Lambda} \middle| \begin{matrix} (f_1, F_1, t), (f_j, F_j)_{2,P} \\ (w_j, W_j)_{1,Q} \end{matrix} \right] = NF(t), \tag{10}$$

$$\ddot{\mathrm{x}} + \omega \underset{(p,q)}{\overset{(a,b,c,d,e)}{\mathrm{S}}} \left[y \left(1 + \frac{x}{L} \right)^{\nu'} \right] \Gamma_{P,Q}^{M,N} \left[z \left(1 + \frac{x}{L} \right)^{\nu} \middle| \begin{matrix} (f_1, F_1, t), (f_j, F_j)_{2,P} \\ (w_j, W_j)_{1,Q} \end{matrix} \right] = NF(t), \tag{11}$$

$$\ddot{\mathrm{x}}+\omega \overset{(a,b,c,d,e)}{\underset{(p,q)}{\mathrm{S}}}\left[y\left(\frac{x}{L}\right)^{\Lambda}\right]{}^{(\Gamma)}I^{0,n:m_1,n_1;m_2,n_2}_{p_l,q_l,r;p_{l^{(1)}},q_{l^{(1)}},r^{(1)};p_{l^{(2)}},q_{l^{(2)}},r^{(2)}}\left[\begin{array}{c|c} z_1\left(\frac{x}{L}\right)^{\nu} & A^* \\ z_2\left(\frac{x}{L}\right)^{\lambda} & B^* \end{array}\right] = NF(t), \quad (12)$$

where

$A^*=\left(e_1,E_1^{(1)},E_1^{(2)},s\right),\left(e_j,E_j^{(1)},E_j^{(2)}\right)_{2,n},\left(e_{jl},E_{jl}^{(1)},E_{jl}^{(2)}\right)_{n+1,p_l},$
$(e_j^{(1)},E_j^{(1)})_{1,n_1},\left(e_{jl^{(1)}}^{(1)},E_{jl^{(1)}}^{(1)}\right)_{n_1+1,p_l^{(1)}},(e_j^{(2)},E_j^{(2)})_{1,n_2},\left(e_{jl^{(2)}}^{(2)},E_{jl^{(2)}}^{(2)}\right)_{n_2+1,p_l^{(2)}}$
and
$B^*=\ldots,\left(f_{jl},F_{jl}^{(1)},F_{jl}^{(2)}\right)_{m+1,q_l},\left(f_j^{(1)},F_j^{(1)}\right)_{1,m_1},\left(f_{jl^{(1)}}^{(1)},F_{jl^{(1)}}^{(1)}\right)_{m_1+1,q_l^{(1)}},$
$\left(f_j^{(2)},F_j^{(2)}\right)_{1,m_2},\left(f_{jl^{(2)}}^{(2)},F_{jl^{(2)}}^{(2)}\right)_{m_2+1,q_l^{(2)}}.$

Under the effect of external periodic force, these NoLDEs defined in (10), (11) and (12) used in the theory of resistance less circuits. To solve these Nonlinear differential equations, we use Hermite, Legendre and Jacobi polynomials.
Now, we derive some new integrals as theorems that will use to solve the above given NoLDEs.

Theorem 1:

$$\int_{-\infty}^{\infty}x^{2\sigma}e^{-x^2}H_n(x)\overset{(a,b,c,d,e)}{\underset{(p,q)}{\mathrm{S}}}\left(yx^{2\rho'}\right)\Gamma^{M,N}_{P,Q}\left[zx^{2\rho}\left|\begin{array}{l}(f_1,F_1,t),(f_j,F_j)_{2,P}\\(w_j,W_j)_{1,Q}\end{array}\right.\right]dx=\sqrt{\pi}2^{n-2\sigma}L_1(k)$$
$$\Gamma^{M,N+1}_{P+1,Q+1}\left[z2^{-2\rho}\left|\begin{array}{l}(-2\sigma-2\rho'k,2\rho),(f_1,F_1,t),(f_j,F_j)_{2,P}\\(w_j,W_j)_{1,Q},(n/2-\sigma-\rho'k,\rho)\end{array}\right.\right], \quad (13)$$

where,

$$L_1(k)=\sum_{k=0}^{\infty}\frac{(\alpha_1)_k\ldots(\alpha_p)_k}{(\beta_1)_k\ldots(\beta_q)_k}\frac{(c)_{kd,e}}{\Gamma_e(ka+b)}\frac{y^k}{k!}2^{-2\rho' k}.$$

Proof: By using the results of (6) and (9) in (13), we arrive at

$$\int_{-\infty}^{\infty}x^{2\sigma}e^{-x^2}H_n(x)\left[\sum_{k=0}^{\infty}\frac{(\alpha_1)_k\ldots(\alpha_p)_k}{(\beta_1)_k\ldots(\beta_q)_k}\frac{(c)_{kd,e}}{\Gamma_e(ka+b)}\frac{\left(yx^{2\rho'}\right)^k}{k!}\frac{1}{2\pi i}\int_L\phi(s,t)(zx^{2\rho})^s ds\right]dx,$$

here $\phi(s,t)$ defined in (7).
Provided under the given condition, interchange the order of contour integral

and integral. We get,

$$\sum_{k=0}^{\infty}\frac{(\alpha_1)_k\dots(\alpha_p)_k}{(\beta_1)_k\dots(\beta_q)_k}\frac{(c)_{kd,e}}{\Gamma_e(ka+b)}\frac{y^k}{k!}$$
$$\frac{1}{2\pi i}\int_L\phi(s,t)z^s\left[\int_{-\infty}^{\infty}x^{2(\sigma+\rho'k+\rho s)}e^{-x^2}H_n(x)dx\right]ds.$$

By using improper integral given below

$$\int_{-\infty}^{\infty}x^{2\sigma}e^{-x^2}H_n(x)dx=2^{n-2\sigma}\sqrt{\pi}\frac{\Gamma(2\sigma+1)}{(\sigma-n/2+1)}. \tag{14}$$

After little simplification we get the desire result.

Theorem 2:

$$\int_{-1}^{1}(1+x)^{\Lambda-1}P_n(x)\overset{(a,b,c,d,e)}{\underset{(p,q)}{\mathrm{S}}}\left[y\,(1+x)^{\nu'}\right]$$
$$\Gamma_{P,Q}^{M,N}\left[z\,(1+x)^{\nu}\,\middle|\,\begin{matrix}(f_1,F_1,t),(f_j,F_j)_{2,P}\\(w_j,W_j)_{1,Q}\end{matrix}\right]dx=2^{\Lambda}L_2(k)\Gamma_{P+2,Q+2}^{M,N+2}$$
$$\left[z2^{\nu}\,\middle|\,\begin{matrix}(1-\Lambda-\nu'k,\nu),(1-\Lambda-\nu'k,\nu),(f_1,F_1,t),(f_j,F_j)_{2,P}\\(w_j,W_j)_{1,Q},(\Lambda-\nu'k-n,\nu),(1-\Lambda-\nu'k+n,\nu)\end{matrix}\right], \tag{15}$$

where,

$$L_2(k)=\sum_{k=0}^{\infty}\frac{(\alpha_1)_k\dots(\alpha_p)_k}{(\beta_1)_k\dots(\beta_q)_k}\frac{(c)_{kd,e}}{\Gamma_e(ka+b)}\frac{y^k}{k!}2^{\nu'k}.$$

Proof: By using the known result given in (p.316, eq.15, [8]), we can get the proof of the Theorem 2 in similar manner as we did in the Theorem 1 .

Theorem 3:

$$\int_{-1}^{1}(1-x)^{\lambda}(1+x)^{\delta}x^nP_n^{(\lambda,\delta)}(x)\overset{(a,b,c,d,e)}{\underset{(p,q)}{\mathrm{S}}}(yx^{\rho})$$
$${}^{(\Gamma)}I^{0,n:m_1,n_1;m_2,n_2}_{p_l,q_l,r;p_{l^{(1)}},q_{l^{(1)}},r_{(1)};p_{l^{(2)}},q_{l^{(2)}},r_{(2)}}\left[\begin{matrix}z_1x^{\nu}\\z_2x^{\mu}\end{matrix}\,\middle|\,\begin{matrix}A^*\\B^*\end{matrix}\right]=2^{\lambda+\delta+n+1}L_3(k)$$
$${}^{(\Gamma)}I^{0,n+2:m_1,n_1;m_2,n_2}_{p_l+2,q_l+1,r;p_{l^{(1)}},q_{l^{(1)}},r_{(1)};p_{l^{(2)}},q_{l^{(2)}},r_{(2)}}\left[\begin{matrix}z_12^{\nu}\\z_22^{\mu}\end{matrix}\,\middle|\,\begin{matrix}C^*\\D^*\end{matrix}\right], \tag{16}$$

where,

$$A^*=\left(e_1,E_1^{(1)},E_1^{(2)},s\right),\left(e_j,E_j^{(1)},E_j^{(2)}\right)_{2,n},\left(e_{jl},E_{jl}^{(1)},E_{jl}^{(2)}\right)_{n+1,p_l},$$
$$(e_j^{(1)},E_j^{(1)})_{1,n_1},\left(e_{jl^{(1)}}^{(1)},E_{jl^{(1)}}^{(1)}\right)_{n_1+1,p_l^{(1)}},(e_j^{(2)},E_j^{(2)})_{1,n_2},\left(e_{jl^{(2)}}^{(2)},E_{jl^{(2)}}^{(2)}\right)_{n_2+1,p_l^{(2)}}$$
$$B^*=\dots,\left(f_{jl},F_{jl}^{(1)},F_{jl}^{(2)}\right)_{m+1,q_l},\left(f_j^{(1)},F_j^{(1)}\right)_{1,m_1},\left(f_{jl^{(1)}}^{(1)},F_{jl^{(1)}}^{(1)}\right)_{m_1+1,q_l^{(1)}},$$

$\left(f_j^{(2)}, F_j^{(2)}\right)_{1,m_2}, \left(f_{jl^{(2)}}^{(2)}, F_{jl^{(2)}}^{(2)}\right)_{m_2+1,q_l^{(2)}}$
$C^* = (-\lambda - n - \rho k, \nu, \mu), (-\delta - n - \rho k, \nu, \mu), \left(e_1, E_1^{(1)}, E_1^{(2)}, s\right),$
$\left(e_j, E_j^{(1)}, E_j^{(2)}\right)_{2,n}, \left(e_{jl}, E_{jl}^{(1)}, E_{jl}^{(2)}\right)_{n+1,p_l}, (e_j^{(1)}, E_j^{(1)})_{1,n_1},$
$\left(e_{jl^{(1)}}^{(1)}, E_{jl^{(1)}}^{(1)}\right)_{n_1+1,p_l^{(1)}}, (e_j^{(2)}, E_j^{(2)})_{1,n_2}, \left(e_{jl^{(2)}}^{(2)}, E_{jl^{(2)}}^{(2)}\right)_{n_2+1,p_l^{(2)}}$
$D^* = \ldots, \left(f_{jl}, F_{jl}^{(1)}, F_{jl}^{(2)}\right)_{m+1,q_l}, (-1 - \lambda - \delta - 2(n - \rho k), 2\nu, 2\mu),$
$\left(f_j^{(1)}, F_j^{(1)}\right)_{1,m_1}, \left(f_{jl^{(1)}}^{(1)}, F_{jl^{(1)}}^{(1)}\right)_{m_1+1,q_l^{(1)}}, \left(f_j^{(2)}, F_j^{(2)}\right)_{1,m_2},$
$\left(f_{jl^{(2)}}^{(2)}, F_{jl^{(2)}}^{(2)}\right)_{m_2+1,q_l^{(2)}}$

and

$L_3(k) = \sum_{k=0}^{\infty} \frac{(\alpha_1)_k \ldots (\alpha_p)_k}{(\beta_1)_k \ldots (\beta_q)_k} \frac{(c)_{kd,e}}{\Gamma_e(ka+b)} \frac{y^k}{k!} 2^{\rho k}$.

Proof: By using the result given in (p.261, eq.15, [15]), we can get the proof of the Theorem 3 in similar manner as we did in the Theorem 1 .

3 Polynomials and Linear Approximation

Here, we solve the NoLDEs given in (10), (11) and (12) by using Hermite, Legendre and Jacobi polynomials respectively.

3.1 Hermite Polynomials and Linear Approximation

Here, we solve the NoLDE given in equation (10) as follows:

$$\ddot{\mathrm{x}} + f(x) = NF(t), \tag{17}$$

where

$$f(x) = \omega \overset{(a,b,c,d,e)}{\underset{(p,q)}{\mathrm{S}}} \left[y \left(\frac{x}{L}\right)^{2\Lambda'} \right] \Gamma_{P,Q}^{M,N} \left[z \left(\frac{x}{L}\right)^{2\Lambda} \middle| \begin{matrix} (f_1, F_1, t), (f_j, F_j)_{2,P} \\ (w_j, W_j)_{1,Q} \end{matrix} \right], \tag{18}$$

which can be written in terms of Hermite polynomials in the interval (–L, L), We get

$$f(x) = \sum_{n=0}^{\infty} \eta_n H_n \left(\frac{x}{L}\right), \tag{19}$$

where coefficient η_n is defined by

$$\eta_n = \frac{\int_{-\infty}^{\infty} f(Lx) H_n(x) x^{2\rho} e^{-x^2} dx}{\int_{-\infty}^{\infty} \left[H_n(x)\right]^2 e^{-x^2} dx}. \tag{20}$$

The series given in equation (20) truncated after two terms then, we get a linear approximation $f^*(x)$ as follows:

$$f^*(x) = \eta_0 H_0\left(\frac{x}{L}\right) + \eta_1 H_1\left(\frac{x}{L}\right). \tag{21}$$

Now, we can write linear approximation $f^*(x)$ by using equation (18) as

$$f^*(x) = \omega \overset{(a,b,c,d,e)}{\underset{(p,q)}{\mathrm{S}}} \left[y\left(\frac{x}{L}\right)^{2\Lambda'} \right] \Gamma_{P,Q}^{M,N} \left[z\left(\frac{x}{L}\right)^{2\Lambda} \middle| \begin{matrix} (f_1, F_1, t), (f_j, F_j)_{2,P} \\ (w_j, W_j)_{1,Q} \end{matrix} \right], \tag{22}$$

putting $H_0(x) = 1$ and $H_1(x) = 2x$ in (21), we have

$$f^*(x) = \eta_0 + 2\eta_1\left(\frac{x}{L}\right). \tag{23}$$

To obtain the values of η_0 and η_1, we consider $n = 0, n = 1$ and using equation (18) in (22), then we have

$$\eta_0 = \frac{\int_{-\infty}^{\infty} \omega \overset{(a,b,c,d,e)}{\underset{(p,q)}{\mathrm{S}}} \left(y x^{2\Lambda'} \right) A_H H_0(x) x^{2\rho} e^{-x^2} dx}{\int_{-\infty}^{\infty} \left[H_0(x)\right]^2 e^{-x^2} dx}, \tag{24}$$

and

$$\eta_1 = \frac{\int_{-\infty}^{\infty} \omega \overset{(a,b,c,d,e)}{\underset{(p,q)}{\mathrm{S}}} \left(y x^{2\Lambda'} \right) A_H H_1(x) x^{2\rho} e^{-x^2} dx}{\int_{-\infty}^{\infty} \left[H_1(x)\right]^2 e^{-x^2} dx}, \tag{25}$$

where

$A_H = \Gamma_{P,Q}^{M,N} \left[z x^{2\Lambda} \middle| \begin{matrix} (f_1, F_1, t), (f_j, F_j)_{2,P} \\ (w_j, W_j)_{1,Q} \end{matrix} \right]$

Further, using Theorem 1 and result (p.193, eq.(6), [15]) with $n = 0$ in equation (24), we get

$$\eta_0 = 2^{-2\sigma} \omega L_1(k) \Gamma_{P+1,Q+1}^{M,N+1} \left[z 2^{-2\rho} \middle| \begin{matrix} (-2\sigma - 2\rho' k, 2\rho), (f_1, F_1, t), (f_j, F_j)_{2,P} \\ (w_j, W_j)_{1,Q}, (-\sigma - \rho' k, \rho) \end{matrix} \right], \tag{26}$$

similarly, we can obtained

$$\eta_1 = 2^{-2\sigma} \omega L_1(k) \Gamma_{P+1,Q+1}^{M,N+1} \left[z 2^{-2\rho} \middle| \begin{matrix} (-2\sigma - 2\rho' k, 2\rho), (f_1, F_1, t), (f_j, F_j)_{2,P} \\ (w_j, W_j)_{1,Q}, (1/2 - \sigma - \rho' k, \rho) \end{matrix} \right]. \tag{27}$$

Now, on replacing $f(x)$ by $f^*(x)$ and using (23), we can express (17) as

$$\ddot{\mathrm{x}} + \eta_0 + 2\eta_1\left(\frac{x}{L}\right) = NF(t), \tag{28}$$

If $\delta^2 = 2\eta_1/L$ and $\delta_1^2 = \eta_0$, then (28) can be written as

$$\ddot{\mathrm{x}} + \delta^2 x + \delta_1^2 = NF(t). \tag{29}$$

Apply Laplace transform in equation (29) to find the approximate solution under the given constraints

$$y = L(L-1) \text{ and } \dot{\mathrm{x}} = 0 \text{ if } t = 0,$$

$$x^* = \left[L(L-1) + \frac{\delta_1^2}{\delta}\right] \cos \delta t - \frac{\delta_1^2}{\delta} + \frac{N}{\delta} \int_0^t F(u) \sin \delta(t-u) du. \tag{30}$$

The obtained approximate solution is general in nature.

3.2 Legendre Polynomials and Linear Approximation

The main objective of this section is to solve the NoLDE defined in (11) as follows:

$$\ddot{\mathrm{x}} + f(x) = NF(t), \tag{31}$$

where

$$f(x) = \omega \overset{(a,b,c,d,e)}{\underset{(p,q)}{\mathrm{S}}} \left[y \left(1 + \frac{x}{L}\right)^{\nu'} \right] \Gamma_{P,Q}^{M,N} \left[z \left(1 + \frac{x}{L}\right)^{\nu} \middle| \begin{matrix} (f_1, F_1, t), (f_j, F_j)_{2,P} \\ (w_j, W_j)_{1,Q} \end{matrix} \right], \tag{32}$$

which can be written in terms of Legendre polynomials in the interval (–L, L). We get

$$f(x) = \sum_{n=0}^{\infty} \tau_n P_n \left(\frac{x}{L}\right), \tag{33}$$

where coefficient τ_n is defined by

$$\tau_n = \frac{\int_{-1}^{1} f(Lx) P_n(x) (1+x)^{\Lambda-1} dx}{\int_{-1}^{1} [P_n(x)]^2 \, dx}. \tag{34}$$

Truncated the series (34) after two terms. We get a linear approximation $f^*(x)$ as follows:

$$f^*(x) = \tau_0 P_0 \left(\frac{x}{L}\right) + \tau_1 P_1 \left(\frac{x}{L}\right). \tag{35}$$

Now, we can write linear approximation $f^*(x)$ by using equation (32) by

$$f^*(x) = \omega \overset{(a,b,c,d,e)}{\underset{(p,q)}{\mathrm{S}}} \left[y \left(1 + \frac{x}{L}\right)^{\nu'} \right] \Gamma_{P,Q}^{M,N} \left[z \left(1 + \frac{x}{L}\right)^{\nu} \middle| \begin{matrix} (f_1, F_1, t), (f_j, F_j)_{2,P} \\ (w_j, W_j)_{1,Q} \end{matrix} \right], \tag{36}$$

Putting $P_0(x) = 1$ and $P_1(x) = x$ in (35), we have

$$f^*(x) = \tau_0 + \tau_1 \left(\frac{x}{L}\right). \tag{37}$$

Use equation (36) in (34) with $n = 0$ and $n = 1$, to obtain the values of τ_0 and τ_1 respectively as

$$\tau_0 = \frac{\int_{-1}^{1} \omega \underset{(p,q)}{\overset{(a,b,c,d,e)}{\mathrm{S}}} \left[y\,(1+x)^{\nu'}\right] A_L P_0(x)(1+x)^{\Lambda-1} dx}{\int_{-1}^{1} \left[P_0(x)\right]^2 dx}, \tag{38}$$

and

$$\tau_1 = \frac{\int_{-1}^{1} \omega \underset{(p,q)}{\overset{(a,b,c,d,e)}{\mathrm{S}}} \left[y\,(1+x)^{\nu'}\right] A_L P_1(x)(1+x)^{\Lambda-1} dx}{\int_{-1}^{1} \left[P_1(x)\right]^2 dx}, \tag{39}$$

where
$A_L = \Gamma_{P,Q}^{M,N}\left[z\,(1+x)^{\nu} \,\middle|\, \begin{matrix}(f_1,F_1,t),(f_j,F_j)_{2,P}\\ (w_j,W_j)_{1,Q}\end{matrix}\right]$
Further, using Theorem 2 and result (p.175, eq.(12), [15]) with $n = 0$ in (38), we get

$$\tau_0 = \omega 2^{\Lambda-1} L_2(k) \Gamma_{P+2,Q+2}^{M,N+2} \left[z2^{\nu} \,\middle|\, \begin{matrix}(1-\Lambda-\nu'k,\nu),(1-\Lambda-\nu'k,\nu),(f_1,F_1,t),(f_j,F_j)_{2,P}\\ (w_j,W_j)_{1,Q},(\Lambda-\nu'k,\nu),(1-\Lambda-\nu'k,\nu)\end{matrix}\right], \tag{40}$$

Similarly, we can evaluate for $n = 1$

$$\tau_1 = 3\omega 2^{\Lambda-1} L_2(k) \Gamma_{P+2,Q+2}^{M,N+2} \left[z2^{\nu} \,\middle|\, \begin{matrix}(1-\Lambda-\nu'k,\nu),(1-\Lambda-\nu'k,\nu),(f_1,F_1,t),(f_j,F_j)_{2,P}\\ (w_j,W_j)_{1,Q},(\Lambda-\nu'k-1,\nu),(2-\Lambda-\nu'k,\nu)\end{matrix}\right]. \tag{41}$$

Now, on replacing $f(x)$ by $f^*(x)$ and use (37), we can express in (31) as

$$\ddot{\mathrm{x}} + \delta_1^2 + \delta^2 x = NF(t), \tag{42}$$

where $\delta^2 = \tau_1/L$ and $\delta_1^2 = \tau_0$. Apply the Laplace transform in (42) to find the approximate solution under the constraints

$$x = L(L-1) \text{ and } \dot{\mathrm{x}} = 0 \text{ if } t = 0,$$

$$x^* = \left[L(L-1) + \frac{\delta_1^2}{\delta}\right]\cos\delta t - \frac{\delta_1^2}{\delta} + \frac{N}{\delta}\int_0^t F(u)\sin\delta(t-u)du. \tag{43}$$

The obtained approximate solution is general in nature.

3.3 Jacobi Polynomials and Linear Approximation

Here, our aim is to solve the NoLDE given in (12) is as follows:

$$\ddot{\mathrm{x}} + f(x) = NF(t), \tag{44}$$

where

$$f(x) = \omega \overset{(a,b,c,d,e)}{\underset{(p,q)}{\mathrm{S}}} \left[y \left(\frac{x}{L} \right)^{\Lambda} \right] {}^{(\Gamma)} I^{0,n:m_1,n_1;m_2,n_2}_{p_l,q_l,r;p_{l^{(1)}},q_{l^{(1)}},r_{(1)};p_{l^{(2)}},q_{l^{(2)}},r_{(2)}} \left[\begin{array}{c|c} z_1 \left(\frac{x}{L} \right)^{\nu} & A^* \\ z_2 \left(\frac{x}{L} \right)^{\mu} & B^* \end{array} \right], \tag{45}$$

where A^* and B^* are defined in (12), which can be written in terms of Jacobi polynomials in the interval (–L, L). We have

$$f(x) = \sum_{n=0}^{\infty} C_n^{(\iota,\kappa)} P_n^{(\iota,\kappa)} \left(\frac{x}{L} \right), \tag{46}$$

where coefficient $C_n^{(\iota,\kappa)}$ is defined by

$$C_n^{(\iota,\kappa)} = \frac{\int_{-1}^{1} f(Lx) P_n^{(\iota,\kappa)}(x)(1-x)^{\iota}(1+x)^{\kappa} dx}{\int_{-1}^{1} \left[P_n^{(\iota,\kappa)}(x) \right]^2 (1-x)^{\iota}(1+x)^{\kappa} dx}. \tag{47}$$

Truncated the above given series after two terms. We get a linear approximation $f^*(x)$ as follows:

$$f^*(x) = C_0^{(\iota,\kappa)} P_0^{(\iota,\kappa)} \left(\frac{x}{L} \right) + C_1^{(\iota,\kappa)} P_1^{(\iota,\kappa)} \left(\frac{x}{L} \right). \tag{48}$$

Now, we can write linear approximation $f^*(x)$ by using equation (45) by

$$f^* = \omega \overset{(a,b,c,d,e)}{\underset{(p,q)}{\mathrm{S}}} \left[y \left(\frac{x}{L} \right)^{\Lambda} \right] {}^{(\Gamma)} I^{0,n:m_1,n_1;m_2,n_2}_{p_l,q_l,r;p_{l^{(1)}},q_{l^{(1)}},r_{(1)};p_{l^{(2)}},q_{l^{(2)}},r_{(2)}} \left[\begin{array}{c|c} z_1 \left(\frac{x}{L} \right)^{\nu} & A^* \\ z_2 \left(\frac{x}{L} \right)^{\mu} & B^* \end{array} \right], \tag{49}$$

Putting $P_0^{(\iota,\kappa)} = 1$ and $P_1^{(\iota,\kappa)} = \frac{\iota-\kappa}{2} + \frac{(2+\iota+\kappa)x}{2}$ in (48), we have

$$f^*(x) = C_0^{(\iota,\kappa)} + C_1^{(\iota,\kappa)} \left[\frac{\iota-\kappa}{2} + \frac{(2+\iota+\kappa)x}{2} \right]. \tag{50}$$

Use equation (47) in (45) with $n = 0$ and $n = 1$, to obtain the values of $C_0^{(\iota,\kappa)}$ and $C_1^{(\iota,\kappa)}$ with the help of Theorem 3 and aid a result (p.260, eq.(11), [15])

with $n=0$ in equation (47), we get $C_0^{(\iota,\kappa)}$ as follows:

$$C_0^{(\iota,\kappa)} = \frac{\omega L_3(k)\Gamma(2+\iota+\kappa)}{\Gamma(1+\iota)\Gamma(1+\kappa)} {}^{(\Gamma)}I^{0,n+2:m_1,n_1;m_2,n_2}_{p_l+2,q_l+1,r;p_{l^{(1)}},q_{l^{(1)}},r_{(1)};p_{l^{(2)}},q_{l^{(2)}},r_{(2)}} \left[\begin{array}{c|c} z_1 2^{\nu} & C^{**} \\ z_2 2^{\mu} & D^{**} \end{array} \right], \quad (51)$$

where
$C^{**} = (-\iota-\rho k,\nu,\mu),(-\kappa-\rho k,\nu,\mu),\left(e_1,E_1^{(1)},E_1^{(2)},s\right),\left(e_j,E_j^{(1)},E_j^{(2)}\right)_{2,n},$
$\left(e_{jl},E_{jl}^{(1)},E_{jl}^{(2)}\right)_{n+1,p_l},(e_j^{(1)},E_j^{(1)})_{1,n_1},\left(e_{jl^{(1)}}^{(1)},E_{jl^{(1)}}^{(1)}\right)_{n_1+1,p_l^{(1)}},(e_j^{(2)},E_j^{(2)})_{1,n_2},$
$\left(e_{jl^{(2)}}^{(2)},E_{jl^{(2)}}^{(2)}\right)_{n_2+1,p_l^{(2)}}$
$D^{**} = \ldots,\left(f_{jl},F_{jl}^{(1)},F_{jl}^{(2)}\right)_{m+1,q_l},(-1-\iota-\kappa-2\rho k,2\nu,2\mu),\left(f_j^{(1)},F_j^{(1)}\right)_{1,m_1}$
$,\left(f_{jl^{(1)}}^{(1)},F_{jl^{(1)}}^{(1)}\right)_{m_1+1,q_l^{(1)}},\left(f_j^{(2)},F_j^{(2)}\right)_{1,m_2},\left(f_{jl^{(2)}}^{(2)},F_{jl^{(2)}}^{(2)}\right)_{m_2+1,q_l^{(2)}}.$

Similarly, we can obtain $C_1^{(\iota,\kappa)}$ as

$$C_1^{(\iota,\kappa)} = \frac{2\omega L_3(k)\Gamma(3+\iota+\kappa)}{\Gamma(2+\iota)\Gamma(2+\kappa)} {}^{(\Gamma)}I^{0,n+2:m_1,n_1;m_2,n_2}_{p_l+2,q_l+1,r;p_{l^{(1)}},q_{l^{(1)}},r_{(1)};p_{l^{(2)}},q_{l^{(2)}},r_{(2)}} \left[\begin{array}{c|c} z_1 2^{\nu} & C^{***} \\ z_2 2^{\lambda} & D^{***} \end{array} \right], \quad (52)$$

where
$C^{***} = (-\iota-1-\rho k,\nu,\mu),(-\kappa-1-\rho k,\nu,\mu),\left(e_1,E_1^{(1)},E_1^{(2)},s\right),$
$\left(e_j,E_j^{(1)},E_j^{(2)}\right)_{2,n},\left(e_{jl},E_{jl}^{(1)},E_{jl}^{(2)}\right)_{n+1,p_l},(e_j^{(1)},E_j^{(1)})_{1,n_1},$
$\left(e_{jl^{(1)}}^{(1)},E_{jl^{(1)}}^{(1)}\right)_{n_1+1,p_l^{(1)}},(e_j^{(2)},E_j^{(2)})_{1,n_2},\left(e_{jl^{(2)}}^{(2)},E_{jl^{(2)}}^{(2)}\right)_{n_2+1,p_l^{(2)}}$
$D^{***} = \ldots,\left(f_{jl},F_{jl}^{(1)},F_{jl}^{(2)}\right)_{m+1,q_l},(-3-\iota-\kappa-2\rho k,2\nu,2\mu),\left(f_j^{(1)},F_j^{(1)}\right)_{1,m_1}$
$,\left(f_{jl^{(1)}}^{(1)},F_{jl^{(1)}}^{(1)}\right)_{m_1+1,q_l^{(1)}},\left(f_j^{(2)},F_j^{(2)}\right)_{1,m_2},\left(f_{jl^{(2)}}^{(2)},F_{jl^{(2)}}^{(2)}\right)_{m_2+1,q_l^{(2)}}.$

Now, on replacing $f(x)$ by $f^*(x)$ and use equation (50), we can write equation (44) as

$$\ddot{\mathrm{x}} + \delta^2 x + \frac{\iota-\kappa}{2+\iota+\kappa}\left(\delta^2-\delta_1^2\right) = NF(t), \quad (53)$$

where $\delta^2 = \frac{2+\iota+\kappa}{2L}$ and $\delta_1^2 = \frac{2+\iota+\kappa}{(\kappa-\iota)L}C_0^{(\iota,\kappa)}$.
Apply the Laplace transform in equation (53) to find the approximate solution under the constraints

$$x = L(L-1) \text{ and } \dot{\mathrm{x}} = 0 \text{ if } t = 0,$$

$$x^* = \left[L(L-1) + \frac{(\iota-\kappa)\delta}{2+\iota+\kappa}\left(1-\frac{\delta_1^2}{\delta}\right)\right] \cos\delta t - \frac{(\iota-\kappa)\delta}{2+\iota+\kappa}\left(1-\frac{\delta_1^2}{\delta}\right) + \frac{N}{\delta}\int_0^t F(u)\sin\delta(t-u)du. \quad (54)$$

The obtained approximate solution is general in nature.

Similarly, we can prove all of the above results and theorems for lower forms of the incomplete H-function $\gamma_{P,Q}^{M,N}[z]$ and incomplete I-function with two variables ${}^{(\gamma)}I_{p_l,q_l,r;p_{l(1)},q_{l(1)},r_{(1)};p_{l(2)},q_{l(2)},r_{(2)}}^{0,n:m_1,n_1;m_2,n_2}[z_i]$.

4 Conclusion

In this article, we introduced the approximate solution of NoLDE associated with incomplete H-functions, incomplete I-functions with two variables and S-function with the help of Hermite, Legendre and Jacobi polynomials. These obtained results are general and effectively used in the field of Science, Mathematics, Statistics, Economics and finance. These findings can be used to solve the problem of a resistance less circuit involving a nonlinear capacitor under the influence of external periodic force.

References

[1] Bansal, M. K., Jolly, N., Jain, R., and Kumar, D. (2019). An integral operator involving generalized Mittag-Leffler function and associated fractional calculus results. *The Journal of Analysis*, 27(3), 727-740.

[2] Bansal, M. K., Kumar, D., and Jain, R. (2019). Interrelationships Between Marichev–Saigo–Maeda Fractional Integral Operators, the Laplace Transform and the $\overline{H}$-Function. *International Journal of Applied and Computational Mathematics*, 5(4), 1-13.

[3] Bansal, M. K., Kumar, D., Khan, I., Singh, J., and Nisar, K. S. (2019). Certain unified integrals associated with product of M-series and incomplete H-functions. *Mathematics*, 7(12), 1191.

[4] Bansal, M. K., Kumar, D., Singh, J., Tassaddiq, A., and Nisar, K. S. (2020). Some new results for the Srivastava–Luo–Raina M-transform pertaining to the incomplete H-functions. *AIMS Math*, 5(1), 717-722.

[5] Chaurasia V. B. L., and Saxena, V. (2007). Applications of certain special functions to non-linear differential equation involving $\bar{H}$-function. *Acta Ciencia Indica.*, XXXIVM(1), 307-318.

[6] Diaz, R., and Pariguan, E. (2004). On hypergeometric functions and Pochhammer k-symbol. *arXiv preprint math/0405596*.

[7] Daiya, J., and Saxena, R. K. (2015). Integral transforms of the S-functions. *Le Matematiche*, 70(2), 147-159.

[8] Erdélyi, A., Magnus, W., Oberhettinger, F., and Tricomi, F. G. (1953). *Higher Transcendental Functions Vol. II*. New York, Toronto and London: McGraw-Hill Book Company.

[9] Garde R. M. (1967). Applications of Jacobi polynomials to non-linear oscillations–1, Free oscillations. *Proc Nat Acad Sci India*. 37, 119-120.

[10] Jayarama, P., Madam, V. N. T., and Kurumujji, S. K. (2014). A study of I-function of several complex variables. *International Journal of Engineering Mathematics*, 2014.

[11] Kumar, D., Singh, J., Purohit, S. D., and Swroop, R. (2019). A hybrid analytical algorithm for nonlinear fractional wave-like equations. *Mathematical Modelling of Natural Phenomena*, 14(3), 304.

[12] Kumar, D., Singh, J., Prakash, A., and Swroop, R. (2019). Numerical simulation for system of time-fractional linear and nonlinear differential equations. *Progr. Fract. Differ. Appl*, 5(1), 65-77.

[13] Prasad, Y. N. (1986). Multivariable I-function. *Vijnana Parishad Anusandhan Patrika*. 29(4), 231-235.

[14] Prym, F. E. (1877). Zur theorie der gamma function. *The Journal fur die Reine und Angewandte Mathematik*. 82, 165–172.

[15] Rainville, E. D. (1960). *Special functions (Vol. 5)*. New York.

[16] Saxena, R. K., and Kushwaha, R. S. (1970). Applications of Jacobi polynomials to non-linear oscillations. *In Proceedings of the National Academy of Sciences, India*. 40, 65-72.

[17] Sharma, M. (2008). Fractional integration and fractional differentiation of the M-series. *Fractional calculus and applied analysis*, 11(2), 187-191.

[18] Sharma, C. K., and Mishra, P. L. (1991). On the I-function of two variables and its properties. *Acta Ciencia Indica Math*. 17, 667-672.

[19] Sharma, R., Singh, J., Kumar, D., and Singh, Y. (2022). Certain unified integrals associated with product of the general class of polynomials and incomplete I-functions. *International Journal of Applied and Computational Mathematics*, 8(1), 1-11.

[20] Singh, P. (2007). Applications of Hermite, Legendre and Jacobi polynomials and linear approximation to some non-linear differential equations associated with H-function. *Vijnana Parishad Anusandhan Patrika*. 50(1), 41-61.

[21] Singh, J., Kumar, D., and Bansal, M. K. (2019). Solution of nonlinear differential equation and special functions. *Mathematical Methods in the Applied Sciences*, 43(5), 2106-2116.

[22] Singh, J., Kumar, D., Baleanu, D., and Rathore, S. (2018). An efficient numerical algorithm for the fractional Drinfeld–Sokolov–Wilson equation. *Applied Mathematics and Computation*. 335, 12-24.

[23] Singh, J., Secer, A., Swroop, R., and Kumar, D. (2019). A reliable analytical approach for a fractional model of advection-dispersion equation. *Nonlinear Engineering*, 8(1), 107-116.

[24] Srivastava, B. M. (1975). Solvable potentials for the Chebyshev and associated Laguerre equations. *Jnanabha Sect A*. 5, 181-187.

[25] Srivastava, B. M., and Singh, F. (1976). Application of Jacobi polynomials to non-linear differential equation associated with H-function. *Vijnana Parishad Anusandhan Patrika*. 19(1), 25-34.

[26] Srivastava, H. M., Saxena, R. K., and Parmar, R. K. (2018). Some Families of the Incomplete H-Functions and the Incomplete $\overline{H}$-Functions and Associated Integral Transforms and Operators of Fractional Calculus with Applications. *Russian Journal of Mathematical Physics*, 25(1), 116-138.

SEAIQHRDP mathematical model Analysis for the transmission dynamics of COVID-19 in India

M. Ankamma Rao[1] and A.Venkatesh[2*]

[1,2]Department of Mathematics,
AVVM Sri Pushpam College (Affiliated to Bharathidasan University),
Poondi, Thanjavur(Dt), Tamilnadu, India-613 503.

December 28, 2022

Abstract

Mathematical modeling is one of the most used techniques for analyzing and preventing the transmission of COVID-19. To control this pandemic, it is essential to classify the infected population. So in this article, a new SEAIQHRDP model was formulated to investigate the transmittal dynamics of COVID-19. This model contains nine compartments Susceptible(S) class, Exposed(E) class, Asymptomatic(A) class, Infected(I) class, Quarantined(Q) class, Hospitalized(H) class, Recovered(R) class, Death(D) class, and Insusceptible (P) class. This model was fitted to the daily and cumulative confirmed COVID-19 cases in the period between 30^{th} January 2020 and 13^{th} January 2021 in India. Sensitivity analysis concerning R_0 was performed to classify the significance of parameters. Contour plots for R_0 were executed and the effect of various parameters on the infected classes had shown graphically. The necessity of stringent face mask usage and social seclusion is highlighted by optimal control analysis as a key factor in the dramatic reduction of infection rates. So the optimal control technique was adopted to lessen the disease mortality by taking both nonpharmaceutical and pharmaceutical intervention strategies as control functions and comparing infectives and recoveries with and without controls.

Keywords: : mathematical model, Stability analysis, Basic reproduction number, Sensitivity analysis, optimal strategy
Subject Classification: 00A71

1 Introduction

The world has been trembling with a new infectious disease COVID-19. The World Health Organization (WHO) has declared it was a universal pandemic on 11^{th} March 2020 [14]. originally The COVID-19 disease was revealed in December 2019 in Wuhan, Hubei, China. Later it increased rapidly and spread in all countries in the world. As of August 28^{th}, 2022, the total confirmed cases of 596,873,121 and death cases of 6,459,684 of COVID-19 had been reported to WHO [15]. On January 30^{th}, 2020 the first COVID-19 case [28] was placed in Kerala, India. A total of 44,389,176 confirmed cases and 527,556

*Corresponding author: avenkateshmaths@gmail.com

death cases were placed in India as of August 28^{th}, 2022. Initially, some countries implemented strictly non-pharmacological interventions namely as use of face masks social distancing, and hygiene to resist the extent of the COVID-19 pandemic. Due to these safety measures, the virus spread slowed down gradually but not ceased completely. Since the vaccination process had started, the COVID-19 cases decreased day by day and it became under control. But still now in some countries COVID- cases raises unexpectedly.

Mathematical modeling is a prominent technique for forecasting and controlling the transmission dynamics of epidemic diseases. Alexander Krämeret al.[1] H.W. Hethcote [16], R.M.May & R.M Anderson, [38] Brauer F & Chavez CC) [6]. Some standard mathematical models such as SIR, SEIR, SEIAR, SEIRD, etc. were broadly used to estimate the future trend of a pandemic. The standard SIR model Kermack WO & McKendrick [20] described the spread of the virus using the compartments of susceptible, infected, and recovered. By incorporating the new compartments, we get new models to detect the communication dynamics of contagious diseases. An SEIR model by Mwalili S et al. cite 26 was developed by adding an Exposed compartment to the SIR model which contained distinctive reaction and administration activity factors. This model is used widely to forecast the direction of the COVID-19 graph in China among other countries. Through the SEIR model, the influence of control strategies was studied by Lin Q et al.[22] and formulated the SEIR extension model. A generalized SEIR model Read JM et al.[34] was advanced in the latent period to cover the communication dynamics of COVID-19. During the incubation period, it consists of one more compartment as asymptomatic individuals in the SEIR model. The isolated class in SEIJR was interchanged with the asymptomatic class in SEIAR. By using this model, Bailey et al [2] displayed related properties to the SEIJR model Peng L et al. [30]. General models such as SIR, SEIR, SEIRD, SEIJR, etc. were not suitable for forecast the effect of the widespread disease since they comprise a finite number of parameters and disregarded essential classes such as asymptomatic infected, quarantine, Hospitalization, etc. SIDARTHE model of Giordano et al.[11] is an extension of the SEIR model which consists of undetected as well as detected infected populations.

The field of FDEs has developed greatly over the past few decades as a result of its applicability in numerous branches of research and technology. To study malaria transmission, Rehman, Attiq ul, and colleagues devised a 9 compartment FDE model [35]. By considering both the government's activity and the individual's response, Danane, Jaouad et al.[8] established a seven-compartment FDE model. Supriya, Yadav, and colleagues [42] created the FDE model to investigate the COVID-19 trend using an effective and potent analytical q-HASTM approach. By Jagdev Singh, a fractional guava fruit model with memory effect was developed [41]

In general, before showing any symptoms an individual exposed to the virus will become infectious i.e. pre-symptomatic through an incubation period of 5 days Liu C et al. [23]. Many reports have shown that a huge number of individuals who were exposed to the virus did not show any symptoms i.e., they all remain asymptomatic. The pre-symptomatic or asymptomatic individuals were capable to diffuse the virus to others. Since the reported asymptomatic cases in India are high, it was necessary to include the asymptomatic class in the epidemiological model. As for the total of parameters and accurateness model, the above-discussed models were not perfect for long-term predictions. Therefore one more compartment dead population had been incorporated in the SEIAR model presented through Huang et al.[15] to improve the accurateness model for long-term prediction.

Raj Kishore et.al [33] developed the SEIQRDP model by including the quarantine class (Q) and insusceptible class (P) and predicted the number of active cases. By

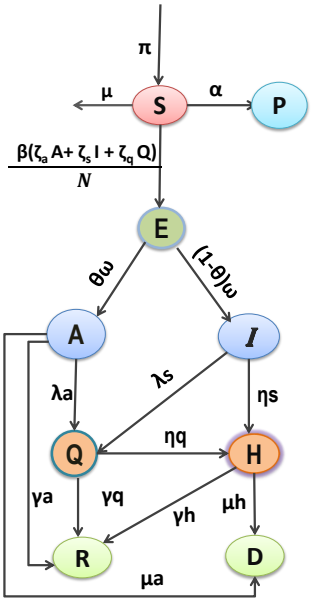

Figure 1: Flow Chart of SEAIQHRDP model

incorporating an asymptomatic class Singh HP et al [39] introduced the SEAIQRDT model and forecast the confirmed cases. When the best optimal control technique is used early in a pandemic, the intensity of epidemic peaks tends to decline, spreading the maximum impact of an epidemic across a longer time. Massad, Eduardo et al [25] developed an optimal control model to analyze the effect of vaccination on the zika virus. To analyze the COVID-19 trend in the future, Bandekar SR and Minighosh [3] devised an 11 compartments mathematical model. They then employed an optimal control strategy to reduce the disease fatality.

By taking into account all of the aforementioned discussions, We developed a new SEAIQHRDP model by including a new class—hospitalization—to the SEAIQRDP model in order to examine the transmission of COVID-19. Later an optimal control strategy with three control variables was applied to the proposed model to moderate the outspread of COVID-19 optimally.

The following sections in this manuscript were systematized as follows: SEAIQHRDP model formulation was presented in section 2. In section 3 The elementary properties of the recommended model such as positivity and boundedness, disease-free equilibrium's local stability, and R_0 expression in various parameters were executed. Section 3 finished Parameter estimation, model fitting, and model justification. Sect.5 performed the sensitive analysis concerning R_0 and the impact of parameters on infected populations. Section 6 implemented and solved an optimal control problem analytically. The work ends with the conclusion in Section 7

2 Model formation

By considering all the above discussions, in this study, a new mathematical model SEAIQHRDP was formulated. In this model, the class S(t) contained the susceptible individuals at time t, the class E(t) contained exposed individuals (these were contaminated but does not contaminate others within the reaction time), the class A(t)

contained asymptomatic infected individuals (despite no symptoms appeared in them but capable to infect others), the class I(t) contains the symptomatic individuals (these persons having symptoms and were capable to infect others), the class Q(t) contained the quarantined individuals (these were infected but isolated), the class H(t) contained the hospitalization individuals (these were infected and undergo medical treatment), the class R(t) contained the recovered individuals, the class D(t) contained the death individuals, and the class P(t) contained the insusceptible individuals those are incapable of getting infected due to either pre-isolated or following the WHO rules strictly.

Let Λ and μ be the constant recruitment rate and normal death rate in the susceptible population. Let β be the virus contact rate. Let ζ_a, ζ_q, and ζ_s be the adjustment factors for asymptomatic infected, symptomatic infected, and quarantine populations. $\beta\zeta_a$, $\beta\zeta_q$ and $\beta\zeta_h$ were the virus transmission factors of asymptomatic, symptomatic, and quarantine populations to susceptible populations. These were time-dependent factors in computations. This model has the potency of disease is $\triangle = \frac{\zeta_a A + \zeta_s I + \zeta_q Q}{N}$.

Let α be the protection rate at which the susceptible individuals move to insusceptible individuals. This included the influence of control measures. Let θ be the fraction at which the exposed individuals move to asymptomatic individuals. Then $(1-\theta)$ is the fraction at which exposed individuals move to symptomatic infected individuals at a velocity ω. Let λ_a and λ_s be the quarantine rates at which the asymptomatically infected individuals and symptomatically infected individuals were quarantined. Let η_s and η_q hospitalization rates at which the symptomatic and quarantine populations had certain complications due to severe symptoms shall be hospitalized. Let γ_a, γ_q, and γ_h be the recovery rates at which the asymptomatic infected, quarantined, and hospitalized individuals were recovered from the disease. There will be a possibility to die, in asymptomatic individuals before getting symptoms and after admitting to the hospital. Let μ_a and μ_h be the mortality rates of asymptomatic and hospitalized individuals. By using all the above conditions, The relation between these nine compartments and corresponding parameters were shown in Figure.1 and table 1

The arrangement of nonlinear differential equations for the proposed model in India was

$$\frac{ds}{dt} = \Lambda - \beta \triangle S - (\alpha + \mu)S \tag{1.1}$$

$$\frac{dE}{dt} = \beta \triangle S - (\omega + \mu)E \tag{1.2}$$

$$\frac{dA}{dt} = \theta\omega E - (\lambda_a + \gamma_a + \mu_a + \mu)A \tag{1.3}$$

$$\frac{dI}{dt} = (1-\theta)\omega E - (\lambda_s + \eta_s + \mu)I \tag{1.4}$$

$$\frac{dQ}{dt} = \lambda_a A + (\lambda_s I - (\eta_q + \gamma_q + \mu)Q \tag{1.5}$$

$$\frac{dH}{dt} = \eta_s I + \eta_q Q - (\gamma h + \mu_h + \mu)H \tag{1.6}$$

$$\frac{dR}{dt} = \gamma_a A + \gamma_q Q + \gamma_h H - \mu R \tag{1.7}$$

$$\frac{dD}{dt} = \mu_a A + \mu_h H \tag{1.8}$$

$$\frac{dP}{dt} = \alpha S. \tag{1.9}$$

with non negative primary conditions are $S(0) = S_0$, $E(0) = E_0$, $A(0) = A_0$, $I(0) == I_0$, $Q(0) = Q_0$, $H(0) = H_0$,$R(0) = R_0$, $D(0) = D_0$and $P(0) = P_0$.

Table 1: SEAIQHRDP model parameter's complete depiction.

parameter	description
Λ	Recruitment rate of human
θ	Proportion of exposed individuals
ω	Conversion rate of exposed to asymptomatically infected populace
α	Protection rate of susceptible individuals to insusceptible populace
ζ_a,ζ_s,ζ_q	Adjustment factor for asymptomatic, symptomatic and quarantine populace
β	Transmission rate of virus
λ_a	Quarantine rate of asymptomatic infected populace
λ_s	Quarantine rate of symptomatic infected populace
η_s	Hospitalization rate of symptomatic infected populace
η_q	Hospitalization rate of quarantine infected populace
γ_a	The rate of recovery from asymptomatic infected populace
γ_q	The rate of recovery from quarantine populace
γ_h	The rate of recovery from hospitalization populace
μ_a	The rate of mortality from asymptomatic populace
μ_h	The rate of mortality from hospitalization populace
μ	Normal mortality rate of human populace

3 SEAIQHRDP model analysis

3.1 Positivity and boundedness

Theorem 1. *All the solutions* $(S(t), E(t), A(t), I(t), Q(t), H(t), R(t), D(t), P(t)) \in \mathbb{R}^9_+$ *of the system (1) with primary conditions remain non negative and were uniformly bounded in the region* Ω *for all time* $t \geq 0$.

Proof 1. *Assumed that* $(S(t), E(t), A(t), I(t), Q(t), H(t), R(t), D(t), P(t)) \in \mathbb{R}^9_+$ *be a solution of (1) for* $t \in [0, t_0]$, *where* $t_0 \geq 0$.

From the equation (1.1),

$\frac{ds}{dt} = \Lambda - (\zeta_a A + \zeta_s I + \zeta_q Q)\frac{S}{N} - (\alpha + \mu)S \geq \Lambda - \phi(t)S$

where $\phi(t) = \beta(\zeta_a A + \zeta_s I + \zeta_q Q)\frac{S}{N} + (\alpha + \mu)$

$\Rightarrow \frac{ds}{dt} \geq \Lambda - \phi(t)S$

After integration, $S(t) = S^0 \exp(-\int_0^t \phi(s)\, ds) \int_0^t e^{\int_0^s \phi(u)\, du)} > 0$.

Hence, for all $t \in [0, t_0)$, *we get* $S(t) > 0$

From the equation (1.2),

$\frac{dE}{dt} = (\zeta_a A + \zeta_s I + \zeta_q Q)\frac{S}{N} - (\omega + \mu)E \geq -(\omega + \mu)E$

$\Rightarrow \frac{dE}{dt} \geq -(\omega + \mu)E$

$\Rightarrow E(t) \geq E^0 \exp(-\int_0^t (\omega + \mu)\, ds) \geq 0$

i.e, $E(t) \geq 0$

From the equation (1.3),

$\frac{dA}{dt} = \theta\omega E - (\lambda_a + \gamma_a + \mu_a + \mu)A \geq -(\lambda_a + \gamma_a + \mu_a + \mu)A$

$\Rightarrow \frac{dA}{dt} \geq -(\lambda_a + \gamma_a + \mu_a + \mu)A$

$\Rightarrow A(t) \geq A^0 \exp(-\int_0^t (\lambda_a + \gamma_a + \mu_a + \mu)\, ds \geq 0$

i.e,$A(t) \geq 0$

From the equation (1.4),

$\frac{dI}{dt} = (1 - \theta)\omega E - (\lambda_s + \eta_s + \mu)I \geq -(\lambda_s + \eta_s + \mu)I$

$\Rightarrow \frac{dI}{dt} \geq -(\lambda_s + \eta_s + \mu)I$

$\Rightarrow I(t) \geq I^0 \exp(-\int_0^t (\lambda_s + \eta_s + \mu)\, ds \geq 0$
$i.e, I(t) \geq 0$

From the equation of (1.5),

$\frac{dQ}{dt} = \lambda_a A + (\lambda_s I - (\eta_q + \gamma_q + \mu)Q \geq -(\eta_q + \gamma_q + \mu)Q$
$\Rightarrow \frac{dQ}{dt} \geq -(\eta_q + \gamma_q + \mu)Q$
$\Rightarrow Q(t) \geq Q^0 \exp(-\int_0^t (\eta_q + \gamma_q + \mu)\, ds \geq 0$
$i.e, Q(t) \geq 0$

From the equation (1.6),

$\frac{dH}{dt} = \eta_s I + \eta_q Q - (\gamma_h + \mu_h + \mu)H \geq -(\gamma_h + \mu_h + \mu)H$
$\Rightarrow \frac{dH}{dt} \geq -(\gamma_h + \mu_h + \mu)H$
$\Rightarrow H(t) = H^0 \exp(-\int_0^t (\gamma_h + \mu_h + \mu)\, ds \geq 0$
$i.e,\ H(t) \geq 0$

From the equation (1.7),

$\frac{dR}{dt} = \gamma_a A + \gamma_q Q + \gamma_h H - \mu R \geq \mu R$
$\Rightarrow \frac{dR}{dt} \geq \mu R$
$\Rightarrow R(t) \geq R^0 \exp(-\int_0^t \mu)\, ds \geq 0$
$i.e, R(t) \geq 0.$

Similarly we can prove that $D(t) \geq 0$ *and* $P(t) \geq 0$.

Hence $(S(t), E(t), A(t), I(t), Q(t), H(t), R(t), D(t), P(t))$ *of (1) with primary conditions for all* $t \in [0, t_0]$ *are non negative solutions in* Ω.

We prove that the boundedness of the solutions (S, E, A, I, Q, H, R,D,P) of system (1).

The positivity of the solutions implies that $\frac{dS}{dt} \leq \Lambda - (\alpha + \mu)S$.

From the above equation, we can write that

$\lim_{t\to\infty} supS \leq \frac{\Lambda}{(\alpha+\mu)}$ *and* $S \leq \frac{\Lambda}{(\alpha+\mu)}$.

consider the entire population $N = S + E + A + I + Q + H + R + D + P$.

By derivation of above equation gives $\frac{dN}{dt} \leq \Lambda - (\alpha + \mu)N$ *which leads to* $\lim_{t\to\infty} supN \leq \frac{\Lambda}{(\alpha+\mu)}$.

This implies that $N \leq \frac{\Lambda}{(\alpha+\mu)}$.

$S + E + A + I + Q + H + R + D + P \leq \frac{\Lambda}{(\alpha+\mu)}$.

Hence all the solution trajectories $(S(t), E(t), A(t), I(t), Q(t), H(t), R(t), D(t), P(t)$ *with primary conditions were uniformly bounded in the region*

$\Omega = (S(t), E(t), A(t), I(t), Q(t), H(t), R(t), D(t), P(t)) \in \mathbb{R}^9_+ : 0 \leq (S, E, A, I, Q, H, R, D, P) \leq \frac{\Lambda}{(\alpha+\mu)}$.

3.2 Basic reproduction number

The basic reproduction number, symbolized as R_0, was a prominent parameter in the analysis of contagious disease and it was defined as the total number of secondary cases arising through a primary case in susceptible individuals. If $R_0 > 1$ then the secondary cases were more than one, so that disease will continue in the population and become an epidemic. If $R_0 < 1$ then the secondary cases were less than one, so that disease cannot spread and die out as soon as possible. If $R_0 = 1$ then there is only one secondary case so that the disease is stable. Since at protection rate α population was protected, the susceptible individuals became $S = N(1 - \alpha)$. The disease-free equilibrium point $E^0 = (N(1-\alpha), 0, 0, 0, 0, 0, 0, 0, 0)$ of system (1) exists. Through Next Generation Matrix O.Diekmann et al [29] P.van den Driessche & Watmough [32] and Khajanchi, S et al [21], R_0 value will be calculated mathematically.

$$\mathcal{F} = \begin{pmatrix} \beta\zeta_a(1-\alpha) + \beta\zeta_s(1-\alpha) + \beta\zeta_q(1-\alpha) \\ 0 \\ 0 \\ 0 \\ 0 \end{pmatrix} \&\mathcal{V} = \begin{pmatrix} (\omega+\mu)E \\ -\theta\omega E + (\lambda_a + \gamma_a + \mu_a + \mu)I_a \\ -(1-\theta)\omega E + (\lambda_s + \eta_s + \mu)I_s \\ -\lambda_a I_a - (\lambda_s I_s + (\eta_q + \gamma_q + \mu)Q \end{pmatrix}$$

At disinfection state $E = A = I = Q = H = 0$,The Jacobian of two matrices $\mathcal{F}$ and $\mathcal{V}$ are

$$F = \begin{pmatrix} 0 & \beta\zeta_a(1-\alpha) & \beta\zeta_s(1-\alpha) & \beta\zeta_q(1-\alpha) \\ 0 & 0 & 0 & 0 \\ 0 & 0 & 0 & 0 \\ 0 & 0 & 0 & 0 \end{pmatrix}$$

$$V = \begin{pmatrix} \omega+\mu & 0 & 0 & 0 \\ -\theta\omega & \lambda_a + \gamma_a + \mu_a + \mu & 0 & 0 \\ -(1-\theta)\omega & 0 & \lambda_s + \eta_s + \mu & 0 \\ 0 & -\lambda_a & -\lambda_s & \eta_q + \gamma_q + \mu \end{pmatrix}$$

Therefore R_0 was obtained from equation $R_0 = \rho(FV^{-1})$,where ρ represented the matrix FV^{-1} spectral radius. Hence, the reproduction number was

$$R_0 = \frac{(1-\theta)\beta\omega\zeta_s(1-\alpha)}{(\lambda_s+\eta_s+\mu)(\omega+\mu)} + \frac{\beta\theta\omega\zeta_a(1-\alpha)}{(\lambda_a+\gamma_a+\mu_a+\mu)(\omega+\mu)} + \frac{\beta\zeta_q((1-\theta)(\lambda_a+\gamma_a+\mu_a+\mu)\omega\lambda_s+(\lambda_s+\eta_s+\mu)\theta\omega\lambda_a)(1-\alpha)}{(\lambda_a+\gamma_a+\mu_a+\mu)(\lambda_s+\eta_s+\mu)(\eta_q+\gamma_q+\mu)(\omega+\mu)} \quad (1)$$

3.3 Disease-free equilibrium Stability analysis

The Jacobian matrix J_{E^0} of the classification of equations (1) at the equilibrium point $E^0(\frac{\Delta}{\mu}, 0, 0, 0, 0, 0, 0, 0, 0)$ was
$J_{E^0} =$

$$\begin{pmatrix} -(\alpha+\mu) & 0 & -\beta\zeta_a(1-\alpha) & -\beta\zeta_s(1-\alpha) & -\beta\zeta_q(1-\alpha) & 0 & 0 & 0 & 0 \\ 0 & \omega+\mu & \beta\zeta_a(1-\alpha) & \beta\zeta_s(1-\alpha) & \beta\zeta_q(1-\alpha) & 0 & 0 & 0 & 0 \\ 0 & \theta\omega & -(\lambda_a+\gamma_a+\mu_a+\mu) & 0 & 0 & 0 & 0 & 0 & 0 \\ 0 & (1-\theta)\omega & 0 & -(\lambda_s+\eta_s+\mu) & 0 & 0 & 0 & 0 & 0 \\ 0 & 0 & \lambda_a & \lambda_s & -(\eta_q+\gamma_q+\mu) & 0 & 0 & 0 & 0 \\ 0 & 0 & 0 & \eta_s & \eta_q & -(\gamma_h+\mu_h+\mu) & 0 & 0 & 0 \\ 0 & 0 & \gamma_a & 0 & \gamma_q & \gamma_h & -\mu & 0 & 0 \\ \alpha & 0 & 0 & 0 & 0 & 0 & 0 & 0 & 0 \\ 0 & 0 & 0 & \mu_a & 0 & \mu_h & 0 & 0 & 0 \end{pmatrix}$$

The characteristic equation of the matrix J_{E^0} was $\mid J_{E^0} - \lambda I \mid = 0$
$(\lambda+\mu)(\lambda+(\alpha+\mu))(\lambda^9 + a_1\lambda^8 + a_2\lambda^7 + a_3\lambda^6 + a_4\lambda^5 + a_5\lambda^4 + a_6\lambda^3 + a_7\lambda^2 a_8\lambda + a_9) = 0$
where $a_1 = (A + G + J + K + t + E + I)$
$a_2 = (G+J+K)t + A(G+J+K+t+E+I) + (G+J+K+I+t)E + (G+J+K+E+t)I + BF + CH + G(J+K) + JK)$,
$a_3 = A(G+J+K+E+I)\mu + GE + JE + GI + KE + JI + KI + EI + BF + CH + GJ + GK + JK) + ... + I(J+K)\mu$,
$a_4 = A(GEI + JEI + KEI + BFJ + CGH + BFK + CHJ + CHK + GJK + (EI + BF + CH)\mu + ... + BFKI + GJKE + GJKI$,
$a_5 = A(FK\lambda_a D + GH\lambda_s D + HK\lambda_s D + (BFI + GJE + GKE + GJI + JKE + JKI + F\lambda_a D)\mu + ... + CHJKt + h\mu DII$,
$a_6 = A(BFJKI + GHK\lambda_s D + (BFJI + BFKI + GJKE + GJKI + FK\lambda_a D + GH\lambda_s D)\mu +$

$... + (FK\lambda_a DI + BFJKI)\mu$,
$a_7 = A(GJKEI + CGHJK + FK\lambda_a DI + BFJKI + GHK\lambda_s D)\mu$,
$a_8 = 0$ and $a_9 = 0$
Here $A = (\alpha + \mu)$,B=$\beta\zeta_a(1-\alpha)$ and $C = \beta\zeta_s(1-\alpha)$, $D = \beta\zeta_q(1-\alpha)$, $E = (\mu + \omega)$, $F = \theta\omega$,
$G = (\lambda_a+\gamma_a+\mu_a+\mu)$, $H = (1-\theta)$, $I = (\lambda_s+\eta_s+\mu)$, $J = (\eta_q+\gamma_q+\mu)$, $K = ((\gamma_h+\mu_h+\mu)$.
Hence J_{E^0} is singular because one of the eigenvalues is zero. Therefore at the disease-free equilibrium, the stability of the system (1) does not exists by using eigenvalues.

Theorem 2. *The Disease-Free Equilibrium* $E^0 = (\frac{\Lambda}{\mu}, 0, 0, 0, 0, 0, 0)$ *was locally asymptotically stable for* $R_0 < 1$ *and unstable for* $R_0 > 1$

Since the J_{E^0} has zero eigen value, according to Kermack WO [20] and singh HP[39], the theorem was satisfied that is the Disease-Free Equilibrium $E^0 = (\frac{\Lambda}{\mu}, 0, 0, 0, 0, 0, 0)$ was locally asymptotically stable for $R_0 < 1$ and unstable for $R_0 > 1$.

Table 2: Fitted parameters and their sensitivity indices list of SEAIQHRDP model

parameter	value	References	sensitivity indices
π	varies	-	-
ζ_a	0.4	Gumel AB et al.[12]	0.4547
ζ_s	0.4	Nadim SS et al.[27]	0.2416
ζ_q	0.3	Biswas, Sudhanshu Kumar et al [4]	0.3037
θ	0.7	Fergusonm.N et al. [10]	-0.0015
ω	0.1	R. Li et al. [36]	-0.1048
β	0.9714	evaluated	1.0000
α	0.0016	evaluated	-0.07158
λ_a	0.4614	evaluated	-0.1764
λ_s	0.1143	evaluated	-0.0997
η_s	0.1840	evaluated	-0.1418
η_q	0.0742	evaluated	-0.0948
γ_a	0.1302	evaluated	-0.2757
γ_q	0.1661	evaluated	-0.2088
γ_h	0.1777	evaluated	-0.2278
μ_a	0.0035	evaluated	-0.0207
μ_h	0.1544	evaluated	-0.0233
μ	0.0000391	Worldmeter.info/coronavirus [16]	-0.1070

4 Numerical simulation

In this sector, the numerical simulation of confirmed cases of COVID-19 for India was performed and the simulation results were compared with actual data [21] from 30^{th}, January 2020 to 13^{th}, January 2021. The SEAIQHRDP model fitted to daily and cumulative confirmed coronavirus cases in India which illustrates a satisfactory estimation. The model parameters β, α, λ_a, λ_s, η_s, η_q, γ_a, γ_q, γ_h, μ_a, μ_h and μ were estimated by using a nonlinear least squares regression method (LSQNONLIN function) in MATLAB.

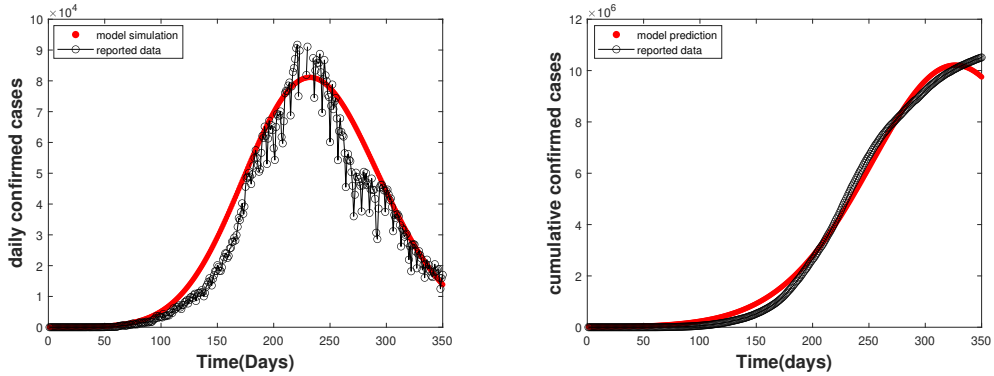

(a) (b)

Figure 2: The model fitting of reported (a) daily confirmed cases and (b) cumulative confirmed cases of COVID-19 in India.

The minimizing error was

$$R(\Phi) = \sum_{t=1}^{n} (Q_t(\Phi) - Q_t\bar{}(\Phi))^2 \tag{2}$$

where $Q_t(\Phi)$ and $Q_t\bar{}(\Phi)$ were a cumulative number of confirmed cases through actual data and model prediction. In Table 2, the values for the estimated and fixed parameters were shown. The fundamental reproduction numberR_0 was determined as 2.089 using the fixed and model parameters in Table 2.

In Figure.2 the curve fitting was taken from 30^{th}, January 2020 to 13^{th}, January 2021 in apicovid19india.org [13] in India. The black curve represented the reported COVID-19 cases and the red curve denoted the model simulation COVID-19 cases.

5 Sensitivity analysis

Sensitivity analysis was used in defining the impact of different factors in the spread of COVID-19. This analysis was used to identify the growth and reduction in basic reproduction numbers concerning numerous parameters. A complete chapter on the sensitivity analysis of the dengue virus was obtained in Rodrigues H et al. [37] and Burattini, M.N et al [6]. Whenever the significant parameters were recognized, different strategies will be executed to get optimum results. To identify such parameters, the sensitivity index of R_0 concerning various parameters was estimated. The normalized sensitivity index of R_0 is defined as

$$\Gamma_q^{R_0} = \frac{\partial R_0}{\partial q} \times \frac{q}{R_0}.$$

where q was the significant parameter, whose sensitivity on R_0 obtained by using normalized forward sensitivity index method Biswas, S et al [5].

The highest sensitive parameter on reproduction number was the parameter whose index was high in magnitude. If the sensitivity of parameter q was positive, R_0 was increased whenever the parameter q increased. Similarly, the sensitivity of parameter q was negative, R_0 was decreased whenever the parameter q increased. From Figure.3

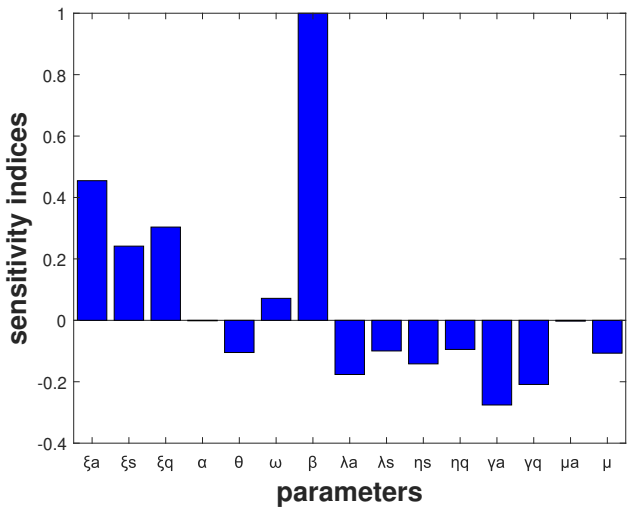

Figure 3: Normalized local sensitivity indices of R_0 with respect to each model parameter.

it was observed the parameters θ, λ_a, λ_s, η_s, η_q, γ_a, γ_q, μ_a have negative indices with R_0 and the parameters ζ_a, ζ_s , ζ_q, β, ω, μ share positive indices with R_0. So that R_0 value increased as the parameters ζ_a, ζ_s and ζ_q increased and R_0 value decreased as the parameters θ, η_s, η_q and γ_q increased. Hence the sensitive analysis determined that the parameters ζ_a, ζ_s, ζ_q, β, θ, η_s,γ_a and γ_q were more effective parameters. The sensitivity indices of various parameters had been displayed in Table 2.

Figure.4(a) represented that R_0 Contour Plot with respect to virus transmission rate (β) and quarantine rate (λ_s) from symptomatic population. This figure described a reduction in R_0 with a decrease in virus transmission rate (β) and an increase in quarantine rate (λ_s) from the symptomatic population. Figure.4(b) explained R_0 Contour Plot with respect to virus transmission rate (β) and hospitalization rate (η_s) from symptomatic population. This figure described a reduction in R_0 with a decrease in virus transmission rate β and an increase in hospitalization rate (η_s) from the symptomatic population. Figure.4(c) displayed R_0 Contour Plot with respect to quarantine rate (λ_a) from asymptomatic population and recovery rate (γ_q) from quarantine population. This figure demonstrated reduction in R_0 with an increase in quarantine rate (λ_a) from an asymptomatic population and an increase in recovery rate (γ_q) from quarantine population. Figure.4(d) expressed the Contour Plot of the Basic Reproduction Number concerning hospitalization rate (η_s) from symptomatic population and hospitalization rate (η_q) from quarantine population. This figure illustrated R_0 rises with a decrease in hospitalization rate (η_s) from the symptomatic population and hospitalization rate (η_q) from the quarantine population.

5.1 COVID-19 Prevalence changes with various parameters

From Figure.5 to Figure.9, It was perceived that the asymptomatic infected and symptomatic infected individuals were reduced if the protection rate (α) from susceptible individuals, quarantine rate (λ_a) from asymptomatic individuals, quarantine rate (λ_s) from symptomatic individuals, hospitalization rate (η_q) from quarantine individuals and hospitalization rate (η_s) from symptomatic individuals increased.

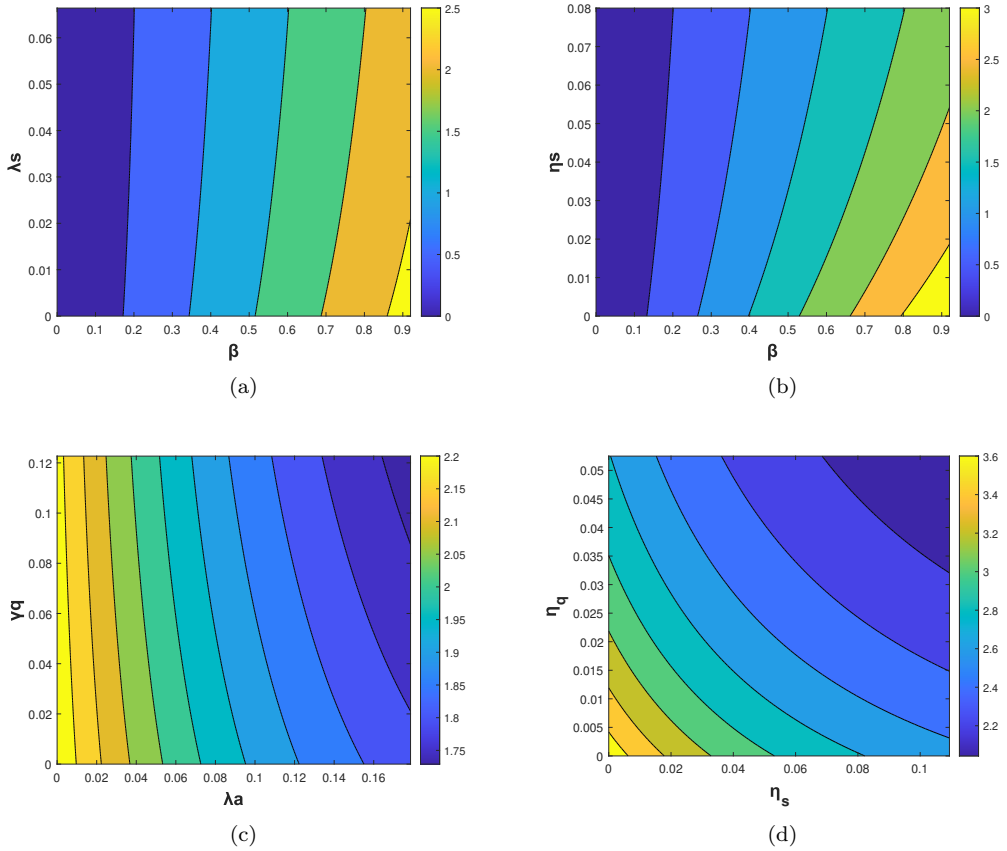

Figure 4: Contour plots of basic reproduction number R_0 with respect to (a) (β, λ_s), (b) (β η_s), (c) (λ_a, γ_q) and (d) (η_s, η_q).

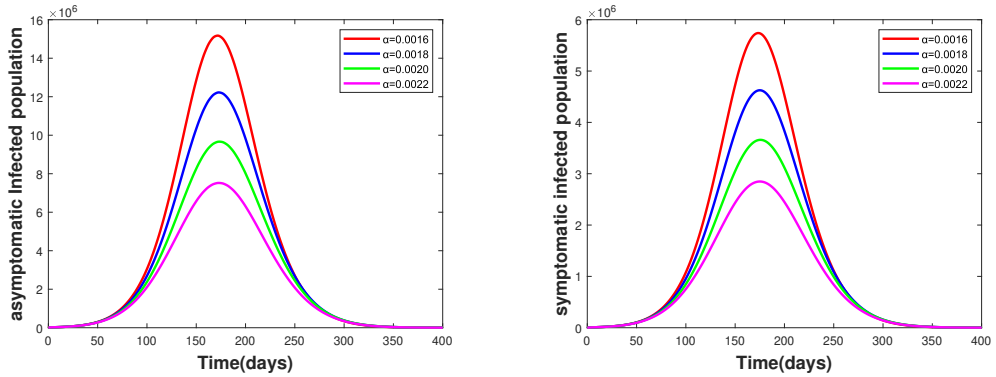

Figure 5: Effect of parameter α on (a) asymptomatic infected populace and (b) symptomatic infected populace

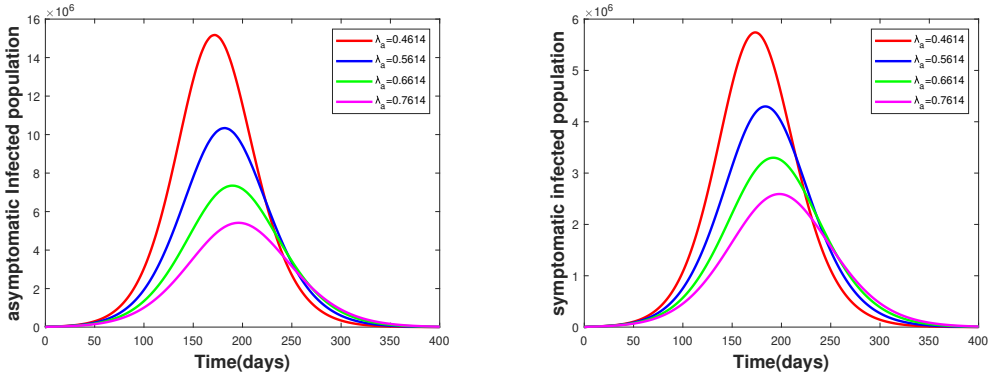

(a) (b)

Figure 6: Effect of parameter λ_a on (a) asymptomatic infected populace and (b) symptomatic infected populace

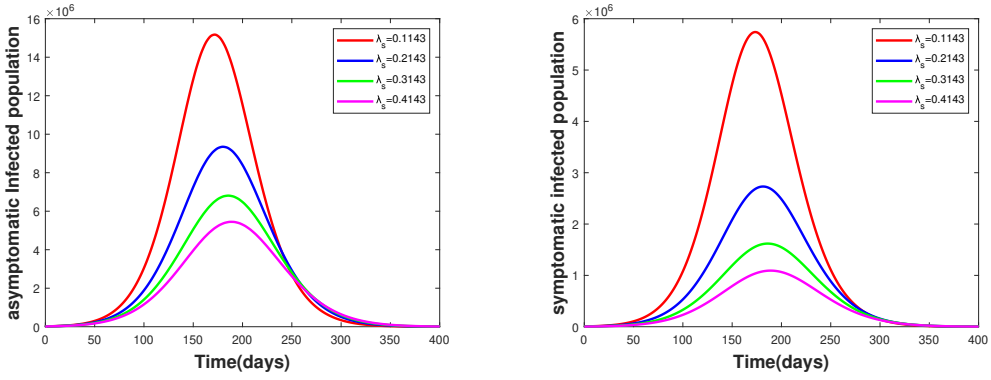

(a) (b)

Figure 7: Effect of parameter λ_s on (a) asymptomatic infected populace and (b) symptomatic infected populace

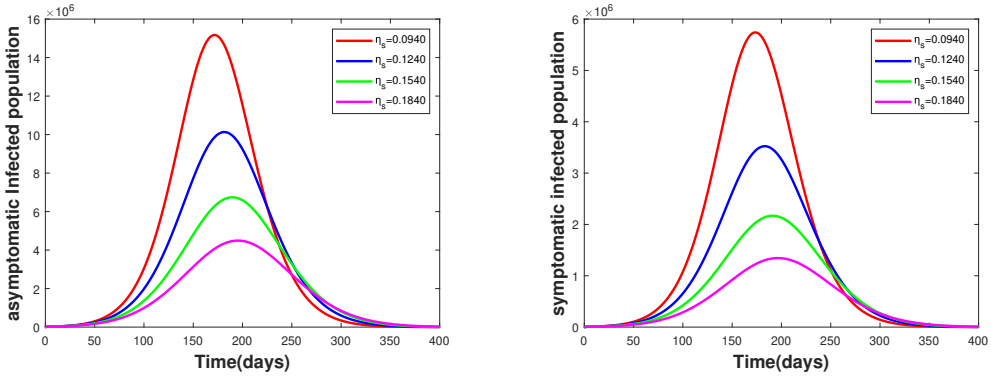

(a) (b)

Figure 8: Effect of parameter η_q on (a) asymptomatic infected populace and (b) symptomatic infected populace

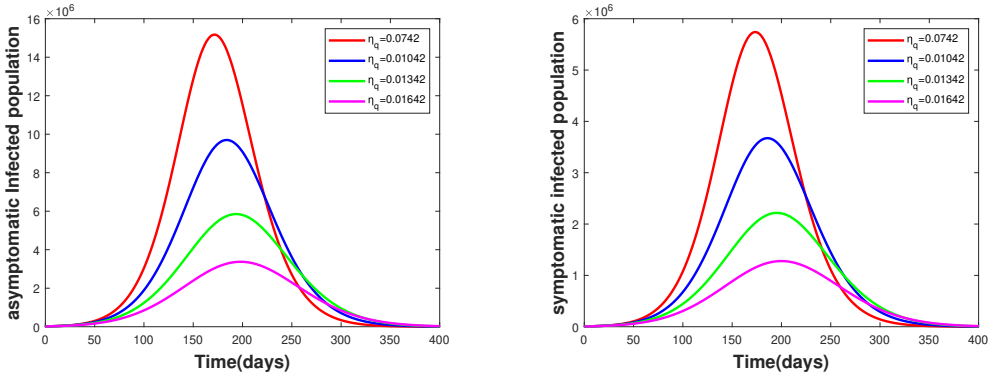

(a) (b)

Figure 9: Effect of parameter η_s on (a) asymptomatic infected populace and (b) symptomatic infected populace

6 Optimal control

6.1 Optimal control problem

The effectiveness of control techniques was crucial in decreasing the spread of the COVID-19 virus. It was essential to improve a policy that minimizes both the number of infected populations and related costs. In this phase, the optimal control technique was a tremendously useful tool for defining such a strategy. Now we study the impact of pharmacological interventions to diminish the spread of the virus. To achieve this, the system(1) can be extended by including three control variables $u_1(t)$, $u_2(t)$ and $u_3(t)$ where
(a) Control $u_1(t)$ represented the degree of protection provided by government interventions. The function of this control variable was to enhance the protection rate α.
(b) Control $u_2(t)$ described the treatment of asymptomatic infected individuals. The function of this control variable was to develop the quarantine rate (λ_a) from asymptomatic infected individuals.
(c) Control $u_3(t)$ characterized the treatment of symptomatic infected (both quarantine and hospitalization) individuals. The function of this control variable was to improve the quarantine rate (λ_s) and hospitalization rate (η_s) from symptomatic infected individuals. The three control variable values were assumed between 0 and 1.
There was no efforts made in these controls if $u_1 = u_2 = u_3 = 0$ and maximum efforts had been placed if $u_1 = u_2 = u_3 = 1$
By considering all the above suppositions, the optimal control model was formulated as

$\frac{ds}{dt} = \pi - \beta\frac{(\zeta_a A+\zeta_s I_s+\zeta_q Q)S}{N} - (\alpha + u_1 + \mu)S$
$\frac{dE}{dt} = \beta\frac{(\zeta_a A+\zeta_s I_s+\zeta_q Q)S}{N} - (\omega + \mu)E$
$\frac{dA}{dt} = \theta\omega E - (\lambda_a + u_2)A + \gamma_a + \mu_a + \mu)A$
$\frac{dI}{dt} = (1-\theta)\omega E - (\lambda_s + u_3 + \eta_s + u_3 + \mu)I$
$\frac{dQ}{dt} = (\lambda_a + u_2)A + (\lambda_s + u_3)I - (\eta_q + \gamma_q + \mu)Q$
$\frac{dH}{dt} = (\eta_s + u_3)I + \eta_q Q - (\gamma_h + \mu_h + \mu)H$
$\frac{dR}{dt} = \gamma_a A + \gamma_q Q + \gamma_h H - \mu R$
$\frac{dD}{dt} = \mu_a A + \mu_h H$
$\frac{dP}{dt} = \alpha S$

Now we detect $u_1(t)$, $u_2(t)$ and $u_3(t)$'s optimal values that minimize the objective functional
$\mathcal{J}(u_1(t), u_2(t), u_3(t))=\int_0^{t_f} (C_1 A + C_2 I + C_3 Q + C_4 H + \frac{1}{2}(C_5 u_1^2 + C_6 u_2^2 + C_7 u_3^2)\, dt$
subject to the system (2), which contained the sum of asymptomatic infected, symptomatic infected, quarantined, and hospitalized population, besides the optimal controls $u_1(t)$, $u_2(t)$ and $u_3(t)$. These were bounded and Lebesgue integral functions Kirschner D et al [9] and S. Lenhart and J.T.Workman [40]). Here The positive coefficients C_1, C_2, C_3, C_4, C_5, C_6 and C_7 were corresponding balancing weight constants parameters of stated infected variables and optimal controls.
The main purpose was to determine the optimal controls variables $u_1^*(t)$,$u_2^*(t)$,$u_3^*(t)$ such that

$$\mathcal{J}(u^*(t)) = \min_{u_1,u_2,u_3 \in U} \mathcal{J}((u_1(t), u_2(t), u_3(t))$$

where Φ= $\{u_1, u_2, u_3$: $u_1, u_2, u_3 /\ u_1, u_2, u_3 : [0, t_f] \to [0, 1]$ are lebsegue integrable$\}$.

Through Pontryagin's maximum principle Pontryagin, L et al [31], we derived the essential conditions for this optimal control problem. The Lagrangian function was given

by
$\mathcal{L}(S,E,A,I,Q,H,R,u_1(t),u_2(t),u_3(t)) = C_1A+C_2I+C_3Q+C_4H+\frac{1}{2}(C_4u_1^2+C_5u_2^2+C_5u_3^2$
The Hamiltonian function $\mathcal{H}$ obtained as
$\mathcal{H} = C_1A + C_2I + C_3Q + C_4H + \frac{1}{2}(C_4u_1^2 + C_5u_2^2 + C_5u_3^2 + \lambda_1\frac{dS}{dt} + \lambda_2\frac{dE}{dt} + \lambda_3\frac{dA}{dt} + \lambda_4\frac{dI}{dt} + \lambda_5\frac{dQ}{dt} + \lambda_6\frac{dH}{dt} + \lambda_7\frac{dR}{dt} + \lambda_8\frac{dD}{dt} + \lambda_9\frac{dP}{dt}$
where λ_1 λ_2, λ_3 , λ_4, λ_5, λ_6 and λ_7 are the adjoint variables.
The of differential equation form of adjoint variables were as follows.
$\frac{d\lambda_1}{dt} = -\frac{\partial\mathcal{H}}{\partial S} = (\lambda_1 - \lambda_2\beta(\frac{(\zeta_aA+\zeta_sI_s+\zeta_qQ)}{N} + (\lambda_1 - \lambda_8(\alpha+u_1) + \lambda_1u_1$
$\frac{d\lambda_2}{dt} = -\frac{\partial\mathcal{H}}{\partial E} = (\omega+\mu)\lambda_2 - \lambda_4 - \lambda_3\theta\omega - \lambda\omega$
$\frac{d\lambda_3}{dt} = -\frac{\partial\mathcal{H}}{\partial A} = -C_1 + (\lambda_1-\lambda_2)\beta\frac{\zeta_aS}{N} + (\lambda_3-\lambda_5)(\lambda_a+u_2) + ((\lambda_3-\lambda_8)\mu_a + \mu\lambda_3$
$\frac{d\lambda_4}{dt} = -\frac{\partial\mathcal{H}}{\partial I} = -C_2 + (\lambda_1-\lambda_2)\beta\frac{\zeta_sS}{N} + (\lambda_4-\lambda_5)(\lambda_s+u_3) + (\lambda_4-\lambda_6)(\eta_s+u_3) + \mu\lambda_4$
$\frac{d\lambda_5}{dt} = -\frac{\partial\mathcal{H}}{\partial Q} = -C_3 + (\lambda_1-\lambda_2)\beta\frac{\zeta_qS}{N} + (\lambda_5-\lambda_6)\eta_q + (\lambda_5-\lambda_7)\gamma_q + \mu\lambda_5$
$\frac{d\lambda_6}{dt} = -\frac{\partial\mathcal{H}}{\partial H} = -C_4 + (\lambda_6-\lambda_7)\gamma_h + (\lambda_6-\lambda_8)\mu_h + \mu)$
$\frac{d\lambda_7}{dt} = -\frac{\partial\mathcal{H}}{\partial R} = \mu\lambda_7$
$\frac{d\lambda_8}{dt} = -\frac{\partial\mathcal{H}}{\partial D} = 0$
$\frac{d\lambda_9}{dt} = -\frac{\partial\mathcal{H}}{\partial P} = 0$

we minimize Hamilton function relating to control variables $u_1^*(t)$,$u_2^*(t)$ and $u_3^*(t)$.
Using the optimal conditions $\frac{\partial\mathcal{H}}{\partial u_1} = 0$, $\frac{\partial\mathcal{H}}{\partial u_2} = 0$ and $\frac{\partial\mathcal{H}}{\partial u_3} = 0$, we get
$\frac{\partial\mathcal{H}}{\partial u_1} = C_5u_1 - \alpha\lambda_1 + \alpha\lambda_9S = 0 \Rightarrow u_1^* = \frac{(\lambda_1-\lambda_9)\alpha S}{NC_5}$
$\frac{\partial\mathcal{H}}{\partial u_2} = C_6u_2 - \lambda_3A + \lambda_5A = 0 \Rightarrow u_2^* = \frac{(\lambda_3-\lambda_5)A}{C_6}$
$\frac{\partial\mathcal{H}}{\partial u_3} = C_7u_3 - ((\lambda_4-\lambda_5+(\lambda_4-\lambda_6)I = 0 \Rightarrow u_3^* = \frac{((\lambda_4-\lambda_5)+(\lambda_4-\lambda_6))I}{C_7}$

6.2 Optimal control model simulation

With the values of the parameters mentioned in Table 2, numerical simulation was conducted for the optimal control problem (2) in MATLAB by using an iterative fourth-order Runge-Kutta method (Kamien, M et al [19] and Lukes, D.L.[24]) for the period [0,400]. The baseline weight parameters were taken as $C_1 = 1$, $C_2 = 1$, $C_3 = 1$, $C_4 = 1$,$C_5 = 40$, $C_6 = 40$ and $C_7 = 45$.

In Figure.10, variations of exposed, asymptomatic infected, symptomatic infected, quarantine, hospitalization, and dead populace with and without control had performed. This figure shows that, in comparison to the infected population without control, the infected population decreased quickly under control.

In Figure.11, variations of recovered and insusceptible Populace with and without control were executed. This graph demonstrates that the disinfected population under control swiftly rose in comparison to the disinfected population without control.

According to Figure.12, the best controls, u_1,u_2 and u_3 combined their efforts extremely well to increase the protection rate (α) from susceptible individuals, the quarantine rates (λ_a, λ_s)from asymptomatic infected and symptomatic infected individuals, and the hospitalization rates (η_q, η_s) from symptomatic and quarantine individuals.

From these figures we perceived that in the presence of optimal control strategy the number of susceptible, exposed, asymptomatic infected, symptomatic infected, quarantined, hospitalized, and dead individuals were reduced rapidly while the number of recovered and insusceptible individuals were increased swiftly comparing with the populations without control strategy.

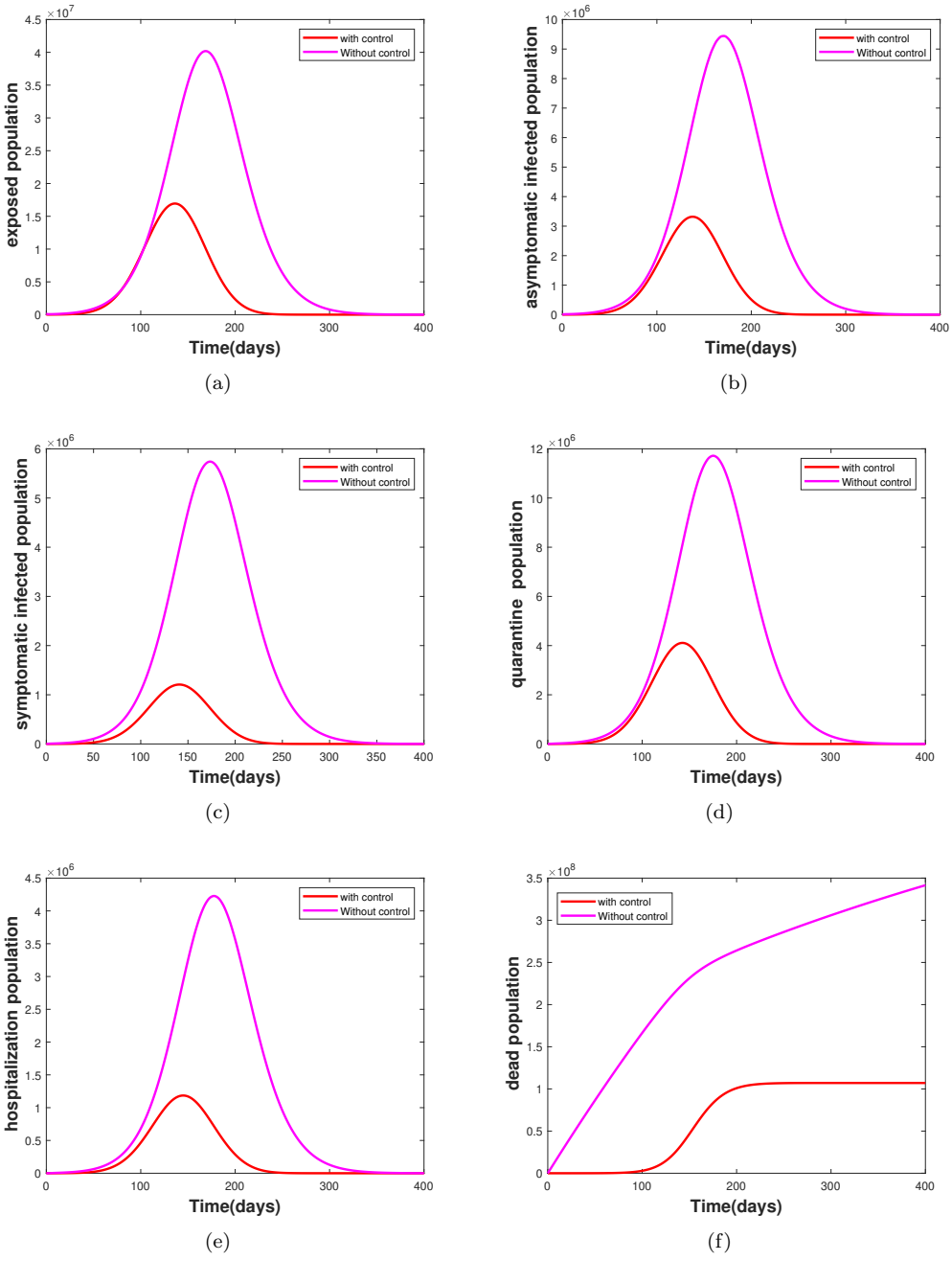

Figure 10: Variations of (a) exposed (b) asymptomatic (c) symptomatic infected (d) quarantine (e) hospitalization and (f) dead populations with and without control

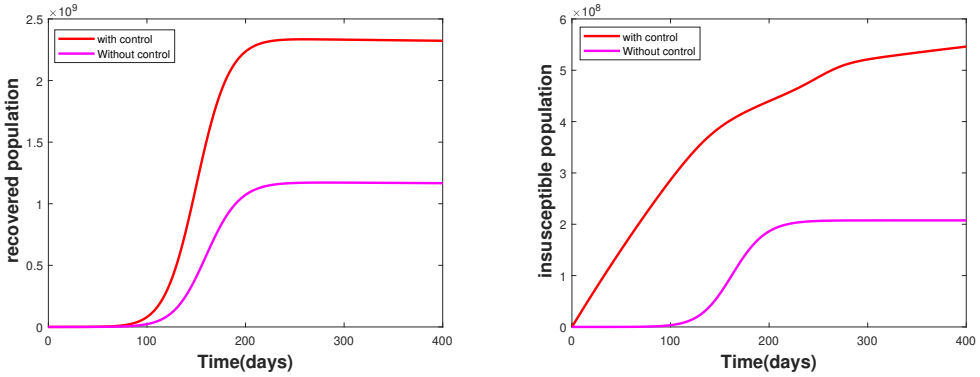

(a) (b)

Figure 11: Variations of (a) recovered (b) insusceptible population with and without control

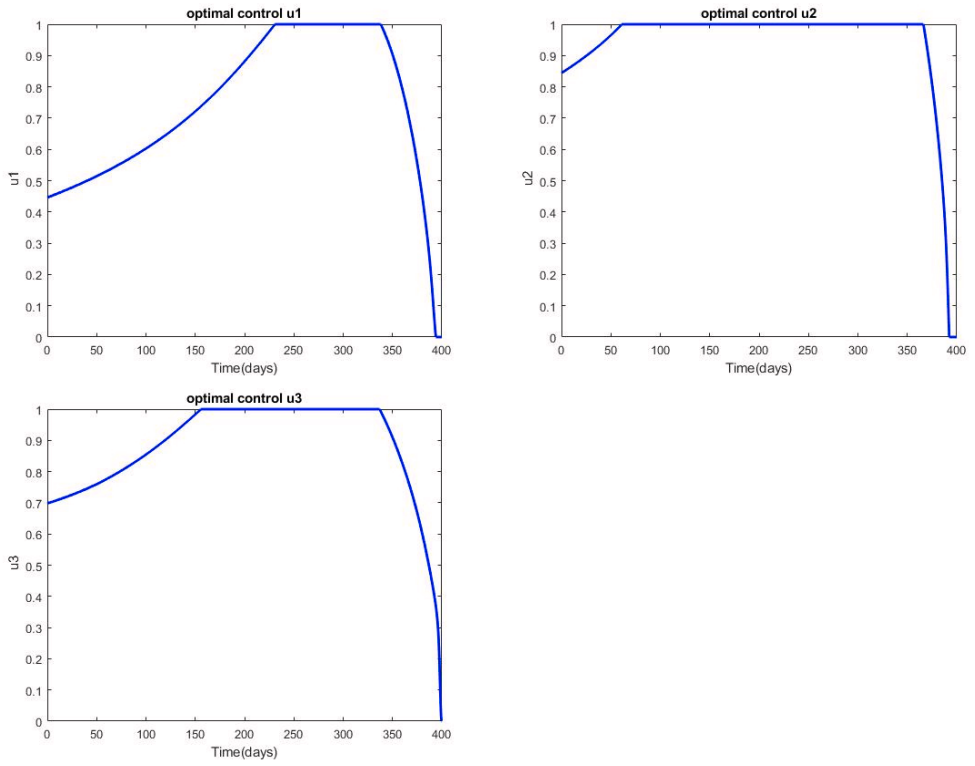

Figure 12: Dynamics of Optimal Controls u_1, u_2 and u_3

7 Conclusion

Epidemiological models aid in understanding the dynamics of infectious illness transmission. The deterministic mathematical model with 9 compartments was thoroughly studied in this paper. First, the elementary properties of the model such as the positivity and boundedness of the SEAIQHRDP model, the expression of R_0, and the local stability of the disease-free equilibrium were performed. Our suggested model has 18 parameters, but we only calculated 11 of them based on the sensitivity analysis. Through sensitivity analysis, it was observed that just eight parameters are very sensitive concerning clinically unwell or infected patients. The time series behavior of the infected populations for 400 days was examined concerning variations in parameters. From this, the spread of infections can be slowed down by increasing the protection rate, hospitalization rate, and quarantine rate. The best optimal control analysis was then carried out by including three control factors, one of which was increased protection, and the other two were improved quarantine and medical facilities for both identified and unidentified affected people. Through the Optimal control strategy, it was found that the infected populations were reduced rapidly, and disinfected populations were increased compared with the infected and disinfected populations without optimal control technique. When the best control approach is used early in a pandemic, the intensity of epidemic peaks tends to decline, spreading the maximum impact of an epidemic across a longer period. Finally, this study leads to the conclusion the rising of infections can be controlled only if the implementation of rapid testing, quarantine centers, and medical facilities. Additionally, we intend to increase the scope of our modeling work by including vaccination and the impact of environmental contaminants in the future.

References

[1] Alexander Krämer, Mirjam Kretzschmar, Klaus Krickeberg. "Krickeberg Modern Infectious Disease Epidemiology." 2010 : 209–221.(2010)

[2] Bai Y, Liu K, Chen Z. " Early transmission dynamics of novel coronavirus pneumonia epidemic in Shaanxi Province [J]." Chin J Nosocomiol 30(6):834–838(2020)

[3] Bandekar SR, Ghosh M." Mathematical modeling of COVID-19 in India and its states with optimal control." Model Earth Syst Environ. 2022;8(2):2019-2034. doi:10.1007/s40808-021-01202-8(2020)

[4] Biswas SK, Ghosh JK, Sarkar S, Ghosh U."COVID-19 pandemic in India: a mathematical model study." Nonlinear Dyn. 2020;102(1):537-553. doi:10.1007/s11071-020-05958-z(2020)

[5] Biswas SK, Ghosh U, Sarkar S. "Mathematical model of zika virus dynamics with vector control and sensitivity analysis.", Infect. Dis. Model. 5, 23–41 (2020)

[6] Brauer F, Chavez CC. "Mathematical models in population biology and epidemiology." Springer, New York, NY. https://doi. org/10.1007/978-1-4614-1686-9 (2012)

[7] Burattini MN, Massad E, Coutinho, FAB. "Estimation of R_0 from the initial phase of an outbreak of a vector-borne infection." Trop. Med. Int. Health 15(1), 120–26 (2010)

[8] Danane J, Hammouch Z, Allali K, Rashid S, Singh J. "A fractional-order model of coronavirus disease 2019 (COVID-19) with governmental action and individual reaction." Math Methods Appl Sci. 2021 Aug 25:10.1002/mma.7759. doi: 10.1002/mma.7759.(2021)

[9] D. Kirschner, S. Lenhart, S. Serbin. "Optimal control of the chemotherapy of HIV." Journal of Mathematical Biology, vol. 35, no. 7, pp. 775–792,(1997).

[10] Fergusonm.N et al Report 9: Impact of non-pharmaceutical interventions (NPIs) to reduce COVID19 mortality and healthcare demand, in https://doi.org/10.25561/77482 (2020).

[11] Giordano G, Blanchini F, Bruno R, Colanary P, Filippo AD, Matteo AD, Colaneri M. "Modelling the COVID-19 epidemic and implementation of population-wide interventions in Italy." Nat Med 26:855–860.(2020)

[12] Gumel AB, Ruan S, Day T, Watmough J, Brauer F, van den Driessche P, Gabrielson D, Bowman C, Alexander ME, Ardal S, Wu J, Sahai BM. "Modelling strategies for controlling SARS outbreaks." Proc Biol Sci. 2004 Nov 7;271(1554):2223-32. (2020)

[13] https://api.covid19india.org/documentation/csv/ Coronavirus outbreak in India. Google sheets

[14] https://www.who.int/director-general/speeches/detail/who-director-general-s-opening-remarks-at-the-media-briefing-on-COVID-19-11-march-2020

[15] https://covid19.who.int

[16] https://www.Worldmeter.info/coronavirus

[17] Huang G, Pan Q, Zhao S, Gao Y, Gao X. "Prediction of COVID-19 outbreak in China and optimal return date for university students based on propagation dynamics". J Shanghai Jiaotong Univ 25:140–146. (2020)

[18] H.W. Hethcote. "The mathematics of infectious diseases". SIAM Review 42.4 ,pp. 599-653. ISSN: 00361445(2000)

[19] Kamien, MI, Schwartz NL. "Dynamic Optimization: The Calculus of Variations and Optimal Control in Economics and Management". Modern Economy, Vol.11 No.7, July 15, 2020 (2020)

[20] Kermack WO, McKendrick AG "A contribution to the mathematical theory of epidemics". Proceedings of the London. Series A Contain Papers Mathematical Phys Charact 115(772):700–721 (1927)

[21] Khajanchi S, Bera S, Roy TK. "Mathematical analysis of the global dynamics of a HTLV-I infection model, considering the role of cytotoxic T-lymphocytes". Math. Comput.Simul. 180, 354–378 (2021)

[22] Lin Q, Zhao S, Gao D, Lou Y, Yang S, Musa S, Wang M, Cai Y, Wang W, Yang L. "A conceptual model for the outbreak of Coronavirus disease (COVID-19) in Wuhan, China with individual reaction and governmental action". Int J Infect Dis 93:211–216.(2020)

[23] Liu C, Ding G, Gong J, Wang L, Cheng K, Zhang D. "Studies on mathematical models for SARS outbreak prediction and warning". Chin Sci Bull 49(21):2245–2251(2004)

[24] Lukes DL. "Differential equations, classical to controlled". Mathematical Science Engineering 162. AcademicPress, New York (1982)

[25] Massad E, Coutinho FAB, Wilder-Smith A. Modelling an optimum vaccination strategy against ZIKA virus for outbreak use. Epidemiol Infect. 2019;147:e196. doi:10.1017/S0950268819000712(2019)

[26] Mwalili S, Kimathi M, Ojiambo V, Gathungu D, Mbogo R. "SEIR model for COVID-19 dynamics incorporating the environment and social distancing." BMC Res Notes. 2020 Jul 23;13(1):352(2020)

[27] Nadim SS, Ghosh I, Chattopadhyay J. "Short-term predictions and prevention strategies for COVID-19." A model-based study. Appl Math Comput. 2021 Sep 1;404:126251.(2021)

[28] NCBI: "First confirmed case of COVID-19 infection in India: a case report." https://www.ncbi.nlm.nih.gov/pmc/articles/ PMC7530459(2020)

[29] O. Diekmann, J. Heesterbeek, J. Metz. "On the definition and the computation of the basic reproduction ratio R_0 in models for infectious diseases in heterogeneous populations." J. Math. Biol. 28, 365–382 (1990)

[30] Peng L, Yang W, Zhang D, Zhuge C, Hong L. "Epidemic analysis of COVID-19 in China by dynamical modeling." medRxiv 2020.02.16.20023465; doi: https://doi.org/10.1101/2020.02.16.20023465(2020).

[31] Pontryagin, L.S., Boltyanskii, V.G., Gamkrelidze, R.V., Mishchenko, E.F. "The Mathematical Theory of Optimal Processes." Wiley-Interscience, New York (1962)

[32] P. van den Driessche, J. Watmough. "Reproduction numbers and sub-threshold endemic equilibria for compartmental models of disease transmission." Math. Biosci. 180(1–2), 29–48(2002)

[33] Raj Kishore, B.Sahoo, D.Swain, Kisor K. Sahu. "Analysis of COVID19 Outbreak in India using SEIR model." arXiv preprint arXiv:2010.13610 (2010)

[34] Read JM, Bridgen JR, Cummings DA, Ho A, Jewell CP. "Novel coronavirus 2019-nCoV: early estimation of epidemiological parameters and epidemic predictions." MedRxiv 2020.01.23.20018549; doi: https://doi.org/10.1101/2020.01.23.20018549 (2020)

[35] Rehman, Attiq ul, Ram Singh, Jagdev Singh. "Mathematical analysis of multi-compartmental malaria transmission model with reinfection." Chaos, Solitons and Fractals, volume 163, 112527, ISSN 0960-0779, https://doi.org/10.1016/j.chaos.2022.112527.(2022)

[36] R Li, Pei S, Chen B, Song Y, Zhang T, Yang W, Shaman J. "Substantial undocumented infection facilitates the rapid dissemination of novel coronavirus (SARS-CoV-2)." Science. 2020 May 1;368(6490):489-493. doi: 10.1126/science.abb3221(2020)

[37] Rodrigues H, Teresa M, Delfim F, Torres M. "Sensitivity Analysis in a Dengue Epidemiological Model." Conference Paper, Open Access Volume 2013, Article ID 721406, https://doi.org/10.1155/2013/721406(2013)

[38] RM May, Anderson RM. "Population biology of infectious diseases." Part II. Nature. 1979 Aug 9; 280(5722): 455-61. doi: 10.1038/280455a0. PMID: 460424(1979)

[39] Singh HP, Kumari p, Singh S. "SEIAQRDT model for the spread of novel coronavirus (COVID-19): A case study in India." Appl Intell (Dordr). 2021;51(5):2818-2837. doi: 10.1007/s10489-020-01929-4. Epub 2020 Nov 13. PMID: 34764566; PMCID: PMC7662031(2020)

[40] S. Lenhart, Workman JT. "Optimal Control Applied to Biological Models, Mathematical and Computational Biology Series." Chapman Hall CRC,(2007)

[41] Singh J, Ganbari B, Kumar D, Baleanu D. "Analysis of fractional model of guava for biological pest control with memory effect." J Adv Res. 2020 Dec 10;32:99-108. doi: 10.1016/j.jare.2020.12.004. PMID: 34484829; PMCID: PMC8408328(2020)

[42] Supriya Yadav, Devendra Kumar, Jagdev Singh, Dumitru Baleanu. "Analysis and dynamics of fractional order Covid-19 model with memory effect." Results in Physics, volume 24,2021, 104017, ISSN 2211-3797, https://doi.org/10.1016/j.rinp.2021.104017 (2021)

On nonempty intersection properties in metric spaces

A. Gupta[1*] and S. Mukherjee[1]

[1]Department of Mathematics,
NIT Meghalaya, Shillong-793003, Meghalaya, India

Abstract

The classical Cantor's intersection theorem states that in a complete metric space X, intersection of every decreasing sequence of nonempty closed bounded subsets, with diameter approaches zero, has exactly one point. In this article, we deal with decreasing sequences $\{K_n\}$ of nonempty closed bounded subsets of a metric space X, for which the Hausdorff distance $H(K_n, K_{n+1})$ tends to 0, as well as for which the excess of K_n over $X \setminus K_n$ tends to 0. We achieve nonempty intersection properties in metric spaces. The obtained results also provide partial generalizations of Cantor's theorem.

Keywords Metric space · Atsuji space · Hausdorff metric · Nested sequence · Cantor's intersection theorem

Mathematics Subject Classification (2020) 54E50 · 54A20

1 Introduction

In metric spaces, there are some marvellous nonempty intersection theorems. Cantor's theorem (see [14]) asserts that in a complete metric space X, the intersection of every decreasing sequence $\{K_n\}$ of nonempty closed subsets of X with diameter $\delta(K_n) \to 0$ has exactly one point. This intersection theorem is widely used in the fields related to mathematical analysis. Kuratowski provided a generalization of Cantor's theorem using Kuratowski measure of non-compactness, α:

$$\alpha(A) = \inf\{\varepsilon > 0 : \exists\ X_i, i = 1, \cdots, n, X_i \subset X, \delta(X_i) < \varepsilon, A = \cup_i X_i\},$$

where A is a subset of a complete metric space X. Kuratowski's theorem (see [6, 15]) states that for each decreasing sequence $\{K_n\}$ of nonempty closed subsets of a complete metric space X with $\lim_{n\to\infty} \alpha(K_n) \to 0$, $\bigcap_{n=1}^{\infty} K_n$ is nonempty

*Corresponding author. *E-mail address:* ajitkumar.gupta@nitm.ac.in

and compact. Later, this theorem is further generalized by Horvath [3] using the same measure of compactness α. In [9], Mitrovic et al. have studied the generalization of Horvath's results; and they applied this generalization for best approximation in [10]. Recently, Souza and Alves [15] extended both Cantor's theorem and Kuratowski's theorem from metric spaces to admissible spaces.

An Atsuji space, which is more general than compact spaces, has the property that each continuous function on it is uniformly continuous. A metric space X is said to be an Atsuji space if the set of limit points X' is compact in X and for each $\epsilon > 0$ the complement of the set $N_\epsilon(X') := \bigcup_{x \in X'} B(x, \epsilon)$, in X, is uniformly discrete, where $B(x, \epsilon)$ denotes the open ball centered at x and with radius ϵ. For a metric space, the property of being an Atsuji space lies in between the compactness and the completeness. A detailed study on Atsuji spaces can be found in [4].

This article presents various results on nonempty intersection of decreasing sequence of nonempty closed bounded subsets in metric spaces and in Atsuji spaces using Hausdorff distance $H(A, B)$ and the functional $\hat{d}$, defined as $\hat{d}(A) = \sup_{x \in A} d(x, X \setminus A)$, where A, B are subsets of a metric space X. These obtained results are also compared with the Cantor's intersection theorem.

The article is organized as follows. Some preliminary results, needed for the rest part of the article, are discussed in Section 2. In Section 3 and Section 4, we consider decreasing sequence $\{K_n\}$ of nonempty closed bounded subsets of a metric space X and discuss their nonempty intersection results in the cases for which the Hausdorff distance $H_n := H(K_n, K_{n+1}) \to 0$, and $\hat{d}(K_n) := \sup_{x \in K_n} d(x, X \setminus K_n) \to 0$, respectively.

2 Preliminaries

Given a metric space (X, d), we denote the set of all nonempty bounded subsets of X and the set of all nonempty bounded closed subsets of X by $B(X)$ and $C_b(X)$, respectively. Further given $A \subset X$, A', A^o, $N_\epsilon(A)$ and ∂A denote the set of all limit points, interior points, ϵ-neighborhood and boundary of A, respectively. The diameter of A is given by $\delta(A) = \sup_{x,y \in A} d(x, y)$.

Definition 2.1. [2] The *Hausdorff distance*, H, of two nonempty subsets A, B of a metric space (X, d) is defined as

$$H(A, B) = \max\left\{\sup_{x \in A} d(x, B), \ \sup_{x \in B} d(x, A)\right\},$$

where $d(x, A) = \inf_{y \in A} d(x, y)$.

It is well-known that the distance function H is a metric, provided A, B are closed and bounded.

Definition 2.2. [7] A sequence $\{x_n\}$ in a metric space (X, d) is said to be *absolutely convergent sequence* if $\sum_{i=1}^{\infty} d(x_i, x_{i+1})$ is finite.

Lemma 2.3. [7] In a metric space X, every Cauchy sequence $\{x_n\}$ contains an absolutely convergent subsequence.

Theorem 2.4. [5] A metric space X is an Atsuji space if and only if each sequence $\{x_n\}$ with $\lim_{n\to\infty} I(x_n) = 0$, has a limit point in X, where $I(x) = d(x, X \setminus \{x\}), x \in X$.

Definition 2.5. [8] A subset S of a metric space X is said to be metrically convex if for any distinct points $x, y \in S$, there is a point $z \in S \setminus \{x, y\}$ that satisfies $d(x, y) = d(x, z) + d(z, y)$.

Theorem 2.6. [8] Consider a complete and metrically convex metric space X. Then, for any distinct points $x, y \in X$, there is a metric segment with the end points x, y.

3 Nonempty intersection results using Hausdorff distance

By a decreasing sequence $\{K_n\}$ of subsets of a metric space X, we mean $K_{n+1} \subset K_n$, $\forall\ n \in \mathbb{N}$, and we denote $H(K_n, K_{n+1})$ by H_n. Clearly $H_n \leq \delta(K_n)$. The following theorem furnishes a partial generalization of Cantor's intersection theorem, which we will discuss in Subsection 3.1. It is well known that, in a metric space X, if for each decreasing sequence $\{F_n\} \subset C_b(X)$ with $\delta(F_n) \to 0$, $\bigcap_{n=1}^{\infty} F_n \neq \emptyset$, then X is complete.

Theorem 3.1. A metric space X is complete if and only if for every decreasing sequence $\{K_n\} \subset C_b(X)$ with $\sum_{n=1}^{\infty} H_n$ converges, $\bigcap_{n=1}^{\infty} K_n \neq \emptyset$.

Proof. Let X be a complete metric space. For $a_1 \in K_1$, $\epsilon > 0$, there exists $a_2 \in K_2$ such that $d(a_1, a_2) \leq H(K_1, K_2) + \epsilon$. Again, for $a_2 \in K_2$ and $\epsilon > 0$ as above, there exists $a_3 \in K_3$ such that $d(a_2, a_3) \leq H(K_2, K_3) + \epsilon^2$. Proceeding this way, we get $d(a_r, a_{r+1}) \leq H(K_r, K_{r+1}) + \epsilon^r,\ r \geq 1$. This implies, $\{a_i\}$ is a Cauchy sequence. Let $a_i \to a \in X$. Then, $a \in \bigcap_{i=1}^{\infty} K_n$.

For the converse, consider a decreasing sequence $\{F_n\} \subset C_b(X)$ with $\delta(F_n) \to 0$. Then, the sequence $\{x_n\} \subset X$ with $x_n \in F_n$ is a Cauchy sequence. So, by Lemma 2.3, it has an absolutely convergent subsequence, say, $\{x_{p_i}\}_{i=1}^{\infty}$. Let K_i be the closure of the set $\{x_{p_i}, x_{p_{i+1}}, x_{p_{i+2}}, ...\},\ i = 1, 2, 3, ...$. Observing $H_i \leq d(x_{p_i}, x_{p_{i+1}})$, we have $\sum_{i=1}^{\infty} H_i < \infty$. Then, by the hypothesis, $\bigcap_{i\in\mathbb{N}} K_i \neq \emptyset$. And hence, $\bigcap_{n\in\mathbb{N}} F_n \neq \emptyset$. This completes the proof. □

Following examples validate the statement of the above theorem.

Example 3.2. Let $K_n = \left[-\frac{1}{n}, \frac{1}{n}\right] \subset \mathbb{R}$. Then $\sum_{n=1}^{\infty} H_n$ converges, and $\bigcap\limits_{n\in\mathbb{N}} K_n = \{0\}$.

Example 3.3. Consider the sequence space $X = (l^p, \|\cdot\|_p)$, for some p with $1 \leq p \leq \infty$ and choose $K_n = \{e_i\}_{i\geq n}$, where $e_i = (\delta_{ij})_{j=1}^{\infty}$. Then $\{K_n\}$ is a decreasing sequence in $C_b(X)$. It can be easily checked that $\sum_{n=1}^{\infty} H_n$ doesn't converge and $\bigcap\limits_{n=1}^{\infty} K_n = \emptyset$.

Example 3.4. Let $X = \mathbb{Q}$ with standard metric. Then X is not complete. Let r be a fixed irrational. Define $K_n = \{x \in X : r - 1/n \leq x \leq r + 1/n\}$. Then $K_n \in C_b(X)$ and decreasing. Although $\sum_{n=1}^{\infty} H_n$ converges, $\bigcap\limits_{n=1}^{\infty} K_n = \emptyset$.

3.1 Comparison with Cantor's theorem

It is worth noting that Examples 3.2-3.4 also validate the result of Cantor's intersection theorem. Therefore it is fairly natural to ask: *What advantage Theorem 3.1 provides over the Cantor's theorem?* The answer lies in the fact that $H_n \leq \delta(K_n)$.

In Cantor's intersection theorem, $\delta(K_n) \to 0$ is the sufficient condition to have nonempty intersection. But in the case when $\delta(K_n) \not\to 0$, Cantor's theorem does not provide a conclusion whether $\bigcap\limits_{n=1}^{\infty} K_n$ is empty or nonempty. In such case, if $\sum_{n=1}^{\infty} H_n$ converges, then Theorem 3.1 ensures $\bigcap\limits_{n=1}^{\infty} K_n$ is nonempty. For instance,

Example 3.5. Let $K_n \subset \mathbb{R}^2$ be the region (including boundaries) bounded by the curves $4n(y - 1/n) = -x^2$, and $4n(y + 1/n) = x^2$, $n \in \mathbb{N}$. Then $\delta(K_n) \not\to 0$, and so Cantor's theorem becomes inconclusive here. However, $\sum_{n=1}^{\infty} H_n$ is convergent, and $\bigcap\limits_{n\in\mathbb{N}} K_n$ is the set $\{(x, 0) : -2 \leq x \leq 2\}$.

3.2 Nonempty intersection in Atsuji space

In Theorem 3.1, we see that the condition "$\sum_{n=1}^{\infty} H_n < \infty$", is sufficient to have $\bigcap\limits_{n\in\mathbb{N}} K_n \neq \emptyset$, in complete metric spaces. A more general condition, namely "$H_n \to 0$", is not sufficient to have the nonempty intersection. For instance,

Example 3.6. The functions e_i, defined as $e_i(t) = t^i, t \in [0, 1], i \in \mathbb{N}$, are in the normed space $X = (C[0, 1], \|\cdot\|_\infty)$, and the sets $K_n := \{e_i\}_{i=n}^{\infty}$, $n \in \mathbb{N}$, are closed bounded subsets of X. Here, $H_n = \|e_n - e_{n+1}\|_\infty \to 0$, but $\bigcap\limits_{n=1}^{\infty} K_n = \emptyset$.

However, in Atsuji spaces, which are also complete, "$H_n \to 0$" is sufficient to have the nonempty intersection.

Theorem 3.7. If X is an Atsuji space, then for each decreasing sequence $\{K_n\} \subset C_b(X)$ with $H_n \to 0$, $\bigcap_{n=1}^{\infty} K_n \neq \emptyset$.

Proof. Given a decreasing sequence $\{K_n\} \subset C_b(X)$ such that $H_n \to 0$. For the sequence $\{K_n\}$, there exists $a_n \in K_n$ (as in the proof of Theorem 3.1) such that for any fixed $\epsilon \in (0,1)$ and for all $n \geq 1$ we have, $d(a_n, a_{n+1}) \leq H_n + \epsilon^n \to 0$, as $n \to \infty$. If $a_n = c$, for infinitely many values of n, then $c \in \bigcap_{n=1}^{\infty} K_n$. Otherwise, if the terms of the sequence $\{a_n\}$ are distinct, except for at most finitely many n, then this implies $I(a_n) \to 0$. Therefore, by Theorem 2.4, $\{a_n\}$ has a limit point lying in $\bigcap_{n=1}^{\infty} K_n$. □

The converse of Theorem 3.7, in general, is not true. That means if "$H_n \to 0$" suffices to have the nonempty intersection property, the space is not necessarily an Atsuji space. This is evident from the following example.

Example 3.8. Consider $X = \mathbb{N} \cup M$ with the standard Euclidean metric on $\mathbb{R}$, where $M = \{n + 1/2m : m, n \in \mathbb{N}\}$. Let $\{K_i\} \subset C_b(X)$ be a decreasing sequence with $H_i \to 0$. Then, as in the proof of Theorem 3.7, there exists $a_i \in K_i$ such that $|a_i - a_{i+1}| \to 0$. It can be shown that either $\{a_i\}$ is eventually constant, say $p \in X$, or $\{a_i\}$ converges to some positive integer k. In either case $\bigcap_{i=1}^{\infty} K_i \neq \emptyset$, as it contains either p or k. Thus we get, for each decreasing sequence $\{K_i\} \subset C_b(X)$ with $H_i \to 0$, $\bigcap_{i=1}^{\infty} K_i \neq \emptyset$, but the space X is not an Atsuji space because $X' = \mathbb{N}$.

We notice that Theorem 3.7 provides a generalization of Cantor's intersection theorem in Atsuji spaces.

4 Nonempty intersection results using $\hat{d}$

Jain and Kundu, in [4], considered a functional $I : X \to \mathbb{R}$ defined as, $I(x) = d(x, X \setminus \{x\})$. Here we consider a more general functional, $\hat{d}$, acting on the subsets of a metric space X, defined by $\hat{d}(A) = \sup_{x \in A} d(x, X \setminus A)$, $A \subset X$. This is also known as the excess of A over $X \setminus A$. This functional gives the radius of the inscribed ball inside a regular body in the Euclidean space $\mathbb{R}^2$. For subsets A, B of a metric space X, we conclude the following as well:

1. $\hat{d}(A) \leq \hat{d}(B)$, if $A \subset B$, and $A \in B(X)$,
2. $\hat{d}(A) = 0$ if and only if $A = \emptyset$ or $A \subset [X \setminus A]'$,
3. For an unbounded set A, $\hat{d}(A)$ can be finite or infinite. For example, in the euclidean space $\mathbb{R}^2$, consider $A_1 = \{(x, 0) : x \in \mathbb{R}\}$, and $A_2 = \{(x, y) : x, y \geq 0\}$, then $\hat{d}(A_1) = 0$, and $\hat{d}(A_2) = \infty$,

4. If $A = X$, then $\hat{d}(A)$ is finite or infinite, depending on X is bounded or unbounded, respectively. (We take $d(x, \emptyset) = \sup\{d(x, A) : A \subset X\},\ x \in X$.)

Proposition 4.1. Let $A, B \in B(X)$. Then

(a) $H(X \setminus A, X \setminus B) \leq \max\{\hat{d}(A), \hat{d}(B)\}$.

(b) $\max\{\hat{d}(A), \hat{d}(B)\} \leq H(A, B)$, provided $A \cap B = \emptyset$.

Proof. (a) For $A, B \in B(X)$, we have

$$\begin{aligned} & H(X \setminus A, X \setminus B) \\ & = \max\{\sup_{p \in X \setminus A} d(p, X \setminus B), \sup_{q \in X \setminus B} d(X \setminus A, q)\} \\ & = \max\{\sup_{p \in B \setminus A} d(p, X \setminus B), \sup_{q \in A \setminus B} d(q, X \setminus A)\} \qquad (4.1) \\ & \leq \max\{\sup_{p \in B} d(p, X \setminus B), \sup_{q \in A} d(q, X \setminus A)\} \\ & = \max\{\hat{d}(B), \hat{d}(A)\}. \qquad (4.2) \end{aligned}$$

(b) Suppose $A \cap B = \emptyset$, then

$$\begin{aligned} H(A, B) &= \max\{\sup_{x \in A} d(x, B), \sup_{y \in B} d(A, y)\} \\ &\geq \max\{\sup_{x \in A} d(x, X \setminus A), \sup_{y \in B} d(X \setminus B, y)\} \\ &= \max\{\hat{d}(A), \hat{d}(B)\}. \end{aligned}$$

□

Remark 4.2. For two subsets A, B with $A \subset B$ in a metric space X, in general, $\hat{d}(B)$ and $H(A, B)$ are not comparable, even in Atsuji spaces.

Theorem 4.3. Let X be an Atsuji space. Then, for each decreasing sequence $\{K_n\} \subset C_b(X)$ with $\hat{d}(K_n) \to 0$, $\bigcap_{n=1}^{\infty} K_n \neq \emptyset$.

Proof. Consider $x_n \in K_n$. Then, $I(x_n) = d(x_n, X \setminus \{x_n\}) \leq d(x_n, X \setminus K_n) \leq \sup_{x \in K_n} d(x, X \setminus K_n) = \hat{d}(K_n)$, which by the hypothesis tends to 0. Hence, using Theorem 2.4, the sequence $\{x_n\}$ has a limit point lying in $\bigcap_{i=1}^{\infty} K_n$. □

The converse of Theorem 4.3, in general, does not hold.

Example 4.4. Consider the set X as in Example 3.8, with the standard Euclidean metric d on $\mathbb{R}$. Let $\{K_i\} \subset C_b(X)$ be a decreasing sequence with $\hat{d}(K_i) \to 0$. Then, as in the proof of Theorem 4.3, there exists $x_i \in K_i \setminus K_{i+1}$ such that $I(x_i) \to 0$. If the range set, $R = \{x_i\}_{i \geq 1}$, is infinite and $R \subset M$,

consider $x_i = n_i + 1/2m_i$. If $\{m_i\}_{i\geq 1} = \{p_1, p_2, ..., p_q\}$, a finite set, then $d(n_i+1/2p_j, X\backslash\{n_i+1/2p_j\}) = d(n_i+1/2p_j, n_i+1/2(p_j+1)) = \frac{1}{2}d(1/p_j, 1/(p_j+1)) \geq \inf_{1\leq j\leq q} \frac{1}{2}d(1/p_j, 1/(p_j+1)) > 0$, which is a contradiction to $I(x_i) \to 0$. Hence, there is a subsequence $\{m_{t_i}\}$ of $\{m_i\}$ with $m_{t_i} \to \infty$ as $i \to \infty$. And so, it can be proved that in the case either $R \subset M$ or $R \not\subset M$; the sequence $\{x_i\}$ has a subsequence converging to some $p \in \mathbb{N}$. Therefore $p \in \bigcap_{i=1}^{\infty} K_i$. Thus we get, for each decreasing sequence $\{K_i\} \subset C_b(X)$ with $\hat{d}(K_i) \to 0$, $\bigcap_{i=1}^{\infty} K_i \neq \emptyset$. Although, the space X is not an Atsuji space.

Theorem 4.5. If X is a metric space, and for each decreasing sequence $\{K_n\} \subset C_b(X)$ with $\hat{d}(K_n) \to 0$, $\bigcap_{n=1}^{\infty} K_n \neq \emptyset$, then X is complete.

Proof. Consider a decreasing sequence $\{F_n\} \subset C_b(X)$ with $\delta(F_n) \to 0$. Then, the sequence $\{x_n\}$ with $x_n \in F_n$ is a Cauchy sequence in X. Let K_n be the closure of the set $\{x_i\}_{i\geq n}$. Since $\{x_n\}$ is Cauchy, for each $\epsilon > 0$, there is an $N \in \mathbb{N}$ such that $\sup_{n\geq N+1} d(x_N, x_n) < \epsilon$, that is, $\sup_{x\in K_{N+1}} d(x_N, x) < \epsilon$, which further implies $\hat{d}(K_{N+1}) = \sup_{x\in K_{N+1}} d(x, X \setminus K_{N+1}) < \epsilon$. Thus $\hat{d}(K_n) \to 0$. So, by the hypothesis $\bigcap_{n=1}^{\infty} K_n \neq \emptyset$. Hence, $\bigcap_{n=1}^{\infty} F_n \neq \emptyset$ and this completes the proof. □

4.1 Comparison with Cantor's theorem

We observe that, in general, $\hat{d}$ and δ are not comparable. For instance,

Example 4.6. Consider a set $X = \{x, y\}$, $x \neq y$, equipped with a metric d. Let $A = \{x\}$. Then, $\hat{d}(A) = d(x, y) > 0$, and $\delta(A) = 0$.

But if $X = \mathbb{R}^2$, with standard Euclidean metric, and $A = B[0, r]$, then $\hat{d}(A) = r < 2r = \delta(A)$.

We shall show that in metrically convex metric spaces, $\hat{d}$ is always dominated by δ.

Lemma 4.7. Let (X, d) be a metric space. Then, for all $x, y \in X$ and $r \in [0, d(x, y)]$, $B[x, r] \cap B[y, d(x, y) - r] = S[x, r] \cap S[y, d(x, y) - r]$, where $S[x, r] := \{z \in X : d(x, z) = r\}$.

Proof. Let us denote $B[x, r] \cap B[y, d(x, y) - r]$ and $S[x, r] \cap S[y, d(x, y) - r]$ by $B^{\cap}$ and $S^{\cap}$, respectively. If $B^{\cap}$ is empty, there is nothing to prove. Let $B^{\cap} \neq \emptyset$ and $z \in B^{\cap}$. We claim $z \notin B_1 \cup B_2$, where $B_1 = B[x, r] \setminus S[x, r]$, $B_2 = B[y, d(x, y) - r] \setminus S[y, d(x, y) - r]$. If possible, let $z \in B_1$. Then $d(x, y) \leq d(x, z) + d(z, y) < r + d(x, y) - r = d(x, y)$, which is a contradiction. Similarly, we prove $z \notin B_2$. Thus, $z \in B^{\cap} \cap [B_1 \cup B_2]^c = B^{\cap} \cap [{B_1}^c \cap {B_2}^c]$, where B^c

denotes the complement of a set B in X. This implies $z \in S^{\cap}$, and so $B^{\cap} \subset S^{\cap}$. Hence, $B^{\cap} = S^{\cap}$. □

Theorem 4.8. Let A be a nonempty bounded proper subset in a complete metrically convex space X. Then $\hat{d}(A) \leq \delta(A)$.

Proof. Let (X, d) be an metrically convex space. By Theorem 2.6, X is a connected metric space too. We shall achieve the conclusion in the following steps.

Step 1 : First we show that for each $\epsilon > 0$ the set $N_\epsilon(A) \setminus A$ is not empty.
Step 2 : We show that for each $\epsilon > 0$ we have $B(a, r+\epsilon) = N_\epsilon(B)$, where $B = B(a, r)$.
Step 3 : Finally we prove that $\hat{d}(A) \leq \delta(A)$.

Step 1. On the contrary, let us assume $N_\epsilon(A) \setminus A = \emptyset$. This implies, A is open and for all $x \in A$, $B(x, \epsilon) \subset A$. Since A is open, $\partial A \not\subset A$. This implies, "$\exists\ b \in \partial A$ such that $b \notin B(x, \epsilon)$ for all $x \in A$", which is a contradictory statement in itself.

Step 2. Observe that, $N_\epsilon(B) \subset B(a, r+\epsilon)$ follows from the triangle inequality. Conversely, suppose $y \in B(a, r+\epsilon)$. If $y \in B$ then $y \in B(y, \epsilon) \subset N_\epsilon(B)$. Suppose $y \in B(a, r+\epsilon) \setminus B$. Then, consider the ball $B(y, \epsilon)$. If $B(y, \epsilon) \cap B = \emptyset$, then $B(y, \epsilon) \cap \partial B = \emptyset$. Therefore, $d(q, y) \geq \epsilon$, for all $q \in \partial B$. By Theorem 2.6 and Lemma 4.7, since $r \in [0, d(a, y)]$, there is a $u \in X$ such that $\psi(r) = u \in B[a, r] \cap B[y, d(a, y) - r] = S[a, r] \cap S[y, d(a, y) - r] = \partial B \cap S[y, d(a, y) - r]$, where ψ is an isometry from $[0, d(a, y)]$ to X. This implies $d(a, y) = d(a, u) + d(u, y) \geq r + \epsilon$, a contradiction. Hence, $B(y, \epsilon) \cap B \neq \emptyset$, and therefore $y \in B(z, \epsilon)$ for some $z \in B$. Thus, $B(a, r+\epsilon) \subset N_\epsilon(B)$.

Step 3. Since $\partial B \neq \emptyset$, $\inf_{p \in X \setminus B} d(a, p) = d(a, q) = r$, for some $q \in \partial B$. Now, let x be an element in A. If $x \in A^{\circ}$, then consider a ball $B(x, r')$, where $r' = \sup\{r > 0 : B(x, r) \subset A\}$. There must be a point in $N_\epsilon(B(x, r'))$ which lies in $N_\epsilon(A) \setminus A$. Hence, $[N_\epsilon(B(x, r')) \setminus B(x, r')] \cap [N_\epsilon(A) \setminus A] \neq \emptyset$. Therefore, $d(x, X \setminus A) = r' \leq \delta(A)$. On the other hand, if $x \in \partial A$, then $d(x, X \setminus A) = 0 \leq \delta(A)$. Hence, $\hat{d}(A) \leq \delta(A)$. □

Since the metric spaces with Takahashi's convex strustures ([12]) and the normed spaces are metrically convex metric spaces, so Theorem 4.8 is applicable to these spaces too. Due to Theorem 4.8, Theorem 4.3 induces a generalization of Cantor's intersection theorem in metrically convex Atsuji spaces.

Example 4.9. Consider the metric space $X = \{(x, y) \in \mathbb{R}^2 : -3 \leq x, y \leq 3\}$, with standard Euclidean metric on $\mathbb{R}^2$. The space X is a metrically convex Atsuji space. Let $K_n \subset X$ be the region (including boundaries) bounded by the curves $n(1 + \frac{1}{n})^2(y - 1/n) = -x^2$, and $n(1 + \frac{1}{n})^2(y + 1/n) = x^2$, $n \in \mathbb{N}$. Here $\delta(K_n) \not\to 0$, and so Cantor's theorem becomes indecisive. However, $\hat{d}(K_n) \to 0$, and $\bigcap_{n \in \mathbb{N}} K_n$ is the set $\{(x, 0) : -1 \leq x \leq 1\}$.

5 Conclusion

For a pair of consecutive elements K_n, K_{n+1} from a decreasing sequence $\{K_n\}$ of nonempty closed bounded subsets of a metric space, it is observed that H_n is less than or equal to the diameter of K_n, where H_n is the Hausdorff distance between K_n and K_{n+1}. Therefore, $H_n \to 0$ is the necessary condition for Cantor's intersection theorem. However, the condition $H_n \to 0$ in not sufficient to have nonempty $\bigcap_{n\in\mathbb{N}} K_n$ in complete metric spaces; extra conditions on H_n is required for that. We have shown that the condition $\sum_{n=1}^{\infty} H_n < \infty$, is sufficient to have nonempty intersection in complete metric spaces; while, $H_n \to 0$ is sufficient to have nonempty intersection in Atsuji spaces. Further, in Atsuji spaces, we have provided sufficient condition for nonempty $\bigcap_{n\in\mathbb{N}} K_n$ using the concept of excess of a set.

Nonempty intersection theorems, and the generalizations of such theorems like Cantor's theorem, Kuratowski's theorem, Horvath's theorem, etc. play an important role to study the best approximations, fixed point results, etc. (for example, see [3, 9, 10, 13]). In case of set-valued mappings, researchers have been studying the fixed point results for mappings from a metric space to the subspaces of the hyperspace of nonempty closed subsets endowed with the Hausdorff distance (for example, see [1, 11]). Findings of this manuscript, can further be applied in these directions.

References

[1] N. A. Assad and W. A. Kirk, Fixed point theorems for set-valued mappings of contractive type, *Pacific J. Math.*, 43, 553–562 (1972).

[2] J. Henrikson, Completeness and total boundedness of the Hausdorff metric, *MIT Undergrad. J. Math.*, 1, 69-80 (1999).

[3] C. Horvath, Measure of non-compactness and multivalued mappings in complete metric topological vector spaces, *J. Math. Anal. Appl.*, 108, 403–408 (1985).

[4] T. Jain, S. Kundu, Atsuji completions: Equivalent characterisations, *Topology Appl.*, 154, 28–38 (2007).

[5] S. Kundu and T. Jain, Atsuji spaces: Equivalent conditions, *Topology Proc.*, 30, 301–325 (2006).

[6] K. Kuratowski, Sur les espaces complets, *Fund. Math.*, 15, pp. 301–309 (1930).

[7] H. M. MacNeille, Extensions of measure, *Proc. Natl. Acad. Sci.*, 24, pp. 188–193 (1938).

[8] A. Martinon, Distance to the intersection of two sets, *Bull. Austral. Math. Soc.*, 70, pp. 329–341 (2004).

[9] Z. D. Mitrovic and I. D. Arandjelovic, Existence of generalised best approximations, *Nonlinear Convex Anal.*, 15, pp. 787–792 (2014).

[10] Z. D. Mitrovic and I. D. Arandjelovic, Generalized scalar equilibrium problem with applications to best and coupled best approximations, *J. Fixed Point Theory Appl.*, 19, pp. 1613–1624 (2017).

[11] S. B. Nadler Jr., Multi-valued contraction mappings, *Pacific J. Math.*, 30, pp. 475–488 (1969).

[12] W. Phuengrattana and S. Suantai, Existence and convergence theorems for generalized hybrid mappings in uniformly convex metric spaces, *Indian J. Pure Appl. Math.*, 45, pp. 121–136 (2014).

[13] T. Shimizu and W.Takahashi, Fixed points of multivalued mappings in certain convex metric spaces, *Topol. Methods Nonlinear Anal.*, 8, pp. 197–203 (1996).

[14] G. F. Simmons, *Introduction to Topology and Modern Analysis*, McGraw-Hill, New York, 1963.

[15] J. A. Souza and R. W. M. Alves, CantorKuratowski theorem in admissible spaces, *Topology Appl.*, 252, pp. 158–168 (2019).

Goal programming approach to solve linear transportation problems with multiple objectives

Vishwas Deep Joshi[1], Keshav Agarwal[2], Jagdev Singh[3]
[1,2,3] Department of Mathematics, JECRC University Jaipur, Rajasthan, INDIA
Email: [1]vdjoshi.or@gmail.com*, [2]keshavaggarwal58@gmail.com, [3]jagdevsinghrathor@gmail.com
*Corresponding author

December 28, 2022

Abstract

In multi-objective transportation, due to the conflicting nature of objectives, no method is available to find the best compromise optimal solution. In this paper, we present a method to obtain a compromised solution for multi-objective transportation problems under a weighted environment. In which, a modified weighted model is presented that provides us with an efficient solution according to the priorities of the decision maker. To measure the efficiency of the method, a numerical example is included and the results are compared with previously reported work for the same numerical problems to illustrate the feasibility and the applicability of the proposed method.

Keywords- Multi-objective optimization; transportation problem; compromise solution; goal programming

1 Introduction

With the growing population of this competitive world the demand for the goods is growing day by day and to fulfil the demands, the businesses have to outperform themselves every time. Due to this, the management of the business faces a lot of challenges and single objective transportation is not enough to meet the needs of this competitive market. Just Minimizing the transportation cost cannot be the only objective, they must take other factors into consideration and solving such type of problem with multiple objectives which need to be fulfilled simultaneously gives birth to a new branch of transportation problem that we call multi-objective transportation problem (MOTP).

In a classic transportation problem, a product is to be transported from m sources to n destinations and there is a penalty p_{ij} associated with transporting a unit of product. This penalty may be cost or delivery time or safety of delivery, or something else depending upon the decision maker (DM). Over a period of time, many algorithms have been developed to obtain initial basic feasible solutions like the North-west corner rule, least cost method, and Vogel's approximation method. Veena Adlakha and Kowalski [2](1997) proposed a very effective algorithm (Absolute point method) that can be used to directly obtain optimal cost without using the MODI method. These methods are applicable when all the decision parameters are given in a precise way, but as already discussed in real life situations, not all transportation problems are single-objective.

Past many years a lot of work has been done in developing an algorithm to solve multi-objective transportation problems. Every algorithm gives varying results and it is very difficult to say which is the best method to obtain a compromised solution (For multi-objective transportation, a compromised solution is a feasible solution that is favoured more by the DM over all other feasible solutions, taking into consideration all criteria contained in the multi-objective function).The quality of the solution totally depends on the DM.

Lee and Moore [7](1973) inspected the optimization of transportation problems with multiple objectives. Isermann and Diaz [6] (1979) formulated different algorithms for all the non-dominated solutions for linear multi-objective transportation problems. The fuzzy programming technique was applied by Bit, Biswal, and Alam [3] (1992) to solve the multi-objective transportation problem. For the first time in the early 1960s, Charnes and Cooper suggested the concept of goal programming (GP) and a very good literature review was given. It has been found extensive in various fields. Since 1960, numerous works have been done and a lot of applications have been proposed. A review of GP formulations and their applications was given by Lee and Olson [8](1999). Edward L. Hannan [4] (1981) illustrated GP with fuzzy goals having a linear membership function. Zangiabadi and Maleki [13](2013) presented the application of fuzzy goal programming to linear MOTP using a non-linear membership function. Despite its recognition and a huge variety of applications, there's no assurance that GP will offer Pareto an optimal solution.

In multi-objective problems, we can assign different weights to the objective according to the importance of the objective and obtain varying results for different weights assigned by the DM. Due to the overlapping existence of priorities, it is rare to find an optimal solution that optimizes all of them at the same. Here in this paper, we have discussed the weighted sum method and the algorithm proposed by Nomani [10](2016) and a comparison has been made with the proposed model with the help of numerical examples. The proposed model is a new weighted method that helps obtain compromised solutions according to the priorities given by the DM for different goals.

2 Multi-objective linear transportation problem (MOLTP)

In today's aggressive environment, a single-objective transportation assignment is insufficient to deal with all real-life decision-making issues. So, to address all real-life conditions on transportation problems, the DM regularly wishes to consider more than one non-commensurable or conflicting objective in transportation problems. The problem wherein more than one target is optimized concurrently is referred to as a multi-objective transportation problem (MOTP). The reason for defining the multi-objective transportation problem in the mathematical programming framework is to optimize numerous objectives concurrently subject to a set of constraints Other than transportation expense the objectives can include shipping time, degradation of goods, secure shipping of items, energy consumption, etc

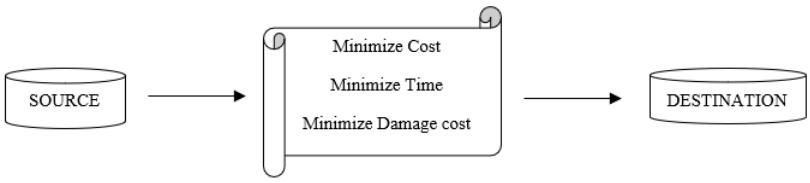

The mathematical model of MOTP is written as follows:

$$Min\ F_k(x_ij) = \sum_{i=1}^{m}\sum_{j=1}^{n} p_{ij}^{k} x_{ij}, \qquad k = 1, 2, \ldots, K$$

Subject to:

$$\sum_{j=1}^{n} x_{ij} = s_i, \qquad i = 1, 2, 3, \ldots, m$$

$$\sum_{i=1}^{m} x_{ij} = dj, \qquad j = 1, 2, 3, \ldots, n$$

$$x_{ij} \geq 0, \quad i = 1, 2, 3, \ldots m, and\ \ j = 1, 2, \ldots, n$$

Where m is no. of source, n is no. of destination, d_n is capacity of destination, s_m is capacity of sources, p_{ij}^{k} is penalty of k^{th} objective, F_k is k^{th} objective and x_{ij} is unknown qty to be shipped.

3 Methods for solving MOLTP

3.1 Weighted sum method

For solving a MOLTP the method of the weighted sum is highly used to obtain varying results for different weights. The basic idea of this method is to assign

weight $n_k \geq 0$ to each objective function F_k and minimize the new objective function $\sum_{k=1}^{K} n_k F_k$ with respect to problem constraints. This method is very easy to use but the solution majorly depends on the weights given by the DM and it should be decided beforehand. Using the weighted sum method, the following normalized single-objective optimization problem is obtained:

$$Minimize \;\; F = n_1 F_1 + n_2 F_2 + \ldots + n_K F_K$$

Subject to:

$$\sum_{j=1}^{n} x_{ij} = s_i, \qquad i = 1, 2, 3, \ldots, m$$

$$\sum_{i=1}^{m} x_{ij} = dj, \qquad j = 1, 2, 3, \ldots, n$$

$$x_{ij} \geq 0, \quad i = 1, 2, 3, \ldots m, and \;\; j = 1, 2, \ldots, n$$

Where the weights $n_k, k = 1, 2, \ldots K$, corresponding to the objective function satisfy the following conditions $n_1 + n_2 + \ldots + n_k = 1 \; k = 1, 2, \ldots K$
Using the above method, single solution points are obtained for different weights that reflect the preferences of the decision-maker. This method fails when DM have no idea about preference.

3.2 Method proposed by Nomani(2016)

In 2016, Mohammad Asim Nomani, Irfan and Ahmed proposed a model to obtain a compromised solution for a MOLTP. This model focuses on converting multiobjective optimization into a new single objective optimization where the objective is to $minimize \; \mu^{'} = \sum \mu(1 - n_k)$, where μ is the general deviation variable for all objectives and n_k is the weight assigned to the k^{th} objective.

Consider the following multi-objective optimization problem:

$$Minimize \; F(x) = [F_1(x), F_2(x), \ldots, F_K(x)]$$

$$Subject \; to \;\; x \in S$$

Where x is an n-dimensional decision maker variable and S is the set of feasible solutions. Each objective is transformed into constraints with an upper bound of $F_k^* + \mu(1 - n_k)$, where F_k^* is an ideal solution obtained when each objective $F_k, k = 1, 2, \ldots, K$ is solved independently of other objectives.
The problem reduces as:

$$Minimize \; \mu^{'} = \sum_{k=1}^{K} \mu(1 - n_k)$$

Subject to:

$$F_k \leq F_k^* + \mu(1 - n_k); \qquad x_{ij} \geq 0$$

In this model, instead of using a deviation variable alone, a factor $(1 - n_k)$ has been introduced. This method is capable of providing a solution even if DM has no priority for objectives.

4 Proposed Method

In this section, we will discuss the proposed method and later we will see a comparison between the results obtained by these three methods. Let us consider a multi-objective optimization problem:

$$Minimize \;\; F(x) = [F_1(x), F_2(x), \ldots, F_K(x)]$$

Like Nomani's model, this model also focuses on converting the multi-objective problem into a single objective problem. The main idea is to minimize the deviation of each objective from its ideal solution. To do so a deviation variable μ was introduced.

The model is formulated as:

$$Minimize\ \mu^{'} = \sum_{k=1}^{K} \mu(1 - n_k)$$

Subject to

$$\sum_{i=1}^{m}\sum_{j=1}^{n} p_{ij}^{k} x_{ij} \leq F_k^* + \frac{\mu(1 - n_k}{(F_u^k - F_l^k)} \quad k = 1, 2, \ldots, K$$

$$\sum_{j=1}^{n} x_{ij} = s_i, \qquad i = 1, 2, 3, \ldots, m$$

$$\sum_{i=1}^{m} x_{ij} = dj, \qquad j = 1, 2, 3, \ldots, n$$

$$0 \leq n_k \leq 1, k = 1, 2, \ldots, K$$

$$x_{ij} \geq 0, i = 1, 2, \ldots, m \;\; and \; j = 1, 2, 3, \ldots, n$$

Here in this model a factor $\frac{1}{(F_u^k - F_l^k)}$ is introduced alongside with existing $\mu(1 - n_k)$. F_u^k and F_l^k represent upper and lower bounds in which the compromised solution will lie. The solution cannot exceed this range. For a k^{th} objective, this range can be obtained by using the ideal allocation. For upper bound max (Solution obtained by substituting others allocation in kth objective) and for lower bound the optimal solution of k^{th} objective is it's lower bound and this lower bound is the ideal solution F_k^*.

Step by Step method:

Step 1: Solve all the K objectives as a single objective problem without considering other objectives.
Step 2: Obtain the range for every objective as stated above.
Step 3: Now develop a model for the problem as described above and define weights for the objectives if DM has any.
Now simply evaluate and a compromised solution will be obtained.

5 Numerical illustration

The first example that we will be considering is used by many authors and they have obtained different solutions. Ringuest and Rinks [11](1987) used this problem to illustrate the MOLTP. In this paper, we have formulated the problem like a real-life problem to make a better understanding of the problem.

Example 1: Let us consider a problem in which Jethalal wants to transport TVs from its 3 Factories situated in Delhi, Mumbai and Bangalore, to the 4 warehouses at Bhopal, Dehradun, Kolkata and Chennai. The Factory capacity of Delhi is 8 thousand TVs, Mumbai is 19 thousand TVs and Bangalore is 17 thousand TVs. The warehouse requirement at Bhopal is 11 thousand TVs, Dehradun is 3 thousand TVs, Kolkata is 14 thousand TVs and Chennai is 16 thousand TVs. Jethalal wants to minimize the transportation cost as well as the safety cost for the TVs. The cost of transportation and safety per unit is given in the table below (in thousands)

Safety,Transportation	**Bhopal**	**Dehradun**	**Kolkata**	**Chennai**
Delhi	1,4	2,4	7,3	7,4
Mumbai	1,5	9,8	3,9	4,10
Banglore	8,6	9,2	4,5	6,1

Solution The first step is to obtain a solution for both the objectives separately ignoring the other objective. The solution obtained is as follows:
$X^1 = (x_{11} = 5, x_{12} = 3, x_{21} = 6, x_{24} = 13, x_{33} = 14, x_{34} = 3)$
$F_1(X^1) = 143(ideal solution), F_1(X^2) = 208,$
Upper and lower bounds of the objective function F_1 is $143 \leq F_1 \leq 208$
$X^2 = (x_{13} = 8, x_{21} = 11, x_{22} = 2, x_{23} = 6, x_{32} = 1, x_{34} = 16)$
$F_2(X^2) = 167(ideal solution), F_2(X^1) = 265,$
Upper and lower bounds of the objective function F_2 is $167 \leq F_2 \leq 265$
Now since we have the bounds, we can formulate the mathematical model of the problem using the proposed model.

$$Minimize\ \mu^{'} = \mu(1 - n_1) + \mu(1 - n_2)$$

Subject to:

$$\sum_{i=1}^{3}\sum_{j=1}^{4} p_{ij}^{1} x_{ij} \leq 143 + \frac{\mu(1 - n_1)}{(208 - 143)}$$

$$\sum_{i=1}^{3}\sum_{j=1}^{4} p_{ij}^2 x_{ij} \leq 167 + \frac{\mu(1-n_2)}{(265-167)}$$

$$\sum_{j=1}^{4} x_{ij} = s_i, \quad i = 1,2,3$$

$$\sum_{i=1}^{3} x_{ij} = d_j, j = 1,2,3,4$$

$$n_1 + n_2 = 1$$

$$0 \leq n_k \leq 1$$

$$k = 1,2; \quad x_{ij} \geq 0$$

Now simply allot the weight to the objective function and solve the LPP. Make sure the weights are non-negative and their sum is exactly equal to 1. We have used Lingo 19.0 to solve the LLP.

	Weights (n_1, n_2)	**Proposed method**	**Nomani**	**Weighted sum**
1	$n_1 = 0.1, n_2 = 0.9$	197;169	186;171	208;167
2	$n_1 = 0.2, n_2 = 0.8$	186;171	176;175	186;171
3	$n_1 = 0.3, n_2 = 0.7$	176;175	172;180	176;175
4	$n_1 = 0.4, n_2 = 0.6$	172;180	168;185	176;175
5	$n_1 = 0.5, n_2 = 0.5$	168;185	164;190	176;175
6	$n_1 = 0.6, n_2 = 0.4$	148;180	160;195	156;200
7	$n_1 = 0.7, n_2 = 0.3$	160;195	156;200	156;200
8	$n_1 = 0.8, n_2 = 0.2$	156;200	154;210	156;200
9	$n_1 = 0.9, n_2 = 0.1$	152;220	150;230	143;265

Comparison of solution of Example 1 by the proposed method, Nomani method, weighted sum

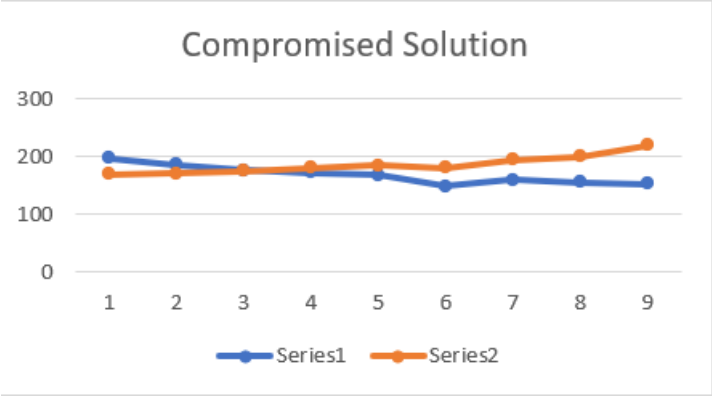

Figure 1 Graphical representation of solution with different priorities

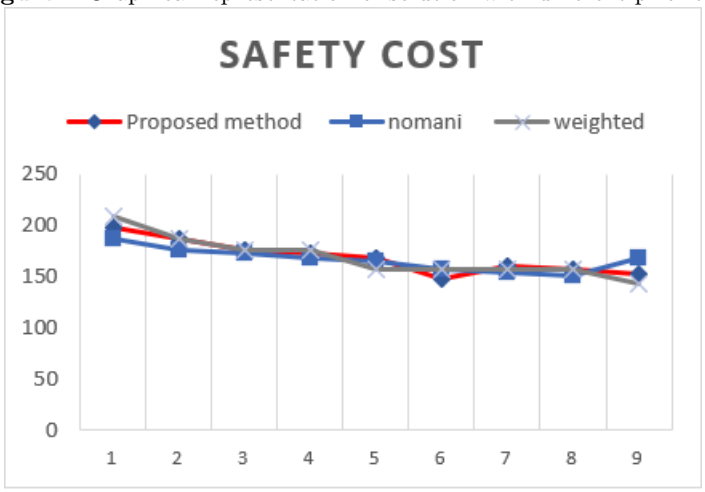

Figure 2 Comparison of safety costs obtained by different methods

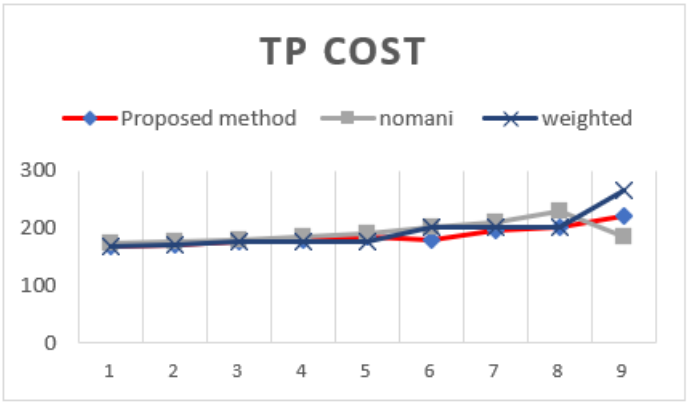

Figure 3 Comparison of TP cost obtained by different methods

Let us now consider a 3-objective problem. This example is already used by authors to compare varying results. Diaz [6](1979) used this example to illustrate the approach. Like the previous problem, we have formulated it like real life problem for better understanding.

Example 2: Madhavi Bhide have a business selling Pickel and she wants to deliver the pickle to various locations across India. She has manufacturing units in Mumbai, Ahmedabad, Chandigarh, and Mirzapur and needs to supply at Ratlam, Nagpur, Patna, Panji, and Kota. The supply capacity of Mumbai is 500 boxes, Ahmedabad is 400 boxes, Chandigarh is 200 boxes, and Mirzapur is 900 boxes. Demand at Ratlam is 400 boxes, Nagpur is 400 boxes, Patna is 600 boxes, Panji is 200 boxes, and Kota is 400 boxes. She wants to minimize the delivery time, transportation cost and packaging cost. The cost time and

packing cost per unit are given below (in hundreds).

Cost,Time,Packing cost	Ratlam	Nagpur	Patna	Panji	Kota
Mumbai	9,2,2	12,9,4	9,8,6	6,1,3	9,4,6
Ahmedabad	7,1,4	3,9,8	7,9,4	7,5,9	5,2,2
Chandigarh	6,8,5	5,1,3	9,8,5	11,4,3	3,5,6
Mirzapur	6,2,6	8,8,9	11,6,6	2,9,3	2,8,1

Solution: The first step is to obtain a solution for all three objectives separately ignoring the other objectives. The solution obtained is as follows:
$X^1 = (x_{13} = 5, x_{22} = 3, x_{23} = 1, x_{31} = 1, x_{32} = 1, x_{41} = 3, x_{44} = 2, x_{45} = 4)$
$F_1(X^1) = 102, F_1(X^2) = 164, F_1(X^3) = 134,$
Upper bound = Max 164,134 = 164
Upper and lower bounds of the objective function F_1 is $102 \leq F_1 \leq 164$
$X^2 = (x_{11} = 3, x_{14} = 2, x_{21} = 1, x_{25} = 4, x_{32} = 2, x_{41} = 1, x_{42} = 2, x_{43} = 6)$
$F_2(X^2) = 72(idealsolution), F_2(X^1) = 141, F_2(X^3) = 122,$
Upper bound = Max 141,122 = 141
Upper and lower bounds of the objective function F_2 is $72 \leq F_2 \leq 141$
$X^3 = (x_{11} = 3, x_{12} = 2, x_{21} = 1, x_{23} = 3, x_{32} = 2, x_{43} = 3, x_{44} = 2, x_{45} = 4)$
$F_3(X^3) = 64(idealsolution), F_3(X^2) = 90, F_3(X^1) = 94,$
Upper bound = Max 90,94 = 94
Upper and lower bounds of the objective function F_3 is $64 \leq F_2 \leq 94$
Now since we have the bounds, we can formulate the mathematical model of the problem using the proposed model.

$$Minimize\ \mu^{'} = \mu(1 - n_1) + \mu(1 - n_2) + \mu(1 - n_3)$$

Subject to:

$$\sum_{i=1}^{4}\sum_{j=1}^{5} p_{ij}^{1} x_{ij} \leq 102 + \frac{\mu(1 - n_1)}{(164 - 102)}$$

$$\sum_{i=1}^{4}\sum_{j=1}^{5} p_{ij}^{2} x_{ij} \leq 72 + \frac{\mu(1 - n_2)}{(141 - 72)}$$

$$\sum_{i=1}^{4}\sum_{j=1}^{5} p_{ij}^{3} x_{ij} \leq 64 + \frac{\mu(1 - n_2)}{(94 - 64)}$$

$$\sum_{j=1}^{5} x_{ij} = s_i, \quad i = 1, 2, 3, 4$$

$$\sum_{i=1}^{4} x_{ij} = d_j, \quad j = 1, 2, 3, 4, 5$$

$$n_1 + n_2 + n_3 = 1 \;\; 0 \leq n_k \leq 1 \quad k = 1, 2, 3$$

Now simply allot the weight to the objective function and solve the LPP. Make sure the weights are non-negative and their sum is exactly equal to 1. We have used Lingo 19.0 to solve the LLP.

	Weights (n_1, n_2, n_3)	**Proposed method**	**Nomani**	**Weighted sum**
1	$n_1 = 0.1, n_2 = 0.9, n_3 = 0.0$	147;76;94	147;76;94	157;72;86
2	$n_1 = 0.2, n_2 = 0.8, n_3 = 0.0$	142;78;98	142;78;98	157;72;86
3	$n_1 = 0.3, n_2 = 0.7, n_3 = 0.0$	134;85;96	134;85;96	142;78;98
4	$n_1 = 0.4, n_2 = 0.0, n_3 = 0.6$	114;99;89	124;109;78	129;126;64
5	$n_1 = 0.5, n_2 = 0.0, n_3 = 0.5$	119;101;91	118;110;83	105;128;84
6	$n_1 = 0.6, n_2 = 0.0, n_3 = 0.4$	117;106;88	117;108;84	105;128;84
7	$n_1 = 0.0, n_2 = 0.3, n_3 = 0.7$	134;93;83	139;99;74	153;89;75
8	$n_1 = 0.0, n_2 = 0.2, n_3 = 0.8$	135;97;78	141;102;72	134;122;64
9	$n_1 = 0.0, n_2 = 0.1, n_3 = 0.9$	141;102;72	140;110;68	134;122;64
10	$n_1 = 0.3, n_2 = 0.3, n_3 = 0.4$	126;92;94	124;99;87	127;104;76
11	$n_1 = 0.3, n_2 = 0.4, n_3 = 0.3$	126;92;94	129;95;87	141;86;82
12	$n_1 = 0.4, n_2 = 0.3, n_3 = 0.3$	124;97;91	124;99;87	112;110;88

Comparison of solution of Example 2 by the proposed method, Nomani method, weighted sum

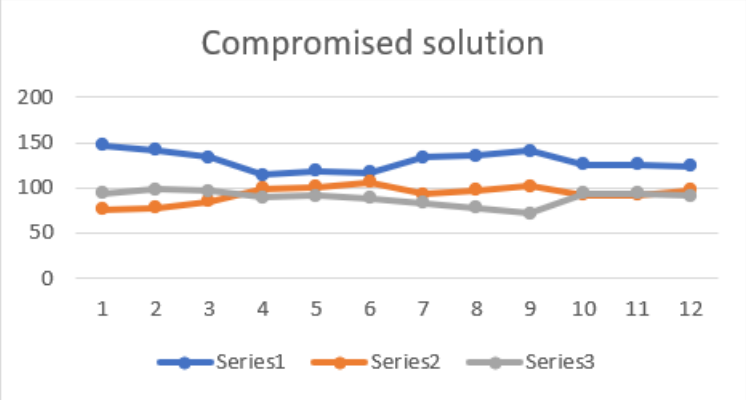

Figure 4 Graphical representation of solution with different priorities

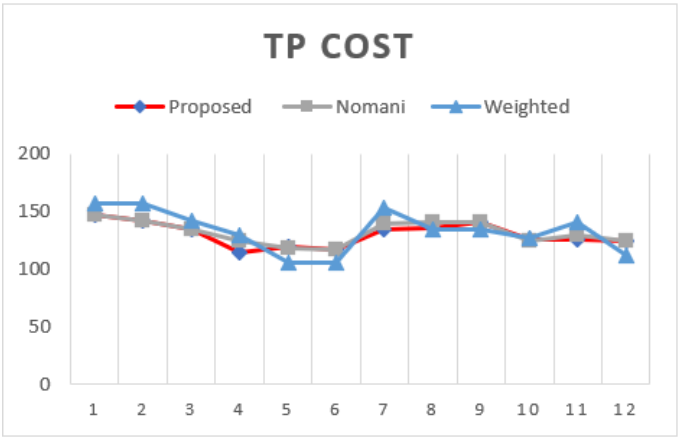

Figure 5 Comparison of transportation costs obtained by different methods

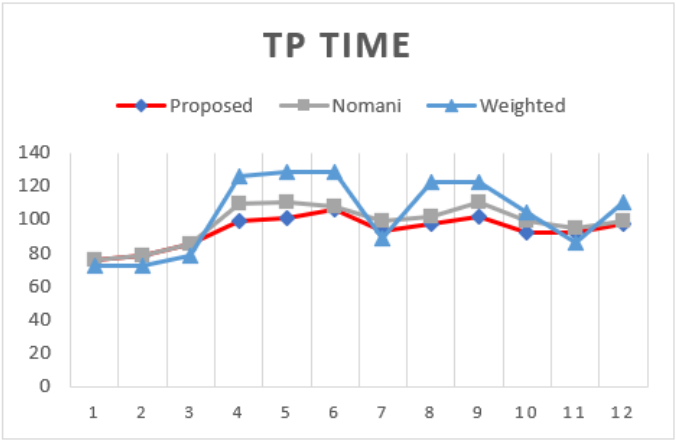

Figure 6 Comparison of transportation time obtained by different methods

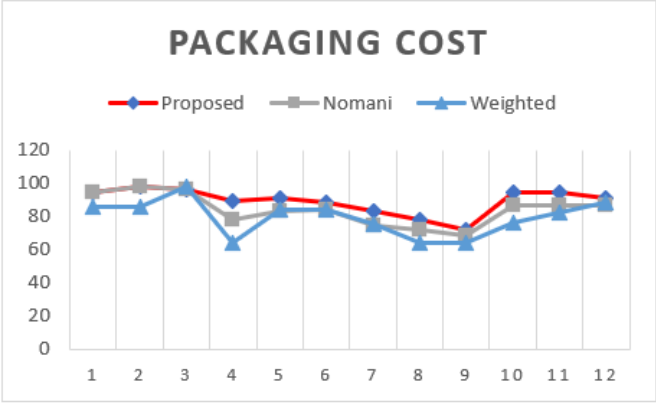

Figure 7 Comparison of packaging cost obtained by different methods

6 Conclusion

In this paper, we discussed a new modified goal programming model and a comparison was made with existing weighted models. The proposed model is capable of providing varying results for a MOTP. LINGO 19.0 was used to solve all the mathematical models. As further development, we plan to extend this method for Fractional MOTP, Rough MOTP and Fixed charge MOTP.

References

[1] Waiel F Abd El-Wahed. A multi-objective transportation problem under fuzziness. *Fuzzy sets and systems*, 117(1):27–33, 2001.

[2] Veena Adlakha and Krzysztof Kowalski. A quick sufficient solution to the more-for-less paradox in the transportation problem. *Omega*, 26(4):541–547, 1998.

[3] AK Bit, MP Biswal, and SS1185389 Alam. Fuzzy programming approach to multicriteria decision making transportation problem. *Fuzzy sets and systems*, 50(2):135–141, 1992.

[4] Edward L Hannan. On fuzzy goal programming. *Decision sciences*, 12(3):522–531, 1981.

[5] Frank L Hitchcock. The distribution of a product from several sources to numerous localities. *Journal of mathematics and physics*, 20(1-4):224–230, 1941.

[6] Heinz Isermann. The enumeration of all efficient solutions for a linear multiple-objective transportation problem. *Naval Research Logistics Quarterly*, 26(1):123–139, 1979.

[7] Sang M Lee and Laurence J Moore. Optimizing transportation problems with multiple objectives. *AIIE transactions*, 5(4):333–338, 1973.

[8] Sang M Lee and David L Olson. Goal programming. In *Multicriteria decision making*, pages 203–235. Springer, 1999.

[9] Gurupada Maity and Sankar Kumar Roy. Solving multi-choice multi-objective transportation problem: a utility function approach. *Journal of uncertainty Analysis and Applications*, 2(1):1–20, 2014.

[10] Mohammad Asim Nomani, Irfan Ali, and A Ahmed. A new approach for solving multi-objective transportation problems. *International journal of management science and engineering management*, 12(3):165–173, 2017.

[11] Jeffrey L Ringuest and Dan B Rinks. Interactive solutions for the linear multiobjective transportation problem. *European Journal of operational research*, 32(1):96–106, 1987.

[12] Rachana Saini, Vishwas Deep Joshi, and Jagdev Singh. On solving a mfl paradox in linear plus linear fractional multi-objective transportation problem using fuzzy approach. *International Journal of Applied and Computational Mathematics*, 8(2):1–13, 2022.

[13] Maryam Zangiabadi and Hamid Reza Maleki. Fuzzy goal programming technique to solve multiobjective transportation problems with some nonlinear membership functions. 2013.

Dynamical analysis of fractional yellow fever virus model with efficient numerical approach

Chandrali Baishya[1,*], Sindhu J. Achar[1], P. Veeresha[2], Devendra Kumar[3]

December 28, 2022

[1]Department of Studies and Research in Mathematics, Tumkur University, Tumkur-572103, Karnataka, India
Email: baishyachandrali@gmail.com, sindhuachar6@gmail.com
[2] Department of Mathematics, CHRIST (Deemed to be University), Bengaluru-560029, India
Email: pveeresha.maths@gmail.com & pundikala.veeresha@christuniversity.in
[3] Department of Mathematics, University of Rajasthan, Jaipur-302004, Rajasthan, India
Email: devendra.maths@gmail.com

Abstract

In this paper, we have projected the theoretical and numerical investigation of the mathematical model representing the yellow fever virus transmission from infected mosquitoes to humans or vise-versa through mosquito bites in the framework of the Caputo derivative. Theoretical aspects of the dynamics of susceptible individuals, exposed individuals, infected individuals, toxic infected individuals, recovered and immune individuals, and susceptible mosquitoes and infected mosquitoes have been analyzed by using the theory of fractional calculus such as boundedness, uniqueness and existence of the solutions. Sufficient conditions for the global stability of the virus-free point of equilibrium are inspected. T validate the theoretical results numerical analysis is performed using the generalized Adams-Bashforth-Moultan method.

Keywords: Predator-Prey, Yellow Fever Virus, Predictor-Corrector Method.
2000 Mathematics Subject Classification: 34A34, 92D30.

---

* Corresponding Author

1 Introduction

Infectious illness outbreaks have become the greatest threat to mankind over time, resulting in the loss of many lives. They may also bring economic and political upheaval if they are not handled properly. Yellow fever (YF) virus which belongs to a family of about 70 viruses was the first human virus discovered. YF is an intense viral disease spread by infected female 'Aedes aegypti' mosquitoes. These mosquitoes are also the vector of Zika virus, dengue and chikungunya [1, 2]. In Africa, sylvatic and peridomestic Aedes species transmit rural and intermediate YF. The incubation period of the virus on the infected individuals is generally 3 to 6 days [3]. Vomiting, nausea, lack of appetite, muscle pain with backache, slight fever, headache, jaundice, and weariness are some of the symptoms that patients experience [4]. Nonetheless, these symptoms fade after four or five days, while other individuals may continue to the infection's toxicity phase, in which 50 percent of instances lead to death within eight to ten days [5]. Although YF is compartmentalized as viral hemorrhagic fever, it causes 1000 times more risk to death than the virus like Ebola [1].

Among the scientific community, the study of disease dynamics has remained a popular issue [6, 7]. To help humankind in fighting against YF by understanding its dynamics mathematically, a few mathematicians have contributed their expertise in modeling this infection [8, 9]. In the recent times, fractional derivatives namely the Caputo, Riemann-Liouville, Gr*ü*nwald Letnikov, Jumarie, and Caputo-Fabrizio are investigated by the researchers in search of new behavioral findings while representing real world problems using such derivatives. Notably, many results associated with memory, hereditary, longrange memory, random walk, anomalous diffusion, non-Markovian processes, and others made the concept of fractional derivatives a highly significant to take into account [10–14]. Over the years, theories of these derivatives have also been developed to a great extent [15–18]. Many phenomena related to mathematical biology and their interdisciplinary fields [18, 19] have been studied using these fractional derivatives [20, 21]. They have been used to model many complex phenomena of disease dynamics [22–24].

This work aims to examine the qualitative nature of the yellow fever virus mathematical model with interaction of seven categories of the population namely susceptible , YF exposed, YF infected, toxic-infected individuals, recovered and immune individuals, susceptible mosquitoes, and infected mosquitoes incorporating the Caputo fractional derivative. Adams-Bashforth-Moulton method has been used to perform the numerical simulation [25–29]. The rest of the paper is structured as follows: in Section 2, we provide some elementary definitions, theorems and lemmas of fractional calculus which is followed by the formulation of the model in Section 3. Sections 4, 5, 6

dispense the existence and uniqueness, boundedness, the existence of various points of equilibrium and their local stability respectively. Sections 7 depicts the numerical method and simulation in detail. Finally, we discuss the concluding remarks in Section 8.

2 Some Essential Theorems

In the present work, we have used the Caputo fractional derivatives because it supports the integer order initial condition. In this section, we have presented certain theorems those have been applied to determine the theoretical results corresponding to the solution of the projected model. The Caputo fractional derivative is denoted by ${}^{C}D$.

Definition 2.1. [15] (Caputo Fractional Derivative) Suppose $g(\mathrm{t})$ is k times continuously differentiable function and $g^{(k)}(\mathrm{t})$ is integrable in $[\mathrm{t}_0, T]$. The fractional derivative of the order α established by Caputo sense for $g(\mathrm{t})$,is

$$ {}^{C}_{\mathrm{t}_0}D^{\alpha}_{\mathrm{t}}\, g(\mathrm{t}) = \frac{1}{\Gamma(k-\alpha)} \int_{\mathrm{t}_0}^{\mathrm{t}} \frac{g^{(k)}(\tau)}{(\mathrm{t}-\tau)^{\alpha+1-k}} d\tau $$

where $\Gamma(\cdot)$ refers to Gamma function, $\mathrm{t} > a$ and k is a positive integer with the property that $k-1 < \alpha < k$.

Lemma 1. [17] Consider the system

$$ {}^{C}_{\mathrm{t}_0}D^{\alpha}_{\mathrm{t}}\, v(\mathrm{t}) = g(\mathrm{t}, v),\ \mathrm{t} > \mathrm{t}_0, \tag{1} $$

choosing the initial condition as $v(\mathrm{t}_0)$, where $0 < \alpha \leq 1$ and $g : [\mathrm{t}_0, \infty) \times \Omega \to \mathbb{R}^n, \Omega \in \mathbb{R}^n$. When $g(\mathrm{t}, v)$ holds the locally Lipchitz conditions concerning to v, Eq.1 has a unique solution on $[\mathrm{t}_0, \infty) \times \Omega$.

Lemma 2. [18] We assume that $g(\mathrm{t})$ is a continuous function on $[\mathrm{t}_0, +\infty)$ satisfying

$$ {}^{C}_{\mathrm{t}_0}D^{\alpha}_{\mathrm{t}}\, g(\mathrm{t}) \leq -\lambda g(\mathrm{t}) + \xi,\ g(\mathrm{t}_0) = g_0, $$

where $\mathrm{t}_0 \geq 0$ is the initial time, $0 < \alpha \leq 1,\ \lambda \neq 0,\ \ (\lambda, \xi) \in \mathbb{R}^2$. Then,

$$ g(\mathrm{t}) \leq (g(\mathrm{t}_0) - \frac{\xi}{\lambda}) E_{\alpha}[-\lambda(\mathrm{t}-\mathrm{t}_0)^{\alpha}] + \frac{\xi}{\lambda} $$

Lemma 3. [18] Let $v(\mathrm{t}) \in \mathbb{R}_+$ be a derivable and continuous function. Then, at any time $\mathrm{t} > \mathrm{t}_0$,

$$ {}^{C}_{\mathrm{t}_0}D^{\alpha}_{\mathrm{t}}(v(\mathrm{t}) - v^* - v^* ln\frac{v(\mathrm{t})}{v^*}) \leq (1 - \frac{v^*}{v}) {}^{C}_{\mathrm{t}_0}D^{\alpha}_{\mathrm{t}}\, v(t), \quad v^* \in \mathbb{R}_+, \quad \forall \alpha \in (0,1). $$

3 Model Formulation

Yusuf and Daniel's [9] work has inspired the mathematical model described in this study. We observe that fractional derivatives influence coexistence. When a new virus emerges, it is never completely eradicated from the world. A fraction of humans will always be infected by that virus in some part of the universe. This nature of the virus's existence prompts us to model YF infection by incorporating fractional derivatives. In this paper, the YF virus mathematical model has been proposed within the population of humans and mosquitoes. It has been assumed that both populations mix freely without any barriers. Since there is a high risk of YF transmission from travelers, their vaccination is essential. It is assumed that some portion of the travelers is vaccinated. Again, a part of the infected population may become toxic. It is also assumed that once an individual becomes toxic, he or she does not recover. In the present model, the human population has been subdivided into five different compartments namely: $S_H(t), E_H(t), I_H(t), T_H(t), R_H(t)$ which represents the density of susceptible, YF exposed, YF infected, toxic-infected individuals, and recovered and immune individuals respectively. In the same way, the mosquito population is divided into two categories: $S_V(t), I_V(t)$ represent the density of susceptible mosquitoes and infected mosquitoes respectively. We have considered the Caputo sense fractional derivative to represent the projected model. The present model is as follows:

$$
\begin{aligned}
{}^{C}_{t_0}D^{\alpha}_{t} S_H &= r + (1-\sigma)\lambda - \theta\beta_1 S_H I_V - \rho S_H - d S_H, \\
{}^{C}_{t_0}D^{\alpha}_{t} E_H &= \theta\beta_1 S_H I_V - \mu E_H - d E_H, \\
{}^{C}_{t_0}D^{\alpha}_{t} I_H &= (1-\xi)\mu E_H - \psi I_H - (d+\Lambda) I_H, \\
{}^{C}_{t_0}D^{\alpha}_{t} T_H &= \xi\mu E_H - (d+\Lambda) T_H \\
{}^{C}_{t_0}D^{\alpha}_{t} R_H &= \psi I_H + \sigma\lambda + \rho S_H - d R_H, \\
{}^{C}_{t_0}D^{\alpha}_{t} S_V &= \nu - \theta\beta_2 S_V I_H - \phi S_V, \\
{}^{C}_{t_0}D^{\alpha}_{t} I_V &= \theta\beta_2 S_V I_H - \phi I_V.
\end{aligned}
\tag{2}
$$

with initial condition $S_H(t_0) = S_H(0)$, $E_H(t_0) = E_H(0)$, $I_H(t_0) = I_H(0)$, $T_H(t_0) = T_H(0)$, $R_H(t_0) = R_H(0)$, where t_0 is the initial time. All the parameters $r, \sigma, \lambda, \theta, \beta_1, \rho, d, \mu, \xi$, $\psi, \Lambda, \nu, \beta_2, \phi$ are non-negative. Where, r is the birth rate of human, σ is the vaccinated proportion of immigrants, λ is the arrival rate of immigrants per individual per time, and θ is the daily biting rate. β_1 and β_2 represent the transmission probability of YF from mosquitoes to human and from human to mosquitoes respectively. ρ is the effective vaccination rate of susceptible humans, d is the natural death rate of human, μ is the rate at which E_H progresses to I_H, ξ is the proportion of E_H which converts to the toxic case, ψ is the recovery rate of human, Λ is the death rate of human-induced due

to YF, ν is the birth rate of mosquitoes, and ϕ is the natural death rate of the vectors.

4 Existence of the solutions

The existence of the solution of the model 2 is demonstrated using the Fixed-Point Theorem. Due to the complex and non-local nature of the system 2, there are no precise algorithms or approaches for evaluating the exact solutions. However, the existence of the solution is assured if certain conditions are met. To initiate the process of establishing the existence of the solution, the system 2 is rewritten as:

$$\begin{aligned}
&{}^{C}_{t_0}D^{\alpha}_{t}[S_H(t)] = \mathfrak{P}_1(t,S_H),\ {}^{C}_{t_0}D^{\alpha}_{t}[E_H(t)] = \mathfrak{P}_2(t,E_H),\ {}^{C}_{t_0}D^{\alpha}_{t}[I_H(t)] = \mathfrak{P}_3(t,I_H),\\
&{}^{C}_{t_0}D^{\alpha}_{t}[T_H(t)] = \mathfrak{P}_4(t,T_H),\ {}^{C}_{t_0}D^{\alpha}_{t}[R_H(t)] = \mathfrak{P}_5(t,R_H),\ {}^{C}_{t_0}D^{\alpha}_{t}[S_V(t)] = \mathfrak{P}_6(t,S_V),\\
&{}^{C}_{t_0}D^{\alpha}_{t}[I_V(t)] = \mathfrak{P}_7(t,I_V).
\end{aligned} \tag{3}$$

The above system can be transformed into Volterra type integral equation as:

$$\begin{aligned}
S_H(t) - S_H(0) &= \frac{1}{\Gamma(\alpha)}\int_0^t \mathfrak{P}_1(\tau,S_H(\tau))(t-\tau)^{\alpha-1}d\tau,\\
E_H(t) - E_H(0) &= \frac{1}{\Gamma(\alpha)}\int_0^t \mathfrak{P}_2(\tau,E_H(\tau))(t-\tau)^{\alpha-1}d\tau,\\
I_H(t) - I_H(0) &= \frac{1}{\Gamma(\alpha)}\int_0^t \mathfrak{P}_3(\tau,I_H(\tau))(t-\tau)^{\alpha-1}d\tau,\\
T_H(t) - T_H(0) &= \frac{1}{\Gamma(\alpha)}\int_0^t \mathfrak{P}_4(\tau,T_H(\tau))(t-\tau)^{\alpha-1}d\tau,\\
R_H(t) - R_H(0) &= \frac{1}{\Gamma(\alpha)}\int_0^t \mathfrak{P}_5(\tau,R_H(\tau))(t-\tau)^{\alpha-1}d\tau,\\
S_V(t) - S_V(0) &= \frac{1}{\Gamma(\alpha)}\int_0^t \mathfrak{P}_6(\tau,S_V(\tau))(t-\tau)^{\alpha-1}d\tau,\\
I_V(t) - I_V(0) &= \frac{1}{\Gamma(\alpha)}\int_0^t \mathfrak{P}_7(\tau,I_V(\tau))(t-\tau)^{\alpha-1}d\tau.
\end{aligned} \tag{4}$$

Theorem 4.1. In the region $\Omega \times [t_0, T]$, where

$$\Omega = \{(S_H, E_H, I_H, T_H, R_H, S_V, I_V) \in \mathbb{R}^7 : max\{|S_H|, |E_H|, |I_H|, |T_H|, |R_H|, |S_V|, |I_V|\} \leq \mathfrak{M}\},$$

and $T < +\infty$, the Lipschitz condition is satisfied and contraction occurs by the kernel $\mathfrak{P}_1$ if $0 \leq \theta\beta_1\mathfrak{M} + \rho + d < 1$.

Proof: We consider the two functions S_H and $\bar{S}_H$ such as:

$$||\mathfrak{P}_1(t,S_H) - \mathfrak{P}_1(t,\bar{S}_H)|| = ||(r + (1-\sigma)\lambda - \theta\beta_1 S_H I_V - \rho S_H - dS_H)$$

$$
\begin{aligned}
&-(r+(1-\sigma)\lambda-\theta\beta_1\bar{S}_H I_V-\rho\bar{S}_H-d\bar{S}_H)||.\\
&\leq(\theta\beta_1\mathfrak{M}+\rho+d)||S_H(t)-\bar{S}_H(t)||\\
&=\zeta_1||S_H(t)-\bar{S}_H(t)||, \qquad (5)
\end{aligned}
$$

where $\zeta_1=\theta\beta_1\mathfrak{M}+\rho+d$. As a result, the Lipschitz condition is met for $\mathfrak{P}_1$ and if $0\leq\zeta_1<1$, then $\mathfrak{P}_1$ follows contraction. Similarly, it can be shown and illustrated in case of the other equations as follows:

$$
\begin{aligned}
&||\mathfrak{P}_2(t,E_H)-\mathfrak{P}_2(t,\bar{E}_H)||\leq\zeta_2||E_H(t)-\bar{E}_H(t)||,\ ||\mathfrak{P}_3(t,I_H)-\mathfrak{P}_3(t,\bar{I}_H)||\leq\zeta_3||I_H(t)-\bar{I}_H(t)||,\\
&||\mathfrak{P}_4(t,T_H)-\mathfrak{P}_4(t,\bar{T}_H)||\leq\zeta_4||T_H(t)-\bar{T}_H(t)||,\ ||\mathfrak{P}_5(t,R_H)-\mathfrak{P}_5(t,\bar{R}_H)||\leq\zeta_5||R_H(t)-\bar{R}_H(t)||,\\
&||\mathfrak{P}_6(t,S_V)-\mathfrak{P}_6(t,\bar{S}_V)||\leq\zeta_6||S_V(t)-\bar{S}_V(t)||,\ ||\mathfrak{P}_7(t,I_V)-\mathfrak{P}_7(t,\bar{I}_V)||\leq\zeta_7||I_V(t)-\bar{I}_V(t)||, \qquad (6)
\end{aligned}
$$

where $\zeta_2=(\mu+d)$, $\zeta_3=(\psi+d+\Lambda)$, $\zeta_4=(d+\Lambda)$, $\zeta_5=(\psi+d+\Lambda)$, $\zeta_6=(\theta\beta_2\mathfrak{M}+\phi)$ and $\zeta_7=\phi$. $\mathfrak{P}_i$, $i=2,3,4,5,6,7$ are the contraction if $0<\zeta_i<1$, $i=2,3,4,5,6,7$. Using system 4, the recursive form can now be written as follows:

$$
\begin{aligned}
\kappa_{1,n}(t)&=S_{H_n}(t)-S_{H_{n-1}}(t)=\frac{1}{\Gamma(\alpha)}\int_0^t(\mathfrak{P}_1(\tau,S_{H_{n-1}})-\mathfrak{P}_1(\tau,S_{H_{n-2}}))(t-\tau)^{\alpha-1}d\tau,\\
\kappa_{2,n}(t)&=E_{H_n}(t)-E_{H_{n-1}}(t)=\frac{1}{\Gamma(\alpha)}\int_0^t(\mathfrak{P}_2(\tau,E_{H_{n-1}})-\mathfrak{P}_2(\tau,E_{H_{n-2}}))(t-\tau)^{\alpha-1}d\tau,\\
\kappa_{3,n}(t)&=I_{H_n}(t)-I_{H_{n-1}}(t)=\frac{1}{\Gamma(\alpha)}\int_0^t(\mathfrak{P}_3(\tau,I_{H_{n-1}})-\mathfrak{P}_3(\tau,I_{H_{n-2}}))(t-\tau)^{\alpha-1}d\tau,\\
\kappa_{4,n}(t)&=T_{H_n}(t)-T_{H_{n-1}}(t)=\frac{1}{\Gamma(\alpha)}\int_0^t(\mathfrak{P}_4(\tau,T_{H_{n-1}})-\mathfrak{P}_4(\tau,T_{H_{n-2}}))(t-\tau)^{\alpha-1}d\tau,\\
\kappa_{5,n}(t)&=R_{H_n}(t)-R_{H_{n-1}}(t)=\frac{1}{\Gamma(\alpha)}\int_0^t(\mathfrak{P}_5(\tau,R_{H_{n-1}})-\mathfrak{P}_5(\tau,R_{H_{n-2}}))(t-\tau)^{\alpha-1}d\tau,\\
\kappa_{6,n}(t)&=S_{V_n}(t)-S_{V_{n-1}}(t)=\frac{1}{\Gamma(\alpha)}\int_0^t(\mathfrak{P}_6(\tau,S_{V_{n-1}})-\mathfrak{P}_6(\tau,S_{V_{n-2}}))(t-\tau)^{\alpha-1}d\tau,\\
\kappa_{7,n}(t)&=I_{V_n}(t)-I_{V_{n-1}}(t)=\frac{1}{\Gamma(\alpha)}\int_0^t(\mathfrak{P}_7(\tau,I_{V_{n-1}})-\mathfrak{P}_7(\tau,I_{V_{n-2}}))(t-\tau)^{\alpha-1}d\tau. \qquad (7)
\end{aligned}
$$

The prerequisites are: $S_{H_0}(t)=S_H(0)$, $E_{H_0}(t)=E_H(0)$, $I_{H_0}(t)=I_H(0)$, $T_{H_0}(t)=T_H(0)$, $R_{H_0}(t)=R_H(0)$, $S_{V_0}(t)=S_V(0)$, $I_{V_0}(t)=I_V(0)$.
By applying the norm to the first equation of the system 7, we obtained

$$
\begin{aligned}
||\kappa_{1,n}(t)||&=||S_{H_n}(t)-S_{H_{n-1}}(t)||\\
&=||\frac{1}{\Gamma(\alpha)}\int_0^t(\mathfrak{P}_1(\tau,S_{H_{n-1}})-\mathfrak{P}_1(\tau,S_{H_{n-2}}))(t-\tau)^{\alpha-1}d\tau||\\
&\leq\frac{1}{\Gamma(\alpha)}\int_0^t||(\mathfrak{P}_1(\tau,S_{H_{n-1}})-\mathfrak{P}_1(\tau,S_{H_{n-2}}))(t-\tau)^{\alpha-1}d\tau||. \qquad (8)
\end{aligned}
$$

Using Lipchitz condition 5, we get

$$||\kappa_{1,n}(t)|| \leq \frac{1}{\Gamma(\alpha)}\zeta_1 \int_0^t ||\kappa_{1,n-1}(\tau)d\tau||. \tag{9}$$

Similarly,

$$\begin{aligned}
&||\kappa_{2,n}(t)|| \leq \frac{1}{\Gamma(\alpha)}\zeta_2 \int_0^t ||\kappa_{2,n-1}(\tau)d\tau||,\ ||\kappa_{3,n}(t)|| \leq \frac{1}{\Gamma(\alpha)}\zeta_3 \int_0^t ||\kappa_{3,n-1}(\tau)d\tau||,\\
&||\kappa_{4,n}(t)|| \leq \frac{1}{\Gamma(\alpha)}\zeta_4 \int_0^t ||\kappa_{4,n-1}(\tau)d\tau||,\ ||\kappa_{5,n}(t)|| \leq \frac{1}{\Gamma(\alpha)}\zeta_5 \int_0^t ||\kappa_{5,n-1}(\tau)d\tau||,\\
&||\kappa_{6,n}(t)|| \leq \frac{1}{\Gamma(\alpha)}\zeta_6 \int_0^t ||\kappa_{6,n-1}(\tau)d\tau||,\ ||\kappa_{7,n}(t)|| \leq \frac{1}{\Gamma(\alpha)}\zeta_7 \int_0^t ||\kappa_{7,n-1}(\tau)d\tau||.
\end{aligned} \tag{10}$$

As a result, it yields
$S_{H_n}(t) = \sum_{i=1}^n \kappa_{1,i}, \quad E_{H_n}(t) = \sum_{i=1}^n \kappa_{2,i}, \quad I_{H_n}(t) = \sum_{i=1}^n \kappa_{3,i}, \quad T_{H_n}(t) = \sum_{i=1}^n \kappa_{4,i},$
$R_{H_n}(t) = \sum_{i=1}^n \kappa_{5,i}, \quad S_{V_n}(t) = \sum_{i=1}^n \kappa_{6,i}, \quad I_{V_n}(t) = \sum_{i=1}^n \kappa_{7,i}.$
This theorem will be used to illustrate the next theorem.

Theorem 4.2. The solution of the fractional model 2 exists and will be unique, if we acquire some t_α such that

$$\frac{1}{\Gamma(\alpha)}\zeta_i t_\alpha < 1,\ \ i = 1,2,3,...,7.$$

Proof: Applying equations 9 and 10 recursively, we have

$$\begin{aligned}
&||\kappa_{1,n}(t)|| \leq ||S_{H_n}(0)||\left[\frac{1}{\Gamma(\alpha)}\zeta_1 t\right]^n,\ ||\kappa_{2,n}(t)|| \leq ||E_{H_n}(0)||\left[\frac{1}{\Gamma(\alpha)}\zeta_2 t\right]^n,\\
&||\kappa_{3,n}(t)|| \leq ||I_{H_n}(0)||\left[\frac{1}{\Gamma(\alpha)}\zeta_3 t\right]^n,\ ||\kappa_{4,n}(t)|| \leq ||T_{H_n}(0)||\left[\frac{1}{\Gamma(\alpha)}\zeta_4 t\right]^n,\\
&||\kappa_{5,n}(t)|| \leq ||R_{H_n}(0)||\left[\frac{1}{\Gamma(\alpha)}\zeta_5 t\right]^n,\ ||\kappa_{6,n}(t)|| \leq ||S_{V_n}(0)||\left[\frac{1}{\Gamma(\alpha)}\zeta_6 t\right]^n,\\
&||\kappa_{7,n}(t)|| \leq ||I_{V_n}(0)||\left[\frac{1}{\Gamma(\alpha)}\zeta_7 t\right]^n.
\end{aligned} \tag{11}$$

As a result, the existence and continuity are established. To illustrate that the above relations formulate the solution of the model 2, we assume the following:

$$S_H(t) - S_{H_0}(t) = S_{H_n}(t) - \Delta_{1n}(t),\ E_H(t) - E_{H_0}(t) = E_{H_n}(t) - \Delta_{2n}(t), \tag{12}$$
$$I_H(t) - I_{H_0}(t) = I_{H_n}(t) - \Delta_{3n}(t),\ T_H(t) - T_{H_0}(t) = T_{H_n}(t) - \Delta_{4n}(t), \tag{13}$$
$$R_H(t) - R_{H_0}(t) = R_{H_n}(t) - \Delta_{5n}(t),\ S_V(t) - S_{V_0}(t) = S_{V_n}(t) - \Delta_{6n}(t), \tag{14}$$

$$I_V(t) - I_{V_0}(t) = I_{V_n}(t) - \Delta_{7n}(t). \tag{15}$$

In order to achieve the desired outcomes, set that

$$||\Delta_{1n}(t)|| = ||\frac{1}{\Gamma(\alpha)} \int_0^t (\mathfrak{P}_1(\tau, S_H) - \mathfrak{P}_1(\tau, S_{H_{n-1}}))d\tau|| \tag{16}$$

This implies,

$$||\Delta_{1n}(t)|| \leq \frac{1}{\Gamma(\alpha)} \zeta_1 ||S_H - S_{H_{n-1}}||t. \tag{17}$$

Continuing the same procedure recursively, we get

$$||\Delta_{1n}(t)|| \leq \left(\frac{1}{\Gamma(\alpha)} \zeta_1 t\right)^{n+1} \mathfrak{M}. \tag{18}$$

At certain t_α, we have

$$||\Delta_{1n}(t)|| \leq \left(\frac{1}{\Gamma(\alpha)} \zeta_1 t_\alpha\right)^{n+1} \mathfrak{M}. \tag{19}$$

From equation [**?**], we observe that $||\Delta_{1n}(t)||$ approaches to 0 as n tends to ∞, provided $\left(\frac{1}{\Gamma(\alpha)} \zeta_1 t_\alpha\right) < 1$. Similarly, it may be demonstrated that $||\Delta_{2n}(t)||$, $||\Delta_{3n}(t)||$, $||\Delta_{4n}(t)||$, $||\Delta_{5n}(t)||$, $||\Delta_{6n}(t)||$, $||\Delta_{7n}(t)||$ tends to 0. Hence the proof. We shall now demonstrate the uniqueness for the solution of the system 2. Let us assume that there is a different set of solutions, namely $\hat{S}_H, \hat{E}H, \hat{I}_H, \hat{T}_H, \hat{R}_H, \hat{S}_V, \hat{I}_V$ for the system 2. Then, as a result of the first equation, we have

$$S_H(t) - \hat{S}_H(t) = \frac{1}{\Gamma(\alpha)} \int_0^t (\mathfrak{P}_1(t, S_H) - \mathfrak{P}_1(t, \hat{S}_H))d\tau. \tag{20}$$

Using the norm, the equation above becomes:

$$||S_H(t) - \hat{S}_H(t)|| = \frac{1}{\Gamma(\alpha)} \int_0^t ||(\mathfrak{P}_1(t, S_H) - \mathfrak{P}_1(t, \hat{S}_H))d\tau||. \tag{21}$$

By applying the Lipschitz condition,

$$||S_H(t) - \hat{S}_H(t)|| \leq \frac{1}{\Gamma(\alpha)} \zeta t ||S_H - \hat{S}_H||.$$

This results in,

$$||S_H(t) - \hat{S}_H(t)|| \left(1 - \frac{(1-\alpha)}{\Gamma(\alpha)} \zeta t\right) \leq 0.$$

Since $\left(1 - \frac{1}{\Gamma(\alpha)} \zeta_1 t\right) > 0$, we much have $||S_H(t) - \hat{S}_H(t)|| = 0$. This implies $S_H(t) = \hat{S}_H(t)$.

5 Boundedness

In this Section, we have established the boundedness of the solution of the system 2.

Theorem 5.1. The solution of the system 2 is uniformly bounded.

Proof. Considering the function, $\mathfrak{L}(t) = S_H(t)+E_H(t)+I_H(t)+T_H(t)+R_H(t)+S_V(t)+I_V(t)$.
and applying fractional derivative on it, we get

$$\begin{aligned} {}^{C}_{t_0}D^{\alpha}_{t}\mathfrak{L}(t)+d\mathfrak{L}(t) &= {}^{C}_{t_0}D^{\alpha}_{t}[S_H(t)+E_H(t)+I_H(t)+T_H(t)+R_H(t)+S_V(t)+I_V(t)] \\ &\quad +d[S_H(t)+E_H(t)+I_H(t)+T_H(t)+R_H(t)+S_V(t)+I_V(t)] \\ &= r+\lambda-\Lambda(I_H+T_H)+\nu-\phi(S_V+I_V)+d(S_V+I_V) \\ &\leq r+\lambda+\nu+dS_V+dI_V. \end{aligned} \tag{22}$$

The solution exists and is unique in
$\mho = \{(S_H,E_H,I_H,T_H,R_H,S_V,I_V)/max\{|S_H|,|E_H|,|I_H|,|T_H|,|R_H|,|S_V|,|I_V|\} \leq \mathfrak{M}\}$.
The above inequality yields,

$${}^{C}_{t_0}D^{\alpha}_{t}\mathfrak{L}(t)+d\mathfrak{L}(t) \leq r+\lambda+\nu+2d\mathfrak{M}.$$

By the Lemma 2, we get

$${}^{C}_{t_0}D^{\alpha}_{t}\mathfrak{L}(t) \leq (\mathfrak{L}(t_0)-\frac{1}{d}(r+\lambda+\nu+2d\mathfrak{M})E_{\alpha}[-\eta(t-t_0)^{\alpha}]+\frac{1}{d}(r+\lambda+\nu+2d\mathfrak{M}) \rightarrow r+\lambda+\nu+2d\mathfrak{M}$$

as $t \rightarrow \infty$. Therefore, all the solution of the system 2 that initiates in $\mho$ remained bounded in
$\Theta = \{(S_H,E_H,I_H,T_H,R_H,S_V,I_V) \in \mho_+ | \mathfrak{L}(t) \leq r+\lambda+\nu+2d\mathfrak{M}+\varepsilon, \quad \varepsilon > 0\}$. □

6 Existence of points of equilibrium

In this section, we find the points of equilibrium of the system 2. We have the following points of equilibrium for the fractional order system 2:

1. The disease-free equilibrium point is $\bar{\mathfrak{I}} = (\frac{r+\lambda(1-\sigma)}{d+\rho},0,0,0,\frac{\rho(r+\lambda)+d\lambda\sigma}{d^2+d\rho},\frac{\nu}{\phi},0)$ and it always exists.

2. The endemic equilibrium point $\tilde{\mathfrak{I}} = (\tilde{S_H},\tilde{E_H},\tilde{I_H},\tilde{T_H},\tilde{R_H},\tilde{S_V},\tilde{I_V})$ exists if $\nu\theta^2\mu\beta_1\beta_2(1-\xi)(r+\lambda(1-\sigma)) > \phi^2(d+\mu)(d+\rho)(d+\Lambda+\psi)$. Coexistence equilibrium point can be obtained by solving the algebraic equations given below:

$$r+(1-\sigma)\lambda-\theta\beta_1\tilde{S_H}\tilde{I_V}-\rho\tilde{S_H}-d\tilde{S_H}=0,\ \theta\beta_1\tilde{S_H}\tilde{I_V}-\mu\tilde{E_H}-d\tilde{E_H}=0,$$

$$(1-\xi)\mu\tilde{E_H} - \psi\tilde{I_H} - (d+\Lambda)\tilde{I_H} = 0,\ \xi\mu\tilde{E_H} - (d+\Lambda)\tilde{T_H} = 0,$$
$$\psi\tilde{I_H} + \sigma\lambda + \rho\tilde{S_H} - d\tilde{R_H} = 0,\ \nu - \theta\beta_2\tilde{S_V}\tilde{I_H} - \phi\tilde{S_V} = 0,$$
$$\theta\beta_2\tilde{S_V}\tilde{I_H} - \phi\tilde{I_V} = 0.$$

Solving these equations we obtain,

$$\tilde{S_H} = \frac{r+\lambda(1-\sigma)}{d+\rho+\tilde{I_V}\theta\beta_1},$$
$$\tilde{E_H} = \frac{\tilde{I_V}\theta\beta_1(r+\lambda(1-\sigma))}{(d+\mu)(d+\rho+\tilde{I_V}\theta\beta_1)},$$
$$\tilde{T_H} = \frac{\tilde{I_V}\theta\mu\xi\beta_1(r+\lambda(1-\sigma))}{(d+\mu)(d+\Lambda+\psi)(d+\rho+\tilde{I_V}\theta\beta_1)},$$
$$\tilde{R_H} = \frac{1}{d}\left(\lambda\sigma + \frac{\rho(r+\lambda(1-\sigma))}{d+\rho+\tilde{I_V}\theta\beta_1} + \frac{\tilde{I_V}\phi^2\psi}{\theta\beta_2(\nu-\tilde{I_V}\phi)}\right),$$
$$\tilde{I_H} = \frac{\tilde{I_V}\phi^2}{\theta\beta_2(\nu-\tilde{I_V}\phi)},$$
$$\tilde{S_V} = \frac{\nu(\nu-\tilde{I_V}\phi)}{\phi(\nu-\tilde{I_V}\phi)+\tilde{I_V}\phi^2},$$
$$\tilde{I_V} = \frac{-\phi^2(d+\mu)(d+\rho)(d+\Lambda+\psi)+\nu\theta^2\mu\beta_1\beta_2(1-\xi)(r+\lambda(1-\sigma))}{\theta\phi^2\beta_1(d+\mu)(d+\Lambda+\psi)+\theta\mu\beta_2(1-\xi)(r+\lambda(1-\sigma))}.$$

Clearly, $\tilde{I_V} > 0$ if $\nu\theta^2\mu\beta_1\beta_2(1-\xi)(r+\lambda(1-\sigma)) > \phi^2(d+\mu)(d+\rho)(d+\Lambda+\psi)$ and hence the endemic equilibrium point exists if this condition is satisfied.

7 Numerical Simulation

Here, we have evaluated the model 2 numerically taking into consideration the influences of various parameters on the dynamics of YF transmission. We have considered the initial values as: $S_{H_0}(t) = 0.62$, $E_{H_0}(t) = 0.23$, $I_{H_0}(t) = 0.1$, $T_{H_0}(t) = 0.05$, $R_{H_0}(t) = 0$, $S_{V_0}(t) = 0.9$, $I_{V_0}(t) = 0.1$. Values of the parameters are considered as:$r = \frac{4.94}{10^5}$, $\theta = 3$, $\beta_1 = 0.6$, $\beta_2 = 0.5$, $\sigma = \frac{0.5}{10^6}$, $\lambda = \frac{1}{10^6}$, $\rho = 0.01$, $d = \frac{4.94}{10^5}$, $\mu = 0.31$, $\xi = 0.15$, $\psi = 0.143$, $\Lambda = \frac{3.5}{10}$, $\nu = 0.051$, $\phi = 0.051$. It is assumed that 50 of the immigrants are vaccinated. From the Figures 1 it is visible that, the daily biting rate θ influences the infected human and infected mosquito population. For $\alpha = 1$, these populations tends to grow and reaches the peak, and thereafter they start to decrease and tend to extinction. As the fractional values are incorporated, it is notable that, there is a delay in extinction of the I_H and I_V population. As the value of α further decreases, we notice that infections in human and mosquitoes are never eradicated. In fact a small portion of population are always with infection.

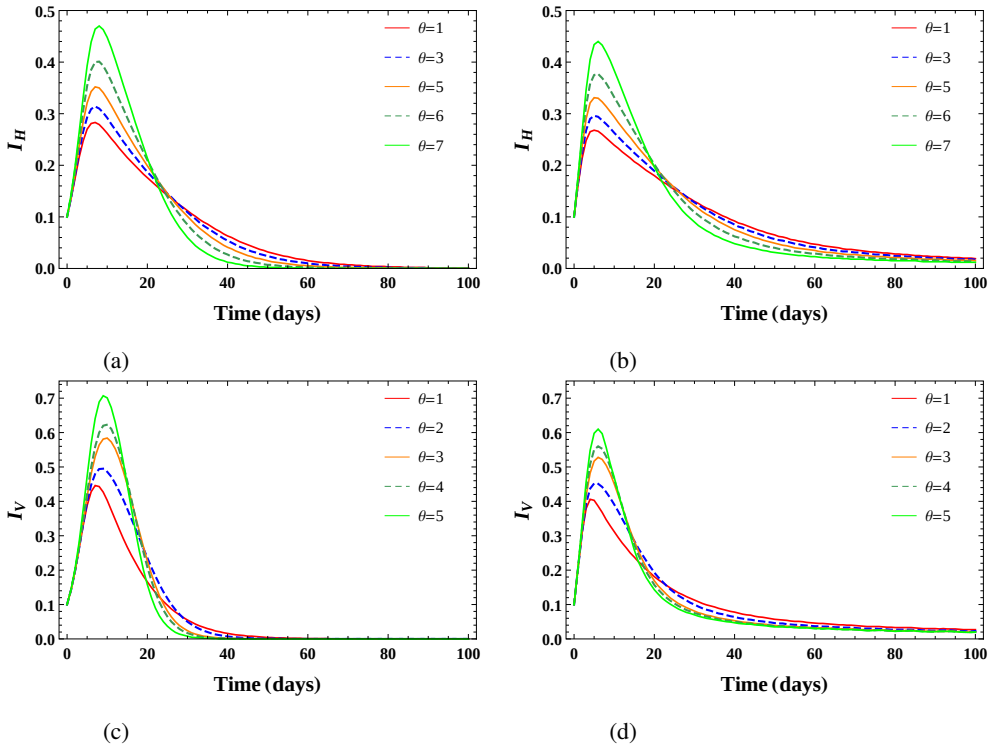

Figure 1: Profile of I_H and I_V for distinct values of θ for (A) $\alpha = 1$, (B) $\alpha = 0.65$, (C) $\alpha = 1$, (D) $\alpha = 0.65$

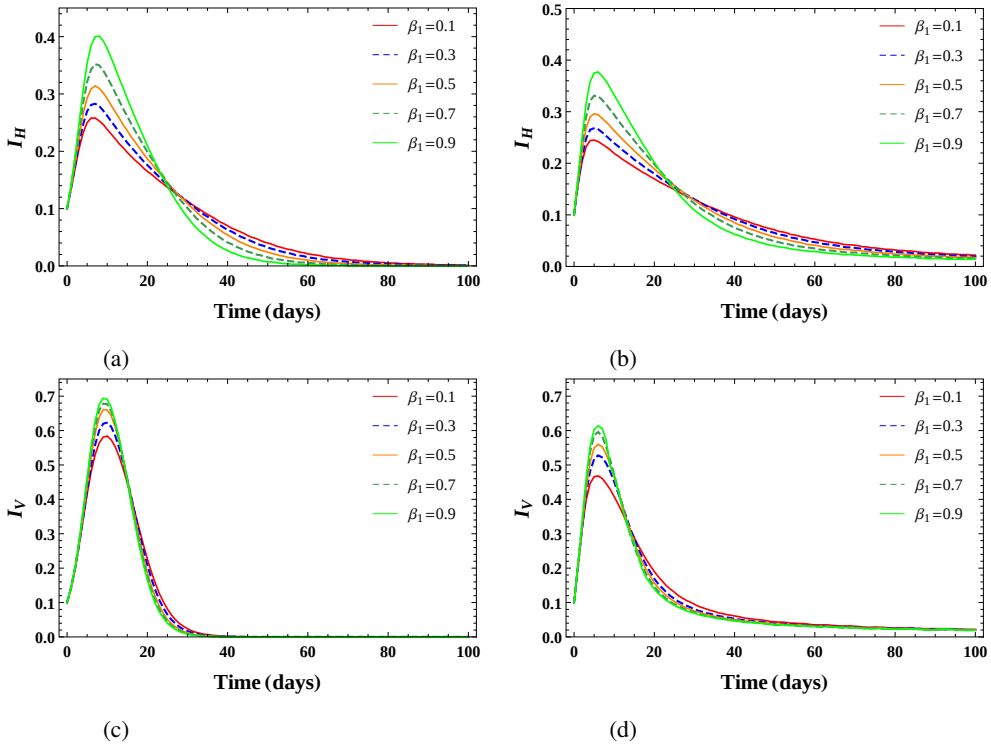

Figure 2: Profile of I_H and I_V for distinct values of β_1 for (A) $\alpha = 1$, (B) $\alpha = 0.65$, (C) $\alpha = 1$, (D) $\alpha = 0.65$

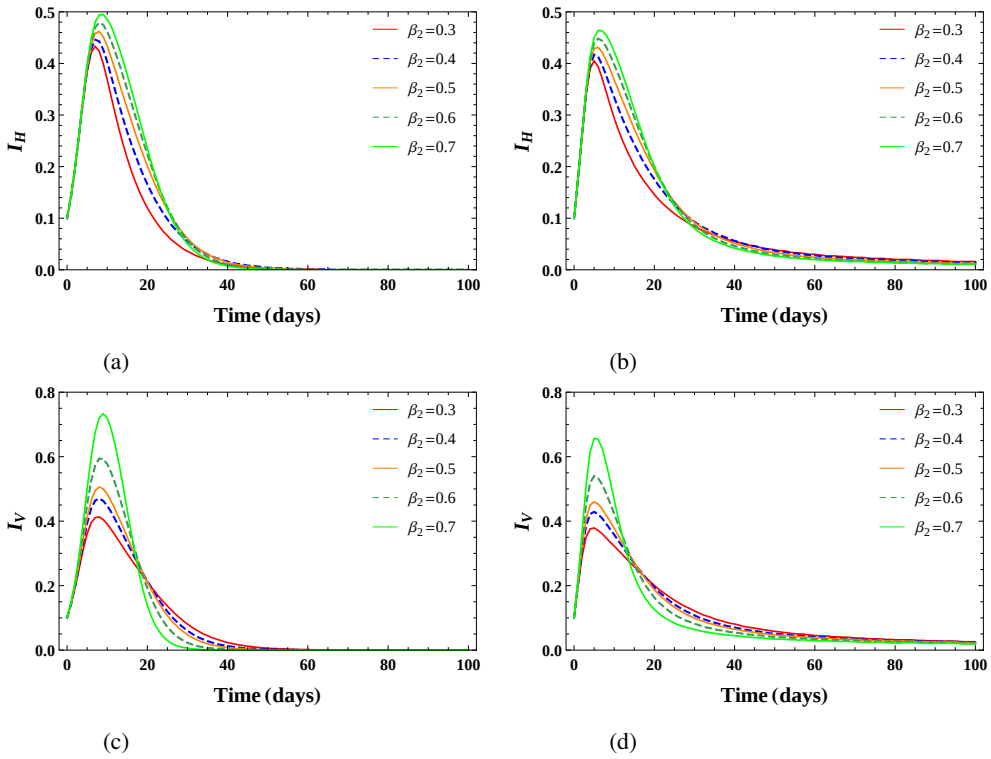

Figure 3: Profile of I_H and I_V for distinct values of β_2 for (A) $\alpha = 1$, (B) $\alpha = 0.65$, (C) $\alpha = 1$, (D) $\alpha = 0.65$

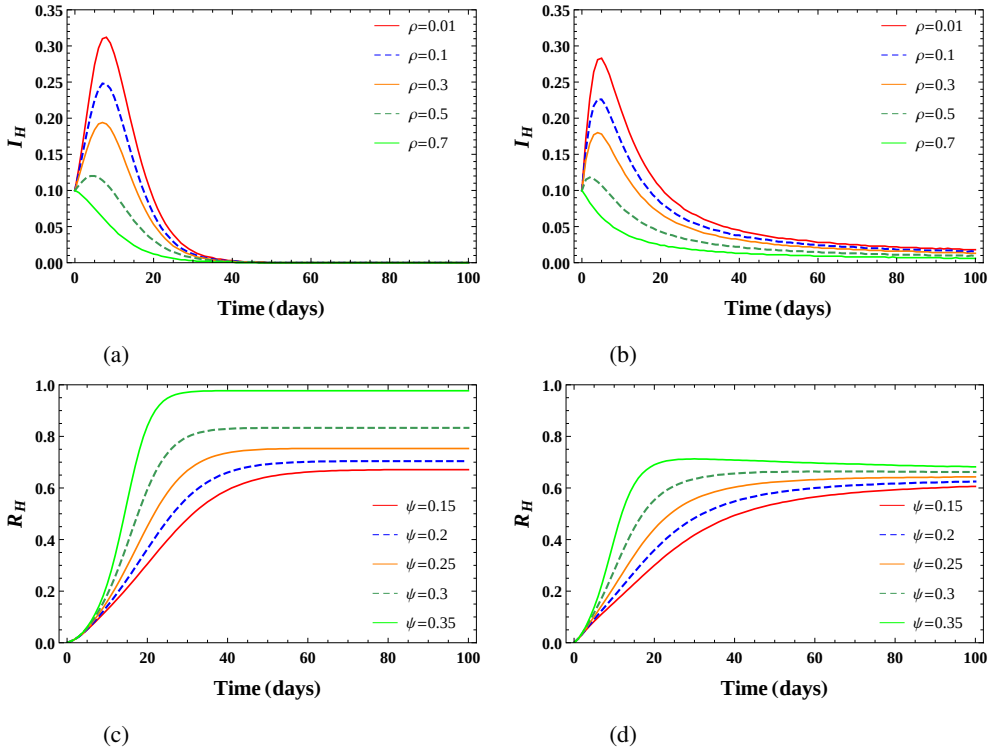

Figure 4: Profile of I_H and R_H for distinct values of (A) ρ and $\alpha = 1$, (B) ρ and $\alpha = 0.65$, (C) ψ and $\alpha = 1$, (D)ψ and $\alpha = 0.65$

The variations in the profiles of I_H and I_V for different values of β_1 are depicted in Figures 2. Figures 3 shows the variation in the profile of I_H and I_V for distinct values of β_2. From the above graphs it is visible that, as the value of β_1 and β_2 increases, the I_H and I_V population tends to grow and attains maximum value. Subsequently, they start decreasing and reach nullity which results in extinction of the I_H and I_V population. But decrease in the value of fractional derivative results in existence of the infection among the populations for longer duration. Figure 4 represents the varied profile of I_H for discrete values of effective vaccination rate of susceptible population. From the figure it is notable that, as the vaccination rate increases, the infected host population keeps on decreasing. Further, as the time progress, the infection extincts due to the influence of vaccination. As the fractional values are introduced, a fall in the infected population peak is notable. Figure 4 also depicts the profile of R_H for different recovery rate ψ and various fractional values. It may be observed that, as the value of recovery rate ψ is increased, the total recovery population also increases and leads to reduction of the

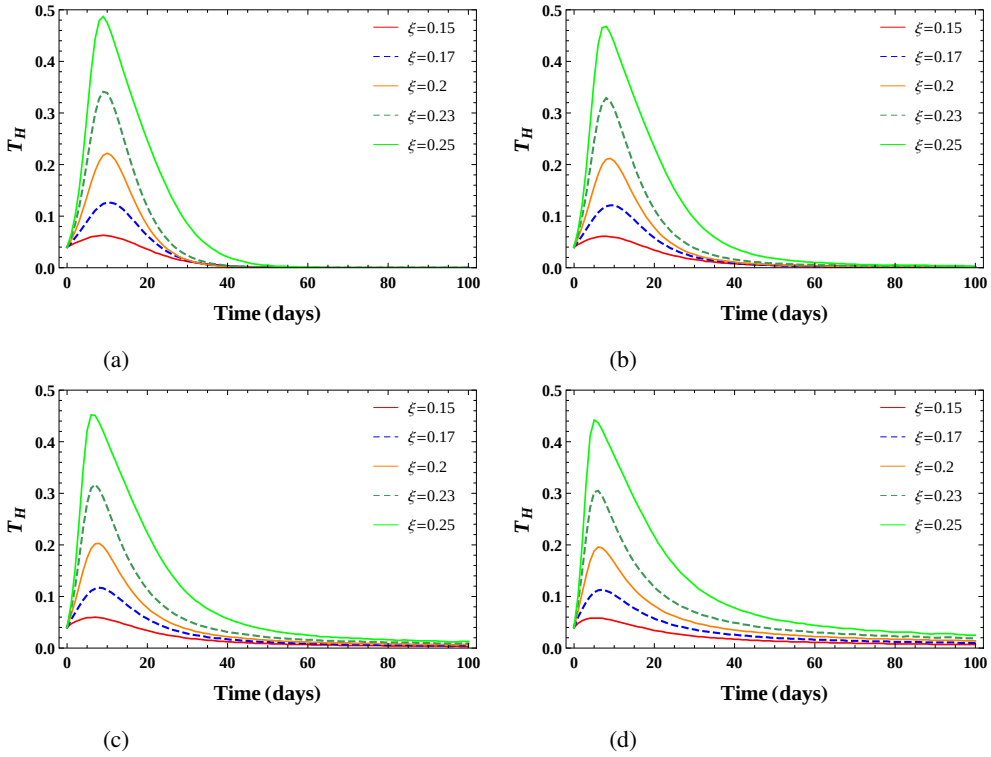

Figure 5: Profile of T_H for distinct values of ξ for (A) $\alpha = 1$, (B) $\alpha = 0.95$, (C) $\alpha = 0.85$, (D) $\alpha = 0.65$

epidemic in the host population.Figure 5 presents the dynamics of the toxic population as the proportion of exposed population deteriorates into toxic case at the rate ξ. As the value of ξ increases, the population of toxic ones grows. Further, since there is no recovery in toxic population, they die and hence population tends to extinction.

8 Conclusion

The fractional dynamics of the YF model is investigated in the present work in Caputo sense. Boundedness, existence, continuity, and uniqueness of the solution have been established. In the figures we have demonstrated the profile of the infected human and infected vectors under the influence of the biting rate, transmission rate from mosquitoes to human and human to mosquitoes, vaccination rate of susceptible population, recovery rate, and toxicity rate in presence of the Caputo fractional derivatives. We have observed that the Caputo derivative provides more realistic information than

that of the classical derivative. The reseason behind this claim is that it does not show the extinction of the infection from the environment. Graphical representations establish that the Adams-Bashfort-Moulton predictor-corrector method gives expected depiction of the results for analyzing the dynamics of the projected model. Numerical analysis of disease dynamics in the framework of various fractional derivatives can enrich the applications of mathematics for betterment of humankind as a future direction of studies of fractional calculus.

References

[1] T. P. Monath, "Dengue and yellow fever-challenges for the development and use of vaccines," *New England Journal of Medicine*, vol. 357, no. 22, pp. 2222–2225, 2007.

[2] T. P. Monath and P. F. Vasconcelos, "Yellow fever," *Journal of clinical virology*, vol. 64, pp. 160–173, 2015.

[3] M. Kung'aro, L. S. Luboobi, and F. Shahada, "Reproduction number for yellow fever dynamics between primates and human beings," *Commun. Math. Biol. Neurosci.*, 2014.

[4] T. P. Monath, "Treatment of yellow fever," *Antiviral research*, vol. 78, no. 1, pp. 116–124, 2008.

[5] T. P. Monath and A. D. Barrett, "Pathogenesis and pathophysiology of yellow fever," *Advances in virus research*, vol. 60, pp. 343–397, 2003.

[6] W. O. Kermack and A. G. McKendrick, "Contributions to the mathematical theory of epidemics-I," *Bulletin of mathematical biology*, vol. 53, no. 1-2, pp. 33–55, 1991.

[7] A. S. Quintero and R. E. Gutierrez-Carvajal, "Modeling the Evolution of SARS-CoV-2 Using a Fractional-Order SIR Approach," *TecnoLogicas*, vol. 24, no. 51, 2021.

[8] L. Esteva, C. Vargas, and H. M. Yang, "A model for yellow fever with migration," vol. 1, no. 6, 2019.

[9] T. T. Yusuf and D. O. Daniel, "Mathematical modeling of yellow fever transmission dynamics with multiple control measures," *Asian Research Journal of Mathematics*, pp. 1–15, 2019.

[10] C. Baishya, "An operational matrix based on the Independence polynomial of a complete bipartite graph for the Caputo fractional derivative," *SeMA Journal*, pp. 1–19, 2021.

[11] M. R. Ali and R. Sadat, "Construction of Lump and optical solitons solutions for (3+ 1) model for the propagation of nonlinear dispersive waves in inhomogeneous media," *Optical and Quantum Electronics*, vol. 53, no. 5, pp. 1–13, 2021.

[12] C. Baishya and P. Veeresha, "Laguerre polynomial-based operational matrix of integration for solving fractional differential equations with non-singular kernel," *Proceedings of the Royal Society A*, vol. 477, 2021.

[13] P. Veeresha, "A numerical approach to the coupled atmospheric ocean model using a fractional operator," *Mathematical Modelling and Numerical Simulation with Applications (MMNSA)*, vol. 1, no. 1, pp. 1–10, 2021.

[14] M. R. Ali, W.-X. Ma, and R. Sadat, "Lie symmetry analysis and invariant solutions for (2+ 1) dimensional Bogoyavlensky-Konopelchenko equation with variable-coefficient in wave propagation," *Journal of Ocean Engineering and Science*, 2021.

[15] I. Podlubny, *Fractional differential equations: an introduction to fractional derivatives, fractional differential equations, to methods of their solution and some of their applications*. Elsevier, 1998.

[16] J. Losada and J. J. Nieto, "Properties of a new fractional derivative without singular kernel," *Progr. Fract. Differ. Appl*, vol. 1, no. 2, pp. 87–92, 2015.

[17] B. Wang and L.-Q. Chen, "Asymptotic stability analysis with numerical confirmation of an axially accelerating beam constituted by the standard linear solid model," *Journal of Sound and Vibration*, vol. 328, no. 4-5, pp. 456–466, 2009.

[18] H. L. Li, L. Zhang, C. Hu, Y.-L. Jiang, and Z. Teng, "Dynamical analysis of a fractional-order predator-prey model incorporating a prey refuge," *Journal of Applied Mathematics and Computing*, vol. 54, no. 1-2, pp. 435–449, 2017.

[19] C. Baishya, S. J. Achar, P. Veeresha, and D. G. Prakasha, "Dynamics of a fractional epidemiological model with disease infection in both the populations," *Chaos: An Interdisciplinary Journal of Nonlinear Science*, vol. 31, no. 4, 2021.

[20] M. A. Dokuyucu, E. Celik, H. Bulut, and H. M. Baskonus, "Cancer treatment model with the Caputo-Fabrizio fractional derivative," *The European Physical Journal Plus*, vol. 133, no. 3, pp. 1–6, 2018.

[21] M. A. Khan, Z. Hammouch, and D. Baleanu, "Modeling the dynamics of hepatitis E via the Caputo–Fabrizio derivative," *Mathematical Modelling of Natural Phenomena*, vol. 14, no. 3, 2019.

[22] E. Ahmed and H. A. El-Saka, "On fractional order models for Hepatitis C," *Nonlinear biomedical physics*, vol. 4, no. 1, pp. 1–3, 2010.

[23] P. Veeresha, D. Kumar, "Analysis and dynamics of the Ivancevic option pricing model with a novel fractional calculus approach," *Waves in Random and Complex Media*, pp. 1-18, 2022.

[24] S. J. Achar, C. Baishya, P. Veeresha, and L. Akinyemi, "Dynamics of fractional model of biological pest control in tea plants with Beddington-DeAngelis functional response," *Fractal and Fractional*, vol. 6, no. 1, 2022.

[25] K. Diethelm, N. J. Ford, and A. D. Freed, "A predictor-corrector approach for the numerical solution of fractional differential equations," *Nonlinear Dynamics*, vol. 29, no. 1, pp. 3–22, 2001.

[26] K. Diethelm and N. J. Ford, "Analysis of fractional differential equations," *Journal of Mathematical Analysis and Applications*, vol. 265, no. 2, pp. 229–248, 2002.

[27] C. Baishya, "Dynamics of fractional stage structured predator prey model with prey refuge," *Indian Journal of Ecology*, vol. 47, no. 4, pp. 1118–1124, 2020.

[28] S. J. Achar, C. Baishya, and M. K. Kaabar, "Dynamics of the worm transmission in wireless sensor network in the framework of fractional derivatives," *Mathematical Methods in the Applied Sciences*, 2021.

[29] C. Baishya, "Dynamics of fractional holling type-ii predator-prey model with prey refuge and additional food to predator," *Journal of Applied Nonlinear Dynamics*, vol. 10, no. 2, pp. 315–328, 2020.

TABLE OF CONTENTS, JOURNAL OF COMPUTATIONAL ANALYSIS AND APPLICATIONS, VOL. 31, NO. 1, 2023